The Impact of Bile Acids on Glucocorticoid Metabolism

Alison Delamere McNeilly

A thesis submitted in partial fulfilment of the requirements of the Degree of Doctor of Philosophy awarded by the University of Edinburgh

March 2006

I hereby declare that this thesis was written by me and that all of the work contained herein was performed by myself except where otherwise stated.

Alison Delamere McNeilly

Abstract

Glucocorticoids regulate a myriad of metabolic and homeostatic processes including lipid and glucose metabolism within the liver and electrolyte balance within the kidney. Circulating levels of active glucocorticoid are regulated tightly by a balance of hypothalamic-pituitary-adrenal (HPA) forward drive, glucocorticoid negative feedback and rates of inactivation. Isoforms of 11β-hydroxysteroid dehydrogenase (11β-HSD1 and 2) interconvert active and inactive glucocorticoids thereby regulating access of glucocorticoids to the corticosteroid receptor (GR). The A-ring reductases (5α- and 5β-reductase) and 3α-hydroxysteroid dehydrogenase (3α-HSD) are involved in both peripheral glucocorticoid metabolism and bile acid biosynthesis. Bile acids are known to regulate their own biosynthesis by feed-forward induction of genes involved in bile acid detoxification and/or excretion and suppression of those involved in biosynthesis. Alterations in hepatic bile acid concentration may therefore influence glucocorticoid metabolism and thus HPA axis activation.

The work in this thesis demonstrates that bile acids and their conjugates are competitive inhibitors of glucocorticoid metabolism by both 11β-HSD1 and 5β-reductase in liver. In vivo, in male Wistar rats, manipulation of hepatic bile acid concentrations by dietary supplementation with chenodeoxycholic acid (CDCA; 1% w/w) suppressed activities of hepatic 5β-reductase and 11βHSD1 activity and caused a reduction in total urinary (mainly 5β-reduced) glucocorticoid metabolites. In response to acute restraint stress bile acid treated animals showed a delay in return to basal corticosterone levels indicative of altered clearance. In addition, adrenal weight and lipid accumulation within the adrenal gland was reduced in bile acid treated animals. Stimulation of bile acid synthesis by cholestyramine (5% w/w) reduced hepatic 5β-reductase activity with animals excreting fewer urinary total (mainly 5β-reduced) glucocorticoid metabolites. Conversely, a reduction in hepatic bile acid content via administration of a fat-free diet induced hepatic 5β-reductase activity accompanied by an increase in total, principally 5β-reduced, urinary metabolites. Animals fed the fat-free diet had larger adrenal glands, and suppressed circulating corticosterone, again suggesting altered HPA axis regulation.

These findings were pursued in rats with bile duct ligation, a pathological model of elevated bile acids. In these animals, reduced activities of 5β-reductase and 11β-HSD1 were also identified. Lastly investigations were made of the impact of bile acids on the renin-angiotensin-aldosterone system (RAAS). Manipulations which increased bile acids concentrations were predicted to reduce the rate of aldosterone inactivation, since it too is a substrate for 5β-reductase. Treatments increasing bile acids were accompanied by a renin-independent increase in aldosterone and associated sodium retention.

Acknowledgements

I would like to thank my supervisors Dr Ruth Andrew and Professor Brian Walker and Dr Chris Kenyon for their guidance, encouragement and support throughout my PhD. I am indebted to everyone in the Department of Endocrinology for their unrelenting patience, advice, scientific input and continuous support, in particular Annick de Vries, Dawn Livingstone, Peter Raubenheimer and Rachel McDonnell. I would like to acknowledge Dr Eleanor Davies and Dr Scott Mackenzie from the Department of Cardiovascular Sciences, Glasgow University for their assistance with real-time PCR, and all the staff at the BRF for their help and advice. I am indebted to the Wellcome Trust and the CVRI for funding and supporting me for the last four years.

Finally I must thank my family and friends, especially my Mother and Father for their continual support and belief in my ability, my twin sister Jane for providing help and encouragement and Perry and Cath who have stuck by me through thick and thin.

Table of Contents

Figures

Chapter 1

Chapter 2

Chapter 3

Chapter 5

Chapter 6

Tables

Chapter 1

Chapter 2

Chapter 3

Chapter 4

Chapter 5

Chapter 6

Abbreviations

A	11-dehydrocorticosterone
ACE	angiotensin converting enzyme
ACTH	adrenocorticotrophic hormone
ACRD	cortisone reductase deficiency
AKR	aldo-keto reductase
AME	apparent mineralocorticoid excess
ANG	angiotensin
ANOVA	analysis of variance
AR	androgen receptor
ARR	aldosterone : renin ratio
ASBT	sodium-dependent bile acid transporter
AUC	area under the curve
B	corticosterone
BARE	bile acid response elements
BDL	bile duct ligation
β-LPH	β-lipotrophin
BSEP	bile salt export pump
CBX	carbenoxolone
CA	cholic acid
CDCA	chenodeoxycholic acid
CE	cholestyrl esters
CF	co-factor
CNS	central nervous system
CRF	corticotrophin releasing factor
CT	cholestyramine
CYP	cytochrome P450
DCA	deoxycholic acid
DEPC	diethylpyrocarbonate
DHEA	dehydroepiandrostenedione
5α-DHT	5α-dihydrotestosterone
DMEM	dulbecco's modified eagle's medium
dNTP	deoxynucleotide triphosphates
5β-THB	5β-tetrahydrocorticosterone
DTT	dithiothreitol
E	cortisone
ER	endoplasmic reticulum
F	cortisol
FBS	fetal bovine serum
FSH	follicle stimulating hormone
FXR	farnesoid X (bile acid) receptor
GA	glycyrrhetinic acid
GCDCA	glyco-chenodeoxycholic acid
GC-MS	gas chromatography mass spectrometry
GH	growth hormone
GR	glucocorticoid receptor
GRE	glucocorticoid response element

7αHCOH	7α-hydroxycholestenone
HDL	high density lipoprotein
H6PDH	hexose-6-phosphate dehydrogenase
HNFα	hepatocyte nuclear receptor 4α
HPA	hypothalamic-pituitary-adrenal
HPLC	high performance liquid chromatography
HSD	hydroxysteroid dehydrogenase
HSP	heat shock protein
I-BABP	ileum bile acid binding protein
IL-1β	interleukin 1β
JNK/c-Jun	c-jun N-terminal kinase
KRB	Hanks Krebs ringer buffer
LCA	lithocholic acid
LDL	low-density lipoprotein
LH	luteinising hormone
LRH-1	liver receptor homologue-1
LXR	oxysterol receptor
M-MLV	murine leukaemia virus
MO-TMS	methoxyamine-trimethylsilimizadole
MR	mineralocortiocid receptor
NH	nuclear hormone
NR	nuclear receptor
NTCP	sodium-dependent taurocholate co-transport peptide
OFN	oxygen-free nitrogen
PBC	primary-biliary cirrhosis
PBS	phosphate buffered saline
PCN	pregnenolone 16α-carbonitrile
PCR	polymerase chain reaction
PEPCK	phosphoenolpyruvate carboxykinase
PFIC1	progressive familial intrahepatic cholestasis type 1
PRL	prolactin
PVN	paraventricular nucleus
PXR	pregnane X receptor
RARα	retinoic acid activated receptor α
RT	room temperature
RXR	retinoic acid X receptor
SDR	Short Chain Dehydrogenase Reductase
SDS	sodium dodecyl sulphate
SEM	standard error of the mean
SHP-1	small heterodimer partner-1
SR-B1	scavenger receptor class B type 1
StAR	Steroidogenic Acute Regulatory protein
SXR	steroid and xenobiotic receptor
TAT	tyrosine amino-transferase
TCDCA	tauro-chenodeoxycholic acid
TNF-∝	tumour necrotic factor ∝
TRH	thyrotrophin-releasing hormone
UDCA	ursodeoxycholic acid

Chapter 1

Introduction

1 Introduction

Cholesterol is the common precursor of both steroid hormones and bile acids. This thesis will address the interaction between enzymes involved in steroid hormone metabolism and bile acid biosynthesis.

1.1 The Endocrine System

Endocrinology describes study of the synthesis, secretion and action of hormones, defined as "chemical messengers which co-ordinate the activities of different cells in a multicellular organism" (Davidson's Medicine, 2004). Classically the endocrine system functions via the release of hormones into the circulation which would then act at a site distant from that of secretion. Many hormones can also act in a paracrine manner, where the factor is not released into the circulation but acts upon adjacent cells, for example regulation of the immune system; an autocrine manner, whereby the factor acts upon the cell of origin, for example neurotransmitters; or an intracrine manner whereby factors act upon the cell within the gland in which they were synthesised. Hormones have diverse biological actions exerting inhibitory or stimulatory roles and can be divided into three broad classes; steroid hormones, peptides or proteins and amino acid derivatives.

1.1.1 *Steroid hormones* - this large class of hormones includes glucocorticoids, mineralocorticoids and sex steroid hormones, all of which are structurally derived from cholesterol.

1.1.2 *Peptides and proteins*- this class encompasses the majority of hormones including adrenocorticotrophin hormone (ACTH), thyrotrophin-releasing hormone (TRH), gonadotrophins such as follicle stimulating hormone (FSH) and leutenising hormone (LH). Proteins belonging to this class include the sex-bindig globulin (SBG).

1.1.3 *Amino acid derivatives* – this class of hormones includes neurotransmitters, thyroid hormones and epinephrine (adrenaline).

This thesis will focus upon the regulation of glucocorticoid action in the liver. Glucocorticoids are steroid hormones synthesised *de novo* in the adrenal gland under control of peptide hormones secreted by the pituitary gland.

1.2 Steroid hormones

1.2.1 Chemistry and nomenclature

Adrenal hormones such as cortisol and aldosterone are steroid hormones which are derived from the common precursor cholesterol. These hormones have a basic structure which is conserved throughout the family. This structure is based upon the steroid nucleus, comprising three cyclohexane rings and one cyclopentane ring. Each steroid is given its unique properties by substitution of chemical groups at various positions on the backbone of the molecule (Figure 1.1)

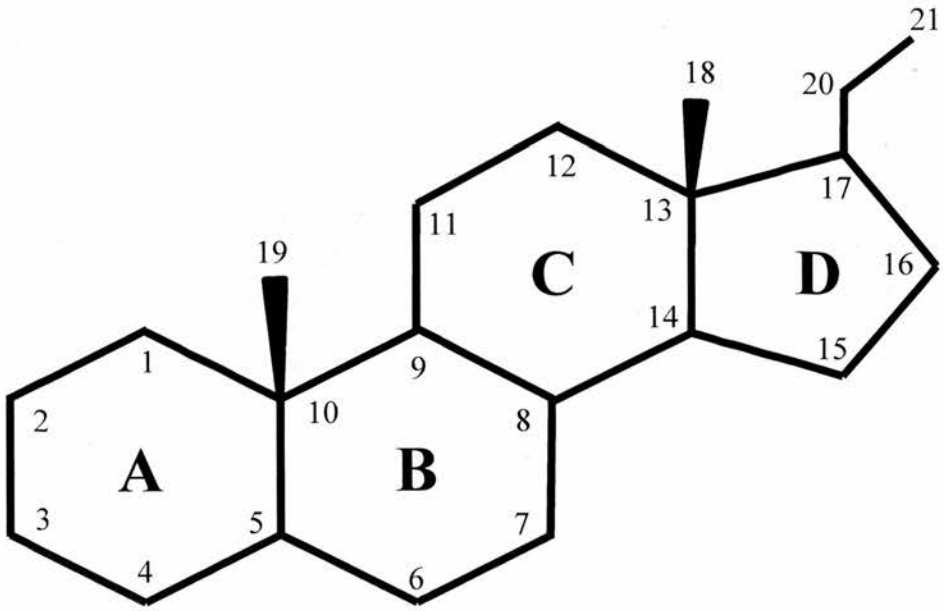

Figure 1.1 Basic steroid ring structure and conventional labeling of pregnane C21 steroid hormones. The four carbon rings are assigned letters and the numbers correspond to individual carbon atoms. Chemical groups are designated by the number of the carbon atom to which they are attached. Stereochemistry of substituents are assigned as their orientation above (β) or below (α) the plane of the molecule.

1.3 Steroid biosynthesis

Steroid hormone are synthesised from the cholesterol by a complex series of reactions carried out within the adrenal gland (Figure 1.2). The conversion of C_{27} cholesterol to 18-, 19-, and 21-carbon steroid hormones involves the irreversible cleavage of a 6-carbon residue from cholesterol to produce pregnenolone (C_{21}) plus isocaproaldehyde in a reaction catalysed by P450-linked side chain cleaving enzyme (P450ssc; CYP11A1; Table 1.1). This enzyme is found primarily within the mitochondria of steroid producing cells. Pregnenolone acts as the common precursor molecule for all C_{18}, C_{19} and C_{21} steroids. Steroid hormones with 21 carbon atoms are known systematically as pregnanes, whereas those containing 19 and 18 carbon atoms are known as androstanes and estranes respectively. Following cleavage of the 6-carbon side chain, pregnenolone is further processed within the cytosol and the final product depends on the cell (tissue) under consideration. The various hydroxylases involved in the directed synthesis of the steroid hormones are members of the cytochrome P450 class of enzymes. Their nomenclature is indicative of the site of hydroxylation (e.g. the 17α-hydroxylase is also identified as P450$_{C17}$). In recent years enzyme nomenclature has been standardised and is summarised in table 1.1.

Trivial name	Previous name	Present name
Cholesterol side chain cleavage	P450$_{SCC}$	CYP11A1
3β-hydroxysteroid dehydrogenase	3βHSD	HSD3B
17α-hydroxylase / 17,20-lyase	P450$_{C17}$	CYP17
21-hydroxylase	P450$_{C21}$	CYP21A2
11β-hydroxylase	P450$_{C11}$	CYP11B1
Aldosterone synthase	P450$_{C11AS}$	CYP11B2

Table 1.1 Nomenclature of rat steroidogenic enzymes.

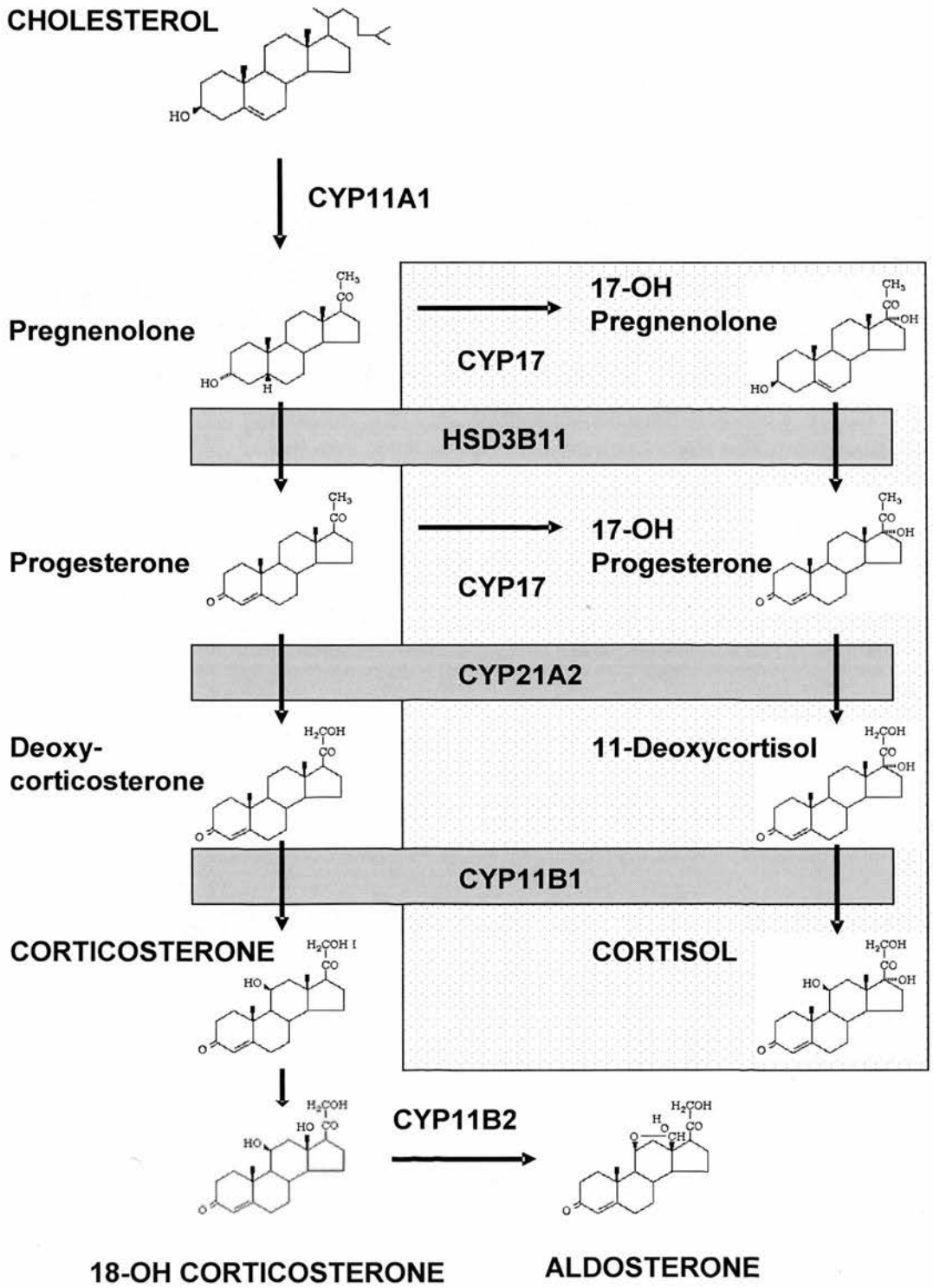

Figure 1.2 Adrenocortical steroid biosynthetic pathway in man. Enzymes and steroid hormone nomenclature are given in bold. Rodents do not express CY17 within the adrenal cortex and therefore steroids can not be 17-hydroxylated. (Reactions within hatched box refer to man only). The major glucocorticoid in rodents is therefore corticosterone.

1.4 Steroid hormones

Corticosteroids are synthesized in the adrenal glands which are located within close proximity of the kidneys. These organs along with the gonads are a major site of production of steroid hormones. Each gland can be divided into two morphologically and biochemically distinct regions, namely the cortex and medulla. The adrenal medulla is embryologically and histologically distinct from the cortex and is part of the sympathetic nervous system. Medullary cells synthesize, store and secrete adrenaline, along with noradrenaline and dopamine. The adrenal cortex which is situated around the perimeter of the adrenal gland is involved in the synthesis of glucocorticoids and mineralocorticoids including cortisol and aldosterone respectively from the common precursor cholesterol. In humans, it also represents a secondary site of androgen synthesis complementing the ovary, testes and placenta. The adrenal cortex can be further subdivided into 3 distinct zones based upon cell type and function (Figure 1.3). Although the pathway to synthesise pregnenolone is common to all zones of the cortex, the exact steroid hormone product is dependent upon the specific enzymes present in the cells of each zone.

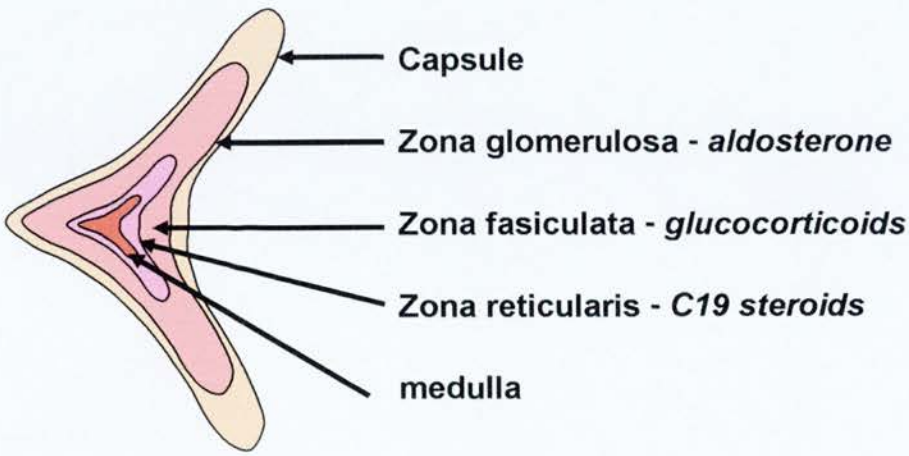

Figure 1.3 Adrenal gland. Zones of the adrenal cortex and the predominating steroid hormone synthesized within each zone

1.4.1 Zona glomerulosa

The outermost zone of the adrenal cortex, the zona glomerulosa is the main site of mineralocorticoid synthesis, primarily aldosterone and also the less potent mineralocorticoid deoxycorticosterone which play a major role in regulating electrolyte balance within the body. Cells within the zona glomerulosa lack the enzyme 17-hydroxylase (CYP17) that converts pregnenolone and progesterone to their C_{17} hydroxylated analogs. As such the pathways to produce glucocorticoids and androgens are not active in these cells. Zona glomerulosa cells express aldosterone synthase (CYP11B2) the enzyme responsible for converting 18-OH corticosterone to aldosterone, the principal and most potent mineralocorticoid.

1.4.2 Zona fasciculata

The zona fasciculata is the primary site of glucocorticoid production in humans of which ~ 95% is cortisol. Cells within the fasiculata express high levels of 11β-hydroxylase (CYP11B1) which is absent from the zona glomerulosa and is responsible for the conversion of 11-deoxycortisol and deoxycorticosterone to the glucocorticoids cortisol and corticosterone. In humans zona fasiculata cells also express CYP17 whose activity is responsible for producing the androgens, dehydroepiandosterone (DHEA) and androstenedione. Rodents do not express CYP17 within the adrenal cortex therefore steroids cannot be 17-hydroxylated. Thus, the major glucocorticoid in the rodent is corticosterone and rodents do not synthesise adrenal androgens.

1.4.3 Zona reticularis

The zona reticularis represents the innermost zone of the adrenal cortex and is the principal site of androgen production (DHEA, DHEA sulphate, and androstenedione in humans). Analogous to the zona fasiculata, zona reticularis cells express both CYP17 and CYP11B1 but not CYP11B2. Thus, cells within the fasiculata and reticularis can synthesize corticosteroids and adrenal androgens, but not aldosterone.

1.5 Steroid metabolism

This thesis will focus upon glucocorticoids, a class of steroid hormones named due to their intrinsic role in glucose metabolism and homoeostasis. The principal active glucocorticoid in man is cortisol (F) and corticosterone (B) in the rodent. This thesis generates data from rodent models and therefore rodent nomenclature will be used throughout.

Glucocorticoid metabolism provides the predominant means of clearing non-sequestered hormone from the circulation, thus influences local circulatory levels and tissue specific responses to hormones. The principal enzymes involved in corticosterone metabolism and the resulting metabolites of corticosterone are shown in figure 1.4. Enzymes directly involved in corticosterone metabolism include the 11β-HSDs, the A-ring reductases (5α- and 5β-reductase and 3α-hydroxysteroid dehydrogenases; 3α-HSDs). Minor pathways of metabolism (not shown) include, 6β-hydroxylation and 20α- and β-reduction.

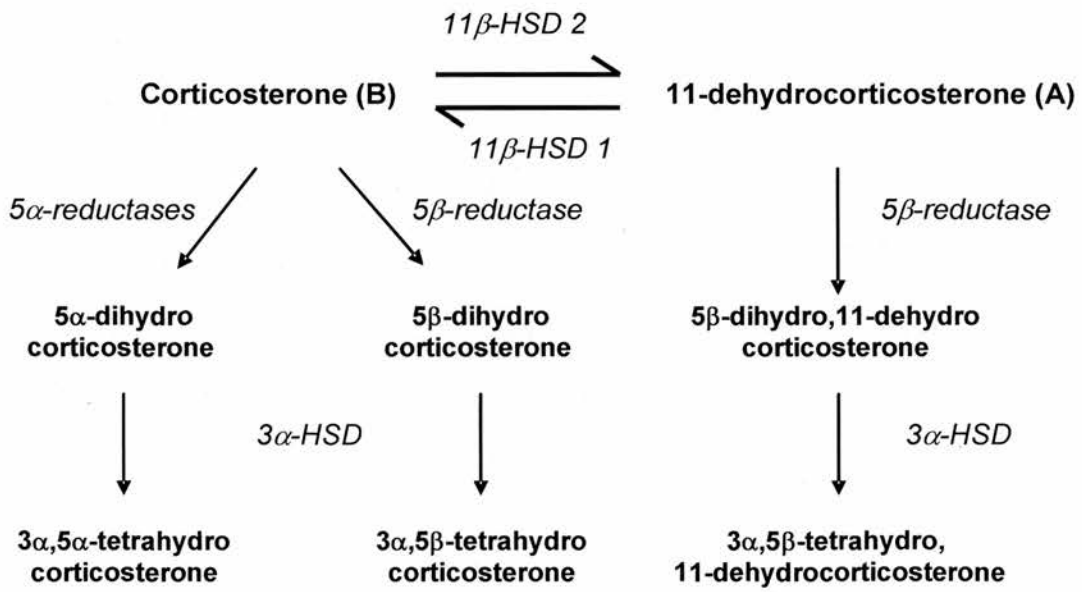

Figure 1.4 Metabolic pathway of glucocorticoid hormones in rat. Principal enzymes involved in glucocorticoid metabolism; HSD = hydroxysteroid dehydrogenase ; 5α and 5β-reductase and 3α-HSD = A-ring reductases

1.5.1 11β-hydroxysteroid dehydrogenase type 1 (11β-HSD1)

11β-HSD type 1 (11β-HSD1), locally regenerates active glucocorticoids from the circulating pool of inert 11-keto forms (Figure 1.5).

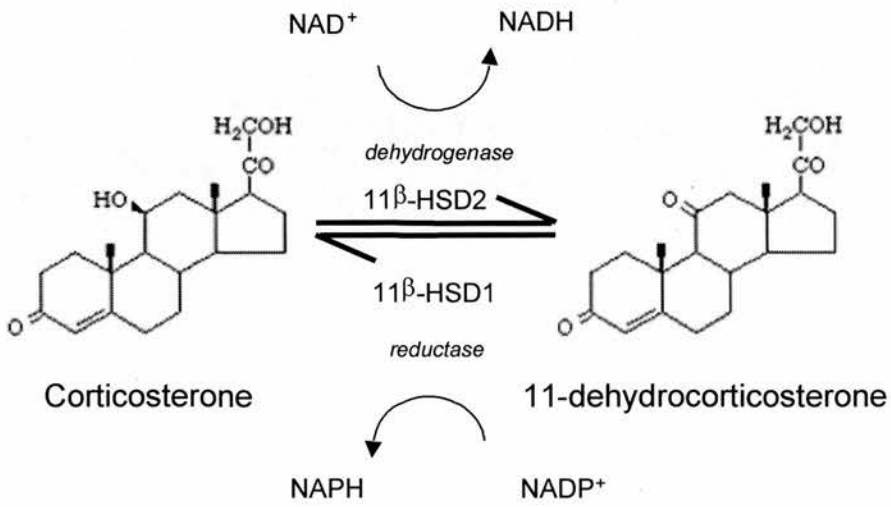

Figure 1.5 Interconversion of active and inactive glucocorticoids by isoforms of 11β-HSD. In situ, 11β-HSD1 acts predominantly in the reductase mode activating corticosterone from 11-dehydrocorticosterone whilst 11β-HSD2 inactivates corticosterone

Within individual tissues 11β-HSD1 mainly acts to locally amplify levels of glucocorticoids thereby ensuring adequate activation of the lower affinity glucocorticoid receptor (GR). This enzyme is a low affinity NADP(H) dependent enzyme which is highly expressed within glucocorticoid target tissues including the liver (Jamieson *et al.* 1995; Bujalska *et al.* 1997), lung (Hundertmark *et al.* 1993), adipose and skeletal tissue (Napolitano *et al.* 1998; Brem *et al.* 1995), adrenal cortex (Shimojo *et al.* 1996) anterior pituitary and certain regions of the brain (e.g. hippocampal and paraventricular nucleus (PVN) neurons (Sakai *et al.* 1992)). These tissues also express high levels of GR and it is thought that 11β-HSD1 modulates glucocorticoid access to these sites (Whorwood *et al.* 1992). Although this isozyme shows bi-directional activity in tissue homogenates and when purified, it acts predominantly as a reductase under physiological conditions and *in vivo.* Mice

homozygous for a targeted disruption of the 11β-HSD1 gene cannot regenerate active corticosterone from inert 11-dehydrocorticosterone (Kotelevtsev *et al.* 1997). Jamieson *et al* (1995) demonstrated that hepatic 11β-HSD1 activity in isolated rat liver acted predominantly as a reductase *in vivo.* The predominating reductase mode of activity relates to the intracellular location of 11β-HSD1 within inner leaflet of the endoplasmic reticulum (ER) rather than any structural features and depends upon co-factor access and supply. The microsomal enzyme hexose-6-phosphate dehydrogenase (H6PDH), which plays an essential role in supplying NADPH co-factor to 11β-HSD1, is also associated within the lumenal side of the ER, directed in the same orientation as the catalytic domain of 11β-HSD1. Mutations within exon 5 of H6PDH which attenuate or abolish H6PDH activity have been identified in individuals with cortisone reductase deficiency (ACRD) (Draper *et al.* 2003). H6PDH deficient mice, which are unable to convert 11-dehydrocorticosterone (11-DHC) to corticosterone, have a reduction in 11β-HSD1 oxo-reductase activity (Lavery *et al.* 2005).

1.5.2 11β-hydroxysteroid dehydrogenase type 2 (11β-HSD2)

11β-HSD type 2 catalyses the oxidation of active corticosteroids to their inactive keto metabolites (Funder *et al.* 1988; Brown *et al.* 1993) protecting the otherwise non-selective mineralocorticoid receptor (MR) from occupation by glucocorticoids (Edwards *et al.* 1988). 11β-HSD2 is a high affinity (low nanomolar Km for cortisol), NAD-dependent dehydrogenase and is widely expressed in fetal tissue including the placenta (Stewart *et al.* 1994). In adults however, this isozyme is expressed in mineralocorticoid-sensitive tissues such at the distal nephron, salivary glands, sweat glands and colonic mucosa (Hirasawa *et al.* 1997; Takahashi *et al.* 1998). Deficiency of renal 11β-HSD2 was originally linked to the syndrome of apparent mineralocorticoid excess (AME), in which glucocorticoids illicitly occupy MR causing sodium retention, hypokalemia and hypertension (Ulick *et al.* 1979) and more recently, genetic mutations within the 11β-HSD2 gene have been identified in patients with this disorder (Wilson *et al.* 1995; Li *et al.* 1997; Lovati *et al.* 1999; Lavery *et al.* 2003). Mutations within 11β-HSD2 also contribute towards the

development of essential hypertension due to illicit activation of MR (Stewart *et al.* 1996; Krozowski *et al.* 1997).

1.5.3 A-ring reduction

The principal routes of cortisol clearance in the liver are catalysed by the hepatic A-ring reduction by the "A-ring reductases" (5α and 5β-Reductase) (Kondo *et al.* 1994; Onishi *et al.* 1991; Russell & Wilson 1994; Tomkins 1956). Reduction of the steroid A-ring $\Delta^{4\text{-}5}$ double bond by 5α and 5β-reductase is rapidly followed by a second reductive step catalysed by 3α-hydroxysteroid dehydrogenase (3α-HSD) (Figure 1.6). The former reactions are rate-limiting. The resulting tetrahydro metabolites (5α or "allo" and 5β-tetrahydrocortisols) are then conjugated, the principal conjugates being glucuronides although some sulphates are formed, making them more water soluble prior to excretion via the kidneys. This two-step reductive pathway, common to several other steroids including the reduction of aldosterone, progestogens and androgens, is not reversible.

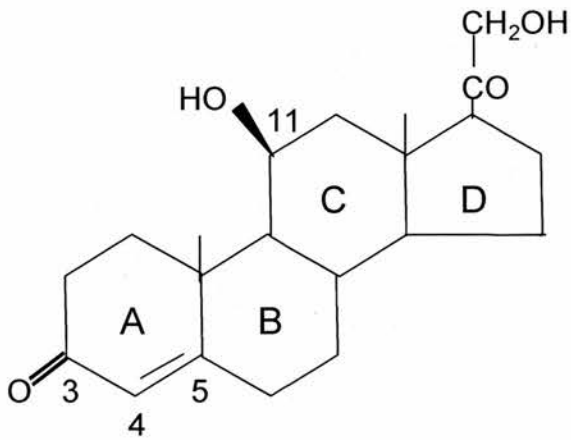

Figure 1.6 Glucocorticoid hydrocarbon skeleton. Structure of corticosterone highlighting sites of action of the hepatic A-ring reductases (5α and 5β-reductase) 3α-HSD and 11β-HSDs respectively.

1.5.3.1 5α-Reductases

5α-reductases catalyse the first step in the reduction of the A-ring, reducing the 4-5 double bond in the A-ring to form 5α-dihydro metabolites. Two isoforms of this enzyme have been cloned (Types 1 and 2) from different genes (Andersson *et al.* 1989a; Andersson *et al.* 1991) and a pseudogene has been identified in man (Jenkins *et al.* 1992). These isoforms differ in both their biochemical characteristics and tissue distribution and also show species specificity and sexual dimorphism (Russell & Wilson 1994). Both isozymes are found within the microsomal and plasma membrane/nuclear sub-fractions and utilise NADPH as a co-factor.

The type 1 enzyme is highly expressed within the liver (Thigpen *et al.* 1993), brain, non-genital skin fibroblasts (Normington & Russell 1992; Andersson & Russell 1990) and to a lesser extent in stromal cells of adipose tissue (Killinger *et al.* 1990). 5α-reductase type 1 is active over a broad range of pH (optimum pH 7.4) and reduces most $\Delta^{4\text{-}5}$ unsaturated steroids with similar efficiency.

In contrast, 5α-reductase type 2 is primarily located within male reproductive tissues e.g. prostrate and seminal vesicles and in regions of the developing central nervous system (CNS) involved in reproductive behaviour (Russell & Wilson 1994) and also within the human but not rat liver. The type 2 isozyme has an optimum pH within the acidic range ≈ pH 5, and is primarily responsible for converting testosterone to active 5α-dihydrotestosterone playing a key role in enhancing local androgen receptor (AR) activation. This amplification process is essential for normal development of the male reproductive development and secondary sexual characteristics. Mutations in the type 2 isozyme in males can result in the condition of male pseudohermaphroditism in which the male genitalia fail to develop properly (Andersson *et al.* 1991). The relative contribution of each isozyme to glucocorticoid metabolism within the liver in humans is as yet unknown but both contribute to first pass metabolism (Andersson & Russell 1990).

Although 5α-reduced glucocorticoids were thought to be biologically inert, recent data has demonstrated that 5α-reduced glucocorticoids can bind and activate GR and therefore have the potential to induce GR responsive genes such as tyrosine

amino-transferase (TAT) and phosphoenolpyruvate carboxykinase (PEPCK) (McInnes *et al.* 2004).

1.5.3.2 5β-Reductase

5β-reductase belongs to the aldo-keto reductase (AKR) super family, a family of cytosolic, monomeric oxidoreductases catalysing the reduction of ketosteroids (i.e. glucocorticoids, mineralocorticoids, androgens and progestogens) and bile acid intermediates. Located within the cytosolic sub-fraction, 5β-reductase catalyses reduction of the steroid 4-5 unsaturated double bond resulting in the generation of *cis* 5β-reduced dihydro metabolites (Tomkins 1956). 5β-reductase is highly expressed within the liver (with much lower expression in the kidney) and utilises NADPH as its preferred co-factor. At present only one form of this enzyme has been cloned in both human and rat (Kondo *et al.* 1994; Onishi *et al.* 1991). A pseudogene has been identified in humans (Charbonneau & The 2001) and there have been reports, as not yet corroborated, suggesting a second 5β-reductase isoenzyme may exist (Furuebisu *et al.* 1987).

1.5.3.3 3α-Hydroxysteroid Dehydrogenases (3αHSD)

The 5α- or 5β- dihydro products of A-ring reduction undergo a further reductive step catalysed by isozymes of 3α-hydroxysteroid dehydrogenases (3α-HSDs), resulting in the formation of tetrahydro metabolites that are conjugated and excreted from the body (Penning 1999). The 3α-HSD isozymes are expressed within the microsomal and cytosolic sub-fractions and utilise NADPH as their preferred co-factor. As with 5β-reductase, these enzymes belong to the AKR superfamily (Jez & Penning 2001) catalysing the reduction of ketosteroids and oxidised cholesterol metabolites. Indeed, the 3α-HSDs perform an array of functions including the hepatic clearance of steroid hormones, the transport and biosynthesis of bile acids, the regulation of androgen metabolism and the formation of neurosteroids (Jin *et al.* 2001). At present 4 genes have been identified in human (AKR1C1-4). These isoforms share >83% sequence identity at the amino acid level but differ in their

biochemical and substrate specificity (Penning *et al.* 2000). Type 1 3α-HSD (AKR1C4) is expressed specifically within the liver and is primarily involved in the metabolism of steroid hormones and the formation and excretion of 5α- and 5β-tetrahydrosteroids. Type II 3α-HSD (AKR1C3) is highly expressed within the prostate where it reduces the potent androgen 5α-dihydrotestosterone (5α-DHT) to 5α-androstane-3α, 17β-diol (a weak androgen) (Lin *et al.* 1997) . Type III 3α-HSD (AKR1C2) is also highly expressed within the prostate and is the only known 3α-HSD isoform capable of activating 5α-androstane-3α, 17β-diol to 5α-DHT (Stolz *et al.* 1993). As high levels of 5α-DHT are linked with abnormal prostate growth, inhibition of AKR1C2 may provide a good strategy for the clinical management of prostate cancer and benign prostate hyperplasia. Also known as human bile acid binding protein, 20α-(3α)-HSD (AKR1C1) is thought to function as an intracellular bile acid transporter (Bahar & Stolz 1999). In contrast only one 3α-HSD protein has been identified in the rat (AKR1C9) (Pawlowski *et al.* 1991). Rat liver 3α-HSD shares 69% sequence identity with the human isoforms and, although more catalytically efficient than the human 3α-HSDs, AKR1C9 lacks 17β- or 20α-HSD activities (Lin *et al.* 1999).

1.5.4 Polar Steroid Metabolism

The 20-reductases (20α and 20β-HSDs) (Abel & Back 1993) and cytochrome P450 microsomal enzyme 6β-hydroxylase (CYP3A)(Waxman *et al.* 1988) are also directly involved in glucocorticoid metabolism generating 20α or β-dihydrocorticosterones and 6β-hydroxycorticosterones respectively. These pathways account for only a small fraction (<10%) of corticosterone metabolites, the majority being excreted as metabolites of the A-ring reductases. In addition to its role in glucocorticoid hydroxylation, CYP3A hydroxylates a number of natural and xenobiotic molecules and is inducible by drugs including the antibiotic rifampicin (Chawla *et al.* 2001). 20α and 20β-HSDs also catalyse the reduction of the tetrahydo metabolites into cortols and cortolones in humans. Finally, P450scc (side-chain cleavage enzyme) and 21-oxidase catalyse the terminal oxidation steps resulting in

the formation of 11-hydroxyetiocholanolone and cortolic/cortolonic acids, respectively.

1.6 Regulation of glucocorticoid secretion

1.6.1 The pituitary gland

The anterior pituitary is responsible for the secretion of a number of types of hormone acting either on endocrine glands or target tissues e.g. glucocorticoid secretion from the adrenal gland is stimulated by ACTH from the pituitary. Further examples are given in Table 1.2. The pituitary gland is composed of two lobes, the anterior and posterior, which are connected via the infundibular stalk to the hypothalamus. Portal vessels within the infundibular stalk carry blood from the median eminence of the hypothalamus to the anterior lobe and nervous fibres to the posterior lobe.

Function	Hormone	Abbreviation
Adrenal glucocorticoid/ mineralocorticoid production	Adrenocorticotrophic hormone	ACTH
Growth	Growth hormone	GH
Thyroid activity	Thyroid stimulating hormone	TSH
Sexual activity and fertility	Luteinising hormone	LH
	Follicle stimulating hormone	FSH
Lactation	Prolactin	PRL

Table 1.2 Functions of anterior pituitary hormones

ACTH release from the anterior pituitary is stimulated by hypothalamic factors such as corticotrophin releasing hormone (CRH), which are carried in the portal circulation. Hypothalamic function in turn is regulated by a variety of stimuli of nervous, hormonal, physiological and metabolic origin. Feedback control by hormones produced in target glands such as the adrenal cortex plays a fundamental role in regulating hormone secretion.

1.6.2 Hypothalamic-pituitary-adrenal (HPA) axis

The levels of active glucocorticoid within the circulation are normally tightly regulated through feed-forward and feed-back mechanisms at the level of the hypothalamus, pituitary and adrenal gland, referred to at the hypothalamic-pituitary-adrenal (HPA) axis (Figure 1.7).

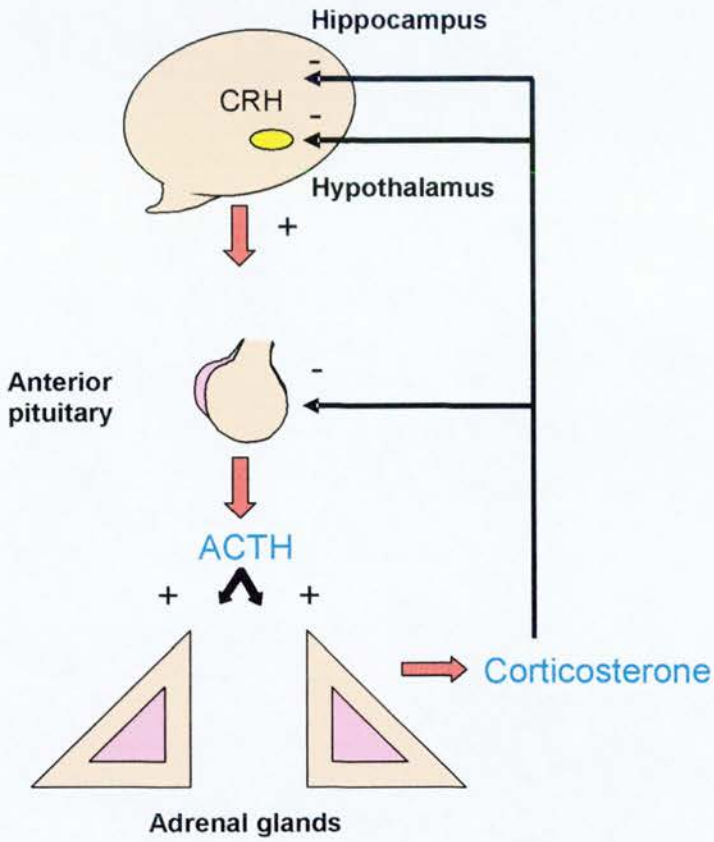

Figure 1.7 Regulation of glucocorticoid synthesis in the rat via the HPA axis. Circulating levels of the active glucocorticoids are detected by the hippocampus, hypothalamus and pituitary which then stimulate or suppress CRH and ACTH secretion accordingly.

Circulatory levels of active glucocorticoid are detected by the hypothalamus and pituitary, which then regulate secretion of ACTH, signaling to the adrenal cortex to stimulate or suppress glucocorticoid synthesis accordingly. For example, when circulating levels of active cortisol are low, increased secretion of corticotrophin releasing hormone (CRH) from the hypothalamus stimulates ACTH secretion from

the anterior pituitary, which in turn induces glucocorticoid biosynthesis. Conversely when glucocorticoid levels are elevated, secretion of CRH and ACTH are reduced thus decreasing the rate of glucocorticoid production. As such the levels of circulating hormone are largely determined by the rates of their biosynthesis and elimination, primarily through glucocorticoid metabolism (Jacobson & Sapolsky 1991; Rask *et al.* 1999).

1.6.3 HPA axis regulation and metabolism

There is now increasing evidence that peripheral metabolism of glucocorticoids and the rate of metabolic clearance play an important role in determining glucocorticoid action in target tissues and HPA axis response. Individuals with an autosomal recessive disorder resulting in 11β-HSD2 deficiency present with the condition of "Apparent mineralocorticoid excess" or AME (Ulick *et al.* 1979), normally diagnosed in childhood with hypokalaemia (polyuria, myopathy), severe hypertension, and complications including stroke and cardiac arrest (Stewart *et al.* 1988). These patients show elevated ratios of the urinary metabolites of cortisol versus cortisone and the half life of [11α^3H]-cortisol is prolonged indicating a deficiency of 11β-dehydrogenase activity (Stewart *et al.* 1988). As such the rate of cortisol metabolite excretion is reduced (consistent with a compensatory fall in HPA axis activation and cortisol production) whilst urinary free cortisol concentrations are elevated (consistent with impaired cortisol metabolism within the kidney) (Ulick *et al.* 1991; Monder *et al.* 1986). The features of AME have since been recapitulated in a transgenic 11β-HSD2 knockout mouse, with a reduction in adrenal size and suppression of the HPA axis (Kotelevtsev *et al.* 1999).

Conversely, where the rate of metabolic clearance is elevated e.g. Cortisone reductase deficiency (ACRD) (Phillipov *et al.* 1996), over stimulation of the HPA axis leads to enhanced production of adrenal steroids. Female sufferers of this disorder often present with hirsutism and menstrual irregularity, whilst males suffer from gonadotrophin-independent pseudo-precocious puberty and hyperandrogenism which are thought to arise due to enhanced ACTH-dependent adrenal androgen secretion. These subjects show elevated excretion of cortisone and total glucocorticoid metabolites consistent with 11β-HSD1 deficiency and compensatory

activation of the HPA axis (Jamieson *et al.* 1999). To date mutations have not been identified in the 11β-HSD1 gene exons or exon/intron boundaries, although in some cases 11β-HSD1 activity is compromised due to impaired co-factor regeneration by H6PDH (Draper *et al.* 2003). Indeed H6PDH deficient mice have increased corticosterone clearance and lower circulating corticosterone demonstrating the important role for co-factor provision in determining directionality of 11β-HSD1 (Lavery *et al.* 2005).

Enhanced 5β-reduction of cortisol and cortisone has also been identified in sufferers suggesting that dysregulation of the A-ring reductases may also contribute to the stimulation of the HPA axis in the manifestation in this condition (Phillipou & Higgins 1985). Likewise, stimulation of the HPA axis is suppressed 11β-HSD1 knockout mice which have heavier adrenal glands to compensate for impaired glucocorticoid reactivation (Harris *et al.* 2001a). In addition, these animals demonstrate an altered responsiveness of the HPA axis which can be corrected by re-expressing this gene within the liver (Harris *et al.* 2001b; Paterson *et al.* 2004). Taken together these findings confirm a fundamental role for metabolism of glucocorticoids in the liver in regulation of the HPA axis.

There is little substantive evidence that changes in activity of the A-ring alter HPA axis activation; however, enhanced glucocorticoid clearance by the 5α- and 5β-reductase is suggested to induce compensatory activation of the HPA axis in idiopathic obesity in order to maintain circulatory glucocorticoid levels (Rask *et al.* 2001; Andrew & Walker 2005).

1.7 Glucocorticoid action

1.7.1 Nuclear hormone receptors

Glucocorticoids exert many of their effects via direct interaction with two types of intracellular receptors: the glucocorticoid (GR; type 2 corticosteroid receptor) and mineralocorticoid (MR; type 1 corticosteroid receptor) receptors. These receptors belong to the nuclear hormone receptor (NHR) superfamily and function as ligand-dependent transcription factors which induce and repress the expression of a range of target genes. Members of this superfamily have three distinct domains: a

ligand-binding domain, a DNA-binding domain and a transcriptional regulatory domain. In the absence of ligand, GR is localised within the cytoplasm as part of a multiprotein complex. When bound by ligand e.g. corticosterone, the resulting complex is a non-DNA-binding oligmer. This complex consist of the heat shock protein 90 (hsp90) dimer which binds to the DNA-binding domain of the receptor along with heat shock protein 70 (hsp70) and FKBP52 (Figure 1.8). Dissociation of the oligomeric complex yields the free GR subunit in the DNA-binding form. The activated receptor forms a homodimer and is translocated to the nucleus through the nucleopore. Once within the nucleus the receptor complex may bind to specific nucleotide sequences in the DNA are referred to as glucocorticoid response elements (GRE) located within the 5' promoter region of target genes modulating their transcription. In contrast to the regulation of these classical GREs, the repression of negatively regulated target genes is mediated by negative GREs (nGREs) or by transrepression of positively acting transcription factors such as AP-1 and NF-κB. Studies by Reichardt et al. (2000) (Reichardt *et al.* 2000) using dimerization-defective GR mutant mice have shown that the repressive mechanisms by direct DNA-binding of GR and by transrepression of other transcription factors can be dissociated. GR can also regulate gene transcription indirectly by cross-talk with other transcription factors such as AP1, NFkB and CREB (Funder 1997). Glucocorticoids can activate both GR and MR but alter fuel metabolism mainly through activation of GR, in sites such as the liver, adipose tissue and skeletal muscle.

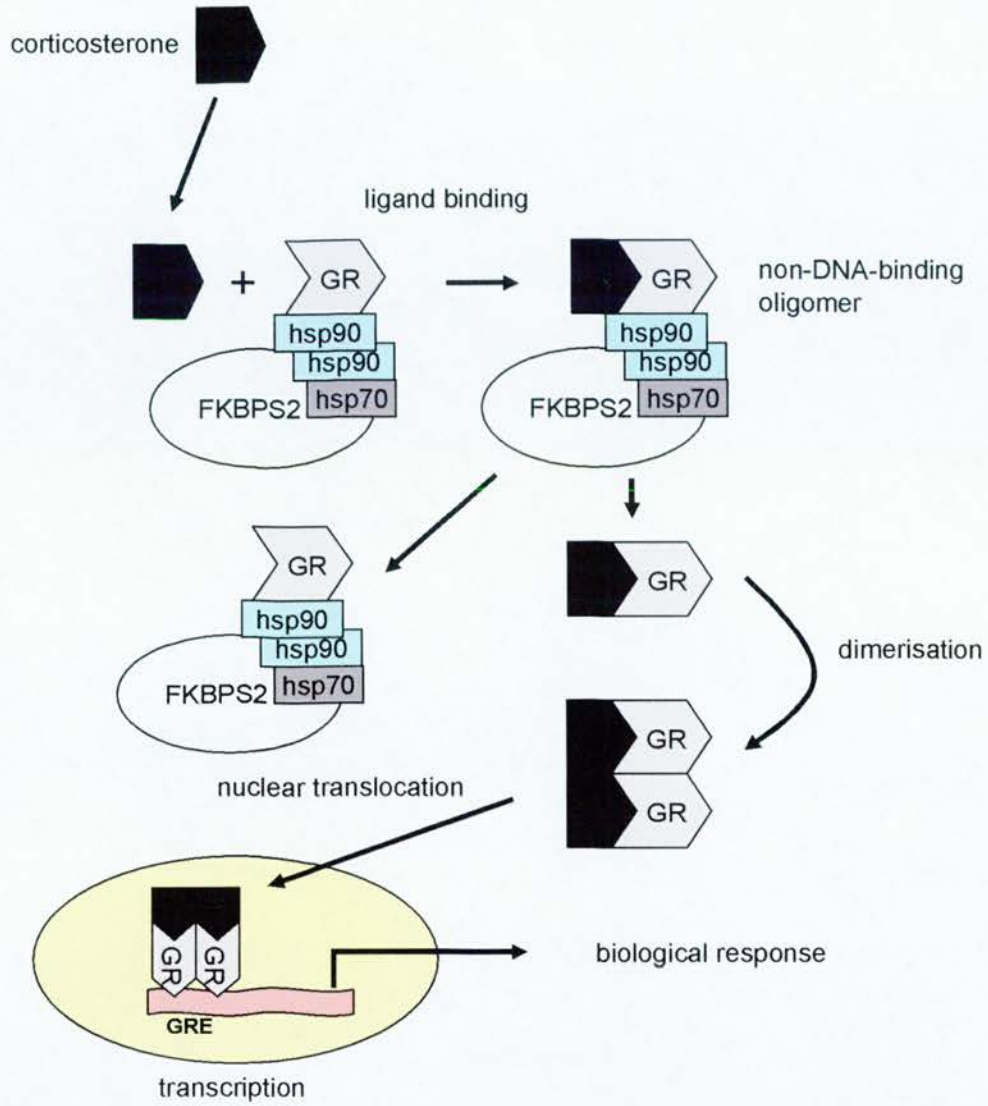

Figure 1.8 Transactivation of glucocorticoid receptor. Corticosterone diffuses through the plasma membrane where it binds to the GR complex. Activation of the oligomer releases GR which forms a homodimer and undergoes cytoplasmic to nuclear translocation. Once within the nucleus GR binds to specific GREs present stimulating transcription of the target gene. GR = glucocorticoid receptor; GRE = glucocorticoid response element; Hsp = heat shock protein; FKBP = Immunophilin FKBP S2.

1.7.2 Orphan nuclear receptors

In addition to acting via the classical nuclear hormone receptors, GR and MR, recent evidence has highlighted several endogenous and exogenous steroids as ligands for the orphan nuclear receptor, pregnane X receptor (PXR; NR1I2) (Kliewer SA *et al.* 1998) alternatively called the steroid and xenobiotic receptor (SXR)(Blumberg *et al.* 1998). PXR binds to DNA as a heterodimer with the 9-*cis* retinoic acid receptor (RXR)(Mangelsdorf & Evans 1995) and is activated by a myriad of compounds including several steroids, synthetic glucocorticoids, anti-glucocorticoids and bile acids (Xie & Evans 2001). Thus activation of PXR may represent a novel steroid signalling pathway that may account for some of the effects of synthetic glucocorticoids and anti-glucocorticoids that are not mediated through the classical GR signalling pathway. 5β-reduced glucocorticoids, namely 5β-dihydrocortisol and 3α,5β-tetrahydrocortisol are thought biologically inert since they do not bind and activated GR. However, 5β-reduced glucocorticoids and also 5β-cholestan-3α,7α,12α-triol, the bile acid precursor and product of 5β-reductase, are potent activators of PXR (Blumberg *et al.* 1998).

Activation of PXR induces expression of the CYP3A family of genes which encode cytochrome P450 hemoproteins involved in the hydroxylation of a broad range of substrates, including endogenous steroid hormones such as corticosterone, progesterone and bile acids and play a crucial role in the detoxification and metabolism of a variety of xenobiotics (Juchau 1990). For example, the human CYP3A4 enzyme is reported to account for 50-60% metabolism of clinical drugs (Maurel 1996). Upon activation, PXR induces CYP3A and inhibits HMG-CoA reductase and cholesterol 7α-Hydroxylase (CYP7A1), the rate limiting enzyme in the cholesterol catabolic pathway resulting in concomitant reductions in sterol biosynthesis and bile acid secretion (Turley & Dietschy 1984; Kliewer *et al.* 1998).

1.8 Roles of glucocorticoids in health and disease

Glucocorticoids regulate a number of key metabolic and homeostatic processes (Andrews & Walker 1999). Their role in carbohydrate and lipid metabolism and the provision of fuel to enable oxidative metabolism within the liver is well recognised. In addition, glucocorticoids are also highly influential in regulating electrolyte balance in the kidney and mediating the stress and immune responses (Munck & Guyre 1986). During times of stress, glucocorticoids provide a long-term signal to reduce many of the acute responses to illness, "re-setting" metabolism in favour of providing immediate energy for the "fight-or-flight" response.

This thesis will focus upon glucocorticoid metabolism and action within the liver. Glucocorticoids play a number of essential roles within the liver including lipid, carbohydrate and protein metabolism. Indeed, glucocorticoids act as potent regulators of key enzymes involved in hepatic gluconeogenesis,inducing transcription of PEPCK, the rate determining step in hepatic gluconeogenesis and tyrosine animo transferase (TAT) thereby promoting glucose production (Nyirenda *et al.* 1998). Likewise, glucocorticoids induce hepatic triglyceride storage (Mantha *et al.* 1999) and promote fat accumulation within the liver (Stravitz & Sanyal 2003). In addition, glucocorticoids activate hepatic CYP3A and induce cholesterol catabolism and bile acid biosynthesis (Kliewer *et al.* 2002).

1.8.1 Regulation of glucocorticoid metabolism

It has become apparent over recent years that tissue-specific regulation of glucocorticoid metabolism can play a fundamental role in determining subsequent action. A number of studies have demonstrated 11β-HSD1 to be regulated by glucocorticoids, C/EBP, peroxisome proliferators-activated receptor-γ agonists and some pro-inflammatory cytokines (TNFα and IL-1β). For example glucocorticoids and insulin have opposing effects upon 11β-HSD1 expression within primary rat hepatocytes, glucocorticoids inducing gene transcription and insulin suppressing 11β-HSD1 transcription (Jamieson *et al.* 1995). Similarly administration of

dexamethasone *in vivo* induced 11β-HSD1 within the liver and hippocampus. These effects were ameliorated following adrenalectomy (Walker & Edwards 1994; Low *et al.* 1994). Likewise, the inflammatory cytokine TNF-α increased activity and expression of 11β-HSD1 within renal cells (Escher *et al.* 1997) while interleukins 5 and 6 induced 11β-HSD1 activity in granulosA cells (Evagelatou *et al.* 1997). 11β-HSD1 is repressed by growth hormones (acting via IGF-1) (Tomlinson *et al.* 2003) and the liver X receptor (LXR) (Stulnig *et al.* 2002). Likewise, sex steroids including estradiol, progesterone and testosterone have also been shown to regulate 11β-HSD1 activity and / or expression (Tomlinson 2005).

5α-Reductase is sexually dimorphically expressed and is under hormonal control. Administration of testosterone to male castrated rats induces the transcription and activity of both 5α-reductase types 1 and 2 within the ventral prostate (Normington & Russell 1992). In contrast, testosterone is a negative regulator of 5α-reductase 1 within the liver (Lopez-Solache *et al.* 1996) and adrenal cortex (Lephart *et al.* 1991). Recent evidence has highlighted a role for insulin in the regulation of 5α-reductase 1, as treatment of obese Zucker rats with the insulin-sensitising drug metformin ameliorated the increase in activity and expression of 5α-reductase 1 within the liver (Livingstone *et al.* 2005). There is some literature showing that GH can induce 5α-reductase 1 activity in isolated female rat hepatocytes (Miller & Colas 1982). In contrast to the 5α-reductases little is known about the regulation of 5β-reductase. Limited reseach suggests that carbenoxolone may inhibit enzyme activity (Latif *et al.* 1990). Indeed, the relative excretion of 5β-tetrahydrocortisol falls following administration of licorice or carbenoxolone (Stewart *et al.* 1987; Monder *et al.* 1989). A recent microarray study has suggested that 5β-reductase may be regulated by the bile acid receptor FXR (Pircher *et al.* 2003; Fukuhara *et al.* 2003). Studies in obese subjects have also demonstrated down-regulation of A-ring reductase activity following weight loss on a very low calorie diet suggesting that nutrition may have a role to play in enzyme regulation. However, specific regulators of this enzyme remain elusive.

1.8.2 Dysregulation of glucocorticoid metabolism

Our understanding of the importance of glucocorticoid hormones in health is largely based upon the pathological consequences of dysregulation in factors governing synthesis, metabolism and /or excretion. Glucocorticoid excess epitomized by "Cushing's Syndrome" leads to insulin resistance/type 2 diabetes, dyslipidemia, central obesity and hypertension (Bujalska *et al.* 1997). Indeed, excessive cortisol secretion in Cushing's syndrome is one of the classical causes of obesity. In the absence of adrenal pathology, the same cluster of clinical and biochemical features are frequently observed together and have been termed the "Metabolic Syndrome or Reaven's syndrome X" (Reaven 1988) and much research has focused upon understanding how and if glucocorticoid actions are altered in this condition. Conversely chronic glucocorticoid deficiency results in "Addison's Disease" first described by Dr Addison in 1855, or adrenal insufficiency (Malerbi *et al.* 1988) characterised by weight loss, muscle weakness, fatigue and hypotension.

1.8.3 Transgenic models of glucocorticoid metabolism

The importance of metabolic enzymes in determining tissue responses to glucocorticoids can be illustrated by studying transgenic animals. Targeted disruption of 11β–HSD1 within the mouse prevents corticosterone regeneration (Kotelevtsev *et al.* 1997; Morton *et al.* 2001). Upon starvation, 11β-HSD1 null mice show attenuated activation of the key hepatic gluconeogenic enzymes glucose-6-phosphatase and phosphoenolpyruvate carboxykinase PEPCK, due to intra-hepatic glucocorticoid deficiency. Moreover, these animals resist hyperglycemia induced by stress or obesity indicating that hepatic 11β-HSD1 plays a key role in the regulation of gluconeogenesis (Morton *et al.* 2001). Conversely, mice over-expressing 11β-HSD1 within the liver only, by means of the apoliprotein E promoter have an attenuated metabolic-syndrome-like phenotype with modest insulin resistance, hypertriglyceridaemia, fatty liver and hypertension, but normal weight, fat depot mass and glucose tolerance (Paterson *et al.* 2004). In contrast, transgenic mice showing 2- to 3-fold higher levels of 11β-HSD1 specifically within the adipose

tissue have increased levels of corticosterone within the adipose tissue but unaltered plasma corticosterone (Masuzaki *et al.* 2003). These mice are obese, with fat accumulating predominantly with the visceral depots, hyperphagic and develop all the main features of the metabolic syndrome: glucose intolerance and insulin resistance which can be exacerbated by high-fat feeding, dyslipidemia with elevated levels of free fatty acids and triglycerides, apparent leptin resistance and hypertension with associated activation of the renin/angiotensin/aldosterone system. It has been proposed that tissue specific changes in glucocorticoid metabolism may also contribute to the obese phenotype. The obese Zucker rat (fa/fa), displays many characteristics of obese humans and has proved to be highly informative when investigating the potential mechanisms that are dysregulated in obesity (Livingstone *et al.* 2000). The obese Zucker rat expresses high levels of 11β-HSD1 within the omental adipose tissue and has elevated expression and activity of the A-ring reductases within the liver (Livingstone *et al.* 2005). The mechanisms of dysregulation of glucocorticoid metabolism are poorly understood; however recent evidence demonstrated a role for insulin with the administration of insulin-sensitising drugs normalising 5α-reductase 1 activity in the obese Zucker rat (Livingstone *et al.* 2005).

1.8.4 Obesity

Increasing evidence supports a role for glucocorticoids in the aetiology of idiopathic obesity and the pathophysiological consequences associated with this condition e.g. cardiovascular and respiratory disease, arthritis, depression and features of the "Metabolic Syndrome" – (hypertriglycridaemia, hyperglycaemia and hypertension). Although obese individuals and the genetically obese Zucker rat show increased cortisol or corticosterone production rate, loss of diurnal variation of plasma cortisol levels, and increased responsiveness to cortisol (Andrew *et al.* 1998; Livingstone *et al.* 2000), circulating plasma levels are within the normal range. This apparent paradox has been attributed to an increased rate of metabolic clearance, mediated primarily via action of the A-ring reductases (5α– and 5β-reductase) (Walker *et al.* 2000; Livingstone *et al.* 2000; Andrew *et al.* 1998) and may result in compensatory activation of the HPA axis (Hautanen & Adlercreutz 1993). This may

therefore account for the normal or even lower circulating levels noted in obesity, despite an increase in daily cortisol production. Increases in the expression and/or activity of these enzymes within the liver have been reported in rodent models of obesity (Stewart *et al.* 1999; Livingstone *et al.* 2000).

In addition to changes in hepatic A-ring reductase activity, recent studies have shown tissue-specific alterations in the expression and activity of 11β–HSD1 in obesity (Masuzaki *et al.* 2001b; Rask *et al.* 2001). This enzyme is down regulated in the liver of obese individuals and conversely up regulated in visceral adipose tissue (Wake *et al.* 2003). Reduced reactivation of glucocorticoids within the liver will contribute to HPA axis activation whereas increased exposure to glucocorticoids encourages fat accumulation within the visceral adipose tissue where it may be responsible for "Cushing's disease of the omentum"(Bujalska *et al.* 1997).

It is interesting to note that both 5β-reductase and 11β-HSD1 are also involved in pathways of cholesterol metabolism. Oxysterols, the oxygenated derivatives of cholesterol produced in the liver, play a pivotal role in maintaining cholesterol homeostasis via suppression of target genes involved in cholesterol synthesis including HMG-Co A reductase (Ulven *et al.* 2005). Oysterols act as ligands for the Liver X receptor (LXR)-α and -β which play a role in the regulation of lipid metabolism. Activation of LXR has been shown to down regulate 11β-HSD1 mRNA in adipocytes and liver (Stulnig *et al.* 2002) and glucose-6-phosphatase (Grempler *et al.* 2005) suggesting a novel role of these receptors in endocrine function with the potential to exert positive effects on insulin sensitivity in conditions such as diabetes type 2 and the metabolic syndrome. Moreover, certain oxysterols are ligands for 11β-HSD1 and 5β-reductase and 3α-HSD are involved in the cholesterol catabolism and bile acid biosynthesis. Bile acids act as potent transcriptional regulators of enzymes involved in cholesterol metabolism and bile acid detoxification and elimination via activation of the FXR (Chiang 2002). The increasing depth of knowledge regarding modulators of cholesterol and bile acid metabolism may therefore provide vital clues as to the mechanisms involved in the regulation of 5β-reductase and 11β-HSD1.

1.9 Cholesterol homeostasis and bile acids

The catabolism of cholesterol to hydrophilic bile acids represents the predominant pathway through which cholesterol is eliminated from the body (Danielsson & Sjovall 1975). In the rat 80-90% of cholesterol is catabolized to bile acids whilst in man approximately 50% cholesterol is removed as bile acids and is excreted in faeces (Nathanson & Boyer 1991a). Bile acids stimulate bile flow and facilitating the direct excretion of hepatic cholesterol into bile thereby decreasing whole body cholesterol levels and play a fundamental role in cholesterol homeostasis (Russell 2003a). Newly synthesised bile acids are secreted into the bile and delivered to the lumen of the small intestine where, along with bile acids secreted from the gall bladder, they act as detergent emulsifiers forming mixed micelles of dietary lipids, cholesterol and fat soluble vitamins (Danielsson & Sjovall 1975). This process promotes the absorption of lipids and cholesterol from the body. Solubilization of dietary cholesterol and efficient recycling of bile acids leads to increased levels of whole body cholesterol and suppression of *de novo* biosynthesis.

1.9.1 Enterohepatic circulation

Within the intestine soluble nutrients are taken up by the enterocytes that line the proximal segment of the gut while the remaining bile acids continue to move distally. At the terminal end of the small intestine, bile acids that are transported across the brush border membrane into the enterocyte are taken up by the the sodium-dependent bile acid transporter (ASBT; SLC10A2) a membrane protein. Once within the cell, bile acids bind to and activate the ileum bile acid binding protein (I-BABP) which facilitates the efflux of bile acids to the portal circulation by truncated ABST (tABST) protecting the cell from the detergent actions of intracellular bile acids (Figure 1.9). Bile acids are then carried to the liver within the portal circulation and transported across the apical surface of the hepatocyte by sodium-dependent taurocholate cotransport peptide (NTCP). Once within the hepatocyte bile acids can then re-secreted into bile across the canalicular membrane via the bile salt export pump (BSEP) into the bile duct. During each cycle of the

enterohepatic circulation approximately 95% bile acids are recovered, with those lost in faeces being replaced by new synthesis within the liver (Figure 1.9)(Russell & Setchell 1992).

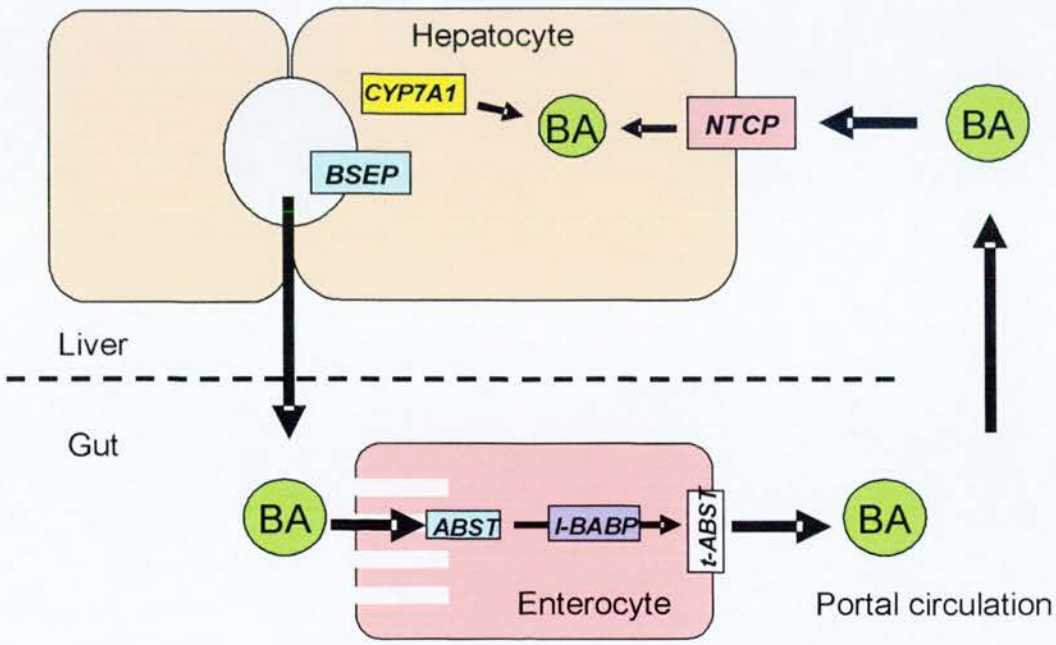

Figure 1.9 Enterohepatic circulation of bile acids. Bile acids are extracted from the portal circulation into the hepatocyte via NTCP and are excreted via BSEP. Within the distal region of the gut they are transported across the enterocytes lining the gut via ASBT and I-BABP and are excreted via t-ABST. These bile acids are then returned to the liver via the portal circulation.

1.10 Pathways of bile acid synthesis

The primary bile acids cholic (CA) acid and chenic (chenodeoxycholic; CDCA) acid in humans and rats are synthesized from cholesterol within the liver by the actions of 17 known enzymes. Two major pathways of bile acid biosynthesis have been described in the mammalian liver, the "Classical" or neutral pathway and the "Alternative" or acidic pathway.

1.10.1 Classical (neutral) pathway

The classical pathway is the main pathway involved in bile acid biosynthesis in man and is initiated by 7α-hydroxylation of cholesterol. This step represents the first and rate-limiting step in the conversion of cholesterol to bile acids in the liver in a reaction catalyzed by the enzyme cholesterol 7α-hydroxylase (CYP7A1), a cytochrome P-450 containing monooxygenase located in the ER membrane (Myant 1977 (Nathanson & Boyer 1991b). This enzyme is subject to complex regulatory mechanisms (Chiang 1998; Danielsson & Sjovall 1975). The subsequent steps involved in the formation of CA and CDCA from cholesterol can be divided into two main categories; those that modify the sterol ring structure or nucleus, e.g. formation of a 5β (A/B, cis) saturated ring system by saturation of the Δ^5double bond, and those that those that oxidize and shorten the side chain of sterol e.g. oxidative cleavage of the side chain between C-24 and C-25 (Chiang 1998) (Figure 1.10). In the Classical pathway, modifications of the steroid nucleus, including hydroxylation at 7α- and 12α- positions, epimerization of the 3β-hydroxyl group and saturation of the steroid nucleus precede the oxidative cleavage of the terminal three carbons of the side chain.

Similarly to the metabolism of pregnene steroids, 5β-reductase and 3α-HSD act upon the A-ring of 7α-hydroxy-4-cholesten-3-one and 7α,12α-dihydroxy-4-cholesten-3-one, the product of a second microsomal cytochrome P-450 enzyme 12α-hydroxylase, to yield a sterol intermediate that is ultimately converted to CDCA and CA respectively (Figure 1.10) (Chiang 2002). The reactions catalysed by 5β-reductase and 3α-HSD are chemically identical to those in glucocorticoid metabolism described previously (Figure 1.11)

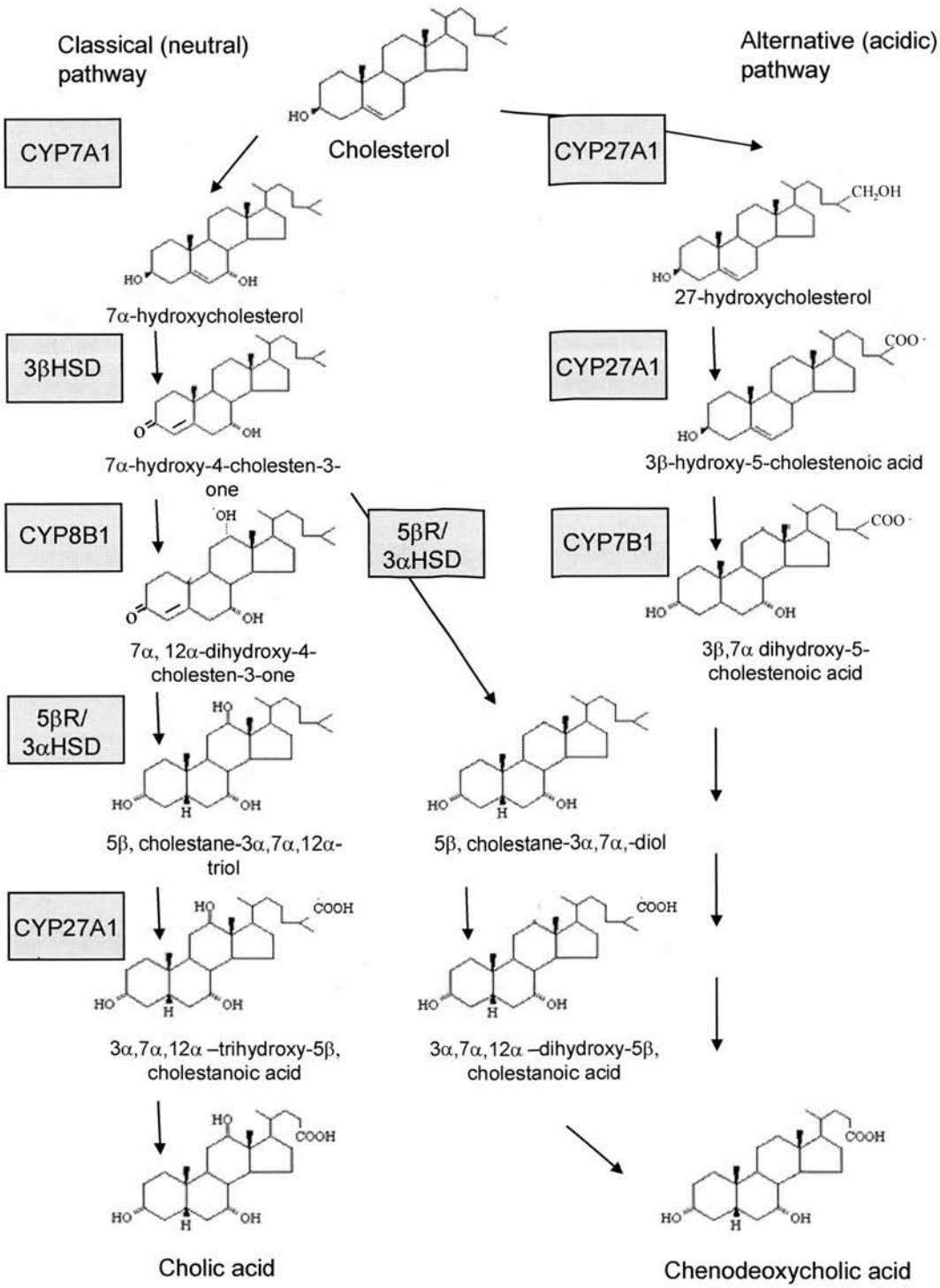

Figure 1.10 Pathways of bile acid biosynthesis. Cholesterol is metabolised via the Classical and Alternative pathway by the action of 17 different enzymes. The resulting primary bile acids chenodeoxycholic acid (CDCA) and cholic acid (CA) are subsequently conjugated to the amino acids taurine and glycine.

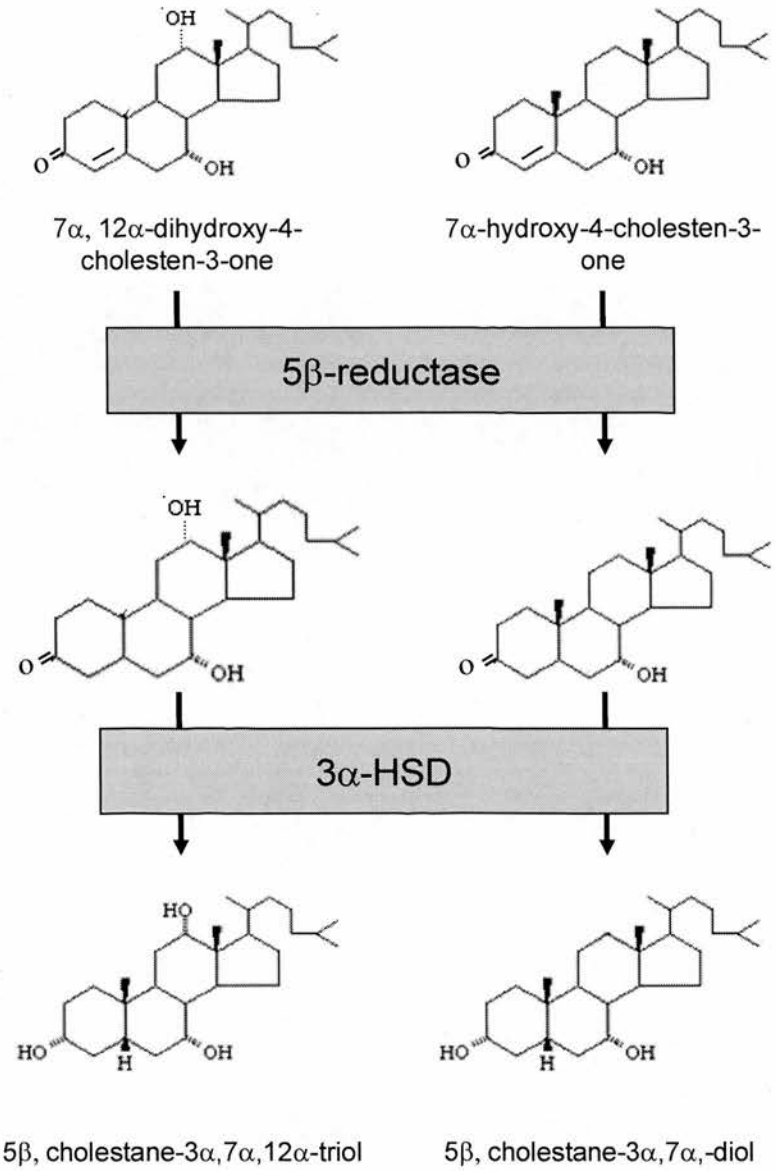

Figure 1.11 A-ring reduction of bile acid intermediates. 5β-Reductase catalyses reduction of the steroid 4-5 double bond and 3α-HSD reduces the oxygen double bond at position 3.

1.10.2 Alternative (acidic) pathway

The alternative pathway is initiated by sterol 27-hydroxylase (CYP27A1), which is expressed in many tissues and converts cholesterol to both 27-hydroxycholesterol and 3β-hydroxy-5-cholestenoic acid (Pikuleva *et al.* 1998) producing predominantly CDCA (Chiang 2002). Oxysterol 7α-hydroxylase (CYP7B1) subsequently converts these intermediates to 7α,27-dihydroxycholesterol

and 3β,7α-dihydroxy-5-cholestenoic acid, respectively. In the alternative pathway, oxidative cleavage of the 3-carbon side chain precedes modification of the steroid nucleus which is performed by the same enzymes as those within the Classical pathway of bile acid biosynthesis (Andersson *et al.* 1989b). 5β-Reductase and 3α-HSD are not directly involved in the alternative pathway of bile acid biosynthesis.

1.10.3 Conjugation

The final step in bile acid synthesis involves the addition of an amino acid, usually glycine or taurine, via an amide linkage to carbon-24 in a reaction catalysed by the peroxisomal enzyme N-acyltransferase (Figure 1.12). Approximately 98% of bile acids excreted from the liver are amidated, which increases their amphipathicity and enhances their solubility, making the cell membrane impermeable the bile acids. The main substrates for N-acetyltransferase are bile acid coenzyme A and either taurine (mice) or taurine and glycine (humans).

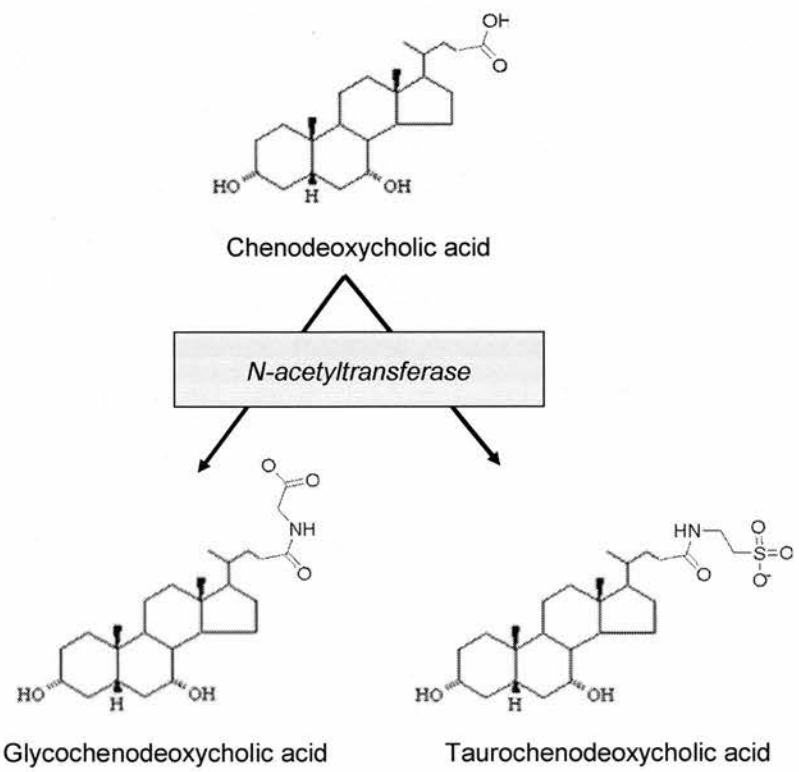

Figure 1.12 Conjugation of chenodeoxycholic acid. N- acetyltransferase catalyses the addition of either taurine or glycine at the C24 carboxylate position of the chenodeoxycholic acid structure via an amide linkage.

1.11 Regulation of bile acid biosynthesis

Cholesterol levels and bile acid synthesis are tightly regulated by a number of factors including diet, bile acids and hormones. Indeed the mechanisms responsible for regulating bile acid synthesis, elimination and detoxification have been an area of much research in the past decade and it is now widely recognised that bile acid "negative feedback" plays an integral role in regulating bile acid synthesis (Shefer *et al.* 1969). Bile acid synthesis is stimulated in response to increases in newly synthesized cholesterol (Myant & Mitropoulos 1977) and following biliary drainage of bile acids by bile fistula (Danielsson & Sjovall 1975). The accumulation of bile acids induces feedback inhibition of CYP7A1 and sterol 12α-hydroxylase (CYP8B1) imposed by enterohepatic re-circulation of bile acids, thus repressing bile acid synthesis.

1.11.1 Competitive inhibition of synthetic enzymes

A principle mechanism whereby bile acids regulate their own synthesis is via inhibiting the activity of enzymes involved in their own biosynthesis. Indeed bile acids act as competitive inhibitors of enzymes involved in cholesterol catabolism including CYP7A1 and 27-hydroxylase (CYP27A1), the rate determining enzymes in the Classical and Alternative pathways of bile acid biosynthesis respectively. It has not been reported whether bile acids feedback and regulate other enzymes in the biosynthetic pathway such as 5β-reductase and 3α-HSD however bile acids have been shown to act as competitive inhibitors of the 5β-reduction of aldosterone (Latif *et al.* 1994) and human type 4 3α-HSD (AKR1C1) acts as a bile acid binding protein.

1.11.2 Bile acids as transcriptional regulators

Bile acids also act as signalling molecules that can activate nuclear receptors thereby regulating the transcription of enzymes involved in cholesterol and bile acid metabolism (Parks *et al.* 1999). The identification of two bile acid response elements

(BAREs), AGGTCA-like repeating within the promoter sequence of CYP7A1 (Chiang & Stroup 1994) which bind a number of nuclear receptors including the retinoic acid receptor α (RXRα) and hepatocyte nuclear receptor 4α (HNFα) led to the hypothesis that, bile acids may exert these effects via nuclear receptors which regulate basal transcription as well as bile acid negative feedback (Stroup *et al.* 1997b) reducing intracellular bile acid concentrations within the hepatocyte. Since then several members of the nuclear receptor (NR)1 family of nuclear receptors, including the oxysterol receptors (LXRα and β), the bile acid receptor (FXR; NR1H4) and PXR have been shown to be activated by micromolar concentrations of bile acids, lipids or sterols (Chiang 2002). Figure 1.13 demonstrates the central roles for LXR and FXR in the co-ordinated regulation of bile acid synthesis, transport and absorption within the liver and intestine and cholesterol metabolism within the liver and peripheral tissues. The regulation of CYP7A1, the rate determining step in the Classical pathway of bile acid biosynthesis has been studied extensively and the mechanism involved in its regulation are now well characterised. When cholesterol levels within the hepatocytes rise, oxysterols activate LXRα (NR1H3) which stimulates transcription of CYP7A1 and cholesterol metabolism. Rising bile acid levels induce FXR (Forman *et al.* 1995) which in turn activates short heterodimer partner (SHP; NROB2). SHP acts as a negative regulator, which binds to and inhibits liver receptor homologue-1 (LRH-1; NR5A2), which normally activates genes involved in cholesterol catabolism including CYP7A1 (and also CYP8B1). As such bile acid synthesis is reduced. In addition, and through similar receptors bile acid regulate re-uptake into the hepatocyte via FXR mediated regulation of the NTCP.

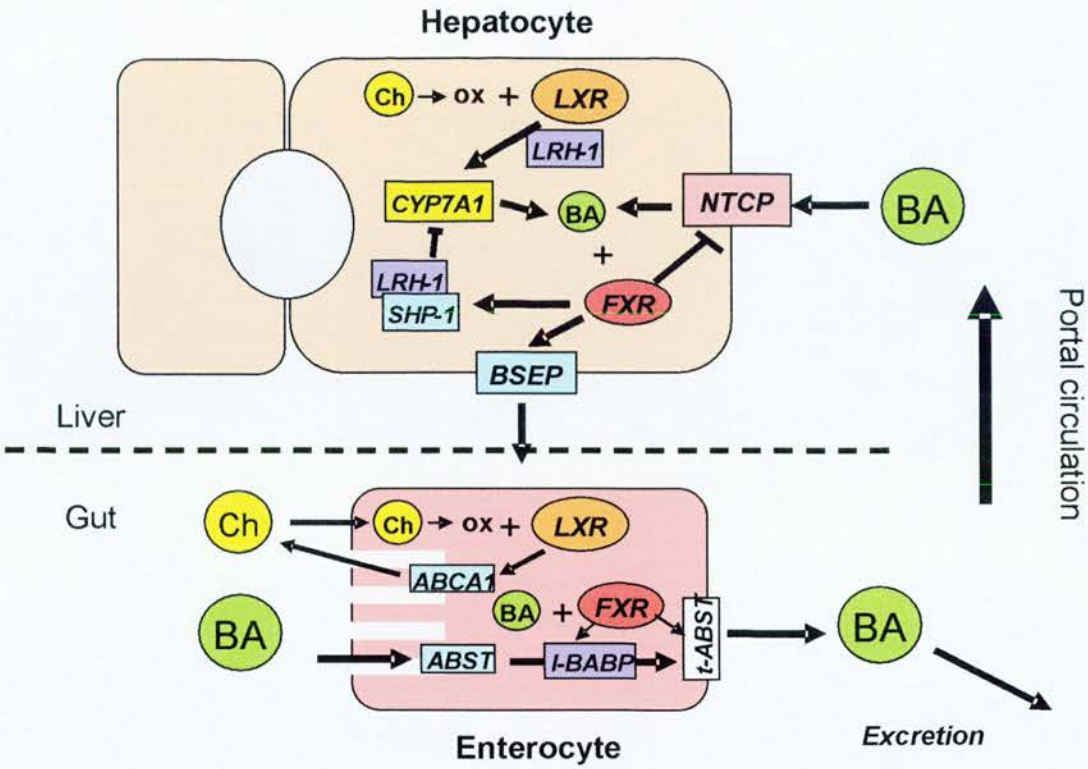

Figure 1.13 The role of FXR and LXR in cholesterol and bile acid biosynthesis. Within the liver cholesterol is converted to bile acids (BA) and also oxidised to oxysterols by sterol hydroxylases. Oxysterols activate LXR which induces CYP7A1. Bile acids also activate FXR which suppresses bile acid uptake via NTCP and induces excretion via BSEP into bile. FXR also inhibits CYP7A1 via SHP-1 and LRH-1. Bile acids are secreted from the gall bladder and reabsorbed in the intestine via ABST. FXR induces IBABP which binds and facilitates the the efflux of bile acids by truncated ABST (t-ABST) into the portal circulation to hepatocytes where they are taken up by NTCP. High levels of cholesterol (Ch) within the enterocyte induce the formation of oxysterols which activate LXR promoting efflux into the intestinal lumen via ABCA1. Within the intestine LXR induces ABCG5/G8 transporters and perhaps MDR2 which is responsible for the excretion of phosphatidylcholine into bile.

Additional SHP-independent pathways exist. For example, repression of CYP7A1 and the Na+-independent organic anion transporter 2 (Oatp2) has been demonstrated via activation of PXR, an orphan nuclear receptor usually associated with the detoxification of xenobiotics and catatoxic steroids (Staudinger JL et al. 2001). Furthermore, bile acids have been demonstrated to activate the stress signalling kinase pathway JNK/c-Jun (c-Jun N-terminal kinase). Indeed taurocholate and the potent JNK activator tumour necrotic factor α (TNFα) have been demonstrated to repress CYP7A1 mRNA expression in cultured primary hepatocytes in a process independent of SHP mediated CYP7A1 repression (Gupta et al. 2001).

1.12 Bile acids and glucocorticoids

It is apparent from the literature presented in the introduction to this thesis that maintaining glucocorticoid and cholesterol homeostasis is an essential requirement for health. That 5β-reductase, 3αHSD and 11β-HSD1 are involved in both cholesterol and glucocorticoid metabolism poses the intriguing prospect that factors common to both pathways may be involved in regulation of these enzymes. Obese individuals and the obese Zucker rat display an altered lipid profile with elevated levels of circulating cholesterol, LDL-cholesterol and triglycerides, in conjunction with altered metabolism and alterations in HPA axis activation (Livingstone *et al.* 2000; Rask *et al.* 2001). Furthermore, liver fat accumulation has been demonstrated to correlate with an increase in 5β-reduced urinary cortisol metabolites, and was independently associated with insulin resistance and hypertriglyceridemia (Westerbacka *et al.* 2003). Cholesterol metabolites (bile acids and oxysterols) are potent signalling molecules, of paramount importance in maintaing hepatic homeostasis and thus may play a role in regulating the activity if hepatic enzymes involved in glucocorticoid metabolism. This raises the possibility that cholesterol and/or bile acids may play a role in regulation of these enzymes common to glucocorticoid metabolism. As such we propose that alterations in bile acid levels may influence glucocorticoid action and metabolism. This in turn may affect activation of the HPA axis. Manipulation of the bile acid pathway may

therefore provide a target for normalising the altered metabolic clearance rate and lipid profile of obese individuals

1.13 Hypothesis and aims

The experiments performed in this thesis were based upon the hypothesis that bile acids may influence glucocorticoid metabolism catalysed by 5β-reductase. This in turn may impact upon activation and/or response of the hypothalamic-pituitary-adrenal (HPA) axis.

The primary aim of this thesis was to investigate the impact of bile acids on glucocorticoid metabolism by addressing the following aims:

1) To investigate the impact of bile acids on the activity of glucocorticoid metabolising enzymes *in vitro* in tissue homogenates or cultured cells.
2) To establish the nature of inhibition by bile acids and the level at which this occurs e.g. pre- or post-transcriptional.
3) To investigate the impact of alterations in hepatic bile acid concentrations on glucocorticoid metabolising enzymes *in vivo* via the administration of a diet supplemented with bile acids (CDCA; 1% w/w) or cholestyramine (CT; 5% w/w) or reducing hepatic bile acid concentrations via the administration of a fat-free diet.
4) To assess the impact of bile acids on HPA axis activation and glucocorticoid target genes following dietary manipulation.
5) To investigate the impact of bile acids on the renin-aldosterone-angiotensin system and adrenal gland physiology.

Chapter 2

Materials and Methods

2.1 Materials

All chemicals and reagents were purchased from Sigma, Poole, UK unless otherwise stated. HPLC grade solvents were from Rathburn Chemicals, Walkerburn, UK. All epi-isomers of steroid standards were from Steraloids, Newport, USA. Radioactive isotopically labelled products were from Amersham, Bucks, UK. Sources other than these are indicated in parenthesis. Solutions were stored at ~21°C (room temperature; RT) unless otherwise stated.

2.2 Commonly used buffers and solutions

Acetate buffer:

Sodium acetate was dissolved in distilled water to achieve a final concentration of 0.2M and the pH was adjusted to 4.6. The solution was stored at 4°C

Alkaline SDS:

Sodium dodecyl sulphate (SDS) and sodium hydroxide was dissolved in distilled water achieve a final concentration of 0.1% (w/v) and 0.2M respectively. The solution was prepared immediately prior to use.

Borate buffer:

Boric acid (8.25g), sodium hydroxide (2.7g), hydrochloric acid (3.5ml) and BSA (Fraction VI; 5g) were dissolved in 1 litre of distilled water and the pH adjusted 7.4. The solution stored at -20°C and thawed at room temperature before use.

Cesium Chloride/TE solution:

Cesium chloride (100g) was dissolved in TE buffer (100ml) (see below).

Charcoal Buffer:

Tris (6.07g), neomycin sulphate (2g), EDTA (1.85g), hydrocholic acid (5M; 5ml) were dissolved in 0.5 litres distilled water. The pH was adjusted to 7.4. BSA (Fraction VI; 5g) was sprinkled on to the surface and allowed to dissolve and the

volume adjusted to 1 litre with distilled water. The solution was stored in volumes of 100ml at -20°C. Prior to use, Dextran T70 (0.062g) was dissolved in 5ml buffer and added to Norit charcoal (0.6g) and buffer (95ml). The solution was stored at 4°C.

Denaturing solution:

Guanidium thiocyanate, sodium citrate and sarcosyl were dissolved in distilled water to achieve concentrations of 4M, 0.025M and 0.5% (w/v) respectively. β-Mercaptoethanol added immediately prior to use to achieve a concentration of 0.1M.

DEPC-treated water:

Diethylpyrocarbonate (DEPC; 5 drops) was dissolved in distilled water (500ml) and inverted to mix. The solution was allowed to stand (RT, 1hr) prior to autoclaving.

Deionised formamide:

Amberlite ion exchange resin (15g ; BDH, Lutterworth, UK) was mixed with formamide (150ml) for 1 hour. The solution was filtered twice through Whattman filter paper (grade #4) to remove the resin.

Hanks Kreb's Ringer Bicarbonate Buffer:

Sodium chloride, potassium chloride, potassium phosphate, calcium chloride, magnesium sulphate and sodium bicarbonate were dissolved in distilled water to achieve concentrations of 118mM, 3.8mM, 1.19mM, 2.54mM, 1.19mM magnesium and 25mM respectively. The pH was adjusted to 7.4 and the buffer stored at 4°C. Glucose (0.2% w/v) was added to the buffer immediately prior to use.

Loading buffer:

Bromophenol blue (0.25% w/v), xylene cyanol (0.25% w/v), Ficoll (25 % w/v) were diluted in DEPC-treated water.

10x MOPS buffer:

3-[N-morpholino]propanesulfonic acid, sodium acetate and EDTA were dissolved in distilled water to achieve concentrations of 0.2M, 50mM and 5mM respectively.

The pH was adjusted to 7 and the solution was autoclaved before use and stored at RT wrapped in foil to avoid exposure to light.

Potassium Acetate:

Potassium acetate (5M; 60 ml), glacial acetic acid (11.5ml) were mixed and the volume adjusted to 100ml with distilled water.

Primary Antibody Buffer:

Normal rabbit serum (1% w/v), Triton X-100 (0.1% v/v), aprotinin (200 KIU/ml; Traysol) were dissolved in stock buffer and prepared immediately prior to use.

Sodium Acetate Buffer:

Sodium acetate (12.30g) was dissolved in distilled water (500ml) to give a final concentration of 30mM and the pH adjusted to 4.8. The solution was autoclaved before use and stored at 4°C.

Sodium Phosphate Buffer:

Sodium dihydrogen orthophosphate dehydrate dissolved in distilled water (500ml) to achieve a final concentration of 40mM and the pH adjusted to 7.4.

Secondary Antibody Buffer:

As for tracer buffer

20x SSC Buffer:

Sodium chloride (175.32g) and sodium citrate (88.23g) were dissolved in 1 litre distilled water to give a final concentration of 30mM. The solution was autoclaved before use and stored at RT.

Stock Buffer:

Sodium phosphate, EDTA and sodium azide were dissolved in distilled water to achieve final concentrations of 63mM, 13mM and 0.02% (w/v) respectively and the pH was adjusted to 7.4. The solution was autoclaved before use and stored at RT.

Standard Buffer:

BSA (Fraction VI; 3.5% w/v) and aprotinin (200 KIU/ml, Traysol) were dissolved in Stock buffer. The solution was autoclaved before use and stored at 4°C.

10x TBE Buffer:

Tris (0.9M; 56g), boric acid (1.9M; 57.5g), EDTA (0.5M; 20ml) were dissolved in distilled water (500ml). The solution was autoclaved before use and stored at RT.

TE Buffer:

Tris-HCl and EDTA were dissolved in distilled water to achieve final concentrations of 10mM and 1mM respectively and the pH adjusted to 8. The solution was autoclaved before use and stored at RT.

Tracer Buffer:

Triton X-100 (0.1% w/v) and aprotinin (200 KIU/ml, Traysol) were dissolved in Stock buffer. The solution was prepared immediately prior to use.

Tris Buffer (50mM, pH7.4):

Tris (12.14g), hydrochloric acid (5M; 10ml), neomycin sulphate (3.5g) and human serum albumin (1.75g) were dissolved in 2 litres of distilled water and the pH adjusted to 7. The solution was stored as 10ml aliquots at -20°C.

Wash Buffer One:

SSC buffer (1x) and SDS (0.1% v/v) were dissolved in DEPC-treated water and prepared immediately prior to use.

Wash Buffer Two:

SSC buffer (0.3x) and SDS (0.1%v/v) were dissolved in DEPC-treated water and prepared immediately prior to use.

2.3 Animal care and maintenance

2.3.1 Animal maintenance

Male Wistar rats were obtained from Harlan Orlac, Bicester, UK at approximately three to four weeks of age or weighing 75-100g. Animals were maintained under controlled conditions of light (lights on, 0800-2000h) and temperature (21°C) and allowed free access to standard rat chow (Special Diet Services, Witham, UK) and drinking water. Prior to any experimental procedures rats were under the care of animal technicians at the Biomedical Research Facilities at the Western General Hospital (Chapter 4) or the Chancellors Building (Chapter 5). During experimental periods, animals were housed individually. Body weight, food and fluid intake were monitored on a daily basis. At all times animals were monitored closely for any signs of distress or ill health. All procedures were carried out according to Home Office guidelines under project license PPL 60/3293 and personal licence PIL 60/9607.

2.3.2 Animal sacrifice and tissue collection

Animals were killed by surgical decapitation in an adjacent room to the one in which they were housed within approximately 1 min of their cage being disturbed to minimize stress to the animals. Trunk blood was collected in EDTA-tubes and plasma prepared by centrifuged (10000g, 10mins, 4^0C) which was then snap frozen on dry ice in Eppendorf tubes, and stored at -80^0C. Tissues (liver, kidneys, adrenal glands, thymus, sub-cutaneous fat, omental fat and peritoneal fat) were dissected carefully within 5mins of sacrifice. Liver, adrenal glands and thymus weights were recorded. Subsequently, several small sections (~100mg) were cut from the upper right hand lobe of the liver and transferred to Eppendorfs for later use. Adrenal glands were carefully cleaned of any residual adipose tissue and transferred to pre-weighed Eppendorfs. All tissues were snap-frozen on dry ice and stored at -80^0C for future analysis.

2.4 Plasma assays

2.4.1 Corticosterone radioimmunoassay

Plasma (10μl) was diluted 1 in 5 in borate buffer and denatured (65°C; 30mins). This allowed corticosterone (B) to dissociate from proteins present within the plasma such as corticosterone binding globulin. A series of solutions representing a range of concentrations of B were prepared (0, 0.6125, 1.25, 2.5, 5, 10, 20, 40, 80, 160, 320 nM) from which a standard curve was derived. Samples or standards (20μl each) were pipetted in duplicate into a 96-well plate with 50μl of a mixture of $[^3H]_4$-1,2,6,7 -B (specific activity 80Ci/mmol;final concentration 1.5nM) and B rabbit anti-rat antibody (1 in 10,000 dilution to achieve ~30% binding; a kind gift from Dr CJ Kenyon) in borate buffer in a total volume of 70μl. Corticosterone present in the plasma and radio-labeled $[^3H]_4$ B were allowed to compete for binding with the anti-body (RT, 2hr). Following incubation, scintillation proximity assay beads (50μl, anti-rabbit-SPA; Amersham, Bucks, UK) were added to each sample and the plate was sealed, inverted to ensure even mixing, covered in foil to avoid exposure to light and incubated (RT,16hr). During this incubation period a binding equilibrium was achieved between antibody/B complex or antibody/ $[^3H]_4$-B complex and the SPA beads. The light induced by β emissions emitted by the SPA beads when they are within close proximity of primary antibody/B complex was measured for 1 min using a Wallac Microbeta Plus counter. The concentration of corticosterone in each sample was calculated from the standard curve constructed following 4-point sigmoidal curve fit analysis where the average response of the duplicates for each standard (Y-axis) was plotted against the concentration of each standard following log transformation (X-axis). The inter- and intra-assay coefficients of variation were 9.2% and 9.4% respectively.

2.4.2 ACTH radioimmunoassay

Adrenocorticotrophic hormone (ACTH) was measured in plasma from animals at baseline and following acute restraint stress. Plasma (25μl) was diluted in

1:4 in Stock Buffer prior to assay. Solutions of ACTH were prepared (0, 3.90, 7.8125, 15.625, 31.25, 62.5, 125, 250, 500, 1000, 2000 pg/ml) by serial dilution from stock human ACTH (Peninsula Laboratories, UK) in Standard Buffer. In each assay a blank (0 ACTH standard) and Non Specific Binding (NSB) (ACTH; 100ng/ml and no antibody) control were included. The blank was used to demonstrate that components within the Standard Buffer did not displace labeled ACTH, whilst the NSB contained standard buffer and ACTH but not primary antibody demonstrated specificity binding of ACTH with the antibody. Primary antibody (rabbit anti-rat)(IgG Corporation USA, IgG-ACTH-1; diluted in Primary Antibody Buffer 1:1000,000 to give approximately 40% binding) was prepared in Stock Buffer (1ml) containing Normal Rabbit Serum (1% w/v), and Aprotinin (200 KIU; diluted in Stock buffer, Traysol, IgG Corporation USA IgG-Aprotinin 100,000 KIU). Diluted samples or standards (100µl in duplicate) were pipetted into 2.5ml polypropylene round bottom tubes (Roche) and incubated with primary ACTH antibody (100µl; RT, 16hr). Following incubation I^{125}ACTH (100µl, 1:1000 in 0.1M acetic acid) was added to each sample and incubated (RT, 7 hrs). A secondary anti-rabbit antibody (ICN Pharmaceuticals, Diagnostic Division: Goat anti-rabbit IgG Precipitation antiserum) was diluted 1:80 in Secondary Antibody Buffer and added (600µl) to each sample and incubated (4°C, 16hr) to achieve an equilibrium between primary and the secondary antibody. Pre-chilled (4°C) Wash buffer (1ml) was added and the anti-body complex precipitated by centrifugation (3000g, 4°C, 30 mins). The resultant supernatant was decanted and the tubes inverted, dabbed gently on tissue to remove any remaining supernatant and allowed to drain upside down in a wire rack leaving an off-white precipitate at the bottom of the test-tube. Activity was counted using a gamma counter (Wallac 1470 Wizard automatic gamma counter; 1 min). The concentration of ACTH in each sample was calculated from a standard curve generated by log/logit curve fit with average emission for the duplicates of each standard on the Y axis (linear) and the corresponding standard ACTH concentration on the X axis (logarithmic). The inter- and intra-assay coefficients of variation were 7.9 and 5.4% respectively.

2.4.3 Renin radioimmunoassay

Plasma renin activity was measured as the generation of angiotensin I from endogenous angiotensinogen present within plasma. Solutions representing a range of concentrations of angiotensin I were prepared (0, 0.8, 1.6, 3.2, 6.4, 12.5, 25, 50, 100, 200, 400 ng/ml) by serial dilution in Tris buffer (50mM, pH 7.4) from stock (1000ng/ml) to allow the construction of a standard curve. Samples and standards (10µl each) were incubated in quadruplicate with rabbit anti-rat Angiotensin I primary antibody at 4°C. Following centrifugation (2000g, 4°C, 1min) two of the four tubes were allowed to remain at 4°C and samples in the other two tubes were incubated (37°C, 30 mins) on a shaking platform. Iodinated Angiotensin I (I^{125} - Angiotensin I; Amersham, UK) was prepared in Tris buffer (50mM, pH 7.4) and 150µl (containing approximately 4-5000cpm I^{125} Angiotensin I) added to each sample. Following, centrifugation (2000g, 4°C, 1min) samples were incubated (4°C, 18hrs). Angiotensin I generated by endogenous renin present within the plasma was separated from solution by the addition of a charcoal suspension (250µl) to which free peptides present within the solution will bind. Following centrifugation (3000g, 4°C, 15mins) the resultant supernatant was aspirated from the samples leaving a charcoal pellet at the base of the RIA cup. Radioactivity in the pellet was counted using a gamma counter (Wallac 1470 Wizard automatic gamma counter; 1 min). Renin activity was calculated as ng/ml/hr following curve fit analysis with average emission for the duplicates of each standard on the Y axis (linear) and the corresponding standard angiotensin 1 concentration on the X axis (logarithmic). The limit of detection was 1.5ng/ml/hr. The inter- and intra-assay coefficients of variation were 6.5 % and 5.4% respectively.

2.4.4 Aldosterone ELISA

Quantification of plasma aldosterone was quantified using a commercially available kit (Coat-a-Count®, DPC, Gwynedd, UK). This assay is a solid-phase radioimmunoassay based an aldosterone-specific antibody which is immobilized to the wall of a polypropylene tubes. A calibration curve was prepared using supplied calibrators (0, 25, 50, 100, 200, 600, 1,200 pg/ml). In addition a blank (deionized water), a non-specific binding (NSB, 0 calibrator alone) and total count (T, ^{125}I-

aldosterone alone) controls were analysed. Plasma and standards (200µl each) were pipetted in duplicate into tubes coated with antibody. Iodinated aldosterone (1ml) was added to each sample and the samples subjected to centrifugation (1000g, RT, 1min) The samples were incubated (RT, 18hrs) then the supernatant decanted (apart from T) and any visible signs of moisture removed by striking the tubes against absorbent tissue and allowing them to drain for 2-3 mins. Activity was counted in a gamma counter (Wallac 1470 Wizard automatic gamma counter; 1 min) and concentration determined from a logit-log representation of the standard curve. The concentration of aldosterone in samples was calculated by interpolation from a standard curve of percent bound against concentration following non-linear curve fit analysis. This assay is sensitive to 11pg/ml. The inter- and intra-assay coefficients of variation were 6.5 % and 5.4% respectively.

2.4.5 Insulin ELISA

Insulin concentrations in plasma were measured using a commercially available kit (Crystal Chem, IL, USA). This assay works on a dual reaction principle. During the first reaction insulin binds to a mouse anti-insulin monoclonal antibody coated on a microplate well. A mouse anti-insulin antibody is subsequently added to each well thus a mouse anti-insulin monoclonal antibody/insulin/anti-insulin antibody complex is immobilized on the microplate well. A horse radish peroxidase (POD)-conjugated anti-mouse antibody in turn binds to the anti-insulin antibody complex immobilized in the microplate well. The bound POD conjugate is detected following its reaction with *o*-phenylenediamine substrate solution and absorbance of product measured at a wavelength of 492nm. Solutions representing a range of concentrations of insulin (0, 156, 313, 625, 1250, 2500, 5000, 10000 pg/ml) were prepared from rat insulin stock solution (10000 pg/ml) by serial dilution in Diluent 2 (supplied with kit) to allow construction of a standard curve. Samples and standards (10µl each) were incubated in duplicate in plastic tubes with a mixture of iodinated insulin (^{125}I-insulin; 1,000cpm per sample) and insulin primary antibody in buffer (total volume 75µl) (RT, 4hr). Two tubes with ^{125}I-insulin (total count; T) and two with ^{125}I-insulin and buffer but no antibody (non-specific binding; NSB) were included in the assay as controls. Amerlex™-M magnetic separation beads (60µl)

were then added to each sample and incubated (RT, 10 mins). The beads were harvested by centrifugation (1000g, 4°C, 10 min), the supernatant discarded and the radioactivity associated with the pellet counted in a gamma counter (Wallac 1470 Wizard automatic gamma counter; 1 min).The concentrations of insulin in samples were determined from a standard curve generated by logit/log curve fit with mean absorbance value for each standard on the Y axis (linear) and the corresponding standard insulin concentration on the X axis (logarithmic). The inter- and intra-assay coefficients of variation were 6.3% and 3.5% respectively.

2. 5 Quantitative analysis of bile acids

2.5.1 Serum bile acids

Bile acid concentrations were measured in serum, faeces and cytosol enzymatically using a commercially available kit (Sigma-Aldrich Ltd, Poole, UK). This assay utilizes the oxidative properties of 3α-HSD. During the oxidation of bile acids to 3-oxo bile acids by 3α-HSD, an equimolar amount of nictotinamide adenine dinucleotide (NAD^+) is reduced to NADH (reaction 1). The NADH is subsequently oxidised to NAD^+ with concomitant reduction of nitro blue tetrazolium salt (NBT) to formazan, a reaction catalysed by the enzyme diaphorase (reaction 2). Formazan has an absorption maximum at 530nm, thus the intensity of colour produced is proportional to the concentration of bile acids within the sample.

(1) 3α-Hydroxybile Acids + NAD^+ $\xrightarrow{3\alpha\text{-HSD}}$ 3-Oxo Bile Acids + NADH

(2) NADH + NBT $\xrightarrow{\text{Diaphorase}}$ NAD^+ + Formazan

Figure 2.1 Enzymatic reactions involved in the determination of bile acids in bodily fluids

Bile acid Test Reagents (A; 2.5mM NAD, 0.61mM NBT, 625U/l Diaphorase) and buffer (pH7) and (B; 1250U/l 3α-HSD) were reconstituted in deionized water according to manufacturers' instructions and immediately mixed by inverting several times. A Test reagent was prepared by combining Reagent A (4ml) with Reagent B (1ml), and a Blank reagent prepared by combining Reagent A (4ml) with deionized water (1ml) The reagents were then heated (37^0C, 15 mins). Solutions representing a range of concentrations of bile acids (0, 5, 25, 50, 100, 200μM) were prepared by serial dilution using the supplied calibrator set. In each assay Calibrator (200μM bile acid) and Control (deionized water) samples were quantified. Samples or controls (5μl) were pipetted in quadruplicate into a 96 well plate and Test or Blank reagents (125 μl) were added to the corresponding samples. The plate was shaken briefly to mix and incubated (37^0C, 5min). Absorbance was measured at 530nm using a microplate reader (OPTImax tunable microplate reader) and the concentration of bile acids calculated using Softmax Pro software by subtracting Blank absorbance from the corresponding Test absorbance as follows:

$$\text{Bile Acid concentration } (\mu M) = \frac{AST - ASB}{ACT - ACB} \times \text{Concentration of Calibrator}$$

Where: AST = Absorbance of Sample with Test reagent

ASB = Absorbance of Sample with Blank reagent

ACT = Absorbance of Calibrator with Test reagent

ACB = Absorbance of Calibrator with Blank reagent

2.5.2 Hepatic bile acids

For measurements of hepatic bile acids, tissue (100μg wet weight) was homogenised in double distilled water (1ml, 37^0C). Bile acids were extracted from the homogenate (100μl) by incubation with ethanol (1ml, 85^0C, 1 min) according to the method described by Miyata *et al* (2004). Following centrifugation (1000g, RT, 5 mins) supernatant (~ 1ml) was removed and transferred to glass culture tubes. This

process was repeated twice. The resultant supernatant (3 x 1ml fractions) was reduced to dryness under a stream of oxygen free nitrogen (OFN) at 60^0C and the residue reconstituted in deionized water (20μl). Bile acid concentration was then measured as described in section 2.5.1 and expressed as μmoles/mg tissue.

2.5.3 Fecal bile acids

Fecal bile acids were measured according to methods described by Moundras *et al* 1997. Faeces (1g from a 24hr collection) were incubated (60^0C, 90mins) in KOH (O.5M, 10 vol). Hexane (1ml) was added to the resultant suspension (100μl) and the sample vortexed briefly and the organic and non-organic layers allowed to separate. The upper organic layer containing neutral sterols was removed and retained for analysis and the process repeated. The resultant fraction (2ml) was reduced to dryness under OFN at 60^0C and the residue reconstituted in deionized water (20μl). Bile acid concentration was then measured as described in section 2.51 and expressed as μmoles/g faeces.

2.6 Spectrophotometric assays

2.6.1 Hepatic triglycerides

Hepatic triglycerides were measured in liver homogenates using Triglyceride reagent (ThermoTrace®, UK) with an assay based upon the methods described previously by McGowan *et al* (McGowan *et al.* 1983) and Fossati *et al* (Fossati & Prencipe 1982). Triglycerides were hydrolyzed enzymatically by hepatic lipase to yield free fatty acids and glycerol. The glycerol was then phosphorylated by adenosine triphosphate (ATP) in the presence of glycerol kinase (GK) to produce glycerol-3-phosphate and adenosine diphosphate (reaction 2). Glycerol-3-phosphate was oxidized subsequently to dihydroxyacetone phosphate (DAP) by glycerol phosphate oxidase (GPO) producing hydrogen peroxide (H_2O_2). The H_2O_2 reacted with 4-aminoantipyrine (4 AAP) and 4-chlorophenol (4-CP) catalyzed by peroxidase, resulting in the production of a red dye (Quinoneimine dye). The absorbance of a

Quinoneimine dye at 500nm is proportional to the concentration of triglycerides present in the sample.

	lipase	
(1) Triglycerides + H_20	→	Glycerol + Free Fatty acids
	GK	
(2) Glycerol + ATP	→	Glycerol-3-phosphate + ADP
	GPO	
(3) Glycerol-3-phosphate + O_2	→	DAP + H_20_2
	Peroxidase	
(4) H_20_2 + 4-AAP + 4-CP	→	Quinoneimine dye + $2H_20$

This assay has a linear range of 0 - 10 mmol/l. To quantify hepatic triglycerides, liver (100mg wet weight) was homogenized in isopropanol (10 vol i.e 1ml) in glass culture tubes. The samples were shaken (RT, 45 mins) and the solid matter separated from the supernatant by centrifugation (3000g, 4^0C, 10mins). Triglycerides were quantified in the resultant supernatant. A series of solutions of triglycerides (0, 0.3125, 0.625, 1.25, 2.5mmol/l) was prepared in deionized water by serial dilution from which a standard curve was generated. Samples and calibrator (2.5mmol/l, 10µl each) were incubated in duplicate with Triglyceride reagent (1ml) (37°C, 5mins). Absorbance was then measured at 500nm using Shimadzu® UV-160A visible recording double beam spectrophotometer zeroed against a blank cell containing Triglyceride reagent alone. The concentration of triglycerides was calculated using the following equation:

$$\text{Liver triglycerides (µmol/g)} = \frac{\text{Absorbance of sample}}{\text{Absorbance of calibrator}} \times 25$$

2.6.2 Hepatic glycogen

Hepatic glycogen concentrations were inferred following their conversion to glucose based upon the method described by Van Handel 1965. Liver (50mg) was digested in KOH (1M, 250µl; 95^0C, 30 mins) then excess alkali neutralized with HCl (1M, 250µl). Following digestion, homogenate (100µl) was incubated (30^0C, 2 hrs) in sodium acetate (0.3M, pH4.8) containing amyloglucosidase (10mg/ml) (Roche Molecular Biochemicals). The content of glucose in the supernatant formed following centrifugation (6000g, RT, 10 mins) was measured using glucose hexokinase reagent (Sigma, St.Louis, MO) as described in section 2.63. Glycogen content is inferred from mg glucose produced per g tissue. The inter- and intra-assay coefficients of variation were 4.5% and 1.5% respectively. This assay is linear between 0 and 45mmol/l.

2.6.3 Plasma glucose

Quantification of plasma glucose was performed using Infinity™ glucose hexokinase reagent (ThermDMA, Louisville, CO, USA). This assay works using the Hexokinase / glucose-6-phosphate method in which glucose is phosphorylated by ATP by hexokinase producing ADP and glucose-6-phosphate (G-6-P) (reaction 1). Glucose-6-phosphate is then oxidized to 6-phosphogluconate (6-PG) with the reduction of NAD^+ to NADH by glucose-6-phosphate dehydrogenase (G-6-PDH) (reaction 2). The amount of NADH produced is proportional to the amount of glucose in the sample and can be measured by and increase in absorbance at 340nm.

1. Glucose + ATP $\xrightarrow{\textit{Hexokinase}}$ G-6-P + ADP

2. G-6-P + NAD^+ $\xrightarrow{\textit{G-6-PDH}}$ 6-PG + NADH + H^+

Plasma (3μl) was incubated (37^{0}C, 3mins) in duplicate with glucose hexokinase reagent (450 μl) which contains ATP, hexokinase, NAD^+ and G-6-PDH. The absorbance of NADH in the samples was measured at 340nM using a Shimadzu® UV-160A UV/visible recording spectrophotometer zeroed against a blank cell containing reagent only. The amount of glucose in the sample was calculated from a standard curve (0, 12.5, 25, 50, 100, 200, 400, 800 mg/dL glucose diluted in deionized water) constructed following linear regression analysis with mean absorbance (Y axis) plotted against standard concentration (X axis).The inter- and intra-assay coefficients of variation were <2%.

2.7 Analysis of glucocorticoid metabolites

2.7.1 Extraction of steroids from urine

Rat urine was collected over 72 hours using metabolic cages which minimised contamination of the urine with food or faeces. Urine (10ml) representing the final 24hr of a 72hr collection period containing epi-THB and epi-B (250ng each in ethanol) was passed through Sep-pak C18 columns (Waters, Herts, UK) containing 360mg packing material. Columns were pre-conditioned with methanol (5 ml) followed by water (5ml). A calibration line of A, B, THA, 5β-THB and 5α-THB representing a range of concentrations (0, 10, 20, 50, 100, 150, 200, 250, 300, 400, 500, 600, 800 and 1000ng) was prepared in water (5ml) to which internal standards of epi-THB and epi-B (250ng each) were added. Following application of the sample/standard and internal standards the columns were washed (5ml water) and the steroids eluted from the column with methanol (5ml). The eluant was dried under OFN at 60°C.

2.7.2 Hydrolysis of steroids

Glucocorticoids are conjugated with either glucuronic acid or sulphate to make them more hydrophilic and thus aid in their excretion. Prior to analysis, these esters were hydrolysed. The dried samples (section 2.7.1) were resuspended in sodium acetate buffer (2ml; 0.2M, pH4.6) vortexed thoroughly to ensure the steroids were in solution and β-glucuronidase (100μl; Type H2 from Helix pomatia) added.

β-Glucuronidase enzyme cleaves the glucuronic acid from the steroid and also has sulphatase action to remove sulphate groups. The samples were incubated in a water bath (37°C, 48hr).

2.7.3 Extraction of steroids from hydrolysate

Following hydrolysis, the steroids were re-extracted through the same Sep-pak columns primed as described previously with methanol (5ml) and water (5ml). The hydrolysate was applied to the column, the column washed with water (5ml) and the steroid eluted with methanol (5ml). The resultant eluant was evaporated to dryness under OFN (60°C). The dried steroids were dissolved in a mixture of ethyl acetate and water (15:1), vortexed thoroughly and the upper organic phase removed and evaporated to dryness under OFN (60°C) into Reacti-Vials ® (3.5ml).

2.7.4 Derivatisation of steroids

The extracted steroids underwent two sequential derivatisation steps in order to mask polar groups which could interfere with the chromatography of the resulting steroids. Firstly, samples were incubated (60°C, 30min) with methoxyamine.HCl (2%) in dry pyridine (50μl) which reacts with ketone groups. The samples were then reduced to dryness under OFN (60°C) and incubated (100°C, 2h) with trimethylsilylimizadole (50μl; Sigma Aldrich, UK) which reacts with hydroxyl groups.

2.7.5 Extraction of derivatised steroids

Following derivatisation, steroids were separated from other reagents using Lipidex 5000 columns prepared by adding Lipidex 5000 (1- 2 cm; Canberra Packard, UK) to glass pasteur pipettes loosely plugged with silanised glass wool. The Lipidex was prepared in mobile phase (cyclohexane; hexamethylsisilazane; pyridine; 98:1:1) and the columns washed with mobile phase (3 x 1ml) prior to use. The samples were then mixed with mobile phase (1ml) applied to the columns and allowed to drip through the columns. A further 2ml mobile phase was applied to the column to ensure all steroids were eluted from the column. The samples were subsequently

reduced to dryness under OFN (60°C) and reconstituted in decane (60μl; Sigma Aldrich, UK) in preparation for analysis by GC-MS.

2.8 Measurements of enzyme activity

2.8.1 Subcellular fractionation

Cytosolic and microsomal subfractions were separated by repeat differential centrifugation according to methods described by Fleischer et al (Fleischer & Kervina 1974). Liver (100mg) was homogenized using a Ystral mechanical homogeniser (Scientific Instruments Centre, Liverpool) in sucrose buffer (1ml; 0.25M, pH7.5) containing HEPES (10mM) and dithiothreitol (DTT;1nM). Homogenates were centrifugated (1000g, 4°C, 10min) and the supernatant removed and subjected to further centrifugation (34000g, 4°C, 30 min). Centrifugation (124000g, 4°C, 60 mins) of the resultant supernatant yielded cytosolic and microsomal sub-fractions, for analysis of 5β-reductase and 11β-HSD1 activity respectively.

2.8.2 Determination of concentration of protein

Concentrations of protein in tissue homogenates, cytosolic and microsomal sub-fractions were determined colorimetrically using the Bio-Rad Protein Assay based on the Bradford dye-binding procedure (Bradford 1976). A differential colour change occurs in response to various concentrations of protein. Binding of protein to an acidic solution of Coomassie® Brilliant Blue G-250 dye results in a shift in absorbance maximum from 465nm to 595nm. The Coomassie blue dye binds primarily to basic and aromatic amino acids, especially arginine. The extinction coefficient of a dye-albumin complex solution is constant over a 10-fold concentration range. Dye reagent was prepared by diluting 1 part Dye Reagent Concentrate (Biorad, UK) with 4 parts deionized water and filtered through Whatman #1 filter paper to remove particulates and was prepared immediately prior

to the test. A standard curve (0, 0.05, 0.1, 0.2, 0.3, 0.4, 0.5, 0.6, 0.8, 1.0, 1.2mg/ml) composed of a series of solutions of Bovine Serum Albumin (BSA) (Sigma-Aldrich, Poole, UK) was prepared in deionised water for each experiment. Samples were diluted in appropriate buffer to ensure protein concentrations were within the range of the standard curve. Diluted sample or standard (2µl each) followed by dye reagent (10µl) was pipetted in duplicate into a 96 well plate (Costar, Corning, NY) and incubated (RT, 10min). Absorbance of samples/standards were measured on a microplate reader (Optimax tunable microplate reader) at 595nm using Softmax Pro software (Version 2.0, Microsoft Windows). The protein concentration was determined by interpolation from the BSA standard curve following linear regression analysis with mean absorbance of each sample (Y axis) against concentration of standard (X axis). The inter- and intra-assay coefficients of variation were 5.8% and 4%, respectively.

2.8.3 5β-Reductase activity

5β-reductase catalyzes the conversion of corticosterone to its 5β-dihydro metabolites by reduction of the steroidal ring-A 4-5 double bond. In liver this reaction is rapidly followed by a second reductive step catalysed by 3α-HSD, resulting in the formation of 5β-THB. Measurements of hepatic 5β-reductase activity were determined in cytosolic sub-fractions from liver homogenates. Cytosolic preparations (100µg/ml protein) together with $[^3H]_4$ -1,2,6,7-corticosterone (50 nM), and unlabeled corticosterone (1950 nM) were incubated in duplicate with sodium phosphate buffer (40mM, pH 7.5) containing sucrose (0.32M) and DTT(1mM), NADPH (2mM), glucose-6-phosphate (5mM) and glucose-6-phosphate dehydrogenase (0.1 units/ml) in a total volume of 250µl. Control samples containing buffer, NADPH co-factor and substrate but no protein (Blank) and buffer, substrate, protein but no co-factor (No CF) were included in each assay. Reactions were performed at 37°C for 4 hours. Following incubation, the reaction was terminated by the addition of ethyl acetate (10 vol) and water (1 vol). The upper organic phase containing the steroids was removed and reduced to dryness under a stream of oxygen free nitrogen (OFN, 60°C). The resultant steroid residues were dissolved in

mobile phase (600µl; methanol; acetonitrile; water; 25:15:60). Steroids were quantified by high performance liquid chromatography (HPLC) as described in Section 2.9.1.

2.8.4 11β-HSD1 dehydrogenase activity

In vivo, 11β-HSD1 is mainly a reductase, converting inactive 11-dehydrocorticosterone to corticosterone. However, *in vitro*, the dehydrogenase direction is preferred, and reductase activity is less stable. 11β-HSD1 protein was therefore quantified in the dehydrogenase direction as the conversion of corticosterone to 11-dehydrocorticosterone under conditions in which dehydrogenase activity is proportional to enzyme protein added.

Microsomal preparations (100µg/ml protein) together with $[^3H]_4$ corticosterone (25 nM), were incubated in duplicate with Hanks Krebs Ringer Buffer (KRB; pH7.4) containing glucose (1% w/v) and $NADP^+$ (2mM). Reactions were performed at 37°C for 30mins. Blank and no co-factor controls were included in each assay as for 5β-reductase. Reactions were performed at 37°C for 30 mins. Following incubation, the reaction was terminated as described in section 2.73 and the upper organic phase containing the steroids was removed and reduced to dryness under a stream of OFN (60°C). The resultant steroid residues were dissolved in mobile phase (600µl; methanol; acetonitrile; water; 25:15:60). Steroids were quantified by HPLC as described in Section 2.91.

2.8.5 11β-HSD2 dehydrogenase activity

Renal 11β-HSD2 activity was determined in kidney homogenates as conversion of corticosterone to 11-dehydrocorticosterone as with 11β-HSD1. Kidneys were halved and homogenised in KRB (1ml) as described in section 2.92 and protein concentration was measured as described in section 2.93. Homogenates (50µg/ml) were incubated in duplicate with NAD^+ (2mM), $[^3H]_4$-corticosterone (25 nM) in KRB (total volume 250µl) at 37°C for 30 mins. Blank and no co-factor controls were included in each assay as for 5β-reductase. Following incubation, the

reaction was terminated and steroids recovered and quantified as described in section 2.76. Activity was assessed in renal homogenates that had only been defrosted once.

2.8.6 3α-HSD Activity

Analysis of 3α-HSD activity was performed by measuring the conversion of 5β-dihydrocortiocosterone (5β-DHB) to 5β-tetrahydrocorticosterone (5β-THB). Cytosolic preparations (50μg/ml protein) containing unlabeled 5β-DHB (500ng) were incubated in duplicate with sodium phosphate buffer (40mM, pH 7.5) containing sucrose (0.32M) and DTT (1mM), NADPH (2mM), glucose-6-phosphate (5mM) and glucose-6-phosphate dehydrogenase (0.1 units/ml) as described previously for 5β-reductase activity.

Reactions were performed at 37°C for 10 minutes and terminated by the addition of ethyl acetate (10 vol) and water (200μl). Epi-tetrahydrocorticosterone (epi-THB; 250ng in methanol) was then added as an internal standard. The organic layer was reduced to dryness under a stream of nitrogen at 60°C. Analysis of the conversion of 5β-DHB to 5β-THB was achieved by converting the steroids in the dried steroidal extracts to their methoxime-trimethylsilyl derivatives using a method based upon that reported by Shackleton & Honour (1976) and quantified by gas chromatography-mass spectrometry (GC-MS) as described in section 2.9.2.

2.9 Analysis of steroid metabolites

2.9.1 High pressure liquid chromatography

High pressure liquid chromatography (HPLC) was used to separate and quantify steroids following bioactivity assays. The HPLC system consisted of a auto-injector (Waters 717 plus ; Herts, UK), mobile phase pump set at a constant flow rate (1ml/min), a reverse phase Symmetry® shield C8 column (pore size =5 μm; length =150mm; internal diameter = 3.9 mm; Waters, Ireland) maintained at 35°C. Radioactive metabolites were detected by on-line liquid scintillation counting (Quicksafe Flow 2, Zinsser, Berks, UK; flow rate 2ml/min; model LB-509, Berthold Instrument). Radioactive standards of $[^3H]_4$ A and $[^3H]_4$B were injected at the start of each run to confirm the identity of the steroids. Further confirmation of identity was

achieved using unlabelled steroids, detected by UV detection (Waters λ2487 Dual Absorbance Detector) at λ254nm (B and A) or 195nm (THB). The area under each radioactive steroid peak was integrated using Dionex Chromeleon software (UK) and the proportion each peak represented of the total area of radioactive peaks was used to determine the conversion of substrate to product and hence enzyme velocity. Velocity was expressed as nmoles of product per mg tissue per hour.

2.9.2 Gas chromatography / mass spectrometry

Steroids were quantified by gas chromatography mass spectrometry under the following conditions:

1. Urinary metabolites

Analysis of urinary metabolites was carried out using Voyager electron impact gas chromatography mass spectrometer operated in selected ion mode fitted with a CP sil 5CB capillary column (Varian 100% dimethyl polysiloxane; length 25m, internal diameter 0.32mm, film thickness 0.12μm; Chrompak, UK). The initial oven temperature was 50°C; this was increased by 30°C/min to 200°C, by 8°C/min to 250°C and then by 6°C/min to 300°C, and maintained for 6 minutes. Injection, source and interface temperatures were 280, 200 and 250°C respectively.

2. Bioactivity assays

Products generated in bioactivity assays were analysed using a PolarisQ ion trap electron impact gas chromatography mass spectrometer operated in selected ion mode (Thermo Finnigan) fitted with a Db5MS capillary column (Crossbond 5% diphenyl; 95% dimethyl polysiloxane; length 30m, internal diameter 0.25mm, film thickness 0.25μm; Alltech, Camforth, UK). The initial oven temperature was 150°C; this was increased by 30°C/min to 200°C and then by 8°C/min to 300°C and maintained for 8 minutes. Injection, source and interface temperatures were 240, 200 and 280°C respectively. Ionization was performed in electron impact mode at 70eV.

The mass (m/z) and typical retention times of the ions monitored are shown in table 2.1. Quantification was achieved by integrating the area under each steroidal peak and calculating the ratio of each steroid peak relative to that of the internal

standard. The concentration of steroid was then be determined by interpolation of the calibration line where r>0.99 was deemed acceptable.

Compound	Ion monitored (m/z)	Retention time (min)
Corticosterone (B)	548	14.66 + 14.71
Epi-B	548	14.29±14.46
5α-Tetrahydro-B (5α-THB)	564	12.89
5β-Tetrahydro-B (5β-THB)	564	12.75
Epi-Tetrahydro-B (Epi-THB)	564	13.00

Table 2.1 Mass/charge ratio and retention time of ions monitored by GC-MS.

2.10 Culture of Rat Hepatoma Cells (H4IIE)

The cell line H4IIE, is a rat hepatoma cell line. This cell line retains many of the properties of rodent hepatocytes cells such as a cobblestone appearance and the expression of liver-specific enzymes such as cholesterol 7α-hydroxylase and 5α-reductase 1.

The H4IIE cells were obtained from the European Collection for Animal Cell Culture (ECACC, Sailsbury, UK). Cells were maintained in continuous culture in Dulbecco's Modified Eagle's Medium (DMEM, Sigma, Poole, UK) supplemented with heat inactivated fetal bovine serum (10%, FBS; Labtech International, East Sussex, UK), glutamate (2mM), streptomycin (100IU/ml) and penicillin (100μg/ml; Invitrogen Life Technologies, Paisley, UK) and incubated at 37°C in a humidified atmosphere containing 5% CO_2.

Once a confluent monolayer has formed in 75 cm^2 tissue culture flasks (Costar, Corning, NY), cells were washed in serum-free media and harvested with Trypsin-EDTA (2.5 ml; Invitrogen Life Technologies, Paisley, UK). After incubation (37^0C, 2-3 mins) cells were detached from the flask and an equal volume of complete

media was added to inactivate the trypsin. The cells were collected by centrifugation (1000g, RT, 5mins) and the cell pellet re-suspended in fresh media. Cells were then seeded at the concentration for the required experiment (1.6 x 10^6 cells/ml) or diluted in complete media for continuous culture.

2.11 Qualititative analysis of gene transcription

2.11.1 Isolation of total cellular RNA

Total cellular RNA was isolated from tissues and cells using TRIzol® Reagent (Invitrogen Life Technologies/Life technologies, Inc., Paisley, UK) based upon the method of Chomczynski *et al* (1987). TRIzol is a mono-phasic solution of phenol and guanidine isothiocyanate which disrupts cells and dissolves cellular components, yet maintains RNA integrity. TRIzol (1ml) was added per 100mg tissue or 10cm^2 tissue culture dish and the tissues homogensied (3 x 10sec) using a Ystral homogeniser The samples were incubated (RT, 10mins) to allow complete lysis of nucleoprotein complexes. To isolate total cellular RNA, choloroform (200µl per ml TRIzol) was added, shaken vigorously (15sec) and incubated (RT, 3min). Samples were separated into an upper, clear aqueous phase containing RNA, an interphase containing DNA and a lower organic phase containing protein and cellular debris by centrifugation (12000g, 4°C, 15 mins). The clear aqueous phase containing RNA was transferred to sterile 1.5ml Eppendorfs (1.5ml) and the RNA precipitated by the addition of isopropanol (500ul; BDH, UK). Following incubation (4°C, 10min), the precipitated RNA was harvested by centrifugation (12,000g, 4°C, 10mins). The RNA pellet was washed in ice cold ethanol (75%) followed by further centrifugation (7,500g , 4°C , 5 mins) the wash solution removed and the pellet allowed to air-dry. The RNA pellet was resuspended in 20µl RNAse free H_20 (DEPC H_20), heated at 55-60°C to ensure that the RNA was in solution and quantified spectrophotometrically using a GeneQuant spectrophotometer at λ 260/280 (Pharmacia Diagnostics, UK). The intergrity of purified total RNA was verified by ethidium bromide staining following electrophoresis through a 1.2% agarose gel.

2.11.2 Preparation of complementary DNA (cDNA)

Complementary DNA (cDNA) is a single-stranded DNA complementary to an RNA molecule. cDNA was generated by reverse transcription of total RNA (0.5 - 1μg) using a first-strand cDNA synthesis kit (Promega Ltd, UK). RNA was diluted to give a final concentration of 0.25 -0.5μg/μl. RNA (5μl diluted) was incubated with master mix (25μl; 60°C, 30mins). The master mix contained reverse-transcriptase derived from moloney murine leukaemia virus (M-MLV)(Promega, Southampton, UK), oligo(dT) primer (Promega) which anneals to the poly(A) tail of the mRNA and enables transcription in the 5'-3' direction and deoxynucleotide triphosphates (dNTPs) (Promega) which have energy-rich phosphate groups aiding nucleic acid synthesis. The resultant cDNA was stored at -20°C until required.

2.11.3 Amplification of cDNA by polymerase chain reaction (PCR)

The polymerase chain reaction (PCR) was used to determine transcripts from the genes of interest in H4IIE cells. cDNA (5μl) prepared from H4IIE cell RNA as described in section 2.11 was subjected to PCR amplification using appropriate forward and reverse primers (20pmoles of each; TAG Copenhagen A/S, Denmark; primer sequences are shown in Table 2.2) prepared in primer mix (40μl; Table 2.3) and *Taq*Beads™ polymerase (1 bead per sample; Promega Ltd, UK). Control samples with no RNA (no template) and no reverse transcriptase (no RT) were included in each cycle.

Target	*Position*	*Oligonucleotide sequence 5'-3'*
5β-reductase	249-268	AGGTGGCAGAAGGGAAGGTA
	761-780	AGCGAGGTTAGGAGTTCATC
11βHSD1		AAAGTGATTGTCACWGGGGC CAGCAAA
		ATCCARAGCAAACTTGCTTGC
3α-HSD	252–273	CTTTGGAGCACTTTCCATAGA
	547-567	GTTGCACACAGGCTTGTATTT
CYP7A1	235–253	TTACCTGCAAACTGATGGG
	440-460	GAAAGTGAACACAGAGCATC

Table 2.2. Oligonucleotide primers used for amplification 5β-reductase, 11β-HSD1, 3α-HSDand CYP7A1cDNAs by RT-PCR

Component	**Amount per sample**
10 x buffer	5μl
$MgCl_2$	3μl
dNTPs	1μl
Sense primer (20pmol/μl)	2μl
Anti-sense primer (20pmol/μl)	2μl
Nuclease free water	32μl

Table 2.3 Master mix components for PCR

Thermal cycling was performed using an Eppendorf Thermal Cycler according to table 2.4.

The amplified PCR products (5μl) were separated by electrophoresis on a agarose gel (1.2% w/v) For each gel, DNA fragments of known fragment sizes (1kb ladder; Promega) were resolved to indicate the size of the RT-PCR product.

Conditions				
Denaturation	**Annealing**	**Extension**	**Final Extension**	**No. Cycles**
99°C	55°C	72°C	72°C	34
45 s	30 s	90 s	10 mins	

Table 2.4 Conditions for PCR of genes of interest.

2.11.4 DNA purification

Complementary DNA (cDNA) products generated by RT-PCR were isolated from gel fragments using a gel extraction kit (Roche Molecular Biochemicals). All solutions were provided with the kit which did not identify individual components of each buffer, thus buffers are referred to by the manufacturers chosen names. RT-PCR products were excised carefully from the gel using a sterile scalpel, weighed in a sterile Eppendorf tube and incubated (60°C, 10 mins) with buffer A (50μl/mg gel). The resultant solution containing the RT-PCR product was passed through a filter catch tube to remove any unsolubilised gel fragments. The effluent was discarded and the filter washed twice by centrifugation (1300g, RT, 1min) in wash buffer (100μl/ml gel). Following centrifugation (1300g, RT, 1min), the purified DNA was eluted from the filter in elution buffer (20μl). The concentration of DNA was determined following electrophoresis of the purified DNA (1 or 2μl) and low or high-molecular weight ladder (depending on the molecular weight of the gene of interest, Promega) on an agarose gel (1.2%, w/v; 80V; 60min).The amount of DNA was calculated by comparing the relative intensity of bands to that of the DNA mass ladder. All purified RT-PCR products were verified by sequencing performed using the Applied Biosystems 3730 DNA Analyser at Wellcome Trust Clinical Research Facility, Western General Hospital, Edinburgh.

2.12 Quantification of messenger RNA (mRNA) by Northern blot analysis

2.12.1 Separation of RNA

Total RNA (10 or 20μg) isolated as described in section 2.10 was separated by electophoresis on an agarose formaldehyde denaturing gel (1.2% w/v). All

equipment was soaked in hydrogen peroxide for 2 hours prior to use and rinsed in nuclease free water (x3 times) to minimise contamination. A gel (100ml) was prepared by melting agarose (1.2g) in DEPC water (88ml) then adding formaldehyde (40%; 2ml) and 10x MOPS (10ml). The solution was mixed gently, poured into a gel casting tray with an appropriately sized comb and allowed to set in a fume hood. Once set the gel was transferred to an electrophoresis tank and soaked in 1x MOPS. RNA was diluted in DEPC water to give a concentration of 1 to 2μg/μl. Diluted RNA (10μl) was denatured (55°C, 15min) in mixture containing deionized formamide (10μl), formaldehyde (40%; 2.5μl) and 10x MOPS (2.5μl). Following denaturation, loading buffer (2μl) containing ethidium bromide (1μl per 50μl loading buffer) was added to each sample, mixed gently by pipetting, loaded on to the gel and subjected to electrophoresis (60V, 2-4 hr) or until the front band of the loading dye was ¾ way down the gel. The gel was briefly photographed under UV light (254nm) to check the integrity of the RNA, then soaked in 20x SSC buffer for 15min.

2.12.2 Blotting

Resolved RNA was blotted on to a Zeta-Probe nylon membrane (Bio-Rad Laboratories, Inc. Richmond, Ca) by capillary transfer. A wick of Whatman #1 3MM filter paper was placed over an upturned gel casting tray and placed in a sterile plastic tray containing 20x SSC. The upper left hand corner of the gel was removed for identification, the gel inverted and placed upon the wick. A piece of membrane was cut to the size of the gel, soaked in 20x SSC and placed carefully upon the gel, followed by 3 sheets of Whatmann #1 3MM paper. Saran wrap was placed along all sides of the membrane to ensure that the membrane did not make contact with the wick, which would short circuit the system thus preventing transfer of the RNA to the membrane. Paper towel (approximately 5cm thick) was placed upon the membrane/Whatman paper. A weight was balanced upon the glass plate and the assembly incubated (RT, 16hr) allowing capillary transfer to occur. Following transfer, the membrane was washed in 20x SSC to remove any residual gel fragments and dried between two sheets of Whatman 3MM #1 paper (60°C, 2hr). The RNA was then cross-linked to the membrane under UV light.

2.12.3 Hybridisation to 32P-labelled probe

The dried membrane was soaked in 20xSSC (5min) then placed in a Hybaid hybridisation bottle containing a pre-warmed (55°C) hybridisation buffer of SDS (20%; 3ml) and sodium phosphate buffer (6ml) to which denatured salmon testes DNA (0.5mg/ml; Sigma Aldrich, UK) was added. The membrane was pre-hybridised for at least 2hr at 55°C. Complementary DNA probes were labelled with [α-^{32}P]dCTP (3000Ci/mmol) (Amersham Pharmacia Biotech) using a random primed labelling kit (Roche Molecular Biochemicals). The probe was purified by passing through a NICK column (Amersham Pharmacia Biotech) which removes any unincorporated radioactivity. The NICK column was primed with TE buffer (3ml), the probe applied to the column, the column washed with TE buffer (400μl) and the labelled DNA eluted from the column with TE buffer (400μl). The activity of the probe was checked by mixing probe (1μl) with Cocktail T scintillant (1ml) and counting in a beta counter (1min). Only probes with specific activity > 10,000cpm were used for subsequent hybridisation. The labelled DNA probe was subsequently denatured (100°C, 5min), added to the pre-hybridisation buffer and the membrane hybridized with the probe (55°C, 16hr). Following hybridisation, the probe was discarded and the membrane rinsed in wash buffer one (1x SSC, 0.1% SDS. The membrane was subjected to a further two washes in buffer one (and on wash in buffer two (0.5x SSC, 0.1% SDS; 55°C, 30min). The membrane was wrapped in cling-film and exposed to an imaging screen (Fujifilm, London, UK) for 6hr. The level of hybridized probe was quantified using Fuji FLA2000 fluorescent image analyzer and imaging software (Aida, Raytek Scientific, Sheffield, UK). Membranes were rehybridised with a probe for U1 using the same method, to control for differences in RNA loading and transfer. The level of expression of the gene of interest was expressed as a ratio of the RNA of interest to that of U1 and expressed in arbitary units (A.U).

2.13 Quantification of messenger RNA (mRNA) by real-time PCR

2.13.1 Taqman® real-time PCR

Quantification of 5β-reductase, 3α-HSD and 11βHSD1 in H4IIE cells and hepatic 5β-reductase, 5α-reductase, 11βHSD1, 3α-HSD, angiotensinogen, PEPCK, TAT, SR-B1, HMG Co-A reductase and CYP7A1 was performed with real time PCR primer/probe sets using the ABI PRISM 7900 Sequence Detection System (Applied Biosystems, Southampton, UK). Gene sequences were obtained from Ensembl Gene Browser (http://www.ensembl.org/).Primers and probes were either designed using *Primer Express* Software (Applied Biosystems, Southampton, UK) or purchased directly from Applied Biosystems (Southampton, UK). Primer: Tm 58-60°C, 20-80% GC, length 9-40 bases, <2°C difference between primers, maximum of 2 G/Cs in the last 5 bases at 3' end. Probe: Tm 10°C higher than primer Tm, 20-80% GC, length 9-40 bases, no G on the 5' end, <4 contiguous Gs, must have more Cs than Gs All primer/probe sets were designed with at least one primer or probe spanning an intron to prevent amplification of genomic DNA. Primer and probe sequences used were:

11βHSD1 forward primer 5'- TCA TAG ACA CAG AAA CAG CTT TGA AA-3'; reverse primer 5'-CTC CAG GGC GCA TTC CT-3'; probe 5'-6-FAM-CTG GGA TAA TCT TGA GTC AAG CTG CT CCC-TAMRA-3'

5β-reductase forward primer 5'- GCC TTT AAG CCT GGA GAG GAA-3' reverse primer 5'- ACG TGG CAC ACA GAT TTG ATT T-3'; probe 5'-6-FAM- TGG TAT ATC ACT CGG CCA TTC TCA TCT TTA GGA T-TAMRA-3'

3αHSD forward primer 5'- TCT ATA CTT CAA AGC TTT GGA GCA CTT-3' reverse primer 5'- CCA GTT GAG TGC TTT TCA GTG TCT-3'; probe 5'-6-FAM-TCC AAG CAA GTT CGG ACC AGA TCT G-TAMRA-3'

Cyclophilin A forward primer 5'- CCC ACC GTG TTC TTC GAC AT-3' reverse primer 5'- GAA AGT TTT CTG CTG TCT TTG GA-3'; probe 5'-6-VIC-CAA GGG CTC GCC ATC AGC CGT-TAMRA-3'

All other primer/probe sets were purchased from Applied Biosystems Taqman® Gene Expression Assays on line catalogue (http://www.appliedbiosystems.com/).

cDNA was incubated with 1x Taqman mastermix (Applied Biosystems, Cheshire, UK), primers (25μM) and probe (5μM; 1μl cDNA per 10 μl, made up to volume with NF-water) and transferred to 384 well PCR plates with optical heat sealing cover (Applied Biosystems, Cheshire, UK). Reagents were concentrated at the bottom of the well by centrifugation (1000g, RT, 5mins) and transferred to ABI PRISM 7900 Sequence Detection for cycling/ detection as per manufacturers' instructions. (50°C, 2 min; 95°C, 10 min; 95°C, 15 sec and 60°C, 1 min, repeated for 40 cycles).

Cyclophilin A (liver) or β-actin (adrenal) primers/probes were used to normalize the transcript levels. A standard curve for each primer probe set was generated in triplicate by serial dilution of cDNA pooled from several samples. Each sample was run in triplicate and the mean values of the triplicates were used to calculate transcript level from the standard curve. The results are expressed as a ratio to cyclophylin A or β-actin using the Relative Standard Curve method. In this method a standard curve is generated for both the target and endogenous reference. For each experimental sample, the amount of target and endogenous reference is determined from the appropriate standard curve. The target amount is divided by the endogenous reference amount to obtain a normalized target value.

2.13.2 LightCycler® real-time PCR

One-step real-time quantitative PCR was used to assess the abundance of 11β-hydroxylase (CYP11B1) and aldosterone synthase (CYP11B2) within the adrenal glands and performed using the LightCycler® System (Roche Diagnostics, Mannheim, Germany) and LightCycler® RNA Master Hybridization Probes kit (Roche Diagnostics, Mannheim, Germany). Two pairs of gene sequence-specific hybridization probes homologous to exon 3 of rat *CYP11B1* or *CYP11B2* were designed and synthesized by TIB Molbiol (Berlin, Germany). Each pair of probes consists of a fluorescein-labelled and LightCycler Red 705 labelled probe. The sequences of the oligonucleotide probes are selected such that they hybridize to the

amplified DNA fragment in a head to tail arrangement within close proximity (1-8 base pairs). When the two probes are brought into close proximity, energy transfer - Fluorescence-Resonance Energy Transfer (FRET) between the two dyes results in the excitation of LightCycler Red by fluorescein, leading to the emission of light by LightCycler Red which is detected by the LightCycler apparatus (Roche Diagnostics, Mannheim, Germany).

Primer pairs (RB1 and RB2) were manufactured by MGW-Biotech (Ebersberg, Germany) and were exon-spanning to minimise amplification of any contaminating genomic DNA. The primers used were:

RB1 sense 5' –GTCTATAAACATTCAGTCCAA- 3'

RB1 antisense 5' –ATCTCGGATATGACACTCC- 3'

RB2 sense 5' – GGATGTCCAGCAAAGTCTC- 3'

RB2 antisense 5' – ATTAGTGCTGCCACAATGC- 3'

A master-mix solution was prepared as shown in table 2.6, mixed gently and aliquots (19µl) transferred into pre-cooled LightCycler Capillary tubes (Roche Diagnostics, Mannheim, Germany) along with 1µl RNA (1µg/µl). The capillaries were sealed with stoppers, placed into adapters. Following centrifugation (700g, 5 secs) the capillaries containing the samples were placed into the rotor of the LightCycler instrument (Roche Diagnostics, Mannheim, Germany). Annealing temperatures were 52^0C for CYP11B1 probes and 55^0C for CYP11B2 probes and the cycle programs were performed as described in table 2.6.

Component	Volume	Final concentration
H20, PCR grade	6.2µl	
$Mn(OAc)_2$ stock solution, 50nM	1.3µl	3.25mM
B1 Fluorescein (FL) or B2 Fluorescein (FL)	1µl	0.2µM
B1 LightCycler Red705 dye (LC) or B2 LightCycler Red705 dye (LC)	1µl	0.2µM
Primer RB1 sense or RB2 sense	1µl	0.5µM
Primer RB1 antisense or RB2 antisense	1µl	0.5µM
LightCycler RNA Master Hybridization Probes, 2.7 x conc		1x
Total volume	19µl	

Table 2.5 Master mix solution for LightCycler PCR. Volume column was multiplied by the number of samples plus one additional sample

Cycle Program Data	RT	Denature	Amplification			Cooling
Cycles	1	1	45			1
Analysis mode	None	None	Quantification			None
Temperature targets	S1	S1	S1	S2	S3	S1
Target temperature (°C)	61	95	95	52/55	72	40
Incubation time	20 min	30 s	1 s	15 s	13 s	30 s
Temperature transition rate (°C/s)	20	20	20	20	2	20
Secondary target temperature (°C)	0	0	0	0	0	0
Step size (°C)	0	0	0	0	0	0
Step delay (cycles)	0	0	0	0	0	0
Acquisition mode	None	None	None	Single	None	None

Table 2.6 Parameters for amplification of CYP11B1 and CYP11B2 by LightCycler® real time PCR

Fluorescent data were collected during a single acquisition phase. A standard curve was constructed by sequential 10-fold dilutions of standard mRNA amplified from 1μg tissue RNA. Sample copy number was then interpolated from the standard curve on the base of the samples crossing point. Each sample was measured three times. In each run controls containing no RNA (Blank) were included. Data are expressed as the mean of each triplicate ± S.E.M..

2.14 Histology

2.14.1 Adrenal histology

In order to assess changes in adrenal morphology transverse sections were cut from snap frozen (Hematoxylin and Eosin) or formalin fixed (Oil red O) glands. Glands were fixed to 1cm x 1cm cork tiles using cryomatrix fixation agent and then mounted on to cryostat chucks using water ensuring that the adrenal gland was in the correct orientation. Sections were cut to a thickness of 30 μm (Oil red O) or 15 μm (H and E) and mounted on to super-frosted microscope slides and stained using either H and E to look at gross morphology or Oil red O to assess lipid accumulation.

2.14.2 Hematoxylin and Eosin stain

Hematoxylin is isolated from an extract of logwood, *Hematoxylin campechuanun Linnaeus,* whose oxidation product, hematein, produces a blue/purple colour when combined with a mordant metallic ion such as aluminium salt. The positively charged aluminium hematin complex combines with negatively charged phosphate groups of nucleic acid producing the characteristic blue/purple colour characteristic of hematoxylin stains. Eosin, a xanthene dye was used as a counterstain to demonstrate structural characteristics of the cytoplasm and connective tissue.

2.14.3 Oil red O stain

Oil red O is an oil soluble dye which exhibits greater solubility in lipoid substances such as fat and is therefore frequently used to evaluate normal or abnormal fatty tissue. This stain was utilised to examine fat distribution and accumulation within different zones of the adrenal gland. Frozen sections were allowed to come to room temperature, rinsed briefly in nuclease free water, immersed in propan-2-ol (60%; 30secs) and then submerged in Oil red O (10mins). Following this time the sections were washed thoroughly in nuclease free water to remove any excess dye then immersed in hematoxylin (1min). Slides were rinsed in nuclease free water to remove any excess dye, then briefly immersed in ammonia (1%; 30secs) then rinsed in nuclease free water and mounted using mounting medium.

2.14.4 Liver histology

Lipid accumulation within the liver was assessed in sections (30μm) cut from snap-frozen livers as described for the adrenal gland section 2.14.1. Sections were stained with Oil red O as described in section 2.14.3.

2.15 Statistical analysis

For all experiments using animal tissues individual experiments were conducted using tissues from 8 independent animals (unless otherwise stated). Each assay was performed duplicate and the mean of each duplicate taken as the final value for that individual animal. For all experiments using cultured cell lines, indivdual experiments were performed using cells from 3 sepearate passages. Each assay was performed 6 times and the mean of these 6 cultures taken as the final value for that individual cell passage. All future analysis was performed using the mean of these replicates. The data in each figure represents the mean ± standard error of the mean (SEM). For *in vitro* experiments statistical significance was determined using one way analysis of variance (ANOVA) followed by post hoc least squared difference test for all groups. All analysis was performed using Statistica (Version 9) or Graphpad prism (Version 4). For *in vivo* experiments, where three groups were studied, data were analysed by one-way and repeated measure ANOVA followed by post-hoc least squared difference tests. Where two groups were studied, data were analysed by Students t-tests. All analysis was performed using Statistica (Version 9). For acute restraint stress, analysis of plasma B and ACTH was carried out by measuring area under the curve (AUC) using a Kinetica program (InnaPhase, USA). The following nomenclature was used to denote statistical significance: *$p<0.05$; **$p<0.01$.

Chapter 3

Inhibitory effects of bile acids on glucocorticoid metabolism and HPA axis activation *in vitro*

3.1 Introduction

The liver is the major organ involved with peripheral glucocorticoid metabolism. In this tissue the interconversion of active (cortisol (F) human; corticosterone (B) rodent) and inactive (cortisone (E) human; 11-dehydrocorticosterone (A) rodent) glucocorticoids is mediated by the type 1 isozyme of 11β-HSD (Agarwal *et al.* 1989). 11β-HSD1 is bi-directional, although it acts predominantly in the reductase mode (*in situ*) activating B from A in contrast to the type 2 enzyme (11β-HSD2) found in the kidney and acting as a dehydrogenase, inactivating B to A. Pre-receptor metabolism by 11β-HSD1 plays a key role in determining access of glucocorticoids to the hepatic GR. Indeed, it is evident from humans and rodent models that tissue specific differences in enzyme activity and expression, primarily within the liver and adipose profoundly influence homeostatic and stress responses in health and disease. (Morton *et al.* 2001; Paterson *et al.* 2004; Wake *et al.* 2003). This is exemplified in humans by the syndrome of "Apparent Cortisone Reductase Deficiency" which is characterised by hirsutism, menstrual irregularity in the female and gonadotrophin-independent pseudo-precocious puberty and hyperandrogenism in male and has been attributed to adrenal activation due to impaired hepatic cortisol regeneration or resulting from 11β-HSD1 deficiency (Phillipou *et al.* 1996). Furthermore, administration of carbenoxolone, the hemisuccinate derivative of glycyrrhetinic acid (GA) and inhibitor of hepatic 11β-HSD1 activity (Stewart *et al.* 1987) improves insulin sensitivity (Walker *et al.* 1995b; Andrews *et al.* 2002; Livingstone & Walker 2003; Livingstone *et al.* 2005).

The principle of peripheral reactivation of glucocorticoids by 11β-HSD1 regulating both HPA axis and glucocorticoid action has been elegantly demonstrated in murine models of transgenic over or under expression of the enzyme (Masuzaki *et al.* 2001b; Morton *et al.* 2001; Paterson *et al.* 2004; Kotelevtsev *et al.* 1996). In disorders of insulin resistance associated with obesity the activity of hepatic 11β-HSD1 is often impaired, perhaps as a means of protecting the liver from the action of excess glucocorticoids.

Irreversible glucocorticoid inactivation in the liver is mediated by the "A-ring reductases" (5α and 5β-reductase) which catalyse the reduction of the steroid 4-5 double bond at the A/B ring position (Russell & Wilson 1994; Kondo *et al.* 1994; Okuda & Okuda 1984). This reaction is rapidly followed by a second reductive step catalysed by 3α-HSD resulting in the formation of tetrahydro-metabolites (Okuda & Okuda 1984; Onishi *et al.* 1991). It is poorly understood what causes dysregulation of glucocorticoid metabolic pathways in the Metabolic Syndrome; however it is recognised that these changes contribute to increased glucocorticoid clearance rates and hence hyperactivation of the HPA axis (Seckl *et al.* 2004). A change in the balance of A-ring reduction in favour of 5α-reduction vs 5β-reduction has been demonstrated in insulin resistance and obesity (Livingstone *et al.* 2005; Andrew *et al.* 2000), whereas in hypertension and fatty liver 5β-reduction predominates (Ulick *et al.* 1977; Westerbacka *et al.* 2003)

There is limited evidence that bile acids may act as inhibitors of hepatic enzymes, particularly those integral to bile acid synthesis (Chiang 1998).

Bile acid biosynthesis is under both feed-forward and feed-back control. For example, several enzymes, most notably CYP7A1 and 27-hydroxylase are regulated by concentrations of bile acids, with increased levels resulting in suppression of activity either by acting as competitive inhibitors or transcriptional inhibitors (Gupta *et al.* 2001). Bile acids are endogenous ligands for the Farnesoid X receptor (FXR), which regulates expression of CYP7A1 via interaction with bile acid response elements within the promoter region of CYP7A1 (Malerod *et al.* 2005).

There is limited evidence that bile acids may inhibit metabolism by 5β-reductase and 3αHSD and also influence their transcription (Latif *et al.* 1990). There have been several reports of bile acids inhibiting the activity of 11β-HSD1 (Walker *et al.* 1995a; Monder *et al.* 1989). The experiments presented in Chapter 3 demonstrate detailed characterisation of bile acids as regulators of activity and transcription of enzymes involved in glucocorticoid metabolism.

3.2 Research Aims

The aims of the research in this chapter were

1. To investigate the impact of bile acids and bile salts on the activity of hepatic glucocorticoid metabolising enzymes in tissue homogenates.
2. To investigate the impact of bile acids and bile salts on the activity of glucocorticoid metabolising enzymes in cultured cells.
3. To investigate the impact of bile acids on mRNA abundance of glucocorticoid metabolising enzymes.

3.3 Methods and method development

Methods to measure the metabolism of glucocorticoids were developed *in vitro* and in cultured cells and subsequently used to assess the inhibitory capacity of bile acids on glucocorticoid metabolising enzymes. The procedures for bioactivity bioassays are described in full in section 2.8. In all assays control samples containing buffer, co-factor, corticosterone but no protein (Blank) and buffer, corticosterone, protein but no co-factor (No CF) were included.

3.3.1 11β-HSD1 activity in tissue homogenates

3.3.1.1 Establishing assay conditions of 11β-HSD1

An initial validation experiment was performed in order to establish the optimal conditions under which to perform subsequent kinetic studies. Bioactivity assays were performed as described in section 2.84. A study of the time course of the reaction was performed using protein (100μg/ml) and the velocity of the formation of product quantified after 0, 10, 30, 60 and 90 minutes. All subsequent assays were performed using the optimized first order conditions.

3.3.1.2 Impact of bile acids and bile salts on activity of 11β-HSD1

Bile acids, CDCA, CA and DCA, and Glyco- and tauro-conjugates of CDCA were dissolved in ethanol to give stock solutions of 2M concentration from which solutions of a range of concentrations of bile acid (final concentration x $10^{-2, -3, -4, -5, -6, -7, -8}$ M) were prepared by serial dilution in buffer. Bioactivity assays were subsequently performed in the presence of bile acid or bile salt.

3.3.1.3 Enzyme kinetics of 11β-HSD1

A solution of corticosterone (1mM) was prepared in ethanol and standards prepared by serial dilution in ethanol (final concentrations: 0 – 5μM). Bioactivity

assays were performed in duplicate at each substrate concentration and activity assessed in the absence (Control) and presence of CDCA at the approximate IC50 value (4μM).

3.3.1.4 Impact of bile acids on 11β-HSD1 reductase activity

11β-HSD1 reductase activity was assessed in lysates of human embryonic kidney cells (HEK293) stably transfected with human 11β-HSD1 (kind gift from Dr Scott Webster, University of Edinburgh) prepared by centrifugation (7000g, RT, 5mins). Bioactivity assays were performed in the presence of bile acids as described in section 3.3.1.2 with following modifications. Reaction mixtures were incubated (37°C, 30mins) with the substrate $[^3H]_2$ cortisone (20nM), the human equivalent of 11-DHB. Activity was measured by HPLC as described in section 2.91 with the following modifications: mobile phase (water: acetonitrile: methanol; 60:10:30) and a Reverse phase Symmetry C18 column (length 15cm, internal diameter 3.9mm, pore size 5μm).

3.3.2 5β-reductase activity in tissue homogenates

3.3.2.1 Establishing conditions of 5β-redutase assay

As described for 11β-HSD1 an initial time course study was performed using the bioactivity assay for 5β-reductase as described in section 2.8.5 to establish the optimal conditions under which to carry out subsequent kinetic studies. Bioactivity assays were performed using 40 and 100μg/ml protein and velocity quantified after 0, 1, 2, 4, 8 and 24 hr. Activity was assessed by HPLC as described in section 2.91. All subsequent assays were performed using the optimized first order conditions.

3.3.2.2 Impact of competing substrate (7α-hydroxycholestenone) on 5β-reductase activity

In order to investigate possible substrate competition, bioactivity assays were performed as in 2.8.4 in the presence of 7α-hydroxycholestenone (7αHCOH; final concentrations x $10^{-3,-4,-5,-6,-7,-8}$ M; Steraloids, London, UK), an intermediate cholesterol metabolite produced during the conversion of cholesterol to bile acids and a substrate for 5β-reductase.

3.3.2.3 Impact of bile acids and bile salts on 5β-reductase activity

Bioactivity assays were performed in the presence of endogenous bile acids and bile salts to determine IC50 values as described in sections 3.3.1.2 and 3.3.1.3 respectively. Assays were performed using the optimised conditions established in the validation study (section 3.3.2.1)

3.3.2.4 Enzyme kinetics of 5β-reductase

The impact of CDCA on the kinetics of the reaction catalysed by 5β-reductase was assessed over a range of concentrations of corticosterone as described for 11β-HSD1 (section 3.3.1.4).

3.3.3 3α-HSD activity in tissue homogenates

3.3.3.1 Establishing conditions of 3α-HSD assay

To assess the impact of bile acids on 3α-HSD alone, conditions were optimised for subsequent kinetic analysis. Bioactivity assays were performed as described in section 2.8.6. Activity was measured using the substrate 5β-dihydrocorticosterone (5β-DHB; 1μM), protein (100μg/ml) and velocity quantified after 5, 10, 15, 30, 60 and 120 minutes. Standards of 5β-THB (0, 50, 100, 200, 400,

500, 600, 800, 1000 ng/ml) were included in each assay. An internal standard of epi-THB (250ng) was added to each sample prior to concentrating the samples with OFN (60°C). Samples and standards were subsequently derivatised and quantified by GC-MS as described fully in section 2.9.2.

3.3.3.2 Impact of bile acids and bile salts on 3α-HSD activity

Bioactivity assays were performed in the presence of bile acids and bile salts at the approximate IC50 value calculated for 5β-reductase. Bile acids and bile salts were prepared as described in sections 3.3.1.3 and 3.3.1.4 respectively and bioactivity assays performed using the optimised conditions for 3α-HSD established in section 3.3.3.1.

3.3.4 5α-Reductase 1 activity in cultured rat hepatoma cells

3.3.4.1 Screening of hepatoma cell lines for genes of interest

Due to the instability of hepatic 5α-reductase 1 activity *in vitro* (Eicheler *et al.* 1995), activity cannot be assessed in tissue homogenates and so a cell culture was utilized to examine the effect of bile acids on the 5α-reduction of corticosterone. As with 5β-reductase, the sequential reduction of corticosterone to 5α-THB catalysed by 5α-reductase 1 and 3α-HSD was assessed. Three hepatoma cell lines were screened to determine the presence of mRNA for 5α-reductase 1 and 3α-HSD; rat H4IIE and 2SFAZA and human HepG2 cells. RNA was extracted from cells with Trizol® as described in section 2.11.1. RT-PCR performed with primers for 5α-reductase 1 and 3α-HSD (rat for H4IIE and 2SFAZA and human for HepG2) as described fully in section 2.11.3.

3.3.4.2 Establishing conditions of 5α-reductase 1 activity

Activity of 5α-reductase 1 was quantified in H4IIE cells maintained as described in section 2.10. An initial time course study was performed to ascertain the optimal conditions. Cells were washed in PBS (1M) and fresh media applied 1 hour prior to application of the substrate. Corticosterone (990μM) with $^{3}[H]_{4}$-corticosterone (10μM) were prepared in ethanol giving a final concentration of 1mM. Cells were treated with corticosterone (1μM) and media (1ml) removed at 1, 2, 4, 8 and 16 hours. Steroids were extracted from media by passing through Sep-pak columns (1g) pre-conditioned with methanol (5ml) followed by water (5ml). The column was washed with water (5ml) and steroids eluted with methanol (5ml). The resulting solvent was removed under a stream of OFN (60°C). The dried residue was dissolved in ethyl acetate (2.5ml) and water (200μl) and vortexed thoroughly. The upper organic phase containing the steroids was removed and dried under OFN (60°C). Samples and standards were subsequently derivatised and products quantified by GC-MS as described in 2.9.2.

3.3.4.3 Impact of bile acids on 5α-reductase 1 activity

Cells were prepared as described in section 3.3.4.2. Bile acids (100mM; Sigma Aldrich, UK) were prepared in ethanol as described in section 3.3.1.2 and the cells incubated (37°C, 2 hr) in the presence of corticosterone (1μM) with or without bile acids (100μM; 1:1000 dilution in media; Control cells were treated with ethanol which always <1% v/v). Media was removed and steroids extracted using Sep-pak columns as described in section 3.3.1.2. Samples and standards were subsequently derivatised and activity assessed by GC-MS as described in 2.9.2.

3.3.4.4 3α--HSD activity in cultured cells

An initial time course study was performed in order to establish the optimum conditions under which to assess enzyme activity. Cells were prepared as described in section 3.3.4.2 and incubated with substrate 5β-DHB (1μM prepared in ethanol).

Media (1ml) was harvested after 15, 30, 45, 20, 60, 90 and 120 minutes and steroids extracted using pre-conditioned Sep-pak columns following addition of the internal standard epi-THB (250ng) as described in section 3.3.1.2. Samples and standards were subsequently derivatised and products quantified by GC-MS as described in section 2.9.2.

3.3.4.5 Impact of bile acids on 3α-HSD activity in cultured cells

The impact of bile acids on 3α-HSD activity was assessed as described for 5α-reductase (section 3.342) with the following amendments. Bile acids (1mM; Sigma Aldrich, UK) were prepared in ethanol and the cells incubated (37°C, 15 mins) in the presence of 5β-DHB (1μM) and bile acids (100μM). Media was removed and passed through Sep-pak columns following addition of the internal standard epi-THB (250ng) as described in section 3.3.12. Samples and standards were subsequently derivatised and activity assessed by GC-MS as described in section 2.9.2.

3.3.5 Impact of bile acids on gene transcription

H4IIE cells were maintained as described in section 2.10. On the day of the experiment cells were washed in PBS (1M) and fresh media applied 1 hour prior to application of the bile acid. Bile acids were prepared in ethanol (100mM) and subsequently dissolved in the media (1:1000 dilution). Cells were therefore incubated with bile acids (100μM; 37°C, 16 hr). Control cells were incubated with ethanol (<1% v/v) and maintained as with bile acids treated cells. Following incubation, the media was removed, the cells washed twice in PBS (1M) to remove any residual media/bile acid and RNA extracted using Trizol® as described in section 2.11.1. Abundance of gene transcripts was assessed using Taqman® real-time PCR (2.13.1) with rat primer/probe sets specific for 11β-HSD1, 5β-reductase, 5α-reductase 1 and 3α-HSD. Typical CT values for 11β-HSD1 and 5β-reductase were 32 cycles and for 5α-reductase and 3α-HSD 28 cycles.

3.3.6 Data analysis

The velocity of product generation is described by the Michealis Menten equation (Equation 1), frequently presented as the reciprocal plot of 1/V versus 1/[S]. This Lineweaver –Burk plot yields a straight line with an intercept of 1/Vmax and a slope of Km/Vmax (2).

(1) $$V = \frac{Vmax\,[S]}{Km + [S]}$$

Equation 1 Michealis Menten equation. describing enzyme velocity as a function of time, where V = velocity of the reaction, [S] = substrate concentration, Vmax = maximum velocity and Km= the Michaelis constant or concentration of substrate required to achieve half-maximum velocity

(2) $$\frac{1}{V} = \frac{Km}{Vmax\,[S]} + \frac{1}{Vmax}$$

Equation 2 Lineweaver Burke double reciprocal plot of enzyme kinetics. Competitive inhibition results in a reduction in Km but no change in Vmax. Non-competitive inhibition causes a change in Vmax but no change in Km.

Kinetic parameters of Vmax and Km were calculated using GraphPad Prism Version 4.0. Data were fitted to the Michaelis-Menten equation and an equation of Competitive Inhibition (3)

(3) $$Kmapp = Km \times \frac{(1+I)}{Ki} \qquad Y = Vmax \times \frac{X}{(Kmapp + X)}$$

3.3.7 Statistical analysis

For all experiments using animal tissues individual experiments were conducted using tissues from 6 independent animals (unless otherwise stated). Each assay was performed duplicate and the mean of each duplicate taken as the final value for that individual animal. For all experiments using cultured cell lines, indivdual experiments were performed using cells from 3 separate passages. Each assay was performed 6 times and the mean of these 6 cultures taken as the final value for that individual cell passage. All future analysis was performed using the mean of these replicates. The data in each figure represents the mean ± standard error of the mean (SEM). Statistical significance was determined using one way or repeated measure analysis of variance (ANOVA) followed by post hoc least squared difference test for all groups. All analysis was performed using Statistica (Version 9) or Graphpad prism (Version 4). Significance was set at * $p<0.05$ *vs* Control; **$p<0.01$ *vs* Control.

3.4 Results

3.4.1 11β-HSD1

3.4.1.1 Chromatography of 11β-HSD1

Figure 3.1 shows representative radio chromatograms of $[^3H]_4$ corticosterone (B) and the product of 11β-HSD1 dehydrogenase activity, $[^3H]_4$11-DHC (A). Conversion was not apparent in either blank or no co-factor control samples indicating the absence of non-enzymatic reactions (blank) or background reactions within the enzyme preparation (e.g. due to endogenous co-factor). Reaction products were not evident in blank or no co-factor control samples (Figure 3.1 B).

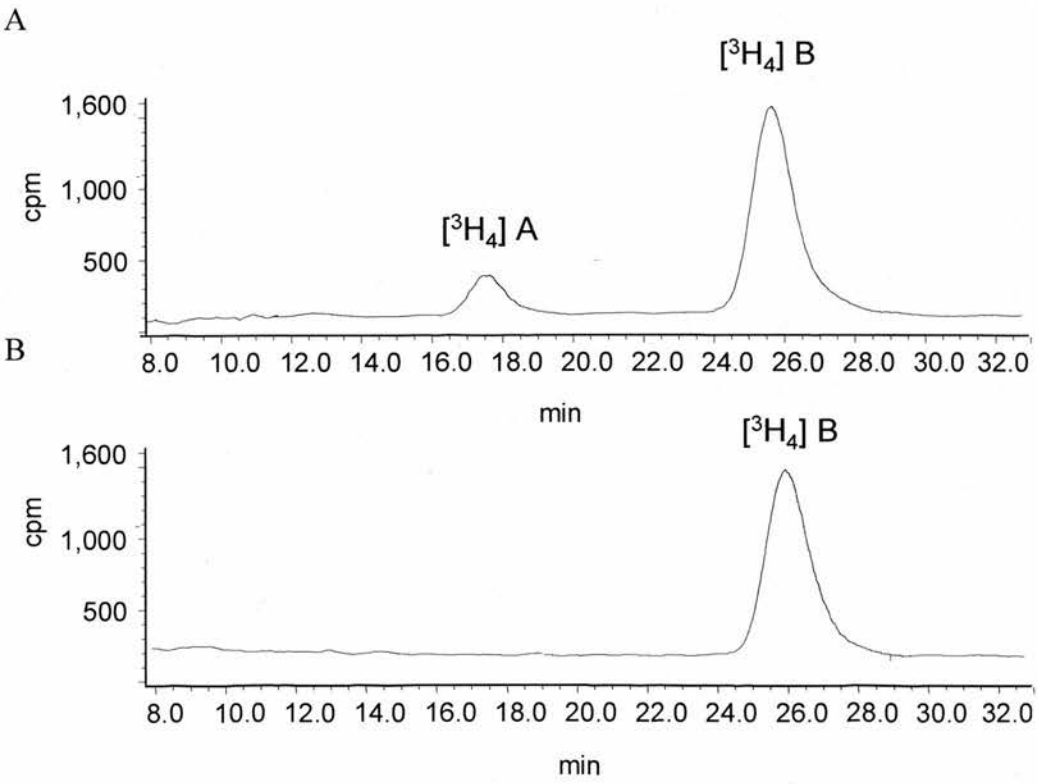

Figure 3.1 Radiochromatograms demonstrating peaks corresponding to $[^3H]_4$ B (Rt 25.9 mins) and $[^3H]_4$ A (Rt 17.5 mins) (A). Products were not are detected in control samples lacking protein (B).

3.4.1.2 Time course of 11β-HSD1 dehydrogenase activity

A study of the time course conversion of $[^3H]_4$ B to $[^3H]_4$ A catalysed by 11β-HSD1 is shown in Figure 3.2. During the initial phase of an enzymatic reaction the reaction proceeds by first order kinetics where velocity is directly proportional to time. Based on this study, all subsequent assays were preformed using 100μg/ml protein with an incubation time of 15 minutes.

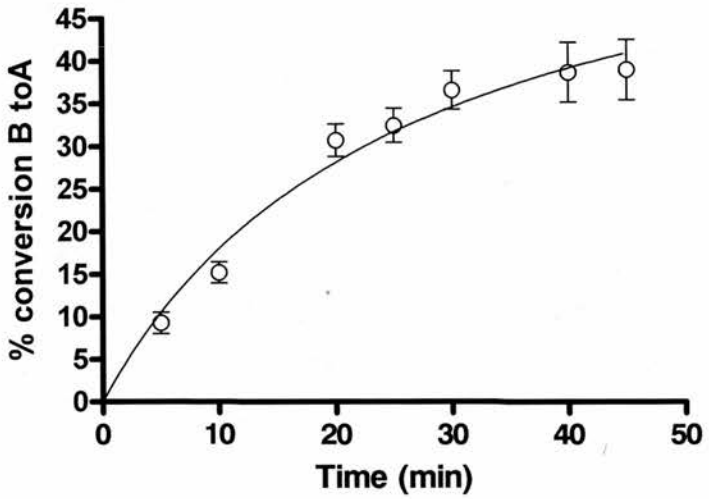

Figure 3.2 Time course of production of $[^3H]_4$ A with time in tissue homogenates. Bioactivity assays were performed in the presence of 100μg/ml protein, co-factor $NADP^+$ and a substrate concentraion of 1μM B. Products were quantified by HPLC as data expressed as the % conversion of $[^3H]_4$ B to $[^3H]_4$ A. Data are mean±SEM, n=6

3.4.1.3 Impact of bile acids on 11β-HSD1 dehydrogenase activity

All bile acids tested inhibited 11β-HSD1 dehydrogenase activity as shown by a dose-dependent reduction in formation of $[^3H]_4$A (Figure 3.3A). Inhibition constants (IC50 values), which represent the concentration of inhibitor which reduces enzyme activity to half that of the maximum, were calculated using Graphpad Prism software. CDCA was the most potent inhibitor of 11β-HSD1 dehydrogenase activity,

with an order of potency CDCA>CA>DCA (Table 3.1). As CDCA was the most potent inhibitor, all subsequent kinetic analysis was performed with this bile acid.

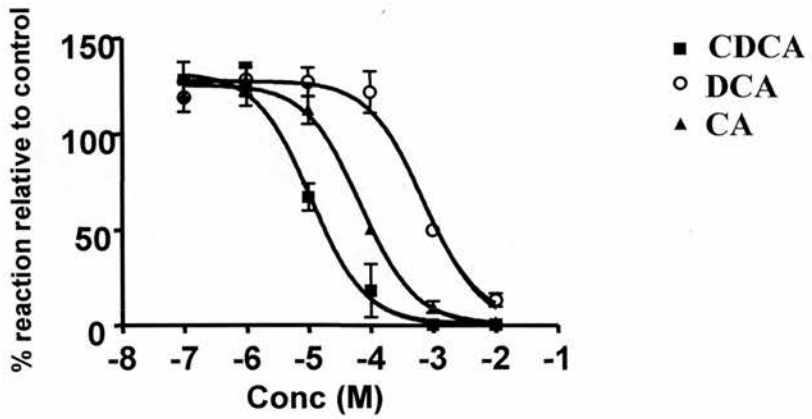

Figure 3.3 A Impact of bile acids on 11β-HSD1 dehydrogenase activity in rat liver homogenates. Chenodeoxycholic acid (CDCA; filled square), cholic acid (CA; filled triangle) and the secondary bile acid deoxycholic acid (DCA; open circle) cause a dose-dependent reduction in 11β-HSD1 dehydrogenase activity in microsomal subfractions isolated from 6 individaul rats. Data are mean; n=6.

	IC50 (μM)
CDCA	22.9±0.1
DCA	784±3.7*
CA	67±1.4*#

Table 3.1 Concentration (IC50) of inhibitor causing 50% inhibition of the rate of the reaction. Data are mean; n=6;*$p<0.05$ *vs* CDCA; $^{\#}p<0.05$ CA *vs* DCA.

3.4.1.4 Impact of bile salts on 11β-HSD1 dehydrogenase activity

Taurine and glycine conjugates of CDCA were equally as potent as the free bile acid (Figure 3.3B; Table 3.2) in inhibitory velocity.

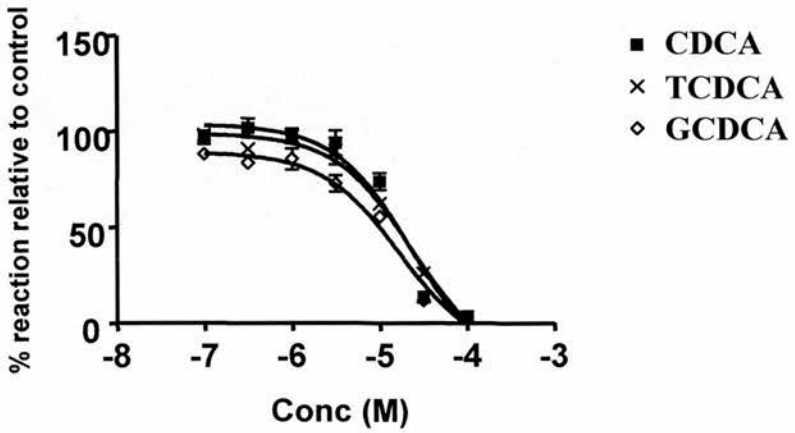

Figure 3.3 B Impact of bile salts on 11β-HSD1 dehydrogenase activity in rat liver homogenates. Glycine (GCDCA; open circle) and taurine (TCDCA; cross) conjugates of CDCA were equally as potent and the free bile acids (CDCA; filled square). Data are mean ± SEM; n=6.

	IC50 (μM)
CDCA	22.9±0.1
GCDCA	16.6±0.1
TCDCA	22.8±0.1

Table 3.2 Concentration (IC50) of inhibitor causing 50% inhibition of the rate of 11β-HSD1 dehydrogenase activity. Data are mean ± SEM; n=6; p=ns.

3.4.1.5 Enzyme kinetics of 11β-HSD1 dehydrogenase activity

Parameters of Km and Vmax were calculated using Michaelis Menten kinetics (Figure 3.4 A).

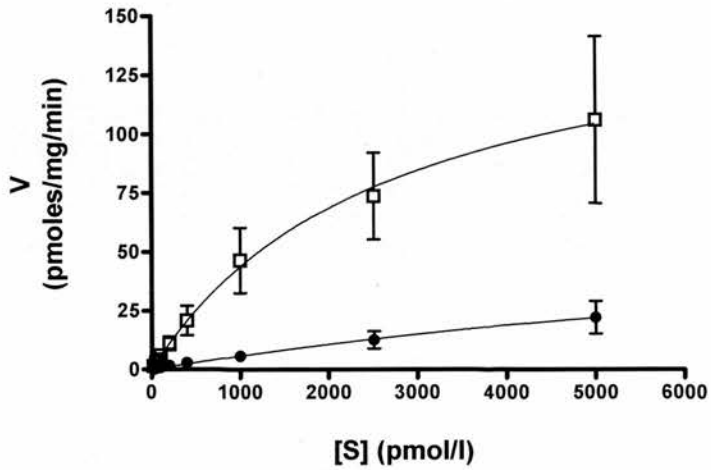

Figure 3.4A Michaelis Menten plot demonstrating inhibition of 11β-HSD1 dehydrogenase activity by CDCA. Data are mean±SEM; n=6; Control (filled circle); CDCA (open square).

Figure 3.4 B illustrates the Lineweaver-Burke double reciprocal plot demonstrating that CDCA acts as competitive inhibitor of enzyme activity

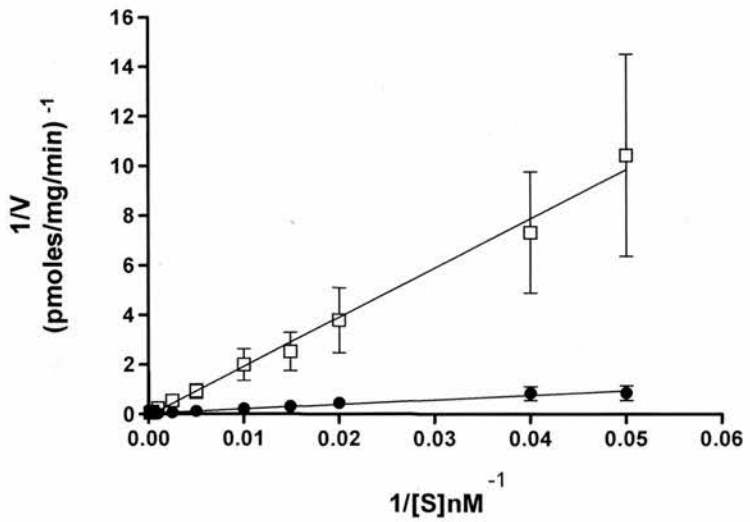

Figure 3.4 B Lineweaver burke plot demonstrating inhibition of 11β-HSD1 by CDCA. CDCA acts as a competitive inhibitor as shown by an increase in Km but not in Vmax. Data are mean ± SEM; n=6; Control (filled circle); CDCA (open square).

Using a global fit model of competitive inhibition, CDCA increased the Km of the reaction but did not alter Vmax (Table 3.3) confirming that CDCA is a competitive inhibitor of 11β-HSD1 dehydrogenase activity.

	11β-HSD1
Vmax (nmoles/mg/hr)	3.6±1.8 v 3.8±1.2
Km (μM)	3.2±1.0 v 12.8±6.1*
Ki (μM)	2.39±0.23
R^2 of curve fit	0.995

Table 3.3 Inhibitory kinetics of CDCA on dehydrogenase activity of 11β-HSD1 measured in rat liver cytosol. CDCA acted as a competitive inhibitor as shown by an increase in Km but not in Vmax. Data are mean ± SEM; n=6; *p<0.05 *vs* Control.

3.4.1.6 Impact of bile acids on 11β-HSD1 reductase activity

Reductase activity of 11β-HSD1 measured in HEK293 cell stably transfected with human 11β-HSD1. Activity assays were preformed using lysates prepared by centrifugation. Reductase activity was significantly reduced in the presence of the primary bile acid chenodeoxcholic acid (CDCA). Inhibition occurred in a dose dependent manner with an IC_{50} value of 3.45μM, (Figure 3.5). Using a global fit model of inhibition, CDCA was a competitive inhibitor of reductase, Ki 3.26±0.34μM.

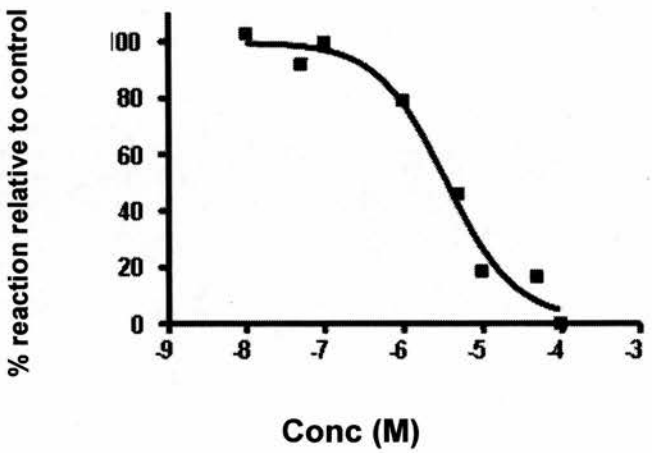

Figure 3.5 Impact of chenodeoxycholic acid (CDCA) on 11β-HSD1 reductase activity. CDCA acted as a potent inhibitor of 11β-HSD1 reductase activity in HEK293 cell lysates in the presence of co-factor $NADP^+$ and a substrate concentraion of 20nM $^3[H_2]$ cortisone. Data are mean±SEM; n=3.

3.4.2 5β-Reductase

3.4.2.1 Chromatography of 5β-reductase

Figure 3.6 A shows representative radiochromatograms of peaks corresponding to $[^3H]_4$B and its 5β-reduced product $[^3H]_4$ 5β-THB. Reaction products were not evident in blank or no co-factor controls (Figure 3.6B).

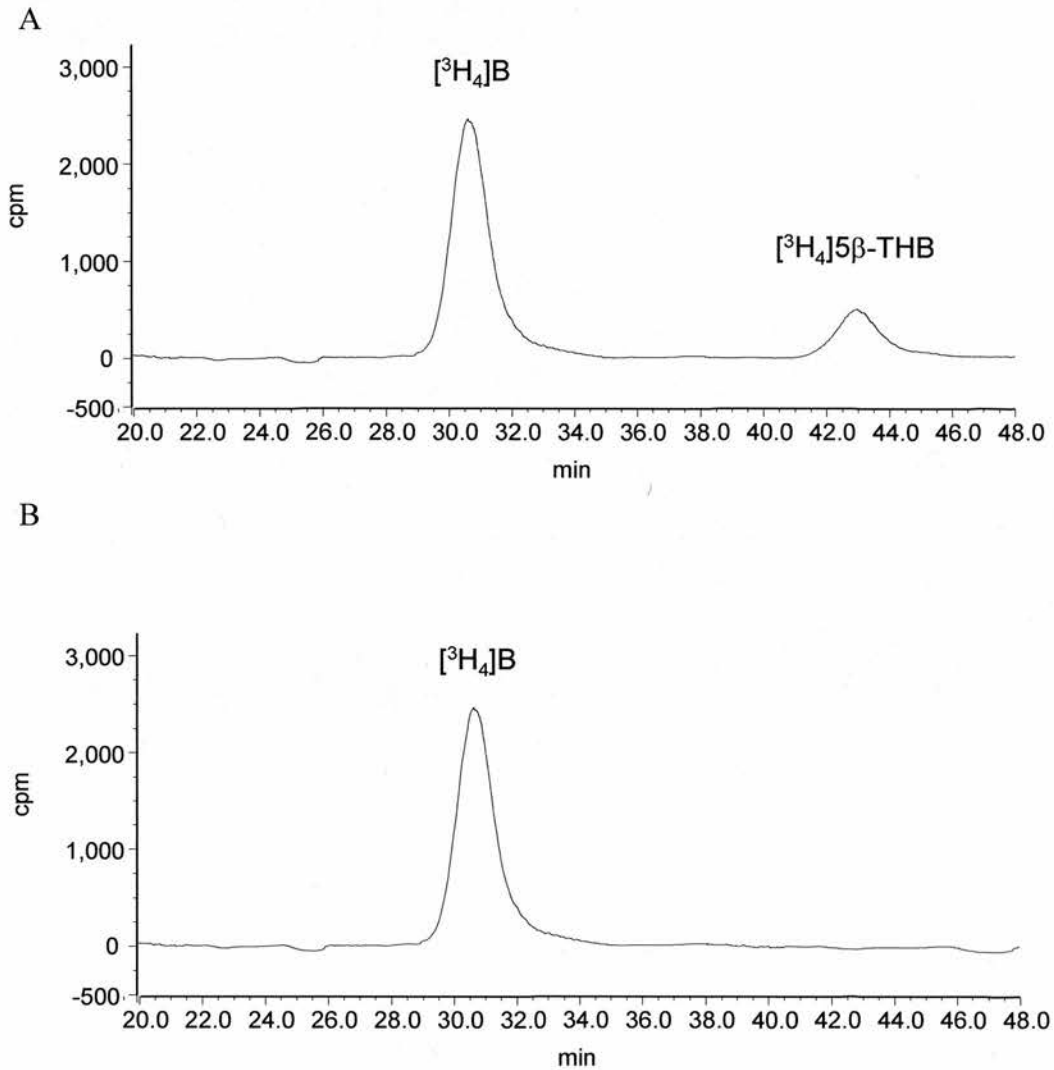

Figure 3.6 Radiochromatograms demonstrating peaks corresponding to $[^3H]_4$B (Rt 30.2 min)and $[^3H]_4$ 5β-THB (Rt 42.5 min). Products were not detected in control samples lacking co-factor NADPH (B).

3.4.2.2 Time course of 5β-reductase activity

Figure 3.7 represents the production of 5β-tetrahydrocorticosterone (5β-THB) from corticosterone (B) in rat liver cytosol with time. For subsequent kinetic studies 100μg/ml protein was used with an incubation time of 4 hr. These conditions ensured that activity was measured during the initial linear phase of the reaction where reaction velocity is directly proportional to protein concentration and time.

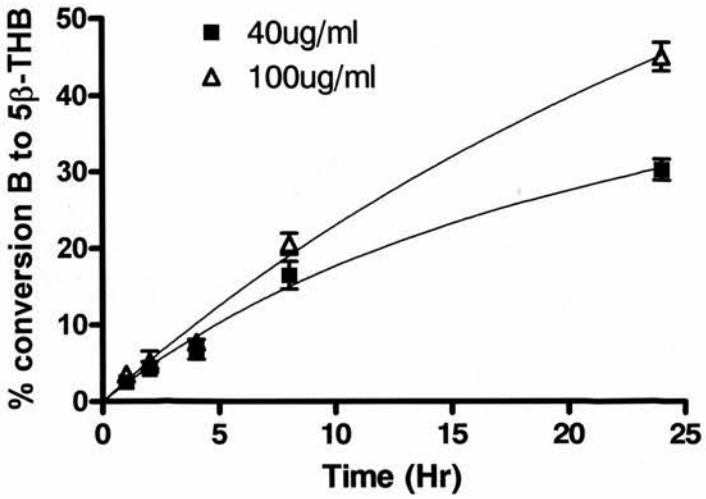

Figure 3.7 Representative time course of production of $[^3H]_4$5β-THB with time. Bioactivity assays were performed in the presence of 100μg/ml protein isolated from 6 animals, co-factor NADPH and 1μM substrate (B) for 4 hr. Activity were quantified by HPLC and data expressed as the % conversion of $[^3H]_4$B to $[^3H]_4$5β-THB. Data are mean±SEM, n=6

3.4.2.3 Impact of bile acids on 5β-reductase activity

The activity of 5β-reductase was significantly reduced in the presence of all bile acids tested (Figure 3.8A). Inhibition occurred in a dose-dependent manner with an order of potency CDCA>DCA>CA. Calculation of the IC50 value for each bile acid confirmed CDCA to be the most potent inhibitor of enzyme activity (Table 3.4).

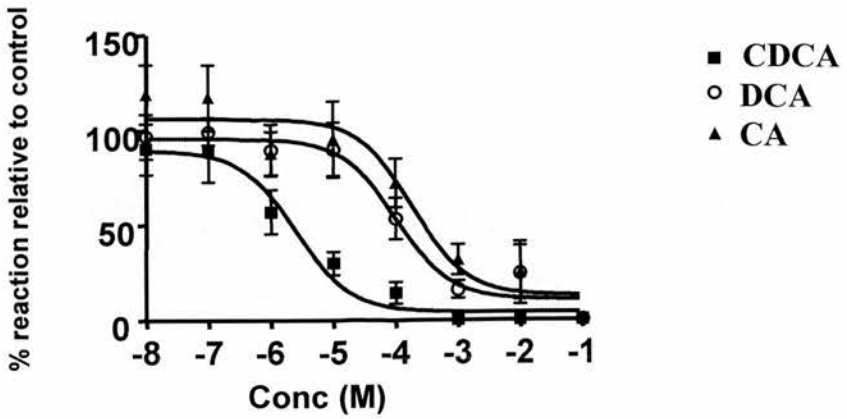

Figure 3.8 A 8A Impact of bile acids on enzyme 5β-reductase activity. Chenodeoxycholic acid (CDCA; filled square), cholic acid (CA; filled triangle) and the secondary bile acid deoxycholic acid (DCA; open circle) caused a dose-dependent reduction in 5β-reductase activity measured in rat liver cytosol isolated from 6 animals per group. Data are mean; n=6.

	IC50 (μM)
CDCA	2.67±0.18
DCA	78.1±1.89*#
CA	665±4.65*

Table 3.4 Concentration (IC50) of inhibitor causing 50% inhibition of the rate of the reaction catalysed by 5β-reductase. Data are mean ± SEM; n=6;*p<0.05 *vs* CDCA; #p<0.05 *vs* DCA.

3.4.2.4 Impact of bile salts on 5β-reductase activity

Conjugation with glycine or taurine did not alter the inhibitory potency of CDCA upon 5β-reductase (Figure 3.8 B; Table 3.5).

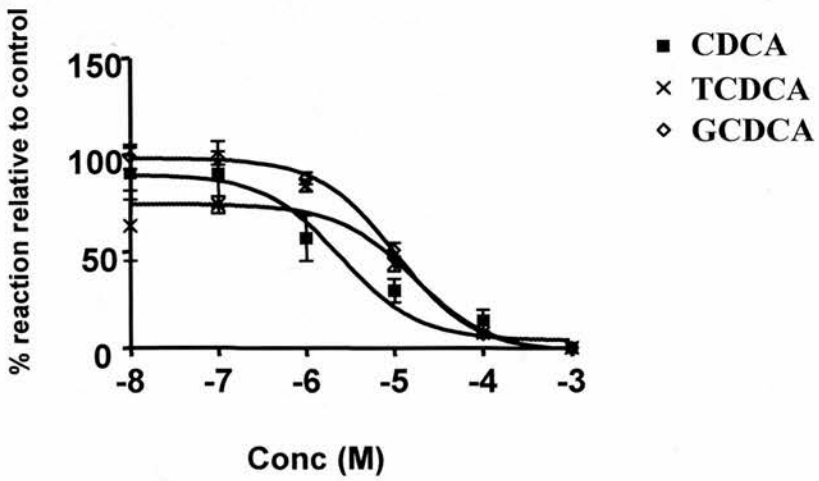

Figure 3.8 B Impact of bile acids and bile salts on 5β-reductase enzyme activity. GCDCA (open circle) and TCDCA (cross) were equally as potent as unconjugated free CDCA (filled square) as inhibitors of 5β-reductase activity. Data are mean ± SEM; n=6.

	IC50 (μM)
CDCA	2.28±0.29
GCDCA	1.66±0.03
TCDCA	2.28±0.29

Table 3.5 Concentration (IC50) of inhibitor causing 50% inhibition of the rate of the reaction ctalysed by 5β-reductase. Data are mean ± SEM; n=6;p=ns.

3.4.2.5 Enzyme kinetics of 5β-reductase

Figure 3.9 demonstrates that CDCA acts as a competitive inhibitor of 5β-reductase activity (Figure 3.9A). Competitive inhibition was confirmed by a global fit model (Figure 3.9B; Table 3.6).

A

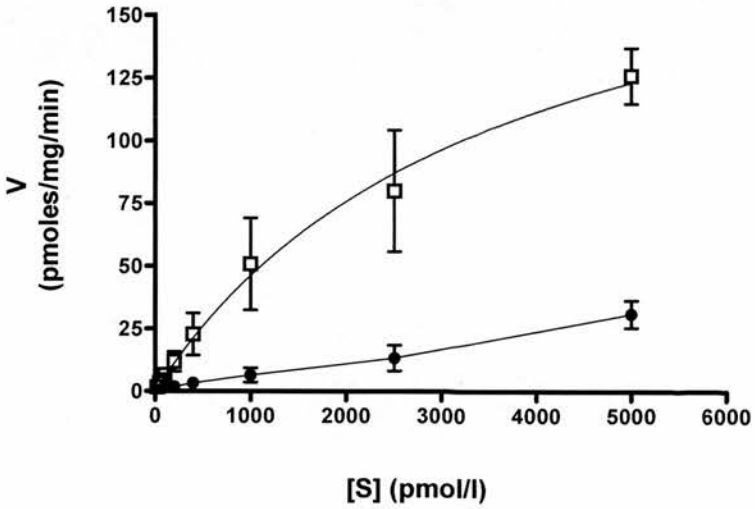

Figure 3.9 A Michaelis Menten plot demonstrating inhibition of 5β-reductase by CDCA. Data are mean ± SEM; n=6

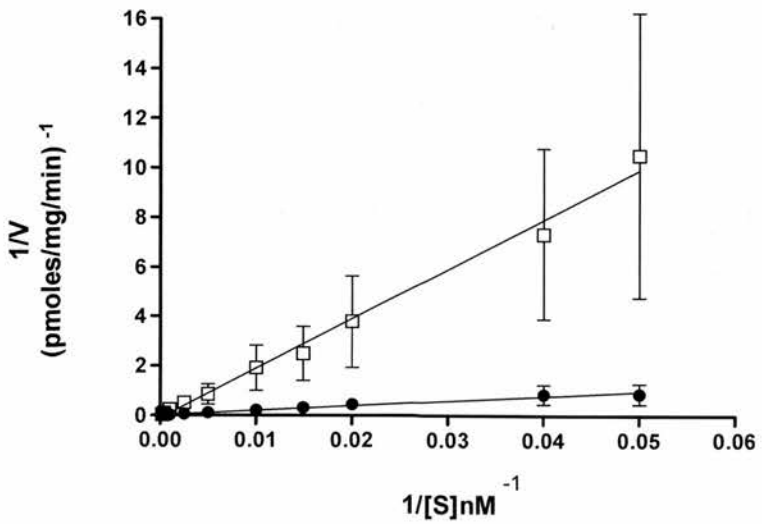

Figure 3.9 B Lineweaver Burke plot demonstrating inhibition of 5β-reductase by CDCA. Data are mean ± SEM; n=6.

Global fit modelling of competitive inhibition from which the inhibitory constant (Ki) could be calculated demonstrated that CDCA acts as a competitive inhibitor of 5β-reductase (Table 3.6).

	5β-reductase
Vmax (nmoles/mg/hr)	27.6±.04 *vs* 15.4±0.8
Km (μM)	10.7±0.8 *vs* 11.9±1.0
Ki (μM)	9.19±0.4
R^2 of curve fit	0.998

Table 3.6 Inhibitory kinetics of CDCA on activity of 5β-reductase. Data are mean±SEM; n=6

3.4.2.6 Impact of 7α-hydroxycholestenone on 5β-reductase activity

7α-Hydroxycholestenone (7α-HCHO) is an intermediate cholesterol metabolite in the catabolic breakdown of cholesterol to bile acids, and a substrate of 5β-reductase. 7α-HCHO did not influence activity of 5β-reductase at any of the concentrations examined (Figure 3.10)

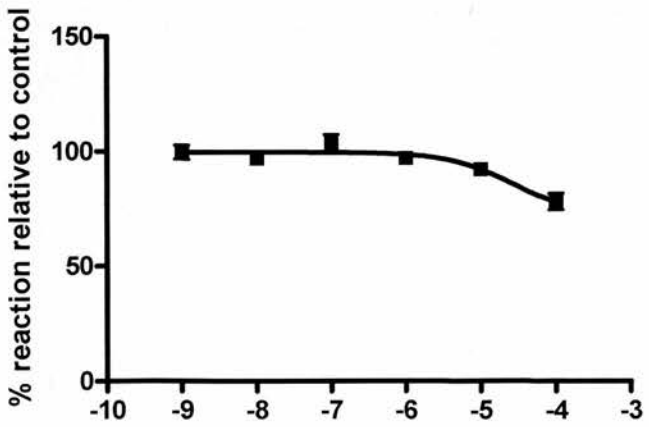

Figure 3.10 Impact of 7αHCOH on activity of steroid 5β-reductase. 5β-reductase activity was determined by measuring the conversion of [$^3H_4$]B to [$^3H_4$]5β-THB in rat liver cytosol in the absence (control) and presence of 7αHCOH . Data are expressed as mean ± SEM; n = 6 per group.

3.4.3 3α-HSD

3.4.3.1 Mass chromatography of 3α-HSD

Figure 3.11 represent a mass chromatogram showing methoxyamine-trimethylsilimizadole (MO-TMS) derivatives of corticosterone (B), the 5α- and 5β-reduced metabolites of corticosterone (5α- and 5β-THB) and the 11α-isomer epi-THB which was used as an internal standard. The stereo epi-isomer is of the same mass as both 5α- and 5β-THB but has a different retention time.

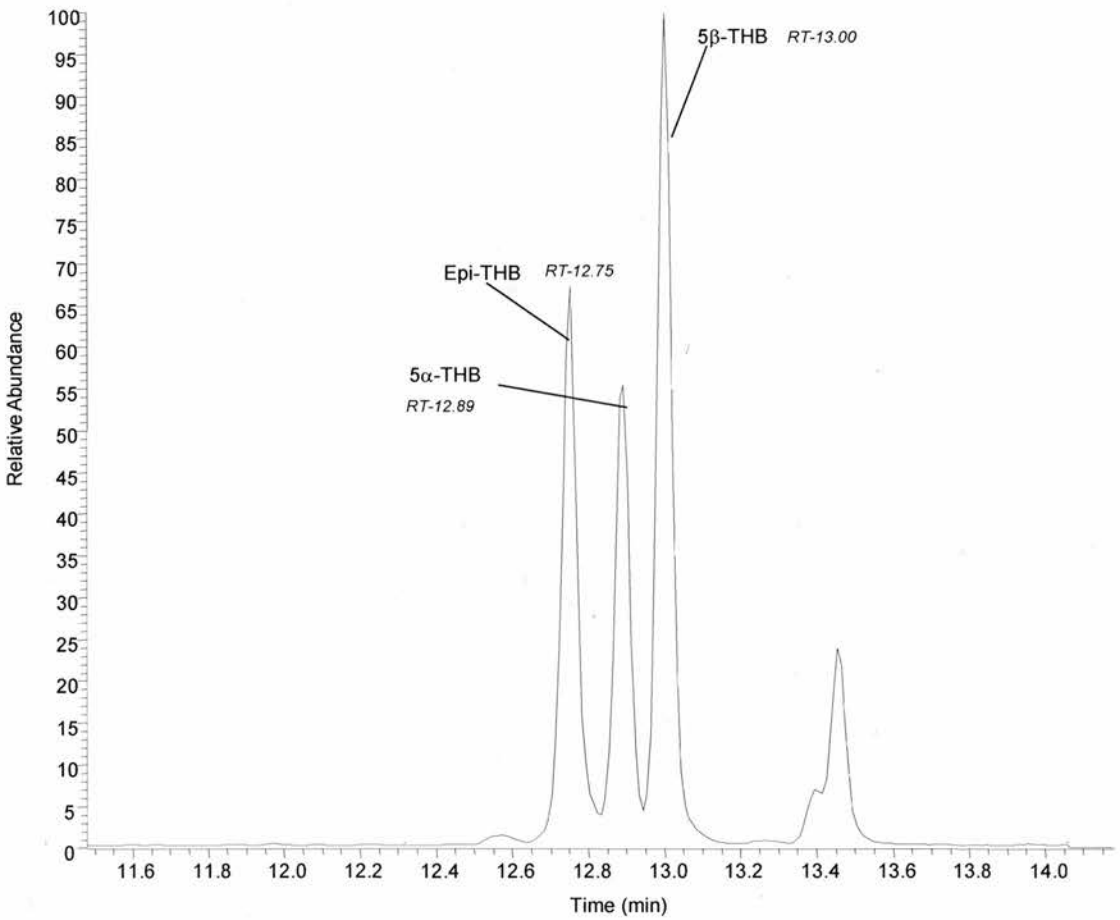

Figure 3.11 Mass chromatogram of methoxyamine-trimethylsilimizadole (MO-TMS) derivatives (m/z 564) 5α- and 5β-reduced corticosterone. 5α-THB = 5α-tetrahydrocorticosterone Rt 12.59 min, 5β-THB =5β-tetrahydrocorticosterone Rt 13.00 min, epi-THB = internal standard Rt 12.75 min. RT = retention time in minutes.

3.4.3.2 Time course of 3α-HSD activity

Figure 3.12 represents the production 5β-THB with time by 3αHSD. Product accumulated in a linear manner in relation to velocity until 40 min when reaction velocity began to plateau indicating that either substrate was becoming depleted or that there was end-product inhibition of the reaction. Conversion was not apparent in the blank and no co-factor controls. As such all subsequent assays were performed using 50μg/ml protein with an incubation time of 20 minutes.

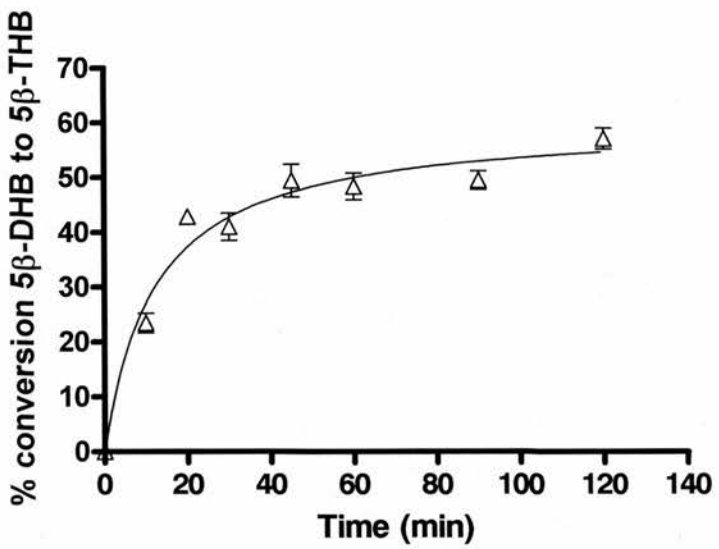

Figure 3.12 Representative time course of production of 5β-THB from 5β-DHB by 3αHSD in rat liver cytosol. Activity assays were performed in the presence of 50μg/ml protein, co-factor NADPH and 1μM 5β-DHB substrate. Products were quantified by GC-MS and data expressed as the % conversion of 5β-DHB to 5β-THB. Data are mean±SEM, n=6 per group

3.4.3.3 Impact of bile acids and bile salts on 3α-HSD activity

The presence of bile acids and bile salts did not influence activity of 3α-HSD alone (Figure 3.13). These findings indicate that the inhibitory potential of bile acids

demonstrated in 3.5 is mediated predominantly through 5β-reductase. As such further kinetic studies were not performed on 3α-HSD alone.

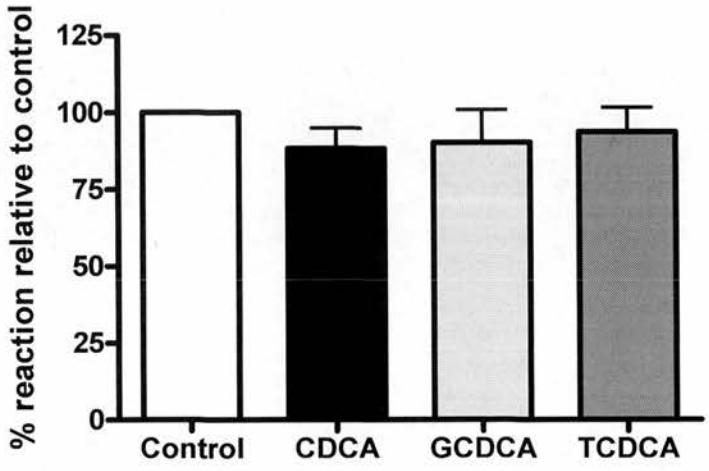

Figure 3.13 Lack of effects of bile acids on activity of 3α-HSD. 5β-DHB (1μM) was incubated with rat liver cytosol in the presence of chenodeoxycholic acid (CDCA), TCDCA and GCDCA (10^{-6}M). 3α-HSD activity was determined by measuring the conversion of 5β-DHB to 5β-THB in the absence (control) and presence of bile acids. Data are expressed as mean ± SEM; n = 6 per group; p=ns.

3.4.4 5α-Reductase 1

3.4.4.1 PCR screening of hepatoma cell lines

Due to the instability of hepatic 5α-reductase 1 activity in disrupted cells *in vitro*, hepatic cell lines (Table 3.7) were screened to identify a hepatoma cell line expressing this gene. All cell lines expressed low levels of 11β-HSD1 and 5β-reductase mRNA, with variable levels of abundance of mRNA of 5α-reductase 1 and 3α-HSD (Table 3.7). The H4IIE cell line, a rat hepatoma cell line expressed highest levels of mRNA both of 5α-reductase 1 and 3α-HSD and was used subsequently to assess the impact of bile acids on 5α-reductase 1 activity and gene transcription.

	Species	11β-HSD1	5β-reductase	5α-reductase 1	3α-HSD
H4IIE	rat	+	+	++	+++
2SFAZA	rat	+	+	+	++
HepG2	human	+	+	+	++

Table 3.7 RT-PCR screening of hepatoma cell lines. RNA (1μg) was reverse transcribed and subjected to PCR using specific primer sequences (section 2.11.3)Abundance is expressed semi-quantitatively relative to a liver positive control. +++ = high abundance, ++ = moderate abundance, + = low abundance.

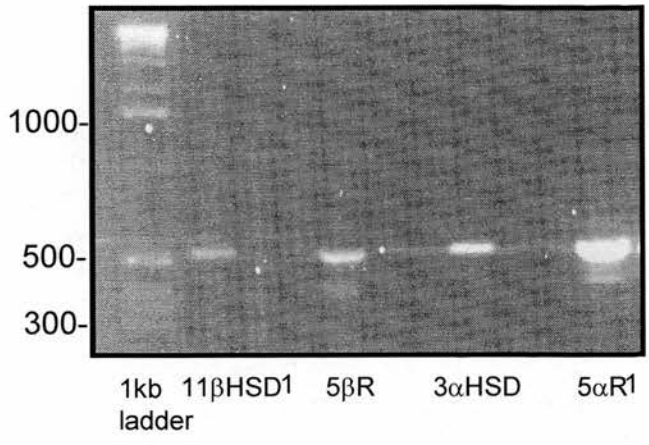

Figure 3.14 RT-PCR gel of enzyme expression in H4IIE cells. RT-PCR was performed on RNA isolated from H4IIE cells to establish presence or absence of enzymes.

3.4.4.2 Time course of 5α-reductase 1 activity in cultured cells

A mass chromatogram demonstrating a peak corresponding to the MO-TMS derivative of 5α-THB with m/z 564 was shown previously in figure 3.11. The activity of 5α-reductase 1, assessed by the velocity of conversion of corticosterone to 5α-tetrahyrocorticosterone (5α-THB), was linear over a 4 hour period with product accumulation directly proportional to time (Figure 3.15). The velocity plateaued at after 8 hours suggesting that either substrate became depleted or there was end product inhibition. A 2 hour incubation period was therefore selected for all subsequent assays

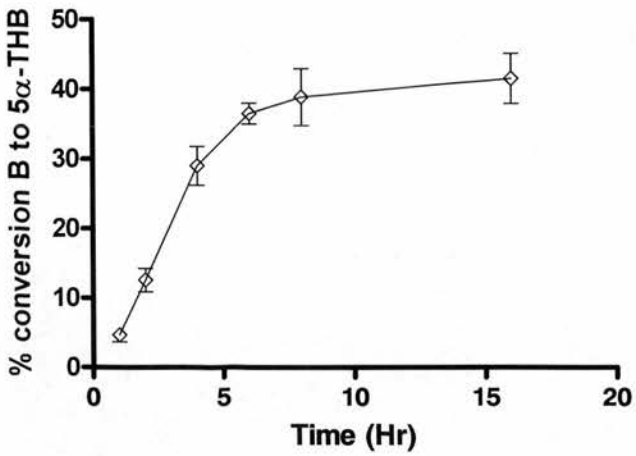

Figure 3.15 Representative time course of production of 5α-THB from B by 5α-reductase 1 and 3αHSD activity in H4IIE cells. Cells were incubated in the presence of corticosterone (1μM). Products were quantified by GC-MS and expressed as the % conversion of B to 5β-THB. Data are mean±SEM of 6 assays performed using cells from 3 independent passages.

3.4.4.3 Impact of bile acids on 5α-reductase 1 activity in cultured cells

Bile acids did not influence the rate of 5α-reduction of corticosterone in H4IIE cells (Figure 3.16).

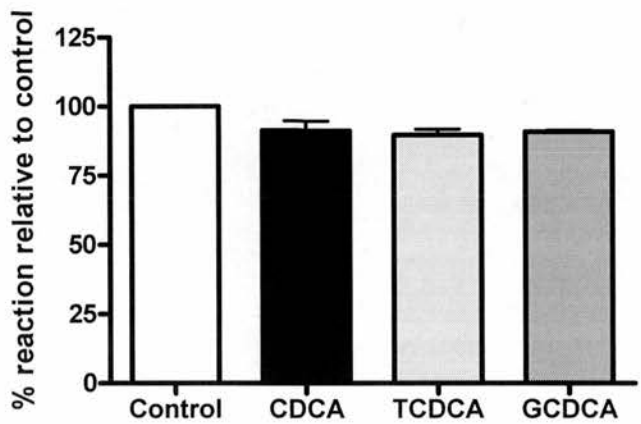

Figure 3.16 Impact of bile acids on 5α-reductase 1 activity in rat hepatoma H4IIE cells. Cells were incubated in the presence of chenodeoxycholic acid (CDCA), glyco-CDCA (GCDCA) and tauro-CDCA (TCDCA) (100μM) and substrate corticosterone (1μM). The conversion of corticosterone to 5α-THB is expressed relative to control (100%). Data are mean±SEM; n=6, p=ns.

3.4.5 Impact of bile acids on gene transcription

The transcription of cholesterol 7α-hydroxylase (CYP7A1) is repressed by bile acids (Chiang 1998). CYP7A1 was therefore used as a positive control. As anticipated CYP7A1 transcript abundance was suppressed in the presence of CDCA and the bile salts (GCDCA and TCDCA)(Figure 3.17). CDCA and glyco- and tauro-conjugates of CDCA did not alter abundance of 5β-reductase (Figure 3.18 A), 5α-reductase 1 (Figure 3.18 B), 11β-HSD1 (Figure 3.18 C) or 3α-HSD (Figure 3.18 D).

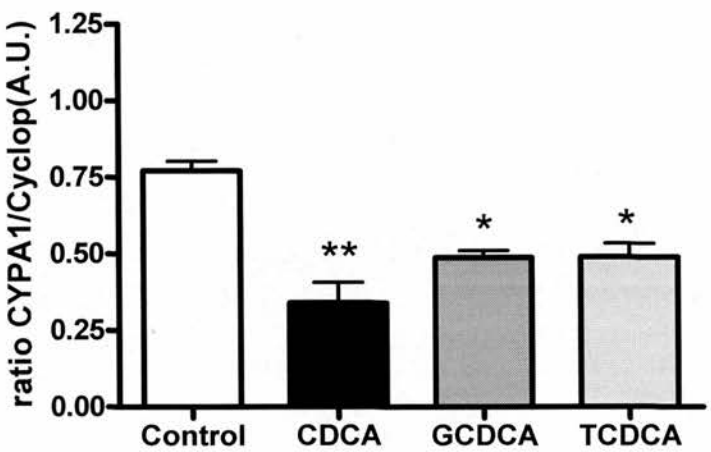

Figure 3.17 Effect of bile acids and bile salts on transcription of CYP7A1. H4IIE cells were incubated in the presence of CDCA, GCDCA and TCDCA (100μM) for 16 hours. The abundance of gene transcript was quantified by Taqman® real time PCR. mRNA abundance is expressed as a ratio to the house keeping gene cyclophilin A. Values are Mean±SEM. Each experiment was performed in triplicate.*p<0.05; **p<0.01 *vs* Control.

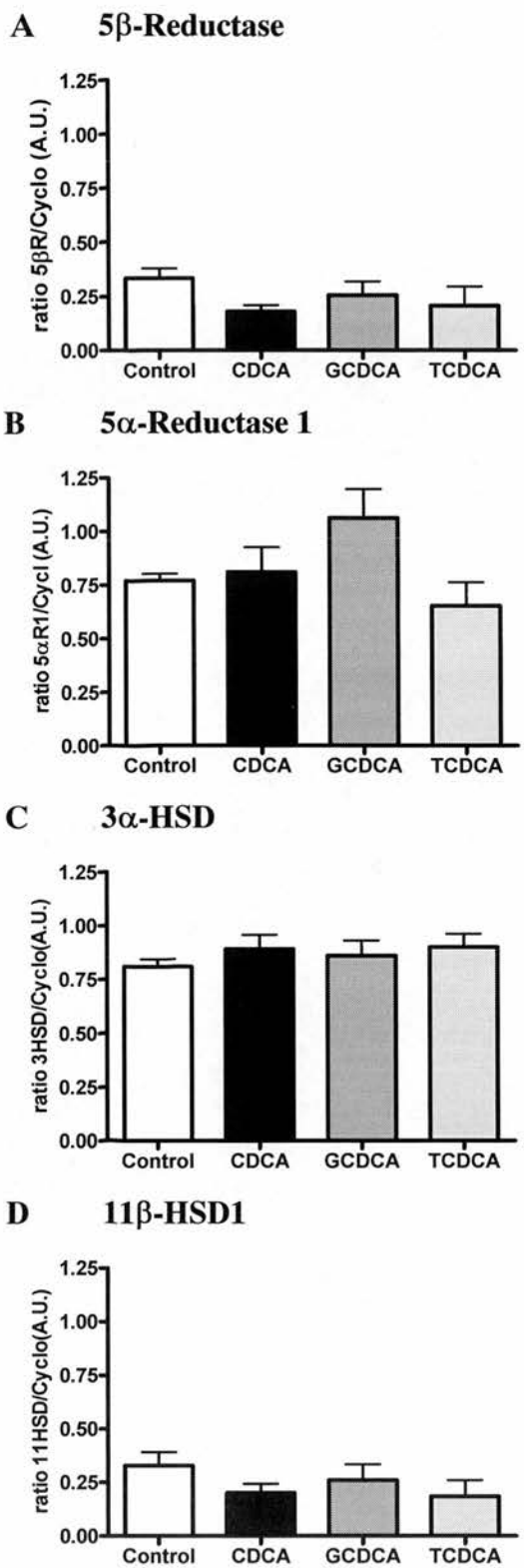

Figure 3.18 Lack of effect of bile acids and bile salts on transcription of 5β-reductase (**A**), 5α-reductase 1 (**B**), 3α-HSD (**C**) and 11β-HSD1 (**D**) mRNA. H4IIE cells were incubated in the presence of CDCA, GCDCA and TCDCA (100μM) for 16 hours. The abundance of gene transcript was quantified by Taqman® real time PCR. mRNA abundance is expressed as a ratio to the house keeping gene cyclophilin A. Values are Mean±SEM. Each experiment was performed in triplicate.

3.5 Discussion

In this chapter, data are presented showing that the primary bile acids CDCA and CA and the secondary bile acid DCA are competitive inhibitors of the glucocorticoid metabolising enzymes, 5β-reductase and 11β-HSD1 dehydrogenase in hepatic tissue homogenates and of 11β-HSD1 reductase in cell lysates. Conjugation of the most potent inhibitor CDCA with glycine or taurine did not alter the inhibitory potency of CDCA. In contrast to our finding with 5β-reductase and 11β-HSD1, bile acids did not inhibit 5α-reductase 1 activity in cultured cells or 3α-HSD activity in tissue homogenates. Enzyme inhibition occurred at a post-transcriptional level as bile acids, both free and conjugated did not reduce transcript abundance of 5β-reductase, 5α-reductase, 3α-HSD or 11β-HSD1.

Chenodeoxycholic acid possesses a 3α,5β-ring A steroidal configuration similar to other known competitive inhibitors of 11β–HSD1 including glycyrrhetinic acid (GA)(Monder *et al.* 1989; Morris *et al.* 1992) and carbenoxolone (CBX)(Andrews *et al.* 2003; Livingstone & Walker 2003). The competitive inhibition of 11β-HSD1 exerted by bile acids is therefore as predicted. A key catalytic residue motif, Y-S-A-S-K is present within the core structure of 11β-HSD1 and the crystal structure of human 11β-HSD1 has recently been reported (Hosfield *et al.* 2005).This motif along with the recently identified essential interactions between Asn-111 and the active site residues are highly conserved across the Short Chain Dehydrogenase Reductase (SDR) family of enzymes to which 11β-HSD1 belongs (Obeyesekere *et al.* 1998). These highly conserved residues play a fundamental role in maintenance of the active site configuration by orientating the substrate/inhibitor within the active site, and catalysing proton transfer to and from reduced and oxidised reaction intermediates (Shafqat *et al.* 2003). Site-directed mutagenesis of residues within the active site of the enzyme diminishes enzyme activity (Obeyesekere *et al.* 1998). The *cis*-orientated A/B ring juncture of CDCA also gives the molecule flexibility in a similar manner to the steroidal detergent CHAPS (Lakshmi & Monder 1985b). Studies have demonstrated that this detergent is accommodated within the active site of 11β-HSD1 via its A-ring which is localised to the catalytic region of the enzyme. This is the opposite conformation to

glucocorticoids in which the D-ring penetrates the active site of the enzyme suggesting that bile acids may bind in the reverse orientation to the natural ligand within the active site of the enzyme in similar manner to that demonstrated between ursodeoxycholic acid and 3α-HSD (Jin *et al.* 2001).

The inhibitory potency of CDCA has also been reported by Lakshmi and Monder 1985, who utilised the detergent like properties of bile acids to disrupt lipid membranes and purify 11β-HSD1 protein (Lakshmi & Monder 1985a). The latency observed in Figure 3.3A where enzyme activity was above control levels in the presence of low concentrations of bile acids prior to inhibition is similar to that described for 11β-HSD oxidase activity on disruption of the lipid environment (Lakshmi & Monder 1985a). CDCA, one of the two primary acids and the most prevalent in the rat, was the most potent inhibitor of 11β-HSD1 inhibiting both dehydrogenase and reductase activity of 11β-HSD1 with equal potency. It is unlikely that these effects are due to the detergent properties of bile acids as CDCA was significantly more potent that either CA or DCA. Using a global fit model, CDCA was a competitive inhibitor of 11β–HSD1 (dehydrogenase and reductase activity).

In similar manner to 11β-HSD1, bile acids acted as potent competitive inhibitors of 5β-reductase, a member of the AKR superfamily (AKR1D). Although very little is known about this enzyme, limited data have shown that bile acids can act as inhibitors of 5β-reduction of aldosterone (Latif *et al.* 1990) with the same order of potency for inhibition of 5β-reductase (CDCA<DCA<CA) as demonstrated for glucocorticoids here. In addition, recent purification and protein modelling of rat 3α-HSD (AKR1C9) may provide some insight into the nature of the binding pocket and catalysis of this enzyme and other associated enzymes (Jez *et al.* 1996). Rat liver 3α-HSD (AKR1C9) is highly homologous to steroid 5β-reductase. Indeed a single point mutation (H117E) within a conserved catalytic tetrad (Tyr55, Lys84, His117 and Asp50)(Bennett *et al.* 1997) of AKR1C9 introduces 5β-reductase activity (Jez & Penning 1998a), suggesting the two genes are the result of divergent evolution. One may anticipate that bile acids interact with 5β-reductase in a similar manner. The binding pocket of AKR1C9 has been modelled by crystaling with ursodeoxycholate. This bile acid binds backwards relative to testosterone in the binding pocket of

AKR1C9 with the A-rings of the two steroids at the opposite end of the pocket (Jin *et al.* 2001). Interaction between the catalytic tetrad of 5β-reductase and the carboxylate moiety of the bile acids may account for the inhibition of enzyme activity seen *in vitro*. In addition, if the A-ring is involved in inhibition (Jin *et al.* 2001) it is understandable why conjugation with either glycine or taurine via an amide bond at position 24 of the D-ring did not impact upon the inhibitory potential of the bile acids as, this should be extruded from the active site of the enzyme.

Rat 3α-HSD/DD (AKR1C9) is the single dominant species of 3α-HSD/DD mRNA present in the rat liver (Lin *et al.* 1999) and has 67% sequence identity at the protein level with the four human isoforms of 3α-HSD. AKR1C9 is frequently used as model for the human AKR1C subfamily (Pawlowski *et al.* 1991). Indeed, AKR1C1 represents the human orthologue of rat AKR1C9. AKR1C2 (3αHSDIII) is a bile acid binding protein and the protein structure has been determined by crystallography with UDCA (Jez & Penning 1998b; Jin *et al.* 2001). Co-factor and substrate bind two distinct highly conserved active sites within the protein with the nicotinamide moiety of the co-factor positioned at the core of the (α/β)8 barrel and the carboxylate moiety of the bile acid anchored deeply in the core active site of the protein by interactions between Tyr55 and His117 (Penning *et al.* 2004). These residues along with Lys84 and Asp50 form a catalytic tetrad which acts as a "proton-relay" in which Tyr55 acts as a general acid/base catalyst (Schlegel *et al.* 1998). Despite these similarities, by comparing the steroid binding pockets of AKR1C2 and AKR1C9 one sees that AKR1C2 possess a relatively large substrate channel allowing the steroid a degree of freedom to occupy several different orientations within the active site of the enzyme, whilst still maintaining contact with the hydrophobic residues which line the binding pocket. In contrast, the steroid binding cavity of AKR1C9 appears to limit the entry of substrates, which may therefore restrict interaction between inhibitor and enzyme (Jin *et al.* 2001). Indeed, the position in AKR1C9 corresponding to the oxyanion hole formed by the tetrad of AKR1C2 into which ursodeoxycholate binds is occupied by the C3 ketone of testosterone in the AKR1C9 complex (Heredia *et al.* 2003) suggesting different moieties may be involved in steroid and bile acid interaction within the rat and human isosforms, perhaps explaining the lack of inhibition observed. The lack of

inhibition may also be related to a difference in one of the key amino acid residues within the catalytic tetrad (Tyr24, Val54 and Trp227), highly conserved in the AKR superfamily and thought to be essential for catalytic efficiency of AKR1C9 (Jin *et al.* 2001). In the rat enzyme, position 54 is a Leu rather than the Val in human AKR1C2. The position of Val54 appears to be critical for this inhibition and is thought to partially explain the functional differences between AKR1C1 and AKR1C2 (Matsuura *et al.* 1997) and along with Tyr24 and Trp227 plays a crucial role in the binding of UDCA within the oxyanion hole of AKR1C2. It is therefore possible that the amino acid substitution may explain why rat 3αHSD is not inhibited by bile acids and also suggests that the human orthologue AKR1C1 may not be inhibited.

5β-Reductase catalyses the rate determining step in the dual reduction of glucocorticoids to their 5β-tetrahydro metabolites. All members of the AKR superfamily follow a sequential ordered bi-bi mechanism in which co-factor binds first and leaves last (Penning 1999). Although the binding and release of co-factor are thought to be the rate determining steps for overall catalysis of aldehyde and aldose reductase reactions (Grimshaw *et al.* 1995), AKR1C2 and AKR1C9 lack a salt-link "safety-belt" which is present in members of the aldehyde reductase (AKR1A) and aldose reductase (AKR1B) subfamilies (Jin *et al.* 2001). As such, the conformational changes associated with co-factor binding may be only partially rate-determining. Furthermore, as bile acids were shown to act as competitive inhibitors of enzyme activity, it is unlikely that co-factor binding will interfere with substrate binding. Alternatively, it is possible that 3α-HSD has a higher affinity for the substrate 5β-DHB than for bile acids. In support of this, activity of 3α-HSD was 16 fold faster than that of 5β-reductase in tissue homogenates, with standard assay times of 15 minutes and 4 hours respectively. Conversion of 5β-DHB to 5β-THB and a rapid on-off time of substrate/enzyme may therefore limit access of bile acid to the active site of the enzyme.

Due to the instability of 5α-reductase 1 in hepatic tissue preparations (Eicheler *et al.* 1995), the activity of 5α-reductase activity was assessed in the H4IIE hepatoma cell line which expressed only the type 1 isozyme in keeping with rat liver. Although 5β-reductase was also expressed within this cell line its abundance was much less. One may have anticipated a compensatory up-regulation in the velocity of

5α-reductase 1 in the presence of more substrate due to inhibition of 5β-reductase. However it is hard to interpret this interaction with such stark differences in abundance in this cell line. These differences were demonstrated by cell based activity assays where only 4% corticosterone was metabolised by 5β-reductase within a 24 hour period (data not shown), whilst nearly 40% corticosterone had been reduced by 5α-reductase 1 within the same time span.

In cultured cells it was also possible to investigate the impact of bile acids on transcription of the 11β-HSD1, 5α- and 5β-reductase 1 and 3α-HSD. Several enzymes involved in the catabolism of cholesterol to bile acids including CYP7A1 and CYP8B1 are regulated at the level of gene transcription by bile acids (Chiang 1998). In support of this, CYP7A1 mRNA abundance was significantly reduced in H4IIE cells treated with CDCA indicating that the bile acid transporters are present within this cell line. Despite this, transcript abundance of 5β-reductase, 5α-reductase 1, 3α-HSD or 11β-HSD1 were not altered following bile acid treatment. In recent years, bile acids have been identified as endogenous ligands for several nuclear hormone receptors including the liver X receptor α (LXRα;NR1H3)(Willy *et al.* 1995) and the farnesoid X receptor (FXR;NR1H4) (Forman *et al.* 1995). Several bile acids including CDCA and its glycine and taurine conjugates bind and activate FXR at physiologic concentrations (Malerod *et al.* 2005; Miyata *et al.* 2005). Moreover, Makishima *et al* 1999 demonstrated that the rank order in which bile acids activate FXR correlates with the repression of CYP7A1 in a hepatocyte-derived cell line with CDCA being significantly more potent than DCA, CA or the tertiary bile acid lithocholic acid (LCA)(Makishima *et al.* 1999). These findings indicate that FXR plays a key role in the negative effect of bile acids on gene expression. Although FXR response elements (FXRE's) have been identified in the promoter regions of both mouse and human forms of the intestinal bile-acid binding protein (I-BABP) which is stimulated by bile acids, these elements were not identified in the promoter region of CYP7A1 (Landrier *et al.* 2003). It has now been demonstrated that bile acids exert their inhibitory effects on CYP7A1 gene expression via indirect mechanism. FXR regulates the expression of small heterodimer partner 1 (SHP-1), an atypical orphan member of the nuclear receptor which lacks a functional DNA binding domain. SHP-1 interacts and represses the transcriptional activities of other

nuclear receptors including the liver receptor homolog 1 (LRH-1; NR5A2), an orphan receptor that binds as a monomer to response elements within the promoter of CYP7A1 inducing transcription (Goodwin B *et al.* 2000). A potential FXR response element has been identified within the up-stream promoter (-15 to +30) of 5β-reductase (unpublished data, O'Flaherty 2006). Recent data would suggest that this response element is expressed at low levels in 5β-reductase, as use of the specific FXR agonist GW4064 at high concentrations was required inorder to induce activation.

Thus bile acids inhibit the activity of glucocorticoid metabolising enzymes as competitive inhibitors at a post transcriptional level. The findings in this chapter would suggest that direct interaction with the functional protein preventing interaction of substrate within the active site of the enzyme is the most likely explanation for the enzyme inhibition. The data presented in this chapter however is performed using two different *in vitro* systems and therefore it is inappropriate to extrapolate these findings to an *in vivo* system where a myriad of factors may influence enzyme activity and expression. It is therefore essential to study the effects of bile acids on glucocorticoid metabolism in an *in vivo* model such as the rat.

Chapter 4

Effect of increased concentrations of bile acids on glucocorticoid metabolism and HPA axis activation *in vivo*

4.1 Introduction

Bile acids represent the predominant means of eliminating excess cholesterol from the body and play an essential role in facilitating the absorption, transportation and elimination of lipid soluble vitamins and dietary fats (Chiang 1998). In excess however, bile acids can be highly cytotoxic leading to progressive liver disease. Bile acid levels within the circulation are under feed-forward and feed-back control resulting in the induction of genes involved in their detoxification and /or elimination e.g. cytochrome P4503A (CYP3A) and suppression of those involved bile acid biosynthesis e.g. CYP7A1. In addition, bile acids act as signaling molecules and play a pivotal role in regulating cholesterol homeostasis in mammals (Parks *et al.* 1999). Bile acids and oxysterols derived from cholesterol act as potent agonists for the nuclear receptors FXR and LXR respectively thus regulating bile acid, cholesterol and triglyceride metabolism in order to maintain lipid homeostasis (Lu *et al.* 2000; Repa & Mangelsdorf 1999).

In Chapter 3, bile acids and bile salts were shown to act as competitive inhibitors of 5β-reductase an enzyme involved in cholesterol catabolism and glucocorticoid metabolism, and also of 11β-HSD1 (reductase and dehydrogenase) in tissue sub-fractions. However, these studies were preformed *in vitro* and therefore do not address potential interactions with factors within the surrounding physiological environment which can have profound effects upon enzyme activity. In this Chapter experiments were performed to test the hypothesis that bile acids inhibit the activity of hepatic glucocorticoid metabolism *in vivo.* Alterations in glucocorticoid metabolism influence HPA axis activation (Harris *et al* 2001) and the regulation of hepatic homeostatic pathways regulated by glucocorticoids e.g. TAT and PEPCK. Enhanced glucocorticoid clearance by the A-ring reductase in obese humans and rodent models of obesity are thought to induce compensatory activation of the HPA axis (Rask *et al.* 2001; Livingstone *et al.* 2000).

Two approaches were used to increase bile acids levels in a rodent model. The first approach was to increase the bile acid pool via the administration of a diet supplemented with the exogenous bile acid CDCA. This method has been used previously to increase hepatic bile acid concentrations (Gustafsson *et al.* 1981). Several studies have demonstrated that this treatment was associated with

suppression of enzymes involved in bile acid biosynthesis and up-regulation of those involved in bile acid detoxification and elimination (Stroup *et al.* 1997a).

In the second approach, bile acid synthesis was increased by administration of a diet supplemented with the bile acid binding resin cholestyramine. Cholestyramine sequesters bile acids within the ileum thus reducing bile acid levels within the enterohepatic circulation and stimulating cholesterol catabolism and bile acid biosynthesis. Several investigators have reported an increase in enzyme activity and bile acid synthesis following dietary administration of cholestyramine (Fukushima *et al.* 1995; Pandak *et al.* 1994). Following these treatments the impact of elevated bile acid concentrations on glucocorticoid metabolism and HPA axis activation *in vivo* was investigated.

4.2 Research aims

The aims of the research in this chapter were:

1. To investigate the effect of elevated levels of bile acids following administration of CDCA and of increased bile acid synthesis following administration of a bile acid sequesterant cholestyramine on pathways of glucocorticoid metabolism *in vivo.*
2. To assess the effect of each diet on HPA axis activation
3. To assess the effect of each diet on glucocorticoid responsive pathways within the liver.

4.3 Methods and method development

4.3.1 Animals

Male Wistar rats (3-4 weeks; Harlan Orlac, Bicester UK) were maintained as described in section 2.3.1. Animals were matched for age and weight and allocated into three groups of eight. Control group received standard rat chow. A second group received standard rat chow supplemented with chenodeoxycholic acid (CDCA; 1% w/w) and a third group received standard rat chow supplemented with cholestyramine (CT; 5% w/w). Animals were housed singly and maintained on their respective diets for 4 weeks. Body weight, food and fluid intake were recorded on a daily basis.

4.3.2 Administration of diet

Standard rat chow was ground manually using a hand rotor creating a fine powder. CDCA or cholestyramine were mixed with the powdered chow each day. Control animals received powdered chow alone. Each day animals received chow (approximately 50g) in glass containers which were placed in shallow metal tins to catch chow dropped or spilled by the animal during feeding. Each morning (approximately 0800h), rats received a fresh pot of chow and any food left from the previous day collected, separated from any debris e.g. saw dust or faeces by sifting through a tea-strainer and weighed. Fluid intake was recorded daily.

4.3.3 Restraint stress

An acute restraint stress test was performed to assess changes in HPA axis activation. Rats were handled for approximately 5 minutes between 0700 and 0800 hrs for 7 days prior to initiation of the test to obtain low basal corticosterone levels. On the day of the experiment, blood was obtained by tail venesection into EDTA-microtubes, and the rats were immediately placed in restraint tubes for 20 minutes. After the 20 minute stressor, a second blood sample was taken as above and the animals were placed back into their original cages where they were allowed free

access to food and water. Further blood samples were taken by tail venesection at 20, 40, 60 and 90 mins post stress. All blood samples were collected into EDTA-microtubes and centrifuged (1000g, RT, 10min). The resultant plasma was frozen on dry ice and stored at -80°C.

4.3.4 Metabolic cages

To study food and fluid intake and steroid metabolite excretion rats were housed singly in metabolic cages (Techniplast, Exton, PA.,US). Animals were placed in the cages after 3 weeks on their respective diets where they remained for 6 days. Body weight, food and fluid intake were monitored daily. Faeces and urine were collected over the final 72 hours and stored a -20°C for subsequent analysis. The animals were then placed back into their original cages for a minimum of 1 day prior to sacrifice.

4.3.5 Animal sacrifice and tissue collection

Animals were killed by surgical decapitation and tissue and blood samples collected and stored as described in section 2.3.2.

4.3.6 Analysis of hepatic enzyme activity

Activities of hepatic cytosolic 5β-reductase (substrate conc: 25nM and 2μM) and 3α-HSD (substrate conc: 2μM) and microsomal 11β-HSD1 (substrate conc: 25nM and 2μM) were measured in tissue subfractions as described in sections 2.8.3, 2.8.4 and 2.8.6.

4.3.7 Abundance of transcripts

Transcript abundance of hepatic 5β-reductase, 5α-reductase 1, 3αHSD, 11βHSD1, angiotensinogen, TAT, PEPCK and CYP7A1 were quantified using Taqman® real-time PCR as described in section 2.13.1

4.3.8 **Analysis of plasma hormones and intermediate metabolites**

Plasma corticosterone, insulin and glucose were measured as described in sections 2.4.1, 2.4.5 and 2.6.3.

Plasma cholesterol, HDL cholesterol, triglycerides and non-esterified fatty acids were quantified by dry slide chemistry using a Vitros analyzer. This work was performed by Dr P Ashby, Clinical Biochemistry Department, Western General Hospital, Edinburgh.

4.3.9 Analysis of liver fat intermediates

Hepatic triglyceride and glycogen concentrations were measured in tissue homogenates using Triglyceride reagent and glucose hexokinase reagent respectively as described in sections 2.6.1 and 2.6.2.

4.3.10 Analysis of urinary steroids

Steroids were extracted from aliquots of urine (10ml) collected over a 72hr collection for each animal and derivatised along with epi-corticosterone and epi-tetrahydrocorticosterone as internal standards (described in full in section 2.7). Analysis was performed by GC-MS (section 2.9.2) and data presented as concentrations excreted per animal per 24hr.

4.3.11 Bile acid analysis

Plasma, hepatic and faecal total bile acid concentrations were measured by enzyme-colorometric method using Total bile acid kit (sections 2.5.1, 2.5.2 and 2.5.3).

4.3.12 Histology

Liver morphology was assessed in transverse sections prepared as described in section 2.14.1 and lipid accumulation determined by staining with Oil red O (section 2.14.3)

4.3.13 Statistical analysis

Data were analysed by one-way or repeated measure ANOVA followed by post hoc least squared difference test for all groups. All analysis was performed using Statistica (Version 9) or Graphpad Prism (Version 4). For acute restraint stress, analysis was carried out by measuring area under the curve (AUC) using Kinetica Program (InnaPhase, USA). Individual experiments were conducted in duplicate and data are expressed as mean ± standard error of the mean (SEM). The following nomenclature was used to denote significance *$p<0.05$; **$p<0.01$. In all experiments 8 independent animals were used per group; n=8 unless otherwise stated.

4.4 Results

4.4.1 Effect of CDCA and cholestyramine on physiological parameters

4.4.1.1 Body weight

Baseline body weight of bile acid treated animals was comparable to Control animals. However, cholestyramine (CT) treated animals were significantly heavier than Control and CDCA animals ($p<0.05$; Figure 4.1). The pronounced weight gain of cholestyramine treated animals could be attributed to greater food intake (0.108±0.002 Control; 0.105± 0.002 CDCA; 0.114±0.003 CT g/g body weight; $p<0.05$).

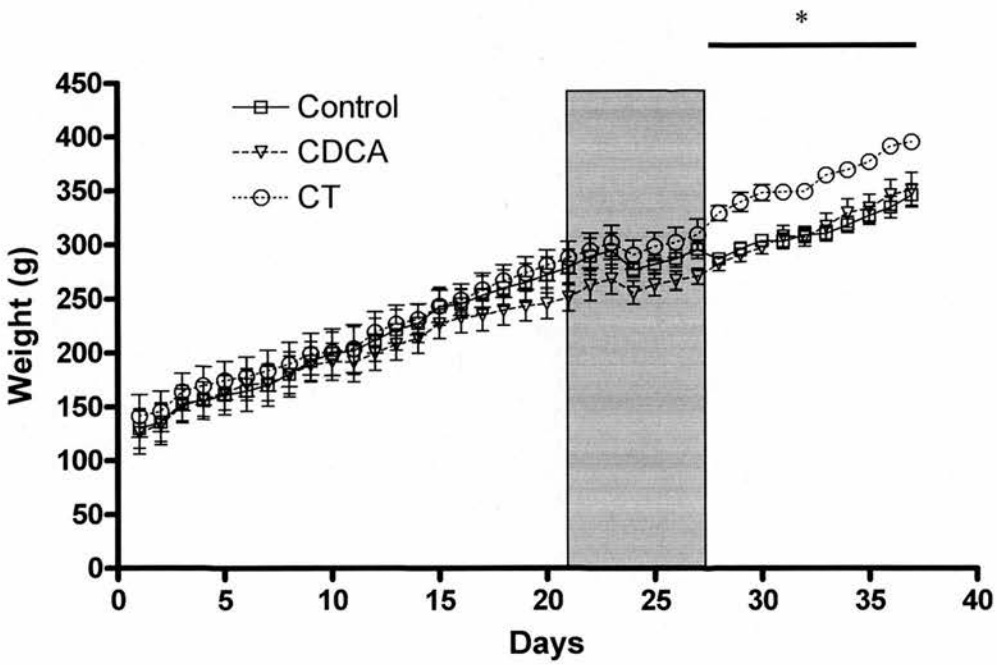

Figure 4.1 Body weight following dietary manipulation. Animals were fed standard chow (Control), chow supplemented with CDCA (1% w/w) or chow supplemented with cholestyramine (CT; 5% w/w) for four weeks and body weight recorded daily. Hatched box = time in metabolic cage. Data are mean±SEM; n=8;*$p<0.05$ Control *vs* CT; CT *vs* CDCA.

4.4.1.2 Organ weight

Animals treated with CDCA but not with cholestyramine had slightly smaller adrenal glands ($p<0.05$, Table 4.1). Thymus and prostate weight were unaltered by either treatment (Table 4.1). Cholestyramine but not CDCA treated animals had smaller livers ($p=0.10$, CDCA; $p<0.05$ CT; Table 4.1) and a reduction in liver glycogen (Table 4.1). Both treatments tended to reduce hepatic triglycerides but this did not reach statistical significance ($p=0.06$, CDCA, $p=0.06$ CT; Table 4.1). Liver histology revealed a marked reduction in lipid accumulation in both treatment groups with fewer, smaller lipid droplets evident in treated livers compared to Control animals (Figure 4.2).

	Control	CDCA	Cholestyramine
Basal body weight (g)	207.5±14	155.8±20*	186.6±18
Body weight change (g)	161.4±7.1	121.9±7.0*	156.9±13.5
Daily food intake (g/g body weight)	0.108±0.002	0.105±0.002	0.114±0.003*
Adrenal weight (mg/g body weight)	0.082±0.006	0.066±0.005*	0.083±0.004
Thymus weight (mg)	0.73±0.04	0.69±0.03	0.73±0.07
Prostate weight (mg/g body weight)	0.83±0.09	0.98±0.13	0.96±0.09
Liver			
Weight (mg/g body weight)	45.3±0.9	43.7±1.06	39.6±1.4*
Glycogen (mg/g)	3.85±0.42	3.44±0.42	2.45±0.32*
Triglycerides (mg/g)	14.7±1.8	10.4±1.5*	10.9±1.3
Cholesterol (mM)	1.89±0.09	2.18±0.11	1.63±0.09
HDL (mM)	1.33±0.08	1.59±0.09*	1.02±0.05*
NEFA (mM)	0.250±0.03	0.275±0.03	0.375±0.04*
Triglycerides (mM)	1.54±0.16	1.25±0.14	1.94±0.23
Plasma (0800h)			
Corticosterone (nM)	78±19	82±26	115±54
ACTH (pg/ml)	27.3±6.3	23.5±5.5	32.6±9.6
Glucose (mg/ml)	8.42+0.73	5.42±0.74*	6.75±0.63
Insulin (ng/ml)	4740±597	2870±577*	3540±357
Bile acids			
Hepatic (μmoles/mg)	38.3±8.89	57.9±8.20	27.7±2.24
Plasma (μM)	28.0±8.75	73.6±15.9*	27.9±4.80
Fecal (μmoles/g)	105.5±0.9	243.3±0.1*	294.9±0.3*
Urine steroids (ng/24hr)			
5β-THB	377±68	213±45*	126±58*
5α-THB	132±32	187±39	107±33
5β-THB:5α-THB	4.15±0.9	1.92±0.5*	0.68±0.03*
Total	508±77	400±47	251±80*

Table 4.1 Changes in physiological parameters following dietary CDCA or cholestyramine. Animals were fed standard chow (Control), chow supplemented with CDCA (1% w/w) or chow supplemented with cholestyramine (CT; 5% w/w) for 4 weeks. Urine and faeces were collected over a 72 hr period and tissues and plasma harvested at cull. Values are mean ±SEM; n=8 per group.

A **Control (x 10)**

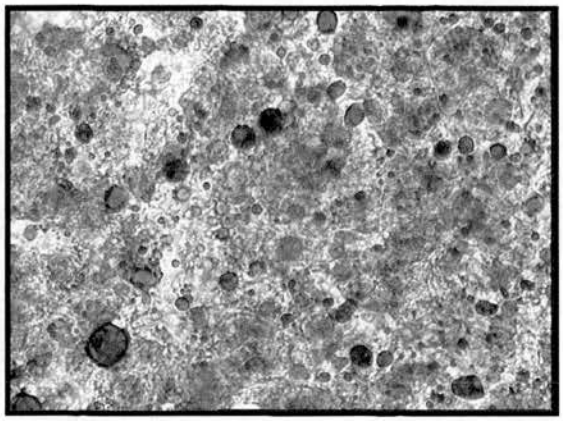

B **CDCA (x 10)**

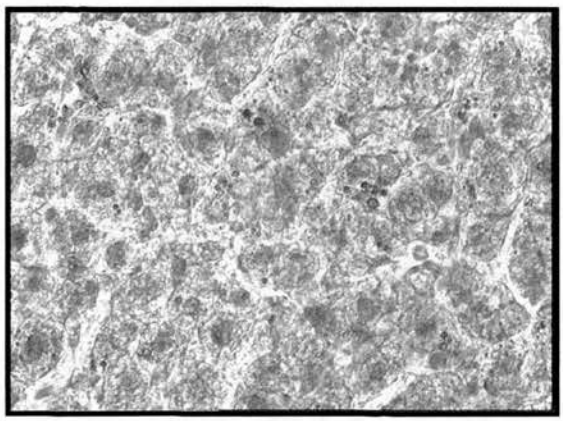

C **Cholestyramine (x 10)**

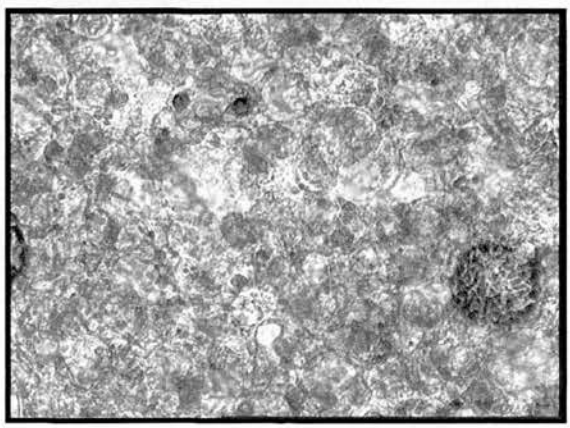

Figure 4.2 Lipid accumulation within the liver following dietary manipulation. Serial transverse sections (30μM) were cut from the liver and stained with stained with the neutral lipid stain Oil red.

4.4.1.3 Bile acids

The total bile acid content of plasma and faeces were significantly elevated following administration of CDCA ($p<0.05$; Table 4.1). Cholestyramine increased bile acid contents of faecal matter ($p<0.05$) but not that of plasma or liver tissue (Table 4.1). Transcript abundance of CYP7A1, the rate determining enzyme in the Classical pathway of bile acid biosynthesis was suppressed following treatment with CDCA and up-regulated following treatment with cholestyramine (Figure 4.3).

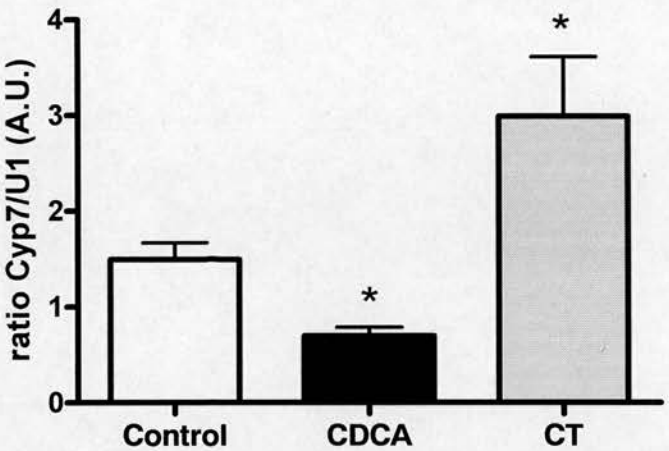

Figure 4.3 Transcript abundance of CYP7A1 following dietary manipulation. mRNA abundance was quantified by northern blot analysis and values corrected for the house keeping gene U1. Data are expressed as mean±SEM, n=8 per group;*$p<0.05$ *vs* Control

4.4.1.4 Blood and serum parameters

Plasma glucose ($p<0.05$) and insulin ($p<0.05$) were significantly reduced in CDCA but not cholestyramine treated animals (Table 4.1). Bile acid treatment caused an increase in plasma HDL cholesterol levels ($p<0.05$) (Table 4.1). The converse was observed with cholestyramine treated animals (Table 4.1). Levels of non-esterified fatty acids (NEFA) were significantly elevated in cholestyramine treated animals ($p<0.05$) but not following bile acid treatment ($p=0.5$; Table 4.1).

4.4.2 Impact of CDCA and cholestyramine on hepatic glucocorticoid metabolizing enzymes

4.4.2.1 Hepatic enzyme activity

Hepatic 11β-HSD1 dehydrogenase activity was decreased with CDCA but not cholestyramine when measured in an assay using 25nM substrate ($^3H_4$ – corticosterone; Figure 4.4 A). Inhibition was not observed when assayed with 2μM substrate (Figure 4.4 B). Changes in enzyme activity were not accompanied by changes in transcript abundance of 11β-HSD1 which were unaltered by either treatment (Figure 4.4 C).

Hepatic 5β-reductase activity was reduced in animals treated with either CDCA or cholestyramine when measured using the lower substrate concentration (25nM; Figure 4.5 A) but not at the higher substrate concentration (2μM; Figure 4.5 B). Abundance of mRNA of 5β-reductase was unaltered by either treatment. In addition, treatment with CDCA and cholestyramine did not influence 3α-HSD activity (Figure 4.5 D) or transcript abundance (Figure 4.5 E). Transcript abundance of 5α-reductase 1 was comparable between groups (0.19±0.05 Control; 0.13±0.03 CDCA; 0.14±0.03 CT AU, p=ns).

A 11β-HSD1 (25nM)

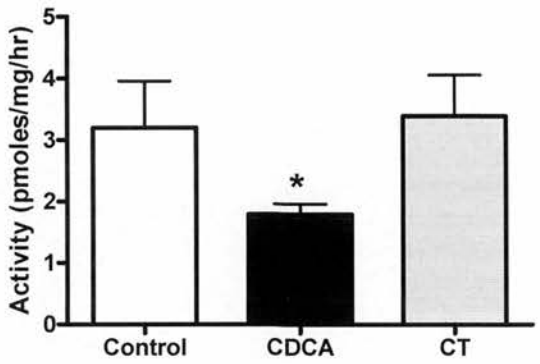

B 11β-HSD1 (2μM)

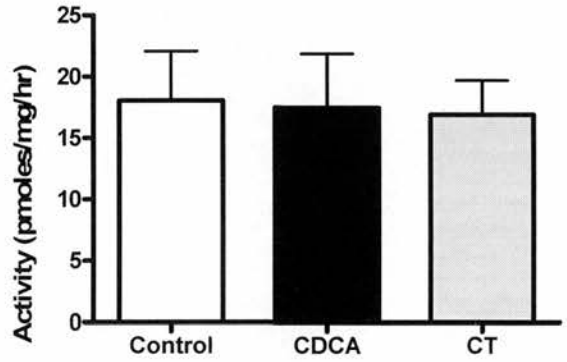

C 11β-HSD1 mRNA

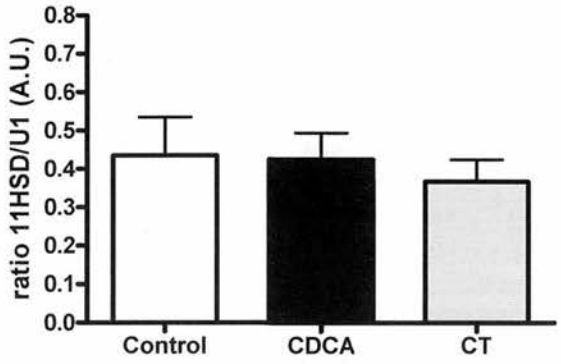

Figure 4.4 11βHSD1 dehydrogenase activity following dietary manipulation. **(A)** Dehydrogenase activity of 11βHSD1 measured in rat liver microsomes was significantly reduced by CDCA but not cholestyramine (CT) when assayed with 25nM corticosterone. **(B)** Inhibition was abolished when assayed at a higher substrate concentration (2μM). **(C)** Transcript abundance of 11βHSD1 was unaltered following dietary manipulation. Data are mean±SEM; n=8 per group; *$p<0.05$ *vs* Control.

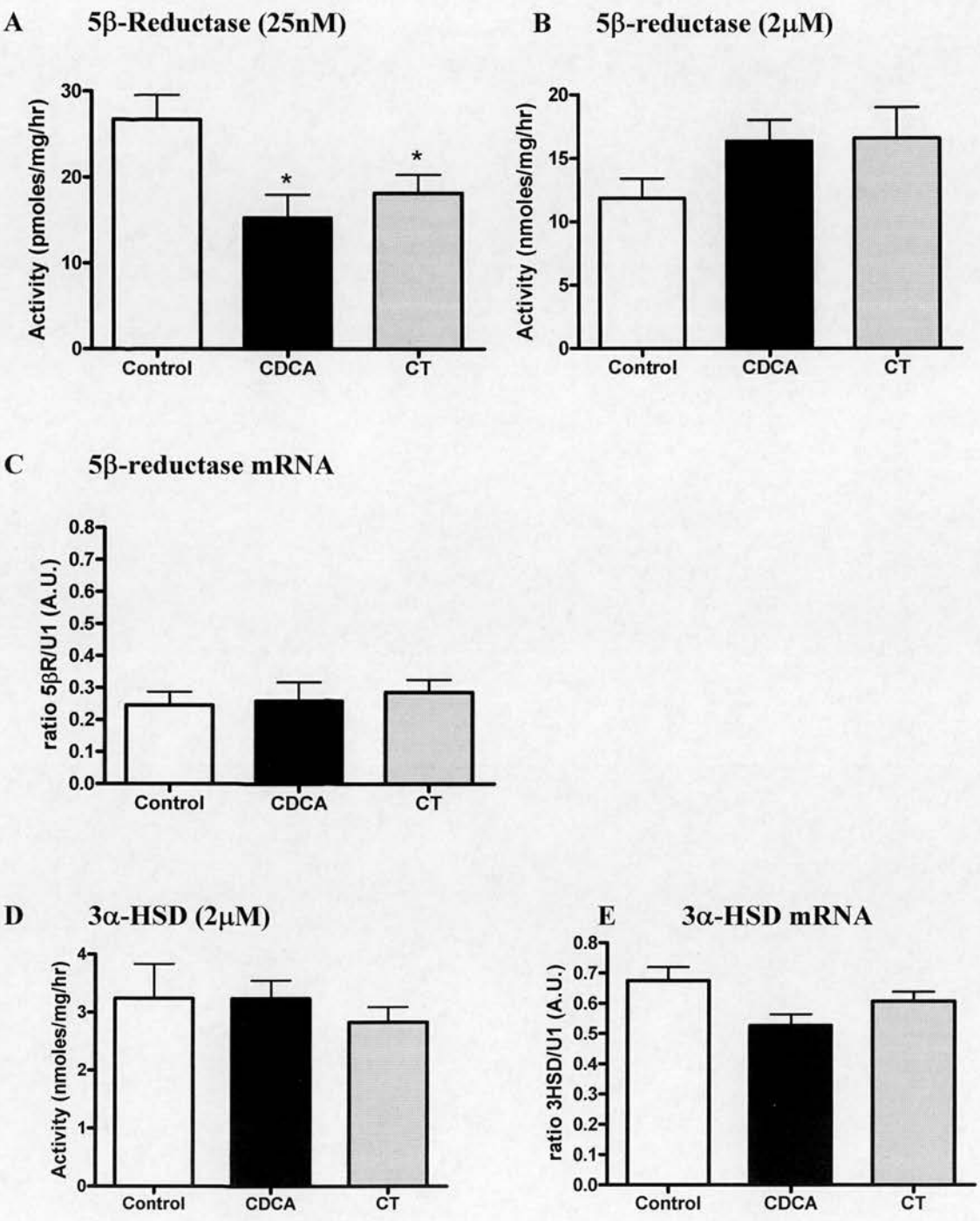

Figure 4.5 5β-reductase and 3α-HSD activity and expression following dietary manipulation. (**A**) Activity of steroid 5β-reductase measured in rat liver cytosol was reduced by treatment with CDCA and cholestyramine (CT) when assayed with 25nM corticosterone. (**B**) Inhibition was abolished at higher substrate concentration (1μM). (**C**) No difference was observed in transcript abundance. (**D**) Dietary manipulation of bile acid concentration did not influence 3α-HSD activity or (**E**) mRNA abundance. Data are mean±SEM; n=8 per group; *$p<0.05$ *vs* Control.

4.4.2.2 Urinary metabolites

Animals treated with cholestyramine excreted lower total quantities of urinary metabolites of corticosterone ($p<0.05$ CT). Both cholestyramine and CDCA treated animals excreted fewer 5β-reduced metabolites ($p<0.05$; Table 4.1). These altered patterns of metabolism were confirmed by changes in the ratio of 5α -to 5β reduced metabolites ($p<0.05$ in both cases). Changes in 11β-HSD1 could not be assessed due to an inability to detect 11-dehydrocorticosterone (A) metabolites within urine.

4.4.2.3 Glucocorticoid-sensitive genes

A reduction in abundance of mRNA of the glucocorticoid sensitive gene angiotensinogen was observed following both treatments (Figure 4.6 A; $p<0.05$). Although a trend towards reduction was observed in TAT (Figure 4.6 B) and PEPCK (Figure 4.6 C) following CDCA treatment and in PEPCK (Figure 4.6 C) following cholestyramine this did not reach statistical significance.

A

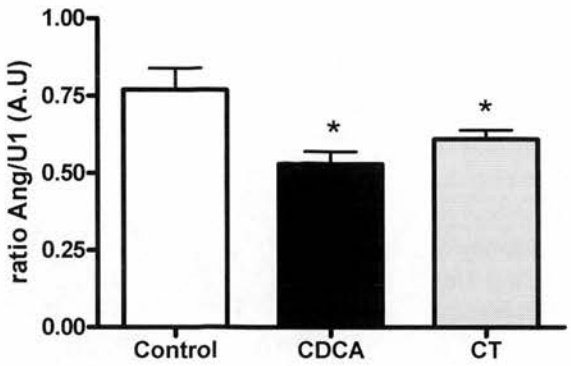

B

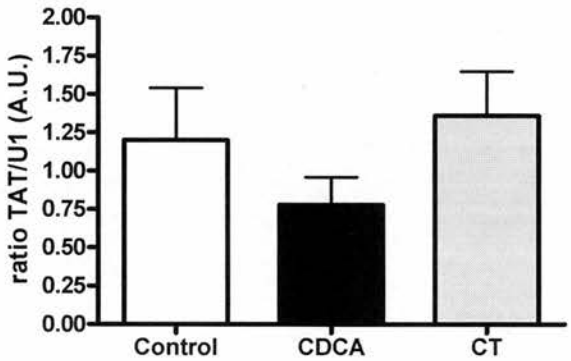

C

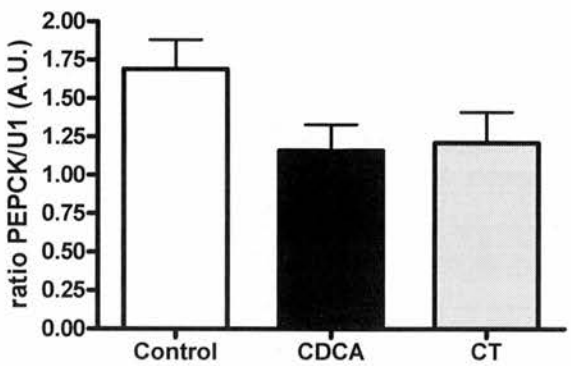

Figure 4.6 Transcript abundance of glucocorticoid-sensitive genes following dietary manipulation. mRNA abundance of hepatic (**A**) angiotensin, (**B**) TAT and (**C**) PEPCK were quantified by northern blot analysis and values corrected for the house keeping gene U1. Data are expressed as mean±SEM, n=8 per group; *p<0.05 *vs* Control.

4.4.3 Effect of CDCA or cholestyramine feeding on HPA axis activation

Baseline plasma corticosterone (Table 4.1; Figure 4.7 A) and ACTH (Table 4.1) levels were comparable between groups. Following acute restraint stress (20 mins) animals treated with CDCA but not cholestyramine showed a delay in the return to basal corticosterone levels compared to Control treated animals (Figure 4.7 A and B). A difference was not apparent in the response of ACTH following acute restraint stress in either treatment group (Figure 4.7 C).

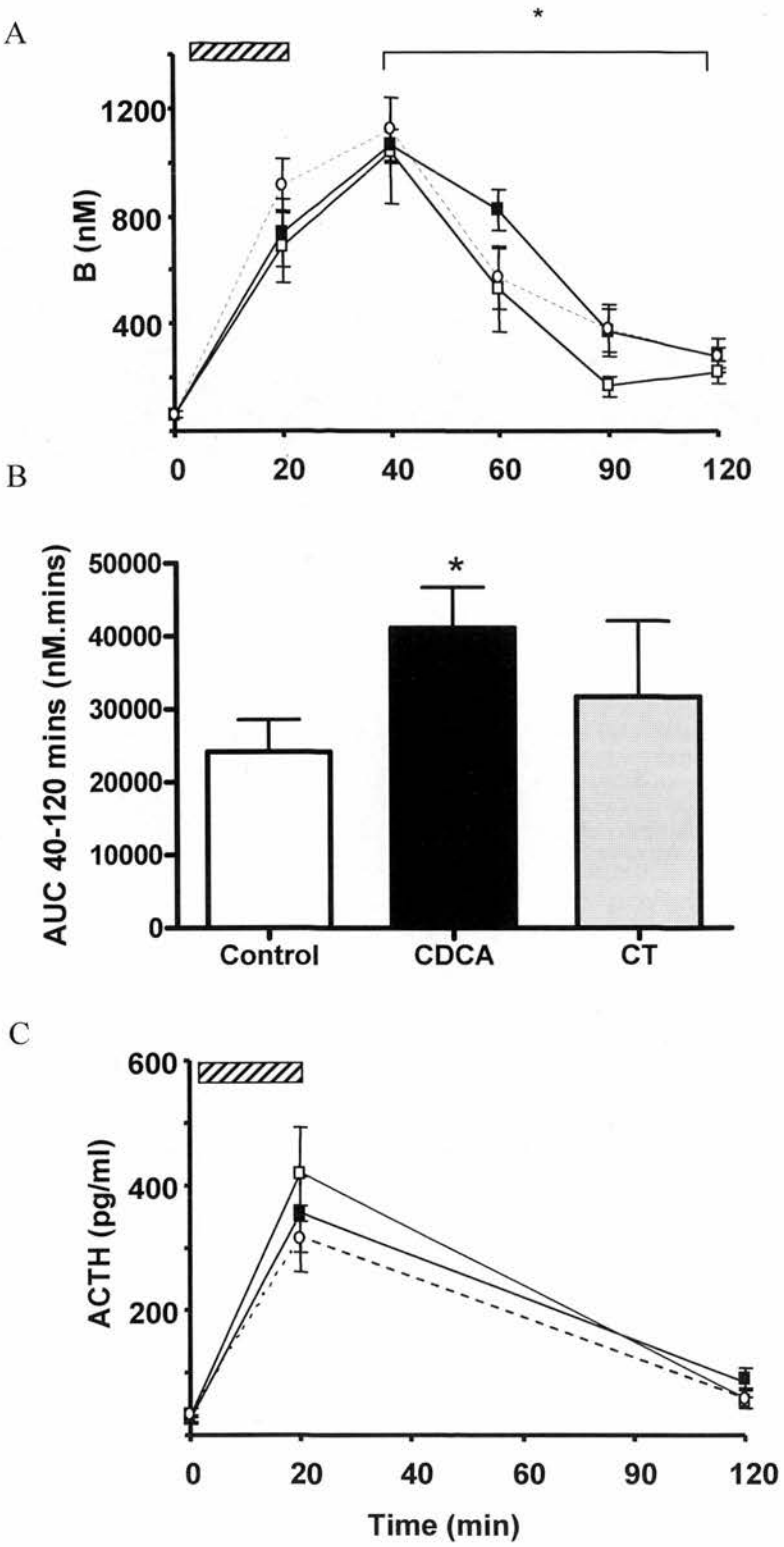

Figure 4.7 Indices reflecting HPA axis response to acute (20 min) restraint stress (hatched box). (**A**) Animals treated with CDCA showed a delay in return to basal corticosterone levels following stress (**B**) calculated as area under the curve (AUC) (**C**) Neither CDCA (filled square) nor CT (open diamond) influenced ACTH levels compared to control (open square). Data are mean±SEM; n=8; *$p<0.05$ *vs* Control.

4.5 Discussion

The data presented in this chapter provide evidence that bile acid induced inhibition of glucocorticoid metabolism also occurs *in vivo.* Dietary administration of CDCA reduced activity of hepatic 5β-reductase and 11β-HSD1 without changes in mRNA or protein levels. Enzyme inhibition was reflected by a reduction in total urinary metabolites of corticosterone, primarily due to a fall in 5β-reduced metabolites. These findings were confirmed by a marked rise in the ratio of 5α:5β-reduced metabolites. Of note, the decline in 5β-reductase activity was not accompanied by a compensatory rise in 5α-reductase 1. Furthermore, despite altered activity, changes were not observed in transcript abundance of 5β-reductase or 11β-HSD1 again suggesting that bile acids are exerting their inhibitory effect at a post-transcriptional level

In this study, two approaches were used to assess the impact of bile acids on glucocorticoid metabolism. The first method, namely the dietary administration of bile acids is a well utilized method of increasing total bile acid content (Pandak *et al.* 1994; Gustafsson *et al.* 1981). The success of this manipulation was evident as transcript abundance of CYP7A1 within the liver was reduced in bile acid supplemented animals. Furthermore, plasma and faecal bile acid contents were elevated in CDCA treated animals when compared to Control animals. The consequences of impaired endogenous bile acid synthesis were also evident from the increase in plasma HDL cholesterol concentrations.

In the second method, bile acid synthesis was stimulated via the administration of cholestyramine, a bile acid binding resin sometimes prescribed to patients with hypercholesterolemia. Cholestyramine sequesters bile acids within the intestine preventing their reuptake into the portal circulation depleting their hepatic levels thereby stimulating cholesterol catabolism into bile acids. It is well established that in response to cholestyramine there is acute up-regulation of CYP7A1 activity and transcription and a reduction in total circulatory cholesterol (Heuman *et al.* 1992; Ren *et al.* 2003; Vlahcevic *et al.* 1996). As anticipated CYP7A1 mRNA abundance was 2-fold greater in Cholestyramine-treated animals compared to Control while HDL cholesterol levels were significantly reduced. In addition faecal bile acid

content of cholestyramine-treated animals was greater than 2-fold that of Control animals; however, hepatic and plasma bile acids were surprisingly unaltered.

As anticipated from the data obtained *in vitro* increasing cytosolic bile acids altered glucocorticoid metabolism with a reduction in total urinary metabolites of corticosterone, primarily due to a reduction in 5β-reduced metabolites. The measurement of urinary metabolites over a 24 hour period provides valuable insight into the overall steady state conditions within the liver, accounting for diurnal fluctuations or acute post prandial changes in enzyme activity or hormone levels. Supplementation of the diet with CDCA and stimulation of bile acid biosynthesis via cholestyramine caused a significant reduction in glucocorticoid clearance over a 24 hour period. In fact cholestyramine appeared to be more potent than CDCA resulting in a 60% reduction in 5β-reduced metabolites and 50% fall in total urinary metabolites of corticosterone. In addition inhibition of hepatic 5β-reductase and 11β-HSD1 was observed in CDCA-treated animals when assayed with low substrate concentration (25nM). This inhibition was abolished when a higher substrate concentration (2μM) was used. These finding corroborate those obtained in Chapter 3, in which bile acids were found to act as a competitive inhibitor of both 5β-reductase and 11β-HSD1. As with CDCA, 5β-reductase activity was inhibited in animals treated with cholestyramine at low (25nM) but not high (1μM) substrate concentration, however, a difference was not observed in 11β-HSD1 activity at either substrate concentration. The disparity between the two models may reflect differences in enzyme localization and bile acid accumulation within the cell. Cholestyramine inhibited 5β-reductase, a cytosolic enzyme, but not 11β-HSD1 whose active site is embedded within the inner leaflet of the endoplasmic reticulum membrane. These findings may reflect the site of bile acid accumulation within the cell. For example cytosolic accumulation may only occur in response to pharmacological loading not due to increased synthesis rates.

Bile acids are reabsorbed within the ileum via active transport mechanisms and carried back to the liver via the portal venous circulation (Myant & Mitropoulos 1977). From the venous circulation they are transported into the hepatic cytosol via high-affinity Na^+-dependent bile salt transporter (Ntcp/NTCP) which can transport only conjugated bile acids and a family of multi-specific organic anion transporters

(Oatps/OATPS) that can mediate sodium independent bile salt uptake along with neutral steroids and organic anions (Trauner & Boyer 2003). It possible that in the presence of excess bile acids these transport mechanisms may be saturated or damaged due to the cytotxicity of the accumulating bile acids within the cells of CDCA treated animals. The bile salt pool undergoes an enterohepatic circulation that is regulated by distinct bile salt transport proteins, including the canalicular bile salt export pump BSEP (ABCB11), the ileal $Na(^{+})$-dependent bile salt transporter ISBT (SLC10A2), and the hepatic sinusoidal $Na(^{+})$-taurocholate cotransporting polypeptide NTCP (SLC10A1), whose expression is regulated by both transcriptional and post-transcriptional mechanism (Trauner & Boyer 2003). This mechanism would protect the hepatocytes from the potential hepatotoxic effects of bile acid accumulation. In support of this hypothesis, bile acids are known to exert feedback regulation on NTCP, the principal hepatic bile acid transporter by bile acid-activated FXR via induction of SHP feedback (Denson *et al.* 2001). Although plasma and fecal bile acid levels were elevated in CDCA-treated animals, there was no apparent change in bile acid content of hepatic tissue homogenates in response to either pharmacological loading with CDCA or the induction of bile acid synthesis with cholestyramine. In the case of CDCA it is possible that intracellular accumulation of bile acids within the cytosol may have been obscured due to dilution with other cellular components when homogenized.

Despite alterations in glucocorticoid metabolism and clearance, there was no difference in transcript abundance of TAT or PECK, enzymes that are known to be regulated by GR. In contrast, angiotensinogen mRNA abundance was reduced by both treatments. It must be noted however, that angiotensinogen is regulated by a number of factors in addition to GR-mediated expression. Indeed, angiotensin II is a potent stimulator of angiotensiogen (Ben Ari & Garrison 1988). Furthermore, a recent study in HepG2 cells demonstrated direct inhibition of human angiotensinogen mediated through the inhibitory effect of SHP on HNF-4 (Yamagata *et al.* 2004). As such, the changes in angiotensinogen expression observed in this study would appear to be independent of alterations in glucocorticoid levels and may be a direct effect of bile-acid-mediated suppression.

The HPA-axis is under both feed-forward and feedback control and the role of glucocorticoid metabolizing enzymes in HPA axis regulation is an area of much research. The paradox that idiopathic obese individuals can have normal or even lower circulatory glucocorticoid levels has been attributed to a reduction in glucocorticoid clearance and compensatory activation of the HPA axis (Hautanen & Adlercreutz 1993). These findings have been recapitulated in the obese Zucker rat (Livingstone *et al.* 2000) where tissue specific alterations in glucocorticoid metabolism are frequently accompanied by changes in HPA axis activation and/or response (Rask *et al.* 1999; Livingstone *et al.* 2000). Indeed, enhanced glucocorticoid clearance, brought about by an increase in activity of the hepatic A-ring reductases (5α- and 5β-reductase) and a reduction in hepatic 11β-HSD1 are associated with compensatory activation of the HPA axis, thus circulatory levels of cortisol are maintained within a normal physiological range (Hautanen *et al.* 1997). The generation of transgenic models including global 11β-HSD1 knock out (Paterson *et al.* 2004; Kotelevtsev *et al.* 1996) and adipose 11β-HSD1 (Morton *et al.* 2004; Masuzaki *et al.* 2001a) over expressing mice support the theory that tissue specific alterations in glucocorticoid metabolizing enzymes play a fundamental role in HPA axis activation. From this work it is clearly evident that one must consider the role that individual tissues play in maintaining whole body glucocorticoid homeostasis.

The A-ring reductases (5α- and 5β-reductase) act as the predominant means of clearing excess glucocorticoids from the body. Bile acid supplementation and induction of synthesis caused a reduction in glucocorticoid clearance, used routinely in humans as an index of glucocorticoid production rates. In addition, HPA axis drive was substantially reduced in bile-acid-treated animals and adrenal gland weight was reduced but only in CDCA-treated animals. Basal levels of corticosterone and ACTH were comparable between all groups, and thymus weight, which may be used to infer circulatory glucocorticoid concentrations, was unaltered by dietary manipulation. Thus it would appear that in the face of diminished 5β-reduction animals reset their HPA axis and maintain circulatory levels of corticosterone. It is hard to predict the change in intracellular corticosterone levels. Diminished regeneration of active corticosterone from inert 11-keto by 11β-HSD1 inhibition would reduce hepatic

concentrations of active steroid, opposing inhibition of 5β-reductase which would predict an increase in corticosterone due to reduced clearance.

HPA axis responsiveness was tested by subjecting animals to a 20 min acute restraint stress. Following restraint, animals treated with CDCA or cholestyramine showed similar peak responses in corticosterone and ACTH 40 minutes post stress which was comparable to Control animals. However, CDCA treated animals showed a delay in the return to basal corticosterone levels. This was most apparent 40-120 minutes post stress in keeping with an impaired clearance of glucocorticoids by 5β-reductase. Although animals treated with cholestyramine also demonstrated a delay in return to basal levels of corticosterone, this was less pronounced than that of CDCA-treated animals and may reflect plasma levels of bile acids which were unaltered in cholestyramine treated animals.

It is interesting to note that CDCA treatment lowered plasma glucose and insulin, reduced triglyceride contents of the liver and impeded lipid accumulation within the liver. This improved metabolic phenotype is very similar to that of 11β-HSD1 null mouse (Kotelevtsev *et al.* 1997). Furthermore, this phenotype was more pronounced in CDCA treated animals in which 11β-HSD1 was potently inhibited. Although it is tantalizing to infer that these effects are mediated through 11β-HSD1 one must also consider the direct impact of bile acids on glucose metabolism. Recent work has established a novel role of FXR in the regulation of peripheral insulin sensitivity and adipocyte function (Cariou 2006). Indeed, treatment with the synthetic FXR agonist GW4064 improved insulin sensitivity of genetically obese ob/ob mice *in vivo.* Furthermore, it has been demonstrated that activation of FXR in db/db mice repressed hepatic gluconeogenic genes and increased hepatic glycogen synthesis and glycogen content by a mechanism that involves enhanced insulin sensitivity (Zhang 2006).

In this study, supplementing the diet with CDCA reduced 11β-HSD1 and 5β-reductase activity within the liver and an altered HPA axis response. In contrast stimulating bile acid synthesis with cholestyramine did not affect 11β-HSD1 activity. It would therefore appear that inhibition of 5β-reductase impacts upon HPA axis activation whilst inhibition of 11β-HSD1 alters glucocorticoid-regulated genes. Where both occur as in CDCA-treated animals, a metabolic phenotype analogous to

the 11β-HSD1 null mouse is observed. Thus disorders with changes in these enzymes could be brought about increased bile acids.

Chapter 5

Effect of decreased bile acids by a fat-free diet on glucocorticoid metabolism and HPA axis activation

5.1 Introduction

In Chapter 4 the concentration of bile acids within the liver was increased by the administration of a diet supplemented with CDCA. In addition, bile acid synthesis was stimulated with cholestyramine. In both models, bile acids inhibited glucocorticoid metabolism, predominantly through their inhibitory effects upon 5β-reductase. In this Chapter, we investigated the impact of lowering hepatic bile acids and bile acid synthesis rates via the administration of a fat-free diet.

Literature was reviewed to determine whether reducing the concentration of cholesterol, the substrate for bile acids would suppress bile acid synthesis rates. Cholesterol is supplied to the liver via four main routes;

1) *De novo* synthesis of cholesterol from acetyl-coenzyme A (CoA).

2) Reverse cholesterol transport from peripheral tissue to the liver by the selective uptake of HDL cholesterol by SR-B1.

3) LDL receptor mediated endocytosis of serum cholesterol esters (CE).

4) Absorption of dietary cholesterol from the intestine and transportation to the liver as chylomicrons by LDL receptor mediated mechanisms (Chiang 2002).

Due to the complex interplay between factors controlling cholesterol biosynthesis, utilisation and elimination, each aspect must be considered in isolation and as part of the whole system. Rats fed a cholesterol-depleted diet compensate for this loss by increasing the rate of *de novo* synthesis (Chiang *et al.* 2001). Supplementation of the diet with fibrous agents such water-soluble NSP guar gum and sodium alginate reduce circulating cholesterol levels and increase their feacal bile acid output by as much as 2 to 3 times due to interuption of the enterohepatic circulation (Seal & Mathers 2001). However, bile acid pool size is normal or even increased (Moundras *et al.* 1997).

It is possible to inhibit the rate of cholesterol synthesis using statins, such as simvostatin and atorvastatin. These agents inhibit 3-hydroxy-3-methylglutaryl-CoA (HMG-CoA) reductase the rate limiting enzyme in cholesterol biosynthesis, thereby reducing cholesterol production and consequently bile acid biosynthesis (Bilheimer *et al.* 1983). Although statins are effective cholesterol lowering agent in humans,

they are ineffective in the rat due to the high basal rate of *de novo* cholesterol synthesis, with bile salt excretion being unaltered (Carella 1999). Lastly, inhibition of cholesterol absorption was considered using agents such as ezetimibe, a potent inhibitor of cholesterol and phytosterol uptake within the proximal jejunum of the small intestine via the Niemann-Pick C1-Like 1 (NPC1L1) transporter (Garcia-Calvo *et al.* 2005). This agent is used for the treatment of hypercholesterolemia effectively lowering circulating plasma cholesterol in humans by 15-20% (Bays *et al.* 2001; Davis, Jr. *et al.* 2004). However, as with statins, ezetimibe absorption does not influence cholesterol biosynthesis or bile acid synthesis in the rat (van Heek *et al.* 2003).

Finally it was determined that hepatic bile acids could be depleted using a synthetic fat-free diet. This diet had previously been used to reduce bile acid synthesis, suppressing it by 63% (Bertolotti *et al.* 1995). By removing all fat from the diet, the functional requirement for bile acids is reduced and consequently recirculation of bile acids along the entero-hepatic axis is much slower. Removal of all fat from the diet necessitated the addition of other component(s), including casein and sucrose. Sucrose has been shown to influence HPA axis independently (Opara *et al.* 1996) and thus it was not possible to compare this directly to normal chow, assuming the only difference was fat. Confounding changes in glucose and lipid homoeostasis, which may also have occurred via administration of the fat-free diet alone, again precluded the use of normal chow as a control diet. Control animals were therefore regarded as animals receiving the fat-free diet supplemented with CDCA (1% w/w; FF/CDCA) to which animals receiving the fat-free diet (FF) were compared.

5.2 Research aims

The aims of the research in this chapter were:

1. To investigate the effect of bile acid depletion on glucocorticoid metabolism.
2. To investigate the effect of bile acid depletion on glucocorticoid action.
3. To investigate the effect of bile acid depletion on HPA axis activation.

5.3 Materials and methods

5.3.1 Animals and animal maintenance

Male Wistar rats (3-4 weeks; Harlan Orlac, Bicester, UK) were maintained as described in section 2.3.1. Animals were matched for age and weight and allocated into two groups of eight. Control group received synthetic fat-free chow supplemented with chenodeoxycholic acid (FF/CDCA; 1% w/w section 5.3.2). The treatment group received synthetic fat-free chow (FF; section 5.3.2). Animals were housed singly and maintained on their respective diets for 4 weeks. Body weight, food and fluid intake were recorded on a daily basis.

5.3.2 Preparation of diet

A synthetic fat-free diet (D05052506) was prepared by Research Diet (Research Diets Inc, NJ, US). The fat was replaced with sucrose (70% w/w) and a standard vitamin and mineral mixture (Table 5.1) in order to achieve a nutritionally and calorifically balanced diet. Chow was prepared in which the fat-free diet was supplemented with CDCA (1% w/w; D05052507) (Research Diets Inc, NJ, US). The synthetic fat-free diet supplemented with bile acid was treated as a "Control" group (Opara *et al.* 1996). Both diets were stored at room temperature.

5.3.3 Metabolic cages

Animals were placed into metabolic cages for 7 days as described in section 4.3.3 after 3 weeks on their respective diets. Faeces and urine were collected over the final 72 hours and stored a -20°C for subsequent analysis. The animals were then placed back into their original cages for at least one day prior to sacrifice.

5.3.4 Animal sacrifice and tissue collection

Animals were killed by surgical decapitation and tissue and blood samples collected and stored as described in section 2.3.2.

5.3.5 Analysis of biochemical parameters

Enzyme activity, plasma hormone levels, liver biochemistry, urinary steroids and bile acid levels were quantified as described in sections 4.3.5 - 4.4.0.

	Bile acid depleted diet (FF)		**Control (FF/CDCA)**	
	gm%	*kcal%*	gm%	*kcal%*
Protein	20.3	*22.2*	20.1	*22.2*
Carbohydrate	71.0	*77.8*	70.3	*77.8*
Fat	0.0	*0.0*	0.0	*0.0*
Total		*100.0*		*100.0*
kcal/gm		*3.65*		*3.61*
Ingredient	**gm**	***kcal***	**gm**	***kcal***
Casein, alcohol extracted	200	*800*	200	*800*
DL-Methionine	3	*12*	3	*12*
Corn Starch	0	*0*	0	*0*
Sucrose	700	*2800*	700	*2800*
Cellulose, BW200	50	*0*	50	*0*
Mineral Mix S10001	35	*0*	35	*0*
Vitamin Mix V10001	10	*40*	10	*40*
Choline Bitartrate	2	*0*	2	*0*
Chenodeoxycholic Acid	0	*0*	10.5	*0*
Total	**1000**	***3652***	**1010.5**	***3652***

Table 5.1 Modified AIN-76A Rodent Diet With Alcohol-Extracted Casein, 70% Sucrose (wt./wt.), No Added Fat and with and without 1% chenodeoxycholic Acid

The sodium content of both diets was 0.3% (w/w).

5.3.6 Abundance of transcripts

Transcript abundance of hepatic target genes were quantified as described in section 4.3.7.

5.3.7 Statistical analyses

Individual experiments were conducted using tissues from 8 independent animals per group (unless otherwise stated). Each assay was performed duplicate and the mean of each duplicate taken as the final value for that individual animal. The data represent the mean ± standard error of the mean (SEM). Results were subjected to Students t-test. All analysis was performed using Statistica (Version 9) or Graphpad prism (Version 4). Significance was set at $*p<0.05;**p<0.01$ *vs* FF/CDCA.

5.4 Results

5.4.1 Effect of fat-free diet on physiological parameters

5.4.1.1 Body weight

Fat-free fed (FF) animals were significantly heavier then Control (FF/CDCA) animals gaining almost twice as much weight as those receiving the bile acid supplemented diet (FF/CDCA; Figure 5.1 A). Weight gain was elevated in the fat free (FF) animals over the duration of study (5.1 B). This was not attributable to a difference in food intake as FF animals ate significantly less food than FF/CDCA animals (Table 5.1).

A

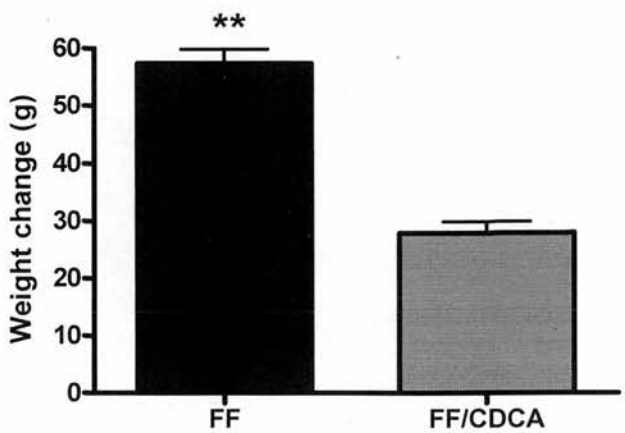

Figure 5.1 A Body weight following dietary manipulation. Animals were fed a synthetic fat-free diet (FF) or fat-free diet supplemented with CDCA (FF/CDCA; 1% w/w) for four weeks and body weight recorded daily. Data represent (A) total weight change (B) course of weight change are mean±SEM; n=8; **p<0.01 *vs* FF/CDCA.

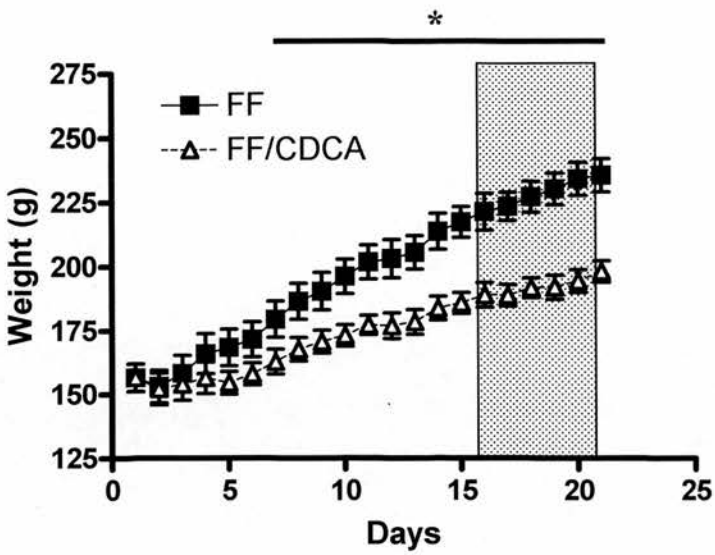

Figure 5.1 B Body weight change following dietary manipulation. Animals were fed a synthetic fat-free diet (FF), or fat-free diet supplemented with CDCA (FF/CDCA; 1% w/w) for four weeks and body weight recorded daily. Hatched box represents time spent in metabolic cage. Data are mean±SEM; n=8; *p<0.05 *vs* FF/CDCA.

5.4.1.2 Organ weight

Adrenal gland weight and plasma corticosterone levels were greater in FF animals compared to FF/CDCA animals (Table 5.2). The difference in adrenal gland weight however was not significant when corrected for body weight (Table 5.2). Removal of bile acids did not influence thymus or prostate weight. Liver weights were also comparable between groups (Table 5.2) however, liver triglyceride ($p<0.05$) but not glycogen ($p=0.1$) levels were elevated in FF animals. Of note adrenal and prostate weight, plasma corticosterone and hepatic triglyceride levels of FF animals were comparable to Control animals fed standard chow for 4 weeks as describded in detail in Chapter 4 (Table 5.2).

	Fat-Free + CDCA	Fat-Free	Control (Chapter 4)
Basal weight (g)	198±4.2	235±6.4*	208±14
Weight change (g)	174.3±4.5	197.1±6.6*	161.4±7.1
Daily food intake (g/g body weight)	0.09±0.003	0.08±0.004*	0.082±0.003
Adrenal weight (mg)	22.9±1.1	29.1±1.4*	27.4
Adrenal weight (mg/g body weight)	0.11±0.003	0.12±0.003	0.082±0.006
Thymus weight (mg)	0.42±0.0	0.53±0.04	0.73±0.04
Prostate weight (mg/g body weight)	0.78±0.13	0.80±0.08	0.83±0.09
Liver weight (mg/g body weight)	33.3±3.1	38.2±3.0	45.3±0.9
Glycogen (mg/g)	6.19±0.78	4.85±0.45	3.85±0.42
Triglycerides (mg/g)	11.2±1.6	18.6±2.1*	14.7±1.8
Corticosterone	52.6±7.4	84.9±10.3*	78.1±19
Glucose (mg/ml)	5.08±0.53	6.22±0.63	8.4±0.7
Insulin (ng/ml)	1781±190	3045±482*	4740±597
Triglycerides (mM)	1.26±0.17	3.08+0.28*	1.5±0.2
Cholesterol (mM)	2.35±0.11	1.81±0.12*	1.89±0.09
HDL cholesterol (mM)	1.58±0.08	1.08±0.11*	1.33±0.08
NEFA (mM)	0.49±0.06	0.43+0.04	0.25±0.03
Bile acids			
Hepatic (μmoles/mg)	34.8±3.6	25.1±7.1	50.5±11.7
Plasma (μM)	108.0±16.34	31.9±6.2*	28.0±8.7
Fecal (μmoles/g)	114.7±15.2	53.9±12.7*	52.8±7.3
Urine (ng/ml)			
5β-THB	178±22	305±26*	377±68
5α-THB	240±27	268±49	132±32
5β:5α-THB	0.96±0.18	1.44±0.39	4.15±0.9
Total	392±51	651±116	508±77

Table 5.2 Changes in physiological parameters following dietary manipulations. Animals were fed a fat-free diet (FF), or fat-free diet supplemented with CDCA (1% w/w; FF/CDCA) for four weeks. Urine and faeces were collected over a 72 hour period and tissues and plasma harvested at cull. Data are expressed as mean±SEM; n=8;*$p<0.05$, FF *vs* FF/CDCA. For comparison animals fed standard chow for 4 weeks as described in detail in Chapter 4.

5.4.1.3 Blood and serum parameters

Plasma insulin but not glucose was elevated in FF animals and plasma triglycerides reduced ($p<0.05$) (Table 5.2). Conversely, plasma total cholesterol ($p<0.05$) and HDL cholesterol ($p<0.05$) were suppressed in fat-free animals whereas plasma NEFA levels were not altered (Table 5.3)

When comparing the lipid profile of animals fed a diet of standard chow (Control animals described in Chapter 4), with those fed the fat-free diet, the FF diet had a major impact upon triglyceride storage and/or utilisation with plasma triglyceride levels almost twice those observed in Chapter 4 Control animals (Table 5.3). NEFA levels were also elevated in FF animals although it must be noted that a different assay was used and data are not completely comparable.

	Control	**FF**
Cholesterol (mM)	1.89±0.11	1.81±0.12
HDL (mM)	1.33±0.08	1.08±0.11
NEFA (mM)	0.25±0.03	0.43±0.04*
Triglycerides (mM)	1.5±0.02	3.1±0.3*

Table 5.3 Plasma lipid profile of animals fed standard chow (Control) compared to fat-free chow (FF) for 4 weeks. Blood was collected at 0800h following decapitation and plasma lipid content assessed. Data are mean±SEM; n=8 per group.*$p<0.05$ Control *vs* FF.

5.4.1.4 Bile acids

The total bile acid content of plasma and faeces were significantly suppressed in FF animals (Table 5.2), corresponding to an increase in mRNA abundance of CYP7A1 (Figure 5.2). Hepatic bile acid concentrations tended to decrease in FF animals but this did not reach statistical significance. Of note, hepatic bile acid concentrations were 2-fold lower in FF animals animals compared to Control animals Chapter 4 (Table 5.2).

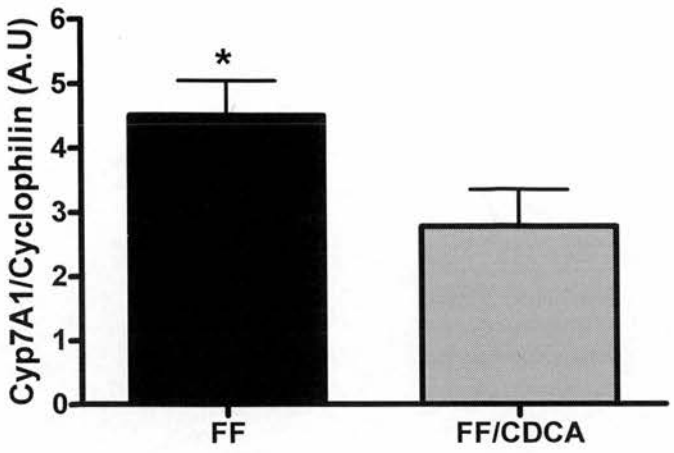

Figure 5.2 Transcript abundance of CYP7A1 following dietary manipulation. mRNA abundance was quantified by Taqman® real-time PCR and values are expressed as a ratio to the house keeping gene cyclophilin A using the Standard Curve method. Data are expressed as mean±SEM, n=8 per group;*p<0.05 *vs* FF/CDCA.

5.4.2 Impact on hepatic glucocorticoid-metabolising enzymes

5.4.2.1 Hepatic enzyme activity

Activity of hepatic 5β-reductase was increased in FF animals when assayed with 25nM substrate (Figure 5.3 A). This difference was abolished at higher substrate concentration (2μM; 1.22±0.26 FF v 1.24±0.18 FF/CDCA nmol/mg/hr; p=ns). A difference was not observed in 11β-HSD1 dehydrogenase activity (Figure 5.3 B) or 3αHSD activity (Figure 5.3 C) between groups.

Transcript abundance of 5β-reductase (Figure 5.4 A), 11β-HSD1 (Figure 5.4 B), 3αHSD (Figure 5.4 C) and 5α-reductase 1 (Figure 5.4 D) were comparable between groups.

A **5β-Reductase (25nM)**

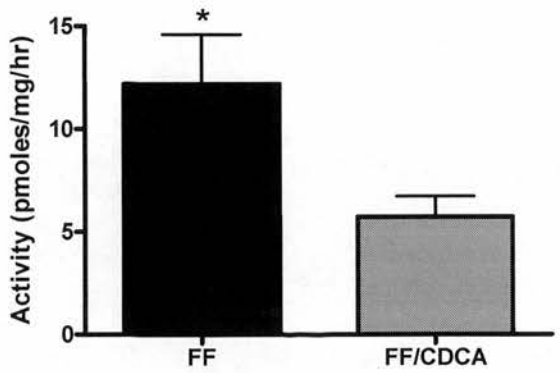

B **11β-HSD1 (25nM)**

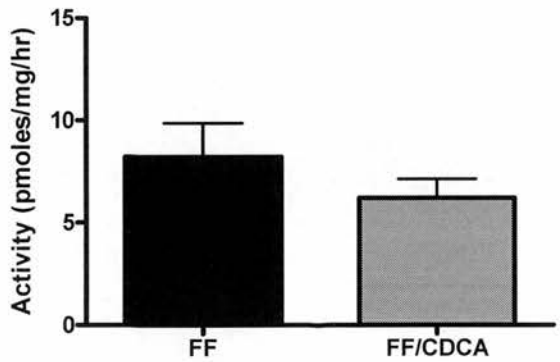

C **3αHSD (2μM)**

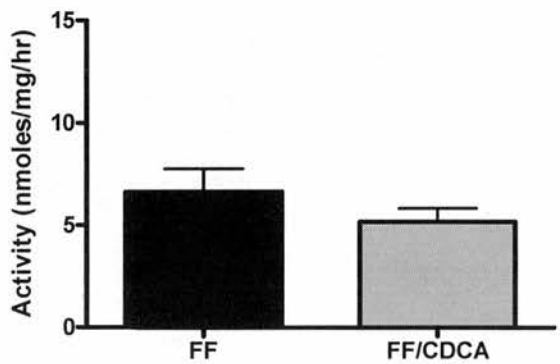

Figure 5.3 Hepatic enzyme activity following dietary manipulation. (**A**) Activity of steroid 5β-reductase and (**B**) 11β-HSD1 when assayed with 25nM corticosterone and (**C**) 3α-HSD when assayed with 2μM corticosterone. 11β-HSD1 or 3α-HSD activity were not influenced by dietary manipulation. Data are mean±SEM; n=8 per group; *$p<0.05$ *vs* FF/CDCA.

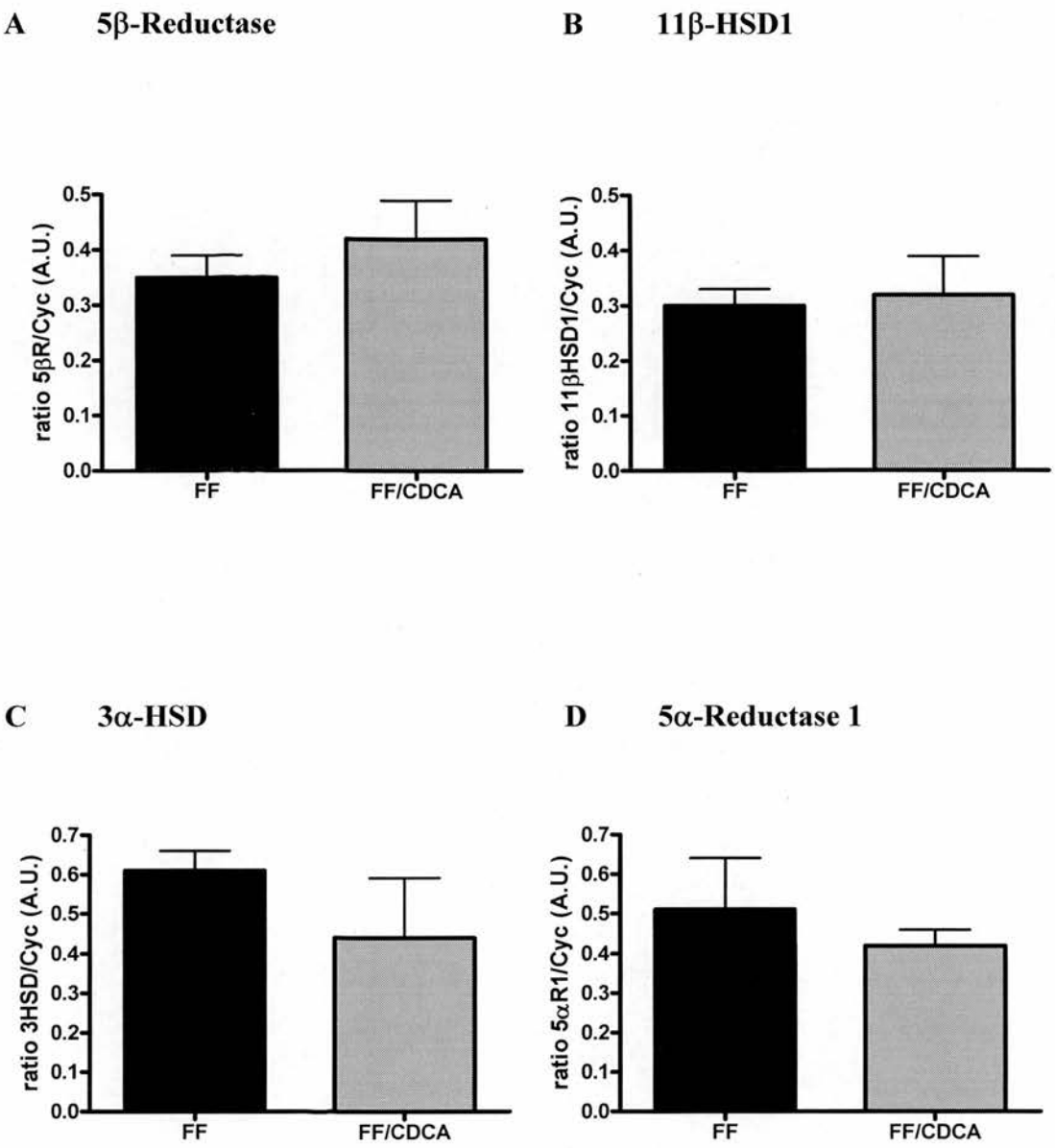

Figure 5.4 Transcript abundance of glucocorticoid metabolizing genes. mRNA abundance of (**A**) 5β-Reductase, (**B**) 11β-HSD1, (**C**) 3α-HSD and (**D**) 5α-Reductase 1 was quantified by Taqman® real-time PCR and values are expressed as a ratio to the house keeping gene Cyclophilin A using the Standard Curve method. Data are expressed as mean±SEM ;n=8 per group; p=ns.

5.4.2.2 Urinary metabolites

Animals receiving FF tended to excrete more total metabolites of corticosterone ($p=0.06$) in their urine, primarily due to an increase in 5β-reduced metabolites ($p<0.05$; Table 5.2). A compensatory change was not observed in the excretion of 5α-reduced corticosterone metabolites (Table 5.2). Changes in 11β-HSD1 could not be inferred due to an inability to detect 11-dehydrocorticosterone (A) metabolites within the urine.

5.4.2.3 Glucocorticoid sensitive genes

Abundance of mRNA for the glucocorticoid-sensitive genes angiotensinogen (0.61±0.02 FF *vs* 0.61±0.03 FF/CDCA AU; p=ns), TAT (0.72±0.08 FF *vs* 0.83±0.13 FF/CDCA AU; p=ns) and PEPCK (0.81±0.22 FF *vs* 0.63±0.14 FF/CDCA AU; p=ns) were not altered in FF animals compared to Control (FF/CDCA) treated animals.

5.5 Discussion

The primary aim of this Chapter was to investigate the impact of bile acid depletion on glucocorticoid metabolism and HPA axis activation. In order to achieve this, animals were fed a synthetic fat-free diet devoid of any cholesterol or fat. This diet reduces hepatic cholesterol synthesis by 65% and bile acid biosynthesis by 63% (Bertolotti *et al.* 1995). In addition recirculation of bile acids along the entero-hepatic axis is delayed due to reduced functional need. Supplementation of the fat-free diet with the bile acid CDCA (1% w/w) enabled glucocorticoid metabolism to be investigated in the presence and absence of bile acids thus providing a model in which to investigate fully the impact of bile acids on glucocorticoid metabolism and HPA axis activation.

The model utilised in this study achieved the required goal as shown by the induction of CYP7A1 mRNA and rise in plasma and faecal bile acid concentration on which were reversed when bile acids were replaced to the diet. However, when considering the findings of this model it is important to consider the impact of the fat-free diet alone on physiological and biochemical parameters. Table 5.2 shows a comparison of the health of animals fed a Standard chow diet (Control animals) from Chapter 4 and the FF animals from this study.

The major differences seen between rats receiving the FF diet and those receiving normal chow were in triglyceride levels (elevated in both plasma and liver) and NEFAs (elevated in plasma). In spite of an increase in triglycerides however, glucose and insulin levels were suppressed in FF animals. This may be attributable to the absence of fat in the diet as triglycerides are normally broken down to fatty acids and monoglycerides by lipases within the intestine during lipolysis. In support of this plasma free-fatty acids (NEFA) were elevated in FF animals compared to Control animals. Replacing bile acids into the diet (FF/CDCA) reversed the changes in plasma and hepatic triglyceride levels whilst plasma NEFA levels were reduced again suggesting that changes in lipolysis are due to the impact of the fat-free diet.

As observed in Chapter 4 bile acids had a major impact upon glucocorticoid metabolism. Animals receiving the FF (bile acid depeleted) diet had elevated levels of 5β-reduced metabolites within their urine which was reversed when CDCA was

added to the diet. In addition, activity of hepatic 5β-reductase was suppressed in FF/CDCA treated animals only when assayed with a low concentration of substrate (25nM). These findings support those obtained in Chapters 3 and 4; namely that bile acids act as competitive inhibitors of hepatic 5β-reductase.

Although the majority of changes in glucocorticoid metabolism mirror those obtained in Chapter 4 there are some inconsistencies which must be considered.

1) Administration of the FF diet supplemented with CDCA did not influence activity of 11β-HSD1. On a background of normal chow however, CDCA acted as potent competitive inhibitor of 11β-HSD1. Interestingly, stimulating bile acid synthesis with cholestyramine also had no impact upon 11β-HSD1 activity. These findings may reflect the change in absolute levels of bile acids achieved within the hepatocytes although this would be hard to measure. 11β-HSD1 is located in the endoplasmic reticulum of the cell which is not easily accessible to bile acids due to the absence of specific bile acid transporters. In support of this hypothesis hepatic bile acid levels were unaltered in FF/CDCA and cholestyramine treated animals. It is possible that on a background of normal chow, supplementation of the diet with bile acids induced hepatotoxicity damaging intracellular organelles and allowing bile acids to gain entry to the ER. Thus only in CDCA-treated animals in Chapter 4 where bile acid levels are elevated above physiological levels is 11β-HSD1 activity inhibited. In it interesting to note that in the absence of changes in 11β-HSD1 a difference in transcription of GR sensitive genes was not observed.

2) Experimental manipulation of the HPA axis was not performed in this protocol, however, "basal" activity was assessed by comparing urinary corticosterone metabolites. The production of corticosterone metabolites within 24 hour urine samples were greater in FF animals compared to both FF/CDCA and animals fed a diet of standard chow (Control animals describded in detail in Chapter 4). This may reflect the removal of metabolic suppression imposed upon 5β-reductase by bile acids and suggest that bile acids produced due to ingestion of a normal chow diet exert a moderate inhibitory effect upon enzyme activity.

3) Adrenal weight was unaltered in FF fed animals after correction for body weight despite a rise in circulating corticosterone levels. In contrast, Chapter 4 CDCA-supplemented animals had smaller adrenal glands but maintained the level of

corticosterone within the circulation. It is not clear why circulatory levels of corticosterone were altered in the FF paradigm and not in the normal chow diet, but it may reflect a resetting of the HPA axis in FF animals, as in both cases these changes were accompanied by an increase in bile acids. It should be noted that the increase in corticosterone concentrations observed in FF compared to FF/CDCA animals was small and the FF animals were less accustomed to handling than those used in Chapter 4. Therefore the small rise in circulatory corticosterone levels may reflect a differential result of stress.

4) Although a comparison has been made between basal corticosterone levels, to assess HPA axis response it is perhaps more appropriate to compare corticosterone levels of FF animals at cull with those obtained from animals examined in Chapter 4 immediately post stress. The fat-free diet in itself could be viewed as a "stressor" thus the rise in circulating corticosterone levels may reflect delayed glucocorticoid clearance due to chronic inhibition of 5β-reductase. Indeed, the prolonged corticosterone peak following acute restraint stress in CDCA treated animals on a normal chow background would support this idea. In CDCA supplemented animals on standard chow diet, reduced clearance due to inhibition of 5β-reductase and lower regeneration due to inhibition of 11β-HSD1 may suppress HPA axis responsiveness, thus accounting for the reduction in adrenal size and maintenance of circulating corticosterone levels in these animals.

The *de novo* synthesis of cholesterol accounts for approximately 50% total body cholesterol production, with diet contributing only a small proportion (~5-10%). Rodents have a high rate of *de novo* cholesterol synthesis which can be acutely regulated in order to maintain cholesterol homeostasis. When given a cholesterol free diet, rodents increase *de novo* synthesis as shown by enhanced activation of HMG-CoA reductase to maintain cholesterol homeostasis. Although hepatic HMG-CoA reductase levels were not assessed in this study, plasma cholesterol and HDL cholesterol (the most prevalent form in the rat) were comparable between FF and Control animals in Chapter 4 indicating that FF animals had achived cholesterol homeostasis.

In summary, the work in this chapter provides further evidence supporting a regulatory role for bile acids in glucocorticoid metabolism. Withdrawl of bile acids

from the diet reverses the inhibiton imposed upon 5β-reductase as demonstrated by enhanced enzyme acitivty and a rise in the urinary excretion of 5β-reduced glucocorticoid metabolites. These changes are also reflected in the lipid profile of bile acid depeleted animals where plasma cholesterol levels comparable with animals fed a standard chow diet. Importantly, supplementing the FF diet with CDCA induces changes in the glucocorticoid and lipid profile analogous to those observed in CDCA supplemented animals in Chapter 4, supporting the hypothesis that bile acids act as inhibitors of glucocorticoid metabolism.

Chapter 6

Impact of bile acids on the renin-angiotensin-aldosterone-system

6.1 Introduction

The experiments described in this thesis so far provide evidence of a novel role for bile acids in the regulation of glucocorticoid metabolism. Bile acids have been shown to act as potent competitive inhibitors of steroid metabolism catalysed by 5β-reductase and 11β-HSD1, *in vitro* both in tissue homogenates and cultured cells (Chapter 3). These findings have been recapitulated *in vivo* by increasing hepatic bile acid content through supplementation of the diet with CDCA or by stimulating bile acid synthesis with the bile acid sequesterant cholestyramine (Chapter 4). Moreover, administration of a fat-free diet incurred the same impact upon glucocorticoid metabolizing enzymes (Chapter 5). The impact of bile acids on other steroidogenic tissues and steroid hormone production and metabolism however, has not been addressed.

In addition to catalyzing the reduction of corticosterone, the A-ring reductases (5α- and 5β-reductase and 3αHSD) are also involved in the reduction of aldosterone. It is possible that dietary manipulation of the bile acid pool may impact upon aldosterone synthesis and/or metabolism with consequences for the associated renin-angiotensin-aldosterone system (RAAS). In support of this, previous work has demonstrated that bile acids inhibit the 5β-reduction of aldosterone (Latif *et al.* 1994). This in turn would lead to suppression of the RAAS and hence activation of MR. Similarly, the licorice derivative glycerrhytinic acid (GA), acts as a potent inhibitor of 5β-reductase and 3α-HSD resulting in the accumulation of aldosterone and 5α-dihydroaldosterone (5α-DHAldo) which act as potent mineralocorticoids (Latif *et al.* 1990). Bile acids may also influence the RAAS through inhibition of 11β-HSD2 (Morris *et al.* 2004; Gomez-Sanchez *et al.* 1996). Illicit activation of MR due to 11β-HSD2 inhibition may contribute towards the sodium retention and potassium excretion observed in patients with biliary obstruction (Stauffer *et al.* 2002) and cirrhosis (Quattropani *et al.* 2001). Previous work using a rodent model of chronic biliary cirrhosis, the bile-duct-ligated (BDL) rat demonstrated that disruption of bile acid flow and the enterohepatic circulation has a major impact on blood pressure with animals having portal hypertension and hypokalemia (Martinez-Prieto

et al. 2000), corroborating the hypothesis that bile acids may also impact upon the RAAS.

However, bile acids may also exert direct effects upon the adrenal gland. Steroid hormones such as corticosterone and aldosterone are synthesized from the common precursor cholesterol within distinct zones of the adrenal cortex. Corticosterone is synthesized primarily within the zona fasciculata (and to a lesser degree within the reticularis) by 11β-hydroxylase (CYP11B1). Aldosterone, a potent mineralocorticoid, is synthesized solely within the zona glomerulosa. CYP11B1 and CYP11B2 genes encode 11β-hydroxylase and aldosterone synthase that catalyse the final steps in the biosynthesis of corticosterone and aldosterone respectively. As the adrenal gland is the primary source of steroid hormones, defects in substrate (cholesterol) supply and/or utilization may have a major impact upon adrenal steroidogenesis.

The experiments presented in this chapter describe detailed analysis of cholesterol uptake and distribution within the adrenal glands of bile acid treated rats and the impact that bile acids have on the RAAS.

6.2 Research aims

The aims of the research in this chapter were:

1. To assess the effect of bile acids on renal function i.e. urinary electrolyte balance and the associated indices of the renin-angiotensin-aldosterone system (RAAS).
2. To investigate the effect of bile acids on 11β-HSD2 activity in the kidney.
3. To investigate the effect of bile acids on adrenal function and morphology.

6.3 Materials and methods

6.3.1 Animals and animal maintenance

Animals examined in this study were those used in Chapters 4 and 5. Animals were maintained according to the procedures described in section 2.3.1

6.3.2 Dietary manipulation

Animals received diets described fully in section 4.3.2 and section 5.3.2. The Na^+ and K^+ contents of normal and fat-free chow are Control: 0.3% Na^+ and 0.6% K^+ Fat-free: 0.1% Na^+ and 0.36% K^+ respectively.

6.3.3 Metabolic cages

After 3 weeks on their respective diets, animals were placed into metabolic cages for 7 days as described fully in section 4.3.3. Faeces and urine were collected over the final 72 hours and stored a -20°C for subsequent analysis. The animals were then placed back into their original cages for at least one day prior to sacrifice.

6.3.4 Animal sacrifice and tissue collection

Animals were killed by surgical decapitation and tissue and blood samples collected and stored as described in section 2.3.2.

6.3.5 Analysis of enzyme activity

Renal 11β-HSD2 activity was determined from whole tissue homogenates as described in section 2.8.5. Steroid products were quantified by HPLC as described in section 2.9.1.

6.3.6 Analysis of plasma hormones and intermediate metabolites

Renin activity was determined by RIA for angiotensin I as described in section 2.4.3. Plasma aldosterone was measured by ELISA using a commercially available kit (Coat-a-Count®, DPC, Gwynedd, UK) as described section 2.4.4.

6.3.7 Analysis of urinary electrolytes

Urinary sodium and potassium was measured from sample specimens (1ml from the final day of collection) by dry-slide chemistry using a Vitros® analyzer. This analysis was performed Dr P Ashby, Department of Clinical Biochemistry, Western General Hospital, Edinburgh.

6.3.8 Quantification of target gene abundance

Transcript abundance of adrenal SR-B1 and HMG Co-A reductase were measured using Taqman® real-time PCR as described in section 2.13.1. Abundance of adrenal aldosterone synthase (CYP11B1) and 11β-Hydroxylase (CYP11B2) was measured by LightCycler® real-time PCR as described section 2.13.2.

6.3.9 Adrenal gland preparation

Adrenal glands were removed and cleaned of any residual adipose tissue. The left adrenal gland was fixed in formalin for 24 hours and then transferred into 70% ethanol solution for histological preparation as described in section 2.14.1. The right gland was snap-frozen on dry ice and stored at -80^{0}C.

6.3.10 Adrenal gland histology

To examine the morphology of the adrenal gland, sections were stained with Hematoxylin and Eosin (H and E) as described in section 2.14.2. To examine lipid

accumulation cryostat sections from frozen adrenals were stained with Oil red O, a neutral lipid stain as described fully in section 2.14.3.

6.3.11 Statistical analysis

Individual experiments were conducted using tissues from 8 independent animals per group (unless otherwise stated). Each assay was performed duplicate and the mean of each duplicate taken as the final value for that individual animal. The data represent the mean ± standard error of the mean (SEM). When three groups were studied, data were analysed by one-way ANOVA followed by post hoc least squared difference tests. When two groups were studied, data were analysed by Students t-tests. All analysis was performed using Statistica (Version 9) or Graphpad Prism (Version 4). The following nomenclature was used to denote significance *$p<0.05$ *vs* Control or FF/CDCA; **$p<0.01$ *vs* Control or FF/CDCA.

6.4 Results

6.4.1 Impact of bile acids on fluid and electrolyte balance

The impact of bile acids on fluid and electrolyte balance are summarized in table 6.1.

	Control	CDCA	CT	FF	FF/CDCA
Fluid Intake (ml/g BW)	0.142±0.006	0.162±0.009*	0.141±0.007	0.089±0.006*	0.145±0.017
Food Intake (g/g BW)	0.108±0.002	0.105±0.002	0.114±0.003	0.085±0.002	0.095±0.004
Urine volume (ml/g BW)	0.041±0.002	0.051±0.006	0.057±0.002*	0.032±0.003	0.047±0.008
Faeces (wet wt g/g BW)	0.051±0.005	0.063±0.003	0.051±0.003	0.0078±0.0005*	0.057±0.012
Urinary Na^+ (mmol/ml)	22.8±1.7	19.3±1.6	21.3±1.5	2.87±0.31*	1.39±0.51
Urinary K^+ (mmol/ml)	34.0±2.5	42.7±2.9	29.9±2.6	5.28±0.46	4.68±1.12
Na:K	0.68±0.04	0.45±0.02**	0.71±0.04	0.54±0.02**	0.28±0.028

Table 6.1 Impact of bile acids on fluid and electrolyte balance. Data represent mean±SEM corrected for body weight; n=8; **p<0.001 *vs* Control or FF/CDCA, *p<0.05 *vs* Control or FF/CDCA

Supplementation of the diet with CDCA (both Control and FF) increased fluid intake. This was accompanied by a rise in the weight of faecal matter produced. Food intake was unaltered by dietary manipulation.

Urinary sodium (Na^+) and potassium (K^+) excretion was greater than 10 higher in Control animals compared to those receiving FF chow, and is likely to be associated with different dietary electrolytes between the two diets. Sodium and potassium content was approximately 3-fold lower in the FF diet (Standard diet: 0.3% Na and 0.6% K compared to 0.1% Na and 0.36% K for FF diet). The estimate of sodium and potassium content of Standard diet is only an approximation as manufacturers indicate that there are likely to be batch variations. Bile acids caused a similar net reduction in urinary sodium excretion. However, as baseline sodium excretion was much higher with the Standard diet the net difference was not statistically significant. Potassium excretion tended to be increased with CDCA treatment but again the effect was not statistically significant. The ratio of urinary sodium to potassium (Na:K) was reduced by CDCA in both control and FF diets. Urinary Na:K values are widely used as an indicator of mineralocorticoid activity. In contrast, cholestyramine did not influence urinary electrolyte excretion. Fluid turnover was increase by both CDCA and cholestyramine.

6.4.2 Impact of bile acids on the renin-aldosterone system

The effects of CDCA and cholestyramine treatment on renin and aldosterone are shown in Table 6.2. Overall FF fed animals had higher levels of both aldosterone and renin than those fed a Control chow, again reflecting the electrolyte content of the FF diet; a low sodium diet is well known to activate the renin-angiotensin system. CDCA in rats fed a Standard control diet increased plasma aldosterone concentration 3.8 fold (Table 6.2). This increase was not caused by activation of the renin-angiotensin system as renin activity was unaltered. Animals receiving FF diet also demonstrated increased concentrations of aldosterone but this was commensurate with activation of the renin-angiotensin system. Cholestyramine did not influence plasma aldosterone or renin levels (Table 6.2).

	Control	CDCA	CT	FF	FF/CDCA
Aldosterone (pg/ml)	70.0±14.8	265.2±64.7*	92.5±30.1	220.6±12.7*	350.1±21.2
Renin (ng/ml/hr)	2.29±0.32	1.77 ±0.34	3.45±0.75	15.2±1.52*	24.1±3.93
ARR	38.3±14.9	160.9±52.1*	35.9±9.9	14.9±2.06	14.8±2.33

Table 6.2 Impact of bile acids on the renin-angiotensin-aldosterone system. Data are mean±SEM; n=8,*p<0.05 *vs* Control or FF/CDCA. ARR = aldosterone:renin ratio

6.4.3 Transcript abundance of adrenal target genes

Aldosterone is synthesized from cholesterol within the zona glomerulosa of the adrenal gland culminating in a reaction catalysed by the enzyme aldosterone synthase (CYP11B2). Transcript abundance of CYP11B2 mRNA was higher in rats fed the FF diet compared to those receiving Standard chow. This difference was exaggerated by CDCA treatment. In contrast, supplementation of Standard control diet with CDCA did not affect CYP11B2 nor plasma renin activity. This reinforces the earlier suggestion that the effects of CDCA on aldosterone are in part independent of the RAAS. Overall, CYP11B1 expression was down-regulated by CDCA in rats fed either Standard control or FF diet. Again CYP11B1 mRNA abundance was not affected by cholestyramine. Lower CYP11B1 expression is consistent with reduced adrenal weights (CDCA treated animals Chapter 4) and urinary 5β-THB excretion (CDCA, CT Chapter and FF/CDCA animals Chapter 5) and probably reflects reduced HPA drive and ACTH stimulation.

	Control	CDCA	CT	FF	FF/CDCA
CYP11B1 ($x10^7$ copy no./μg RNA)	9.13±0.90	7.01±0.74*	8.75±0.16	8.14±1.59*	4.40±0.43
CYP11B2 ($x10^6$ copy no./μg RNA)	1.37±0.14	1.45±0.12	1.41±0.23	8.02±1.45*	15.8±2.4

Table 6.3 Impact of bile acids on the 11β-hydroxylase (CYP11B1) and aldosterone synthase (CYP11B2) gene transcription. mRNA abundance was quantified by Light-cycler real-time PCR Data are mean±SEM; n=8,*p<0.05 *vs* Control or FF *vs* FF/CDCA.

6.4.4 Impact of bile acids on 11β-HSD2 activity

The activity of 11β-HSD2 within whole kidney homogenates was significantly reduced in animals fed normal chow supplemented with either CDCA or cholestyramine (Figure 6.1 A). These findings were recapitulated in FF animals (Figure 6.1 B) with CDCA supplementation of fat-free diet inhibiting 11β-HSD2 activity by approximately 35%.

A

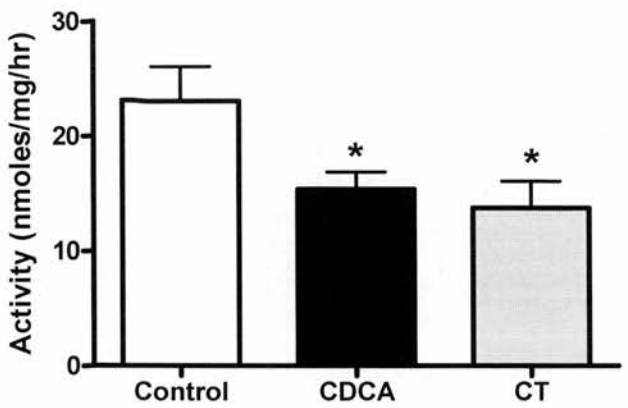

B

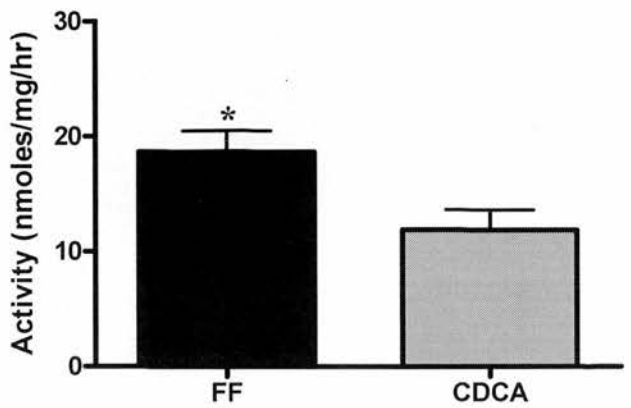

Figure 6.1.11β-HSD2 activity following dietary manipulation. Activity of 11β-HSD2 was reduced by (**A**) CDCA and cholestyramine (CT) and (**B**) CDCA supplementation of a fat-free (FF) diet when assayed with corticosterone (1μM). Data are mean±SEM; n=8;*p<0.05 *vs* Control or FF *vs* FF/CDCA.

6.4.5 Impact of bile acids on adrenal gland morphology

Having observed differences in the RAAS of bile acid treated animals in Chapter 4, a comprehensive study of adrenal gland morphology and lipid accumulation from FF and FF/CDCA animals was performed.

Histological examination of FF and FF/CDCA adrenal glands revealed a difference in the size of zones of the adrenal cortex with a small but significant increase in the size of cells within the inner zona fasiculata in FF animals (Figure 6.2).

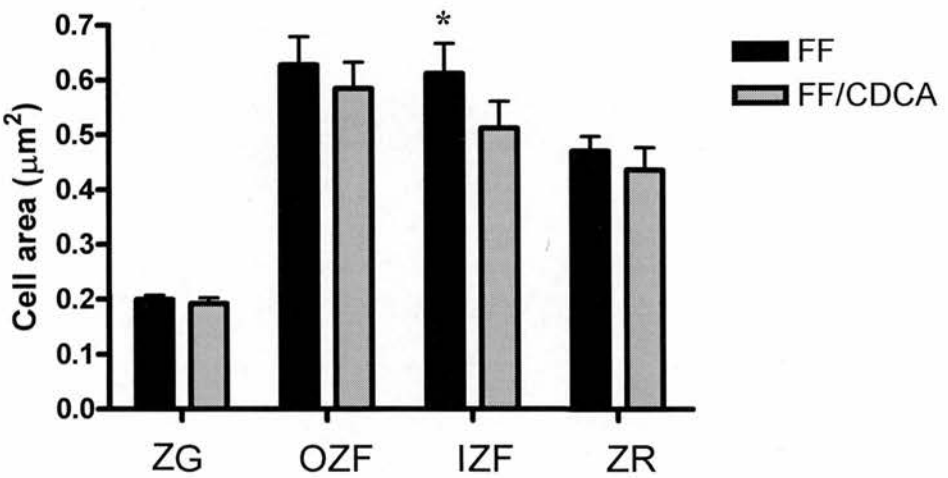

Figure 6.2. Size of zones within the adrenal cortex following dietary manipulation. The size of cell in each zone of the adrenal cortex was measured under x40 magnification by counting the number of cell nuclei in a set area. Cell size was calculated by dividing the total area measured number of nuclei within that area. ZG=Glomerulosa; OZF=Outer zona fasiculata; IZF=Inner zona fasiculata; ZR=zona. Data are mean±SEM; n=6; *$p<0.05$ *vs* FF/CDCA

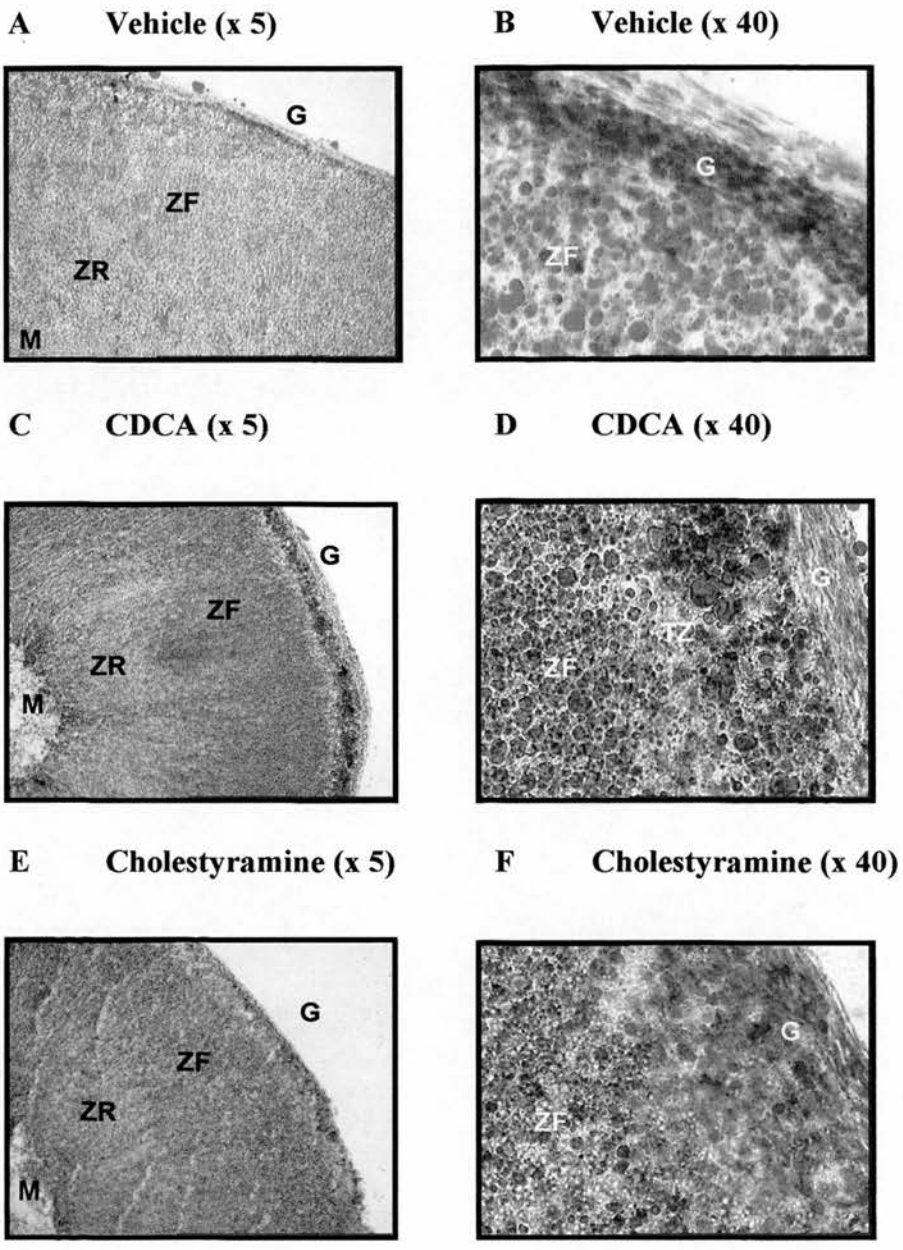

Figure 4.6 Lipid accumulation within the adrenal gland following dietary manipulation. Serial transverse sections (30μM) were cut from the left adrenal gland and stained with the neutral lipid stain Oil red O. G=glomerulosa, ZF=zona fasiculata, ZR=zona reticularis, M=medulla, TZ=zone of transition.

6.4.6 Gene transcript abundance

Transcript abundance of SR-B1, which mediates the selective uptake of cholesterol esters (CE) from HDL within the liver and adrenal glands, was enhanced in FF adrenal glands (Figure 6.4 A), whilst HMG-CoA reductase gene abundance, the rate determining step in cholesterol synthesis was suppressed in FF animals (Figure 6.4 B)

A

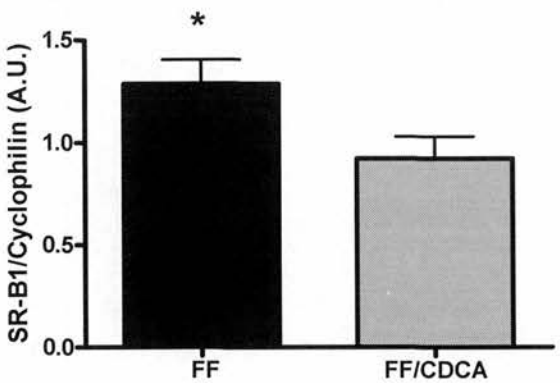

B

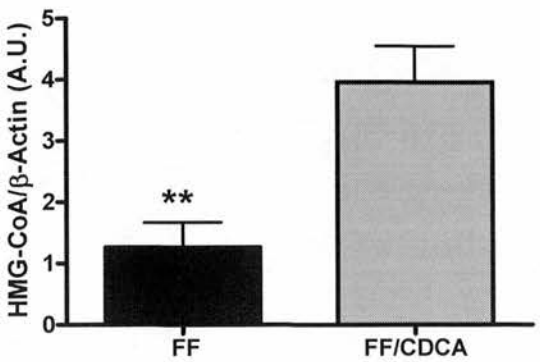

Figure 6.4 Transcript abundance of (**A**) SR-B1 and HMG-CoA reductase following dietary manipulation. mRNA abundance was quantified by Taqman real-time PCR and values are expressed as a ratio to the house keeping gene β-Actin or cyclophilin A. Data are expressed as mean±SEM, n=8 per group;*$p<0.05$ *vs* FF; **$p<0.01$ *vs* FF/CDCA.

6.5 Discussion

The data presented in this chapter provide evidence of an additional role for bile acids in regulation of the renin-angiotensin system (RAAS). Supplementation of both Standard chow and a synthetic fat-free diet (FF/CDCA) with CDCA induced sodium retention concomitant with a reduction in potassium excretion resulting in a fall in the overall sodium to potassium ratio. Plasma aldosterone levels were increased in both CDCA-treated groups, albeit through different mechanisms. In general in FF animals, the rise in plasma aldosterone was accompanied by an increase in renin activity indicating activation of the renin angiotensin system. This was probably due to the low sodium diet and was exaggerated following administration of CDCA. In contrast, renin activity was unaltered in animals receiving the standard diet supplemented with CDCA or cholestyramine. Moreover, CYP11B2 transcript abundance within the glomerulosa was elevated in CDCA-treated FF animals (FF/CDCA) but not in those receiving bile acids on a standard diet. In addition, 11β-HSD2 activity within the kidney was significantly reduced in both bile acid and cholestyramine treated groups. Alterations in lipid accumulation within the adrenal gland were apparent in FF/CDCA animals. These changes were most evidennt within the zona glomerulosa, the outer most region of the adrenal cortex with lipid droplets being smaller and more dispersed. Intruigingly, transcript abundance of SR-B1, the predominant HDL cholesterol transporter within the adrenal gland was down-regulated in FF/CDCA animals whilst that of HMG CoA reductase was enhanced. These findings suggest that bile acids may also alter lipid uptake, synthesis and/or metabolism within the adrenal gland.

The kidney represents one of the most important sites of renin production and release in response to sympathetic stimulation (acting via β_1-adrenoceptors), renal artery hypotension, and decreased sodium delivery to the distal tubules. Angiotensinogen (ANG) is a vasodilatory peptide which is synthesized predominantly within the liver. Proteolytic cleavage of ANG by renin results in the formation of the decapeptide angiotensin I. This in turn acts as the substrate for angiotensin converting enzyme (ACE) which is highly abundant in vascular endothelium, particularly within the lungs. ACE cleaves off 2 amino acids resulting

in the formation of the octapeptide angiotensin II (AII). Angiotensin II acts upon the zona glomerulosa inducing the synthesis of aldosterone. Aldosterone is synthesized from cholesterol within the zona glomerulosa of the adrenal gland by a series of enzymes culimating in the conversion of corticosterone to aldosterone. This reaction is catalysed by the enzyme aldosterone synthase (CYP11B2) in response to hormonal stimulation in the form of AII and ACTH and /or a drop in Na^+ ions and/or rise in K^+ ions within the blood (Ye *et al.* 2003). The elevated levels of CYP11B2 in the adrenal glands of FF/CDCA are likely to be induced in response to the low Na^+ content of the diet. The fact that both CDCA-treated groups had elevated plasma aldosterone levels whilst only those receving the FF/CDCA diet showed alterations in CYP11B2 expression indicate aldosterone synthesis is not the sole factor contributing to the rise in plasma aldosterone.

The function of renal MR is clearly evident in the rare syndrome of "Apparent Mineralocorticoid Excess" (AME) where individuals present with hypertension, hypokalemia and sodium retention together with low plasma aldosterone and low plasma renin activity (Shackleton & Stewart 1990). Similar symptoms e.g. hypertension, hyperkalaemia and suppression of plasma renin activity and aldosterone, manifest following ingestion of large amounts of liquorice. Although these side effects were initially attributed to the direct activation of MR, it has since been demonstrated that glycyrrhetinic acid (GA), the active component of liquorice, acts as a potent inhibitor if 11β-HSD2 activity, thus allowing binding of active glucocorticoids to MR. There is also evidence demonstrating bile acids as inhibitors of 11β-HSD2 in tissue homogenagtes (Morris *et al.* 2004) and cell cultures (Gomez-Sanchez *et al.* 1996). The inhibition of 11β-HSD2, resulting in illicit activation of MR by glucocorticoids plays a role in hypertension due to enhanced Na^+ re-absorption and K^+ excretion (Stewart *et al.* 1987; Monder *et al.* 1989).

The data described in this chapter corroborate these findings with bile acid supplementation of both normal chow (normal chow/CDCA) and a fat-free diet (FF/CDCA) causing a marked reduction in renal 11β-HSD2 activity. In keeping with these findings, a reduction in urinary sodium and an overall decrease in the sodium: potassium ratio (used as an indicator of mineralocorticoid activity) was observed in in animals fed a diet supplemented with CDCA (both standard and fat-free).

Although blood pressure was not measured in this study, the data described here showing a reduction in Na^+: K^+ ratio would suggest that bile acid treated animals may be mildly hypertensive. Indeed, systolic blood pressure is elevated in male Wistar rats following treatment with cholic acid (Wu *et al.* 1999).

In contrast cholestyramine had no impact upon urinary electrolyte levels which again may relate to the concentration of bile acids within the circulation, which were elevated in CDCA-treated animals but not in those receving cholestyramine.

In vitro, cortisol-induced nuclear translocation of MR has been demonstrated following the treatment of HEK293 transfected with human 11β-HSD2 and tagged MR cells with increasing concentrations of bile acids, specifically CDCA (Quattropani *et al.* 2001). This may predict elevated blood pressure and suppression of renin (Kenyon *et al.* 1984). In vivo, continuous infusion of CDCA to Sprague-Dawley rats induced hypertension which persisted over the 14 day duration of the experiment (Morris & Souness 1996). Likewise, bile-acid-dependent inhibition of 11β-HSD2 is thought to be partly responsible for the sodium retention and potassium excretion observed in patients with biliary obstructive disease (Stauffer *et al.* 2002). In addition, the hypokalemia and hypertension induced following ligation of the common bile duct in the rat may in part be attributable to bile acid induced inhibition of 11β-HSD2 (Thiesson *et al,* unpublished data). The fact that CDCA reduced renal 11β-HSD2 activity whilst simultaneously increasing aldosterone is paradoxical. One may normally anticipate aldosterone levels to fall as a consequence of reduced activation of the RAAS when 11β-HSD2 is inhibited as demonstrated in sufferers of AME (Phillipou *et al.* 1996). Interestingly, plasma concentrations of aldosterone were 3-fold greater in FF/CDCA animals compared to those receiving standard chow perhaps reflecting differences in electrolyte content of the diet. Indeed the sodium and potassium content of the FF diet was approximately 3-fold lower than those of standard control diet (control diet: 0.3% Na and 0.6% K *vs* 0.1% and 0.36% for FF diet). Sodium depletion is a potent stimulant of the RAAS, indeed a low sodium diet increased CYP11B2 abundance 57-fold within the adrenal glands of male Wistar rats (Ye *et al.* 2003). Therefore, although plasma aldosterone was increased in both CDCA-treated groups compared to controls, the mechanisms through which this was

induced differ. Plasma renin activity was enhanced in FF/CDCA animals but not in those receiving a normal chow suggesting that in the presence of normal dietary salt the impact of CDCA on plasma aldosterone was independent of the renin angiotensin system. Furthermore, transcript abundance of aldosterone synthase (CYP11B2) the enzyme responsible for aldosterone synthesis was up-regulated in FF/CDCA animals but unchanged in animals fed a standard chow diet supplemented with CDCA supporting the hypothesis that changes in circulating aldosterone induced by bile acids are in part independent of the renin angiotensin system. In summary on normal chow, CDCA caused sodium retention through mechanism independent of the RAAS, perhaps related to impaired inactivation and increased synthesis of aldosterone.

Theoretically, the increase in aldosterone could have been due to reduced clearance of aldosterone, stimulation by other factors (e.g. ACTH or plasma potassium) or greater provision of cholesterol substrate. Reduced clearance occurs with bile-acid-induced inhibition of aldosterone metabolism which may be extrapolated from a reduction in urinary 5β-reduced corticosteroid metabolites. Furthermore, a study performed by Latif in the early 1990's demonstrated the bile acids inhibit aldosterone metabolism catalysed by 5β-reductase (Latif *et al.* 1994). It is unlikely that ACTH is a contributory factor since adrenal weight and HPA activity (see Chapter 4) tended to be reduced not increased in bile acid treated animals. However, cholesterol availability could be an important factor since plasma HDL (the main source of cholesterol for adrenal steroidogenesis in rodents) was increased. Histological examination of the adrenal glands of FF and FF/CDCA animals revealed that bile acid treatment may also interfere with cholesterol uptake and utilization. When stained with Oil-red O, a neutral lipid stain which is commonly used to identify cholesterol, lipid droplets appeared smaller and more numerous within the zona glomerulsoa of CDCA treated animals. Furthermore, a sudanophobic region or "zone of transition" where no lipids were present was evident between the zona glomerulosa and reticularis in the adrenal glands of bile acid treated animals only. This would suggest that bile acids may interfere with cholesterol uptake and/or accumulation within the adrenal gland. The emulsifying properties of bile acids may

have contributed towards the reduction in size of lipid droplets within the adrenal glands of CDCA treated animals.

To understand the mechanisms of altered lipid accumulation within the adrenal gland, factors influencing cholesterol uptake and *de novo* synthesis were investigated. Transcript abundance of SR-B1, the principal HDL transporter in the adrenal gland was reduced in FF/CDCA treated animals which may be anticipated as SR-B1 is an FXR suppressible gene (Malerod *et al.* 2005). These findings argue against lipid accumulation however, as this change would impede cholesterol uptake into the adrenal. It has been demonstrated that adenovirus-mediated hepatic overexpression of SR-B1 on both the sinusoidal and canalicular surfaces of the hepatocyte results in a marked increase in biliary cholesterol and the virtual disappearance of plasma HDL. In addition, SR-B1 attenuate (att) mice which carry a mutation within the promoter of the SR-B1 gene show a reduction in the hepatic uptake of HDL-cholesterol esters (HDL-CE) (Wang & Carey 2002). Moreover, SR-B1 knock-out (KO) mice show impaired biliary cholesterol secretion and increased plasma cholesterol concentrations in large apolipoprotein A-1-containing particles and a low adrenal gland cholesterol content (Altmann *et al.* 2002). HDL-CE clearance from the blood stream is markedly reduced in SR-B1 KO mice while liver and adrenal uptake, are attenuated. The elevated levels of HDL cholesterol and suppression of hepatic and adrenal SR-B1 in FF/CDCA (Chapter 5) treated animals corroborate these findings. Recent studies suggest that the nuclear receptor farensoid X receptor (FXR) may play a role in mediating these effects. $FXR^{-/-}$ mice exhibit reduced expression of hepatic genes involved in reverse cholesterol transport, most notably, that for SR-BI (Lambert *et al.* 2003). Attenuation of SR-B1 gene abundance within the liver is thought to be mediated via the induction of SHP which acts as a negative nuclear receptor induced by FXR, thus by inducing the expression of SHP, LXR/RXR and LRH-1 mediated transactivation of SR-B1 is reduced (Malerod *et al.* 2005). Whether or not bile acids exert their effect on adrenal SR-B1 via the same mechanism is as yet unknown, however the adrenal gland does express both FXR and LRH-1 (Francis *et al.* 2003; Zhang *et al.* 2006) thus a similar mechanism may be at work. It is important to note however that there are at least 2 variants of SR-B1 expressed in the adrenal; SR-B1 and a splice variant SR-B11 which differs from SR-

B1 by an entirely different C-terminal cytoplasmic tail (Webb *et al.* 1998). Transcript abundance of SR-B11 accounts for approximately 30% of the total SR-B1 mRNA in the mouse adrenal (Webb *et al.* 1997). It is possible that the primer sequence used to detect SR-B1 in this study is targeted towards region of the gene common to both transcripts. It is not known whether SR-B1 and SR-BII are expressed differentially across the zones of the adrenal gland and it is still possible that one transcript was upregulated specifically within the zona glomerulosa. A more likely explanation of the increase in cholesterol within the zona glomerulosa is due to the stimulation of HMG CoA-reductase in FF/CDCA animals. This would imply increased *de novo* biosynthesis of cholesterol. The rat is known to have a high rate of *de novo* cholesterol synthesis which enables the animal to maintain cholesterol homeostasis when faced with a cholesterol depleted diet. Whether or not induction of HMG Co-A reductase is related to the fall in SR-B1 transcript abundance is as yet unknown but it is possible that HMG Co-A reductase is enhanced in an attempt to maintain cholesterol homeostasis within the adrenal gland, irrespective of whole body cholesterol levels.

It is interesting to note that cholestyramine did not influence urinary electrolytes or the RAAS, despite reducing activity of 11β-HSD2, again supporting a more complex role for bile acids in regulation of the RAAS. In addition, cholestyramine did not induce changes in adrenal morphology or CYP11B1/2 expression. These findings may relate to the overall level of bile acids achieved within by each diet as the level bile acids within the circulation of cholestyramine treated animals were comparable to control animals. In a similar manner, hepatic 11β-HSD1 activity was only affected in animals where bile acids were administered over and above those synthesised naturally.

In summary the findings of the work in this chapter provide evidence for an additional role for bile acids in regulation of the RAAS, over and above inhibition of 11β-HSD1, perhaps causing bile acid treated animals to be hypertensive. Furthermore, bile acids may impact upon cholesterol uptake and utilisation within the adrenal gland. It is therefore possible that steroid hormone synthesis *per se* and not just glucocorticoid synthesis and metabolism may be affected in that in conditions of elevated bile acids such as obesity, jaundice and biliary cirrhosis.

Moreover, inhibition of HMG Co-A reductase within the adrenal, which may be induced by statins frequently prescribed for hypercholesterolaemia may restrict cholesterol supply for adrenal steroidogenesis and alter blood pressure through a mechanism influencing aldosterone biosynthesis.

Chapter 7

Summary and future work

7.1 Summary and Future Work

The aims of this thesis were to assess the impact of bile acids on glucocorticoid metabolism and potential interaction between factors regulating cholesterol and glucocorticoid homeostasis. The work described in this thesis provides evidence that bile acids are competitive inhibitors of glucocorticoid metabolism mediated by 5β-reductase and 11β-HSD1 *in vitro* both in tissue homogenates and cultured cells. Inhibition occurred at a post-transcriptional level without changes in transcript abundance or protein. These findings were pursued *in vivo* in animal models of bile acid excess and bile acid depletion. In excess, bile acids were potent competitive inhibitors of glucocorticoid metabolism, altering HPA axis response as demonstrated by a prolonged corticosterone response following restraint stress. Converse findings on a fat-free (bile acid) depleted diet confirming could be reversed by bile acid supplementation confirming bile acids as the sole mediators of this inhibition. The inhibitory impact of bile acids was corroborated in model of chronic bile acid excess, the bile-duct-ligated rat, where enzyme activity was reduced 4 fold (McNeilly *et al* unpublished data). In parallel studies bile acids were demonstrated to alter the expression of key steroidogenic enzymes within the adrenal gland, primarily within the zona glomerulosa. These differences were associated with altered expression of aldosterone synthase and 11β-hydroxylase, suggesting a role for bile acids in aldosterone action and sodium: potassium regulation within the kidney.

Glucocorticoids regulate a myriad of metabolic and homeostatic processes including glucose and lipid metabolism within the liver and electrolyte balance within the kidney, the principal organs involved in glucocorticoid metabolism. Levels within the circulation are normally tightly regulated by a combination of HPA axis forward drive and glucocorticoid negative feedback. The importance of these regulatory systems can be exemplified in conditions where the mechanisms controlling glucocorticoid homeostasis are abnormal resulting in glucocorticoid excess in the case of Cushing's syndrome or glucocorticoid deficiency as in Addison's disease. Increasing evidence has supported a role for tissue-specific alterations in glucocorticoid metabolism and/or synthesis in cardiovascular disease

and in particular in the manifestation of idiopathic obesity. Obese humans and the Zucker rat (fa/fa) a model of obesity and insulin resistance display an altered glucocorticoid metabolic profile, with suppressed 11β-HSD1 activity within the liver and enhanced expression and activity within adipose tissue, primarily the subcutaneous tissue (Andrew *et al.* 1998; Livingstone *et al.* 2000; Rask *et al.* 2001). In addition, elevated expression and activity of the A-ring reductases (5α- and 5β-reductase) have been observed (Andrew *et al.* 1998; Andrew & Walker 2005). These changes cause an enhanced rate of glucocorticoid clearance, and compensatory activation of the HPA-axis, and the balance of A-ring reduction often favours 5α-reduction over that of 5β-reduction (although in this case 5α-reductase appears to be the predominant A-ring reductase). Insulin plays a key role in regulating 5α-reductase activity and expression as treatment of the Zucker rat with insulin sensitizing drugs such as metformin reverses these effects (Livingstone *et al.* 2005). Likewise, insulin increases the excretion of 5α-reduced cortisol metabolites in individuals with polycystic ovary syndrome (PCOS) independent of obesity (Tsilchorozidou *et al.* 2003). A number of key regulators of 11β-HSD1 have been proposed, including inflammatory cytokines (Tomlinson *et al.* 2001), diet (Drake *et al.* 2005), steroid hormones (Ricketts *et al.* 1998), peroxisome proliferator-γ (PPARγ) agonists (Berger *et al.* 2001), LXR agonists (Stulnig *et al.* 2002) and pharmacological agents such as carbenoxolone (Walker *et al.* 1995b) and the antidiabetic drug Arylsulfonamidothiazole (Barf *et al.* 2002). Factors controlling 5β-reductase activity and expression however remain elusive.

In addition to its involvement in glucocorticoid metabolism, 5β-reductase also plays a key role in bile acid biosynthesis. Indeed, mutations within 5β-reductase (SRD5B1) have been identified in 3 infants suffering from neonatal cholestatic liver disease. These infants excrete elevated levels of glycine and taurine conjugates of 7α-hydroxy-3-oxo-4-cholenoic acid and 7α,12α-dihydroxy-3-oxo-4-cholenoic acid within their urine and can be treated with CDCA or CA if liver disease is not too far advanced (Lemonde *et al.* 2003). In addition, a recent study has reported improved cholesterol absorption and cholesterol synthesis in patients with 5β-reductase deficiency following treatment with bile acids due to their role in the micellar

solubilisation of cholesterol within the lumen of the gut (Woollett *et al.* 2006). These studies indicate the important role that 5β-reductase plays in cholesterol and bile acid homeostasis. This thesis provides evidence that bile acid levels may also influence the hepatic activity of 11β-HSD1 and 5β-reductase and subsequently impact upon HPA axis activation and hepatic glucocorticoid regulated target genes.

Physiologically bile acids vary in a circadian manner. In rodents, both cholesterol and bile acid synthesis have marked diurnal rhythms that peak synchronously at midnight (Galman *et al.* 2005) thus the rate of hepatic glucocorticoid metabolism may be slower in the evening. To our knowledge the diurnal patterns of A-ring reduced metabolites have not been compared in the literature, although one would predict a reduction in 5β-reduced metabolites when hepatic bile acid synthesis was increased e.g. at night. Interestingly, in obesity the diurnal rhythm of circulating cortisol is flattened with higher trough values (Björntorp & Rosmond 1999). It is possible that these increased levels are associated with exaggeration of the inhibition of steroid metabolism due to an increased drive to synthesise bile acids and eliminate cholesterol. The diurnal rhythm of bile acids in obesity is to our knowledge unknown but circulatory levels are elevated in humans (Halmy *et al.* 1986) and the obese Zucker rat (3-fold higher; McNeilly unpublished data). Physiologically, bile acid synthesis is stimulated following a fatty meal in order to facilitate the absorption of fats (Costarelli & Sanders 2001). Again, this would be predicted to occur at a time when glucocorticoid metabolism may be impaired. Interestingly, a post-prandial rise in circulating cortisol in observed, although this is considered to be more pronounced following the ingestion of protein.

Pathological conditions such as liver cirrhosis and cholestasis are manifest due to the accumulation of bile acids within the liver and bile duct. Likewise obstruction of the bile duct leading to secondary biliary cirrhosis can result in severe jaundice and has serious implications to health. Bile acids and their precursors are cytotoxic when accumulated in excess. For example the genetic defects in cholesterol catabolism can result in the accumulation of highly toxic intermediated including oxysterols and bile acids, leading to liver disease, premature cardiovascular disease or neurological disorders (Russell 2003b). Furthermore, bile acids have been implicated as nephrotoxins increasing the risk of post-operative renal failure in

individuals with obstructive jaundice (Kaler *et al.* 2004). There is scant research investigating glucocorticoid metabolism in such patients although the increase in urinary ratio of (5β-tetrahydrocortisol+5α-tetrahydrocortisol) / tetrahydrocorticosterone has been reported in cholestatic patients which has been attribute to alterations in 11β-HSD1/2 and/or the A-ring reductases (Quattropani *et al.* 2001). Similarly in rats following bile duct ligation, an alteration in the equivalent ratio of corticosterone metabolites has been observed (Ackermann *et al.* 1999). These studies support a role of bile acids in the regulation of glucocorticoid metabolism. The hepatic insult of these patients may resemble that of animals receiving normal chow supplemented with CDCA yielding a state of bile acid excess. Our data predict that under these circumstances 5β-reductase and 11β-HSD1 will both be impaired and this in turn will impact upon activation of the HPA axis and also the RAAS.

The bile-duct-ligated (BDL) rat represents an ideal model in which to assess the progression of bile acid induced enzyme inhibition. Chronic bile duct ligation is frequently used to model liver cirrhosis with cholestasis (Kountouras *et al.* 1984). These animals also show cardiovascular and renal abnormalities. Indeed chronic BDL induces a circulatory hyperdynamic state, with arterial hypotension and increased cardiac output (Green & Better 1995) concomitant with renal alterations including, portal hypertension, sodium retention, a decrease in renal angiotensinogen and increase in renin transcript abundance (Ubeda *et al.* 1994), activation of intra-renal hormones including prostaglandin E2 and thromboxane A2 (Ackerman *et al.* 1996) and an increase in the aldosterone : renin ratio (Thiesson *et al* unpublished data). It is known that the MR protective effect of 11β-HSD2 is diminished in cirrhosis (Ackermann *et al.* 1999), however A-ring reductase activity in these animals has not been studied. Preliminary data generated in collaboration with Dr H Thiesson (Odense, Denmark) revealed that BDL rats exhibit changes in the same enzyme pathways were observed in animals treated with CDCA. It must be noted however that the tissues analysed in this thesis were taken from animals 5-7 weeks after surgery by which stage the animals were in a state of decompensated biliary cirrhosis with hepatic cytotoxicity. It would therefore be interesting to assess enzyme activity and expression at earlier time points, perhaps 1-2 days following surgery and throughout the development of biliary cirrhosis along with HPA axis tests. This

would provide insight into the time course and degree of inhibition exerted by bile acids and permit quantification of bile acid concentrations and a glucocorticoid profile to be determined. It would also be interesting to measure blood pressure in CDCA treated animals as they present with symptoms of a hypertensive phenotype i.e. sodium retention, elevated plasma aldosterone and alterations in the urinary electrolyte balance.

There is much evidence to support a role for glucocorticoid metabolism regulation of the HPA axis and intermediary metabolism. Indeed, hepatic over expression of 11β-HSD1 causes dyslipidemia and hypertension in the absence of obesity (Paterson *et al.* 2004), whilst transgenic mice expressing elevated levels of 11β-HSD1 specifically within the adipose tissue exhibit the full metabolic syndrome with visceral obesity, dyslipidemia, insulin-resistant and diabetes (Masuzaki *et al.* 2001b). These models demonstrate the importance of tissue specific alterations in enzyme activity. Down regulation of hepatic 11β-HSD1 in obesity is thought to protect the liver from the adverse effects of excess glucocorticoids, however, the mechanism is as yet unknown. There are several phenotypic similarities between bile acid treated animals and the 11β-HSD1 null mouse. For example CDCA treated animals have elevated plasma cholesterol and HDL cholesterol, a prolonged corticosterone peak following restraint stress and reduced plasma glucose and insulin analogous to that seen in the 11β-HSD1 knock out mouse. These mice also resist hyperglycemia provoked by stress and obesity and have attenuated activation of the key hepatic gluconeogenic enzymes such as PEPCK suggesting that inhibition of 11β-HSD1 may offer similar metabolic protection from the adverse impact of stress and high fat diet (Morton *et al.* 2004). In support of this, the administration of carbenoxolone, a non-specific 11β-HSD inhibitor has been shown to inhibit hepatic 11β-HSD1 (and enhance insulin sensitivity)(Walker *et al.* 1995b). This property has been suggested as a protective mechanism to reduce the extent of insulin resistance within the liver of diabetic obese patients (Sandeep *et al.* 2005). These findings suggest that bile acids may offer potential physiological but also therapeutic benefits in conditions of dyslipidemia such as obesity, non-alcoholic steatohepatitis (NASH) and myotonic dystrophy. Indeed, administration of a low calorie diet and ursodeoxycholic acid has been shown to reduce the severity of steatosis and improve

serum lipid variable and hepatic inflammatory changes in a rodent model of NASH (Fan *et al.* 2005). In addition, a recent study has shown bile acids act as general metabolic integrators, increasing energy expenditure in brown adipose tissue, thus preventing obesity and insulin resistance via induction of cAMP dependent thyroid hormone activating enzyme type 2 iodothyronine deiodinase (Watanabe *et al.* 2006). In support of this administration of cholic acid has been shown to reverse diet induced obesity and improve glucose tolerance in KK-A^y mice and C57BL/6j mice with diet induced obesity (Ikemoto *et al.* 1997). The findings of this thesis provide an alternative mechanism through which bile acids may improve insulin sensitivity, namely through inhibition of 11β-HSD1 within the liver. However, these beneficial effects may be associated with altered stress and a predisposition to hypertension.

An unexpected finding of this thesis was the impact of bile acids on cholesterol uptake and utilization within the adrenal gland. Bile acid treatment caused a marked rise in plasma aldosterone and altered urinary electrolyte balance suggesting that bile acid may induce a mild state of hypertension. This may be a consequence of impaired aldosterone metabolism by 5β-reductase and as such monitoring blood pressure in bile acid treated animals would therefore be of interest. Likewise a detailed study of adrenal gland morphology and the transcription of steroidogenic genes and enzymes within the cholesterol uptake and transportation pathway including StAR would provide insight into the mechanism through which bile acids exert change in adrenal gland function. Again this may contribute to the increase in blood pressure exhibited in the BDL rat and in conditions such as cholestatic jaundice

It is difficult however to put this work into context with the changes in glucocorticoid metabolism observed in obesity, another condition where one may anticipate bile acid excess.

The obese Zucker rat displays an altered metabolic profile with elevated plasma and fecal bile acids and therefore provides a model in which to investigate the impact of chronic bile acid excess in obesity. Bile acid treated animals and the Zucker rat have similarly elevated levels of bile acids within the circulation, which in the Zucker rat is accompanied by raised corticosterone. However, activity of hepatic 11β-HSD1 is reduced and activity and expression of 5α- and 5β-reductase are increased in the

Zucker rat whereas hepatic enzyme activity of 5β-reductase and 11β-HSD1 are both reduced in CDCA treated animals, without changes in transcript abundance or protein levels. The work in this thesis has demonstrated that bile acids are competitive inhibitors of enzyme activity with bile acids and glucocorticoids competing for the same active site of the enzyme. It is possible that the differences observed between 5β-reductase in the two models is an adaptation to chronic elevation of both substrates (bile acids and glucocorticoids) over an extended period of time which induces an increase in transcript abundance and protein level in order to accommodate the high circulatory levels of the two competing substrates. In the obese Zucker rat however, elevated plasma bile acids were this was associated with a decrease in transcript abundance of 11β-HSD1 within the liver. It is possible that administration of the CDCA within the diet over a longer time period of months as opposed to weeks may have resulted in a decrease in gene transcription similarly to the BDL rat (Thiesson *et al* unpublished data). It would therefore be interesting to investigate the impact of a bile acid supplemented diet on glucocorticoid metabolism in the obese Zucker rat. One may anticipate that in the face of elevated levels of bile acids 5β-reductase activity and expression may be suppressed. This may in turn impact upon HPA axis activation and/or response. Although there was no compensatory increase in 5α-reductase 1 activity or expression in bile acid treated animals it is possible that this may occur in the obesity as previous studies have demonstrated a predominating role for this enzyme in glucocorticoid clearance (Livingstone *et al.* 2000). It is also possible that chronic exposure to elevated levels of bile acids may reduce feedback sensitivity within the Zucker rat thus overwhelming the system with additional bile acids may have no impact on enzyme activity. One must also consider the effects of FXR mediated suppression of enzymes involved in bile acid synthesis, detoxification and elimination as one may anticipate enhanced induction of those involved in bile acid elimination and suppression of those mediating bile acid biosynthesis.

It would also be of interest to examine adrenal morphology and function in the Zucker rat as this thesis has demonstrated that bile acids also impact upon cholesterol uptake and utilization within the adrenal gland characterized by altered lipid accumulation within the zona glomerulosa and a decrease in expression of SR-

B1, the predominating cholesterol transporter in the adrenal gland. An alternative approach would be to administer a fat-free diet to Zucker rats in an attempt to reduce bile acid levels within the circulation and assess glucocorticoid metabolism and cholesterol uptake and utilization within the adrenal gland.

Reference List

Abel SM & Back DJ 1993 Cortisol metabolism in vitro - III. Inhibition of microsomal 6β- hydroxylase and cytosolic 4-ene-reductase. *J Ster.Biochem.Mol.Biol.* **46** 827-832.

Ackerman Z, Karmeli F, Amir G & Rachmilewitz D 1996 Renal vasoactive mediator generation in portal hypertensive and bile duct ligated rats. *J Hepatol.* **24** 478-486.

Ackermann D, Vogt B, Escher G, Dick B, Reichen J, Frey BM & Frey FJ 1999 Inhibition of 11β-hydroxysteroid dehydrogenase by bile acids in rats with cirrhosis. *Hepatology* **30** 623-629.

Agarwal AK, Monder C, Eckstein B & White PC 1989 Cloning and expression of rat cDNA encoding corticosteroid 11β-dehydrogenase. *J Biol.Chem.* **264** 18939-18943.

Altmann SW, Davis HR, Jr., Yao X, Laverty M, Compton DS, Zhu LJ, Crona JH, Caplen MA, Hoos LM, Tetzloff G, Priestley T, Burnett DA, Strader CD & Graziano MP 2002 The identification of intestinal scavenger receptor class B, type I (SR-BI) by expression cloning and its role in cholesterol absorption. *Biochim.Biophys.Acta* **1580** 77-93.

Andersson S, Berman DM, Jenkins EP & Russel DW 1991 Deletion of steroid 5α-reductase 2 gene in male pseudohermaphroditism. *Nature* **354** 159-161.

Andersson S, Bishop RW & Russell DW 1989a Expression cloning and regulation of steroid 5alpha-reductase, an enzyme essential for male sexual differentiation. *J Biol.Chem.* **264** 16249-16255.

Andersson S, Davis DL, Dahlback H, Jornvall H & Russell DW 1989b Cloning, structure, and expression of the mitochondrial cytochrome P-450 sterol 26-hydroxylase, a bile acid biosynthetic enzyme. *J Biol.Chem.* **264** 8222-8229.

Andersson S & Russell DW 1990 Structural and biochemical properties of cloned and expressed human and rat steroid 5 α-reductases. *Proc.Natl.Acad.Sci.U.S.A* **87** 3640-3644.

Andrew R, Phillips DIW & Walker BR 1998 Obesity and Gender Influence Cortisol Secretion and Metabolism in Man. *J Clin.Endocrinol.Metab.* **83** 1806-1809.

Andrew R, Phillips DIW & Walker BR 2000 Influence of gender and body composition on glucocorticoid metabolism in middle-aged humans. *Int J Obesity* **24** S144-S145.

Andrew R & Walker BR 2005 Glucocorticoid Metabolism: Regulation of Tissue Specific Responses in Obesity. In *Trends in Obesity Research*, pp 85-120. Ed Ling P.R. New York: Nova Boimedical Books.

Andrews RC, Herlihy O, Livingstone DEW, Andrew R & Walker BR 2002 Abnormal Cortisol Metabolism and Tissue Sensitivity to Cortisol in Patients with Glucose Intolerance. *J Clin.Endocrinol.Metab b* **87** 5587-5593.

Andrews RC, Rooyackers O & Walker BR 2003 Effects of the 11 β-hydroxysteroid dehydrogenase inhibitor carbenoxolone on insulin sensitivity in men with type 2 diabetes. *J Clin.Endocrinol.Metab* **88** 285-291.

Andrews RC & Walker BR 1999 Glucocorticoids and insulin resistance: old hormones, new targets. *Clin.Science* **96** 513-523.

Bahar RJ & Stolz A 1999 Bile acid transport. *Gastroenterol.Clin.North Am.* **28** 27-58.

Barf T, Vallgarda J, Emond R, Haggstrom C, Kurz G, Nygren A, Larwood V, Mosialou E, Axelsson K, Olsson R, Engblom L, Edling N, Ronquist-Nii Y, Ohman B, Alberts P & Abrahmsen L 2002 Arylsulfonamidothiazoles as a new class of potential antidiabetic drugs. Discovery of potent and selective inhibitors of the 11β-hydroxysteroid dehydrogenase type 1. *J Med.Chem.* **45** 3813-3815.

Bays HE, Moore PB, Drehobl MA, Rosenblatt S, Toth PD, Dujovne CA, Knopp RH, Lipka LJ, Lebeaut AP, Yang B, Mellars LE, Cuffie-Jackson C & Veltri EP 2001 Effectiveness and tolerability of ezetimibe in patients with primary hypercholesterolemia: pooled analysis of two phase II studies. *Clin.Ther.* **23** 1209-1230.

Ben Ari ET & Garrison JC 1988 Regulation of angiotensinogen mRNA accumulation in rat hepatocytes. *Am.J Physiol.* **255** E70-E79.

Bennett MJ, Albert RH, Jez JM, Ma H, Penning TM & Lewis M 1997 Steroid recognition and regulation of hormone action: crystal structure of testosterone and NADP+ bound to 3 α-hydroxysteroid/dihydrodiol dehydrogenase. *Structure* **5** 799-812.

Berger J, Tanen M, Elbrecht A, Hermanowski-Vosatka A, Moller DE, Wright SD & Thieringer R 2001 Peroxisome proliferator-activated receptor-gamma ligands inhibit adipocyte 11beta -hydroxysteroid dehydrogenase type 1 expression and activity. *J Biol.Chem.* **276** 12629-12635.

Bertolotti M, Spady DK & Dietschy JM 1995 Regulation of hepatic cholesterol metabolism in the rat in vivo: effect of a synthetic fat-free diet on sterol synthesis and low-density lipoprotein transport. *Biochim.Biophys.Acta* **1255** 293-300.

Bilheimer DW, Grundy SM, Brown MS & Goldstein JL 1983 Mevinolin and colestipol stimulate receptor-mediated clearance of low density lipoprotein from plasma in familial hypercholesterolemia heterozygotes. *Proc.Natl.Acad.Sci.U.S.A* **80** 4124-4128.

Björntorp P & Rosmond R 1999 Hypothalamic arousal, insulin resistance and Type 2 diabetes mellitus. *Diabetic Med.* **16** 373-383.

Blumberg B, Sabbagh W Jr, Juguilon H, Bolado J Jr, van Meter CM, Ong ES & Evans RM 1998 SXR, a novel steroid and xenobiotic-sensing nuclear receptor. *Genes Dev.t* **12** 3195-3205.

Brem AS, Bina RB, King T & Morris DJ 1995 Bidirectional activity of 11β-hydroxysteroid dehydrogenase in vascular smooth muscle cells. *Steroids* **60** 406-410.

Brown RW, Chapman KE, Edwards CRW & Seckl JR 1993 Human placental 11β-hydroxysteroid dehydrogenase: evidence for and partial purification of a distinct NAD-dependent isoform. *Endocrinology* **132** 2614-2621.

Bujalska I, Kumar S & Stewart PM 1997 Does central obesity reflect "Cushing's disease of the omentum"? *Lancet* **349** 1210-1213.

Charbonneau A & The VL 2001 Genomic organization of a human 5β-reductase and its pseudogene and substrate selectivity of the expressed enzyme. *Biochim.Biophys.Acta* **1517** 228-235.

Chawla A, Repa JJ, Evans RM & Mangelsdorf DJ 2001 Nuclear Receptors and Lipid Physiology: Opening the X-Files. *Science (Lipid Biology Review)* **294** 1866-1870.

Chiang JYL 1998 Regulation of Bile Acid Synthesis. *Front.Biosci.* **3** d176-d193.

Chiang JYL 2002 Bile acid regulation of gene expression: Roles of nuclear hormone receptors. *Endocr.Rev.* **23** 443-463.

Chiang JYL, Kimmel R & Stroup D 2001 Regulation of cholesterol 7α-hydroxylase gene (*CYP7A1*) transcription by the liver orphan receptor (LXRα). *Gene* **262** 257-265.

Chiang JY & Stroup D 1994 Identification and characterization of a putative bile acid-responsive element in cholesterol 7 α-hydroxylase gene promoter. *J Biol.Chem.* **269** 17502-17507.

Costarelli V & Sanders TA 2001 Acute effects of dietary fat composition on postprandial plasma bile acid and cholecystokinin concentrations in healthy premenopausal women. *Br.J Nutr.* **86** 471-477.

Danielsson H & Sjovall J 1975 Bile acid metabolism. *Annu.Rev.Biochem* **44** 233-253.

Davidson's Medicine 1995 Endocrine and metabolic diseases, including diabetes mellitus. In *Principles and practice of medicine 17th Ed.* pp670-720. Ed Edwards CRW, Bouchier IAD, Haslett C and Chilvers ER. Churchill Livingstone, Edinburgh, UK.

Davis HR, Jr., Zhu LJ, Hoos LM, Tetzloff G, Maguire M, Liu J, Yao X, Iyer SP, Lam MH, Lund EG, Detmers PA, Graziano MP & Altmann SW 2004 Niemann-Pick C1 Like 1 (NPC1L1) is the intestinal phytosterol and cholesterol transporter and a key modulator of whole-body cholesterol homeostasis. *J Biol.Chem.* **279** 33586-33592.

Denson LA, Sturm E, Echevarria W, Zimmerman TL, Makishima M, Mangelsdorf DJ & Karpen SJ 2001 The orphan nuclear receptor, shp, mediates bile acid-induced inhibition of the rat bile acid transporter, ntcp. *Gastroenterology* **121** 140-147.

Drake AJ, Livingstone DE, Andrew R, Seckl JR, Morton NM & Walker BR 2005 Reduced adipose glucocorticoid reactivation and increased hepatic glucocorticoid clearance as an early adaptation to high-fat feeding in Wistar rats. *Endocrinology* **146** 913-919.

Draper N, Walker EA, Bujalska IJ, Tomlinson JW, Chalder SM, Arlt W, Lavery GG, Bedendo O, Ray DW, Laing I, Malunowicz E, White PC, Hewison M, Mason PJ, Connell JM, Shackleton CH & Stewart PM 2003 Mutations in the genes encoding 11β-hydroxysteroid dehydrogenase type 1 and hexose-6-phosphate dehydrogenase interact to cause cortisone reductase deficiency. *Nat.Genet.* **34** 434-439.

Edwards CRW, Stewart PM, Burt D, Brett L, McIntyre MA, Sutanto WS, DeKloet ER & Monder C 1988 Localisation of 11β-hydroxysteroid dehydrogenase- tissue specific protector of the mineralocorticoid receptor. *Lancet* **ii** 986-989.

Eicheler W, Seitz J, Steinhoff M, Forssmann WG, Adermann K & Aumuller 1995 Distribution of rat hepatic steroid 5alpha-reductase 1 as shown by immunohistochemistry. *Exp.Clin. Endocr.Diab.***103** 105-112.

Escher G, Galli I, Vishwanath BS, Frey BM & Frey FJ 1997 Tumor necrosis factor alpha and interleukin 1beta enhance the cortisone/cortisol shuttle. *J Exp.Med.***186** 189-198.

Evagelatou M, Peterson SL & Cooke BA 1997 Leukocytes modulate 11β-hydroxysteroid dehydrogenase (11β-HSD) activity in human granulosa-lutein cell cultures. *Mol.Cell Endocrinol.* **133** 81-88.

Fan JG, Zhong L, Tia LY, Xu ZJ, Li MS & Wang GL 2005 Effects of ursodeoxycholic acid and/or low-calorie diet on steatohepatitis in rats with obesity and hyperlipidemia. *World J Gastroenterol.* **11** 2346-2350.

Fleischer S & Kervina M 1974 Subcellular fractionation of rat liver. *Methods Enzymol.* **31** 6-41.

Forman BM, Goode E, Chen J, Oro AE, Bradley DJ, Perlmann T, Noonan DJ, Burka LT, McMorris T, Lamph WW, Evans RM & Weinberger C 1995 Identification of a nuclear receptor that is activated by farnesol metabolites. *Cell* **81** 687-693.

Fossati P & Prencipe L 1982 Serum triglycerides determined colorimetrically with an enzyme that produces hydrogen peroxide. *Clin.Chem.* **28** 2077-2080.

Francis GA, Fayard E, Picard F & Auwerx J 2003 Nuclear receptors and the control of metabolism. *Annu.Rev.Physiol* **65** 261-311.

Fukuhara Y, Hirasawa A, Li XK, Kawasaki M, Fujino M, Funeshima N, Katsuma S, Shiojima S, Yamada M, Okuyama T, Suzuki S & Tsujimoto G 2003 Gene expression profile in the regenerating rat liver after partial hepatectomy. *J Hepatol.* **38** 784-792.

Fukushima K, Ichimiya H, Higashijima H, Yamashita H, Kuroki S, Chijiiwa K & Tanaka M 1995 Regulation of bile acid synthesis in the rat: relationship between hepatic cholesterol 7 α-hydroxylase activity and portal bile acids. *J Lipid Res.* **36** 315-321.

Funder JW 1997 Glucocorticoid and mineralocorticoid receptors: biology and clinical relevance. *Annu.Rev.Med.* **48** 231-240.

Funder JW, Pearce PT, Smith R & Smith AI 1988 Mineralocorticoid action: target tissue specificity is enzyme, not receptor, mediated. *Science* **242** 583-585.

Furuebisu M, Deguchi S & Okuda K 1987 Identification of cortisone 5β-reductase as delta 4-3-ketosteroid 5 beta-reductase. *Biochim.Biophys.Acta* **912** 110-114.

Galman C, Angelin B & Rudling M 2005 Bile acid synthesis in humans has a rapid diurnal variation that is asynchronous with cholesterol synthesis. *Gastroenterology* **129** 1445-1453.

Garcia-Calvo M, Lisnock J, Bull HG, Hawes BE, Burnett DA, Braun MP, Crona JH, Davis HR, Jr., Dean DC, Detmers PA, Graziano MP, Hughes M, MacIntyre DE, Ogawa A, O'neill KA, Iyer SP, Shevell DE, Smith MM, Tang YS, Makarewicz AM, Ujjainwalla F, Altmann SW, Chapman KT & Thornberry NA 2005 The target of ezetimibe is Niemann-Pick C1-Like 1 (NPC1L1). *Proc.Natl.Acad.Sci.U.S.A* **102** 8132-8137.

Gomez-Sanchez EP, Cox D, Foecking M, Ganjam V & Gomez-Sanchez CE 1996 11β-Hydroxysteroid dehydrogenases of the choriocarcinoma cell line JEG-3 and their inhibition by glycyrrhetinic acid and other natural substances. *Steroids* **61** 110-115.

Goodwin B, Jones SA, Price RR, Watson MA, McKee DD, Moore LB, Galardi C, Wilson JG, Lewis MC, Roth ME, Maloney PR, Willson TM & Kliewer SA 2000 A regulatory cascade of the nuclear receptors FXR, SHP-1, and LRH-1 represses bile acid biosynthesis. *Mol.Cell* **6** 517-526.

Green J & Better OS 1995 Systemic hypotension and renal failure in obstructive jaundice-mechanistic and therapeutic aspects. *J Am.Soc.Nephrol.* **5** 1853-1871.

Grempler R, Gunther S, Steffensen KR, Nilsson M, Barthel A, Schmoll D & Walther R 2005 Evidence for an indirect transcriptional regulation of glucose-6-phosphatase gene expression by liver X receptors. *Biochem Biophys.Res.Commun.* **338** 981-986.

Grimshaw CE, Bohren KM, Lai CJ & Gabbay KH 1995 Human aldose reductase: rate constants for a mechanism including interconversion of ternary complexes by recombinant wild-type enzyme. *Biochemistry* **34** 14356-14365.

Gupta S, Stravitz RT, Dent P & Hylemon PB 2001 Down-regulation of Cholesterol 7α-Hydroxylase (*CYP7A1*) Gene expression by bile acids in primary rat hepatocytes is mediated by the c-Jun N-terminal pathway. *J Biol.Chem.* **276** 15816-15822.

Gustafsson BE, Angelin B, Bjorkhem I, Einarsson K & Gustafsson JA 1981 Effects of feeding chenodeoxycholic acid on metabolism of cholesterol and bile acids in germ-free rats. *Lipids* **16** 228-233.

Halmy L, Feher T, Steczek K & Farkas A 1986 High serum bile acid level in obesity: its decrease during and after total fasting. *Acta Med.Hung.* **43** 55-58.

Harris HJ, Kotelevtsev Y, Mullins JJ, Seckl JR & Holmes MC 2001a Intracellular regeneration of glucocorticoids by 11β-hydroxysteroid dehydrogenase (11β-HSD)-1 plays a key role in regulation of the hypothalamic-pituitary-adrenal axis: analysis of 11β-HSD-1-deficient mice. *Endocrinology* **142** 114-120.

Harris HJ, Kotelevtsev YV, Mullins JJ, Seckl JR & Holmes MC 2001b 11β-Hydroxysteroid dehydrogenase type 1 null mice have altered hypothalamic-pituitary-adrenal axis activity: a novel control of glucocorticoid feedback. *Endocrinology* **142** 114-120.

Hautanen A & Adlercreutz H 1993 Altered adrenocorticotropin and cortisol secretion in abdominal obesity: implications for the insulin resistance syndrome. *J Intern.Med.* **234** 461-469.

Hautanen A, Raikkonen K & Adlercreutz H 1997 Associations between pituitary-adrenocortical function and abdominal obesity, hyperinsulinaemia and dyslipidaemia in normotensive males. *J Intern.Med.* **241** 451-461.

Heredia VV, Kruger RG & Penning TM 2003 Steroid-binding site residues dictate optimal substrate positioning in rat 3α-hydroxysteroid dehydrogenase (3α-HSD or AKR1C9). *Chem.Biol.Interact.* **143-144** 393-400.

Heuman DM, Vlahcevic ZR, Pandak WM, Hylemon PB, Kim YS, Lillienau J & Hofmann AF 1992 Effect of cholylsarcosine on hepatic cholesterol and bile acid synthesis and bile secretion in rats. *Gastroenterology* **103** 1641-1648.

Hirasawa G, Sasano H, Takahashi K, Fukushima K, Suzuki T, Hiwatashi N, Toyota T, Krozowski ZS & Nagura H 1997 Colocalization of 11 β-hydroxysteroid dehydrogenase type II and mineralocorticoid receptor in human epithelia. *J Clin.Endocrinol.Metab.* **82** 3859-3863.

Hosfield DJ, Wu Y, Skene RJ, Hilgers M, Jennings A, Snell GP & Aertgeerts K 2005 Conformational flexibility in crystal structures of human 11{β}-hydroxysteroid dehydrogenase type I provide insights into glucocorticoid interconversion and enzyme regulation. *J Biol.Chem.* **280** 4639-4648.

Hundertmark S, Ragosch V, Schein B, Buhler H, Fromm M, Lorenz U & Weitzel HK 1993 11-Beta-hydroxysteroid dehydrogenase of rat lung: Enzyme kinetic, oxidase- reductase ratio, electrolyte and trace element dependence. *Enzyme Protein* **47** 83-91.

Ikemoto S, Takahashi M, Tsunoda N, Maruyama K, Itakura H, Kawanaka K, Tabata I, Higuchi M, Tange T, Yamamoto TT & Ezaki O 1997 Cholate inhibits high-fat diet-induced hyperglycemia and obesity with acyl-CoA synthetase mRNA decrease. *Am.J Physiol* **273** E37-E45.

Jacobson L & Sapolsky R 1991 The role of the hippocampus in feedback regulation of the hypothalamic-pituitary-adrenocortical axis. *End. Rev.* **12** 118-134.

Jamieson A, Wallace AM, Andrew R, Nunez BS, Walker BR, Fraser R, White PC & Connell JMC 1999 Apparent cortsione reductase deficiency: A functional defect in 11β-hydroxysteroid dehydrogenase type 1. *J Clin.Endocrin.Metab.* **84** 3570-3574.

Jamieson PM, Chapman KE, Edwards CRW & Seckl JR 1995 11β-Hydroxysteroid dehydrogenase is an exclusive 11β-reductase in primary cultures of rat hepatocytes: effect of physicochemical and hormonal manipulations. *Endocrinology* **136** 4754-4761.

Jenkins EP, Andersson S, Imperato-McGinley J, Wilson JD & Russell DW 1992 Genetic and pharmacological evidence for more than one human steroid 5α-reductase. *J Clin Invest* **89** 293-300.

Jez JM & Penning TM 1998a Engineering steroid 5 β-reductase activity into rat liver 3 α-hydroxysteroid dehydrogenase. *Biochemistry* **37** 9695-9703.

Jez JM & Penning TM 1998b Engineering steroid 5 beta-reductase activity into rat liver 3 alpha-hydroxysteroid dehydrogenase. *Biochemistry* **37** 9695-9703.

Jez JM & Penning TM 2001 The aldo-keto reductase (AKR) superfamily: an update. *Chem.Biol.Interact.* **130-132** 499-525.

Jez JM, Schlegel BP & Penning TM 1996 Characterization of the substrate binding site in rat liver 3α-hydroxysteroid/dihydrodiol dehydrogenase. The roles of tryptophans in ligand binding and protein fluorescence. *J Biol.Chem.* **271** 30190-30198.

Jin Y, Stayrook SE, Albert RH, Palackal NT, Penning TM & Lewis M 2001 Crystal structure of human type III 3α-hydroxysteroid dehydrogenase/bile acid binding protein complexed with NADP(+) and ursodeoxycholate. *Biochemistry* **40** 10161-10168.

Juchau M 1990 Substrate specificities and functions of P450 cytochromes. *Life Science* **47** 2385-2394.

Kaler B, Karram T, Morgan WA, Bach PH, Yousef IM & Bomzon A 2004 Are bile acids involved in the renal dysfunction of obstructive jaundice? An experimental study in bile duct ligated rats. *Ren.Fail.* **26** 507-516.

Kenyon CJ, Saccoccio NA & Morris DJ 1984 Glucocorticoid inhibition of mineralocorticoid in the rat. *Clin.Science* **67** 329-335.

Killinger DW, Perel E, Daniilescu D, Kharlip L & Lindsay WN 1990 Influence of adipose tissue distribution on the biological activity of androgens. *Ann. New York Acad.Sci.* **595** 199-211.

Kliewer SA, Moore JT, Wade L, Staudinger JL, Watson MA, Jones SA, McKee DD, Oliver BB, Willson TM, Zetterstrom RH, Perlmann T & Lehmann JM 1998 An orphan nuclear receptor activated by pregnanes defines a novel steroid signaling pathway. *Cell* **92** 73-82.

Kliewer SA, Goodwin B & Willson TM 2002 The nuclear pregnane X receptor: a key regulator of xenobiotic metabolism. *Endoc.r Rev.* **23** 687-702.

Kondo K-H, Kai M-H, Setoguchi Y, Eggertsen G, Sjoblom P, Setoguchi T, Okuda K-I & Bjorkhem I 1994 Cloning and expression of cDNA of human delta4-3-oxosteroid 5βreductase and substrate specificity of the expressed enzyme. *Eur. J Biochem.* **219** 357-363.

Kotelevtsev YV, Brown RW, Fleming S, Edwards CRW, Seckl JR & Mullins JJ 1999 Hypertension in mice caused by inactivation of 11β-hydroxysteroid dehydrogenase type 2. *J Clin.Invest.* **103** 683-689.

Kotelevtsev YV, Holmes MC, Burchell A, Houston PM, Scholl D, Jamieson PM, Best R, Brown RW, Edwards CRW, Seckl JR & Mullins JJ 1997 11β-Hydroxysteroid dehydrogenase type 1 knockout mice show attenuated glucocorticoid inducible responses and resist hyperglycaemia on obesity and stress. *Proc.Nat.Acad.Sci.USA* **94** 14924-14929.

Kotelevtsev YV, Jamieson PM, Best R, Stewart F, Edwards CRW, Seckl JR & Mullins JJ 1996 Inactivation of 11β-hydroxysteroid dehydrogenase type 1 by gene targeting in mice. *Endocr.Res.* **22** 791-792.

Kountouras J, Billing BH & Scheuer PJ 1984 Prolonged bile duct obstruction: a new experimental model for cirrhosis in the rat. *Br.J Exp.Pathol.* **65** 305-311.

Krozowski ZS, Stewart PM, Obeyesekere VR, Li K & Ferrari P 1997 Mutations in the 11β-hydroxysteroid dehydrogenase type II enzyme associated with hypertension and possibly stillbirth. *Clin.Exp. Hyperten.* **19** 519-529.

Lakshmi V & Monder C 1985a Evidence for independent 11-oxidase and 11-reductase activities for 11β-hydroxysteroid dehydrogenase: enzyme latency, phase transitions and lipid requirement. *Endocrinology* **116** 552-560.

Lakshmi V & Monder C 1985b Extraction of 11 β-hydroxysteroid dehydrogenase from rat liver microsomes by detergents. *J Steroid Biochem.*. **22** 331-340.

Lambert G, Amar MJ, Guo G, Brewer HB, Jr., Gonzalez FJ & Sinal CJ 2003 The farnesoid X-receptor is an essential regulator of cholesterol homeostasis. *J Biol.Chem.* **278** 2563-2570.

Landrier JF, Grober J, Demydchuk J & Besnard P 2003 FXRE can function as an LXRE in the promoter of human ileal bile acid-binding protein (I-BABP) gene. *FEBS Lett.* **553** 299-303.

Latif SA, Conca TJ & Morris DJ 1990 The effects of the liquorice derivative, glycyrrhetinic acid, on hepatic 3α- and 3β-hydroxysteroid dehydrogenases and 5α- and 5β-reductase pathways of metabolism of aldosterone in male rats. *Steroids* **55** 52-58.

Latif SA, Hartman LR, Souness GW & Morris DJ 1994 Possible endogenous regulators of steroid inactivating enzymes and glucocorticoid-induced Na^+ retention. *Steroids* **59** 352-356.

Lavery GG, Ronconi V, Draper N, Rabbitt EH, Lyons V, Chapman KE, Walker EA, McTernan CL, Giacchetti G, Mantero F, Seckl JR, Edwards CR, Connell JM, Hewison M & Stewart PM 2003 Late-onset apparent mineralocorticoid excess caused by novel compound heterozygous mutations in the HSD11B2 gene. *Hypertension* **42** 123-129.

Lavery GG, Walker EA, Draper N, Jeyasuria P, Marcos J, Shackleton CH, Parker KL, White PC & Stewart PM 2005 Hexose-6-phosphate dehydrogenase knockout mice lack 11beta -hydroxysteroid dehydrogenase type 1-mediated glucocorticoid generation. *J Biol.Chem.* **281** 6546-6551.

Lemonde HA, Custard EJ, Bouquet J, Duran M, Overmars H, Scambler PJ & Clayton PT 2003 Mutations in SRD5B1 (AKR1D1), the gene encoding delta(4)-3-oxosteroid 5β-reductase, in hepatitis and liver failure in infancy. *Gut* **52** 1494-1499.

Lephart ED, Simpson ER & Trzeciak WH 1991 Rat adrenal 5α-reductase mRNA content and enzyme activity are sex hormone dependent. *J Mol. Endocrin.* **6** 163-170.

Li A, Li KZ, Marui S, Krozowski ZS, Batista MC, Whorwood CB, Arnhold IP, Shackleton CL, Mendonca BB & Stewart PM 1997 Apparent mineralocorticoid excess in a Brazilian kindred: Hypertension in the heterozygote state. *J Hyperten.* **15** 1397-1402.

Lin HK, Hung CF, Moore M & Penning TM 1999 Genomic structure of rat 3α-hydroxysteroid/dihydrodiol dehydrogenase (3α-HSD/DD, AKR1C9). *J Ster.Biochem.Mol.Biol.* **71** 29-39.

Lin HK, Jez JM, Schlegel BP, Peehl DM, Pachter JA & Penning TM 1997 Expression and characterization of recombinant type 2 3 α-hydroxysteroid dehydrogenase (HSD) from human prostate: demonstration of bifunctional 3 alpha/17 β-HSD activity and cellular distribution. *Mol.Endocrin.* **11** 1971-1984.

Livingstone DEW, Kenyon CJ & Walker BR 2000 Mechanisms of dysregulation of 11β–hydroxysteroid dehydrogenase type 1 in obese Zucker rats. *J Endocrin.* **167** 533-539.

Livingstone DE, McInnes KJ, Walker BR & Andrew R 2005 Increased A-ring reduction of glucocorticoids in obese Zucker rats: effects of insulin sensitization. *Obes.Res.* **13** 1523-1526.

Livingstone DE & Walker BR 2003 Is 11β-hydroxysteroid dehydrogenase type 1 a therapeutic target? Effects of carbenoxolone in lean and obese Zucker rats. *J Pharmaco.Exper.Ther.* **305** 167-172.

Livingstone DEW, Jones GC, Smith K, Andrew R, Kenyon CJ & Walker BR 2000 Understanding the role of glucocorticoids in obesity: tissue-specific alterations of corticosterone metabolism in obese Zucker rats. *Endocrinology* **141** 560-563.

Lopez-Solache I, Luu-The V, Seralini GE & Labrie F 1996 Heterogeneity of rat type I 5 α-reductase cDNA: cloning, expression and regulation by pituitary implants and dihydrotestosterone. *Biochim.Biophys.Acta* **1305** 139-144.

Lovati E, Ferrari P, Dick B, Jostarndt K, Frey BM, Frey FJ, Schorr U & Sharma AM 1999 Molecular basis of human salt sensitivity: the role of the 11β-hydroxysteroid dehydrogenase type 2. *J Clin.Endocrin.Metab.* **84** 3745-3749.

Low SC, Moisan M-P, Edwards CRW & Seckl JR 1994 Glucocorticoids regulate 11β-hydroxysteroid dehydrogenase activity and gene expression in vivo in the rat. *J Neuroendocrinol.* **6** 285-290.

Lu TT, Makishima M, Repa JJ, Schoonjans K, Kerr TA, Auwerx J & Mangelsdorf DJ 2000 Molecular Basis for Feedback Regulation of Bile Acid Synthesis by Nuclear Receptors. *Mol.Cell* **6** 507-515.

Makishima M, Okamoto AY, Repa JJ, Tu H, Learned RM, Luk A, Hull MV, Lustig KD, Mangelsdorf DJ & Shan B 1999 Identification of a nuclear receptor for bile acids. *Science* **284** 1362-1365.

Malerbi D, Liberman B, Giurno-Filho A, Giannella-Neto D & Wajchenberg BL 1988 Glucocorticoids and glucose metabolism: hepatic glucose production in untreated Addisonian patients and on two different levels of glucocorticoid administration. *Clin.Endocrin.* **28** 415-422.

Malerod L, Sporstol M, Juvet LK, Mousavi SA, Gjoen T, Berg T, Roos N & Eskild W 2005 Bile acids reduce SR-BI expression in hepatocytes by a pathway involving FXR/RXR, SHP, and LRH-1. *Biochem.Biophys.Res.Commun.* **336** 1096-1105.

Manglesdorf DJ & Evans R.M 1995 The RXR heterodimers and orphan receptors. *Cell* **83** 841-850.

Mantha L, Palacios E & Deshaies Y 1999 Modulation of triglyceride metabolism by glucocorticoids in diet-induced obesity. *Am. J Physiol.* **277** R455-R464.

Martinez-Prieto C, Ortiz MC, Fortepiani LA, Ruiz-Macia J, Atucha NM & Garcia-Estan J 2000 Haemodynamic and renal evolution of the bile duct-ligated rat. *Clin.Sci.(Lond)* **98** 611-617.

Masuzaki H, Paterson J, Shinyama H, Morton NM, Mullins JJ, Seckl JR & Flier JS 2001a A transgenic model of visceral obesity and the metabolic syndrome. *Science* **294** 2166-2170.

Masuzaki H, Yamamoto H, Kenyon CJ, Elmquist JK, Morton NM, Paterson JM, Shinyama H, Sharp MG, Fleming S, Mullins JJ, Seckl JR & Flier JS 2003 Transgenic amplification of glucocorticoid action in adipose tissue causes high blood pressure in mice. *J.Clin.Invest* **112** 83-90.

Matsuura K, Deyashiki Y, Sato K, Ishida N, Miwa G & Hara A 1997 Identification of amino acid residues responsible for differences in substrate specificity and inhibitor sensitivity between two human liver dihydrodiol dehydrogenase isoenzymes by site-directed mutagenesis. *Biochem. J* **323 (Pt 1)** 61-64.

Maurel, P. 1996. Cytochrome P450, Metabolic and Toxicological Aspects. 241-270. CRC Press, Inc., Boca Raton, FL.

McGowan MW, Artiss JD, Strandbergh DR & Zak B 1983 A peroxidase-coupled method for the colorimetric determination of serum triglycerides. *Clin.Chem.* **29** 538-542.

McInnes KJ, Kenyon CJ, Chapman KE, Livingstone DE, Macdonald LJ, Walker BR & Andrew R 2004 5α-reduced glucocorticoids, novel endogenous activators of the glucocorticoid receptor. *J Biol. Chem.* **279** 22908-22912.

Miller MA & Colas AE 1982 Multihormonal control of microsomal 5 α-reductase activity in cultured adult female rat hepatocytes. *Endocrinology* **111** 136-143.

Miyata M, Tozawa A, Otsuka H, Nakamura T, Nagata K, Gonzalez FJ & Yamazoe Y 2005 Role of farnesoid X receptor in the enhancement of canalicular bile acid output and excretion of unconjugated bile acids: a mechanism for protection against cholic acid-induced liver toxicity. *J Pharmacol .Exp .Ther.* **312** 759-766.

Monder C, Shackleton CHL, Bradlow HL, New MI, Stoner E, Iohan F & Lakshmi V 1986 The syndrome of apparent mineralocorticoid excess: its association with 11β-dehydrogenase and 5β-reductase deficiency and some consequences for corticosteroid metabolism. *J Clin.Endocrin.Metab.* **63** 550-557.

Monder C, Stewart PM, Lakshmi V, Valentino R, Burt D & Edwards CRW 1989 Licorice inhibits corticosteroid 11β-dehydrogenase of rat kidney and liver: in vivo and in vitro studies. *Endocrinology* **125** 1046-1053.

Morris DJ, Semafuko WEB, Latif SA, Vogel B, Grimes C & Sheff MF 1992 Detection of glycyrrhetinic acid-like factors (GALFs) in human urine. *Hypertension* **20** 356-360.

Morris DJ & Souness GW 1996 Endogenous 11 β-hydroxysteroid dehydrogenase inhibitors and their role in glucocorticoid Na^+ retention and hypertension. *Endocr.Res.* **22** 793-801.

Morris DJ, Souness GW, Latif SA, Hardy MP & Brem AS 2004 Effect of chenodeoxycholic acid on 11β-hydroxysteroid dehydrogenase in various target tissues. *Metabolism* **53** 811-816.

Morton NM, Holmes MC, Fievet C, Staels B, Tailleux A, Mullins JJ & Seckl JR 2001 Improved lipid and lipoprotein profile, hepatic insulin sensitivity, and glucose tolerance in 11β-hydroxysteroid dehydrogenase type 1 null mice. *J Biol.Chem.* **276** 41293-41300.

Morton NM, Paterson JM, Masuzaki H, Holmes MC, Staels B, Fievet C, Walker BR, Flier JS, Mullins JJ & Seckl JR 2004 Novel adipose tissue-mediated resistance to diet-induced visceral obesity in 11 β-hydroxysteroid dehydrogenase type 1-deficient mice. *Diabetes* **53** 931-938.

Moundras C, Behr SR, Remesy C & Demigne C 1997 Fecal losses of sterols and bile acids induced by feeding rats guar gum are due to greater pool size and liver bile acid secretion. *J Nutr.* **127** 1068-1076.

Munck A & Guyre PM 1986 Glucocorticoid physiology, pharmacology and stress. *Adv.Exp.Med.Biol.* **196** 81-96.

Myant NB & Mitropoulos KA 1977 Cholesterol 7 α-hydroxylase. *J Lipid Res.* **18** 135-153.

Napolitano A, Voice MW, Edwards CW, Seckl JR & Chapman KE 1998 11β-Hydroxysteroid dehydrogenase 1 in adipocytes: Expression is differentiation-dependent and hormonally regulated. *J Ster.Biochem.Mol.Biol.* **64** 251-260.

Nathanson MH & Boyer JL 1991a Mechanisms and regulation of bile secretion. *Hepatology* **14** 551-566.

Normington K & Russell DW 1992 Tissue distribution and kinetic characteristics of rat steroid 5 alpha-reductase isozymes. Evidence for distinct physiological functions. *J Biol.Chem.* **267** 19548-19554.

Nyirenda MJ, Lindsay RS, Kenyon CJ, Burchell A & Seckl JR 1998 Glucocorticoid exposure in late gestation permanently programs rat hepatic phosphoenolpyruvate carboxykinase and glucocorticoid receptor expression and causes glucose intolerance in adult offspring. *J Clin.Invest.* **101** 2174-2181.

Obeyesekere VR, Trzeciak WH, Li KZ & Krozowski ZS 1998 Serines at the active site of 11β-hydroxysteroid dehydrogenase type I determine the rate of catalysis. *Biochem.Biophys. Res.Comm* **250** 469-473.

Okuda A & Okuda K 1984 Purification and characterisation of delta4-3-ketosteroid 5β-reductase. *J Biol.Chem.* **259** 7519-7524.

Onishi, Y, Noshiro, M, Shimosato, T, and Okuda, K. 1991 Molecular cloning and analysis of cDNA encoding 3-4-ketosteroid 5β-reductase of rat liver. *Fed.Eur. Biochem.Stud.* 283, 215-218.

Opara EC, Petro A, Tevrizian A, Feinglos MN & Surwit RS 1996 L-glutamine supplementation of a high fat diet reduces body weight and attenuates hyperglycemia and hyperinsulinemia in C57BL/6J mice. *J Nutr.* **126** 273-279.

Pandak WM, Vlahcevic ZR, Heuman DM, Redford KS, Chiang JY & Hylemon PB 1994 Effects of different bile salts on steady-state mRNA levels and transcriptional activity of cholesterol 7 α-hydroxylase. *Hepatology* **19** 941-947.

Parks DJ, Blanchard SG, Bledsoe RK, Chandra G, Consler TG, Kliewer SA, Stimmel JB, WillsonTM, Zavacki AM, Moore DD & Lehmann JM 1999 Bile Acids: Natural Ligands for an Orphan Nuclear Receptor. *Science* **284** 1365-1368.

Paterson JM, Morton NM, Fievet C, Kenyon CJ, Holmes MC, Staels B, Seckl JR & Mullins JJ 2004 Metabolic syndrome without obesity: Hepatic overexpression of 11β-hydroxysteroid dehydrogenase type 1 in transgenic mice. *Proc.Natl.Acad.Sci.U.S.A* **101** 7088-7093.

Pawlowski JE, Huizinga M & Penning TM 1991 Cloning and sequencing of the cDNA for rat liver 3 α-hydroxysteroid/dihydrodiol dehydrogenase. *J Biol.Chem.* **266** 8820-8825.

Penning TM 1999 Molecular determinants of steroid recognition and catalysis in aldo-keto reductases. Lessons from 3α-hydroxysteroid dehydrogenase. *J Steroid Biochem.Mol.Biol.* **69** 211-225.

Penning TM, Burczynski ME, Jez JM, Hung CF, Lin HK, Ma H, Moore M, Palackal N & Ratnam K 2000 Human 3α-hydroxysteroid dehydrogenase isoforms (AKR1C1-AKR1C4) of the aldo-keto reductase superfamily: functional plasticity and tissue distribution reveals roles in the inactivation and formation of male and female sex hormones. *Biochem. J* **351** 67-77.

Penning TM, Jin Y, Steckelbroeck S, Lanisnik RT & Lewis M 2004 Structure-function of human 3 α-hydroxysteroid dehydrogenases: genes and proteins. *Mol.Cell Endocrinol.* **215** 63-72.

Phillipou G & Higgins BA 1985 A new defect in the peripheral conversion of cortisone to cortisol. *J Steroid Biochem.***22** 435-436.

Phillipou G, Palermo M & Shackleton CHL 1996 Apparent cortisone reductase deficiency; a unique form of hypercortisolism. *J Clin.Endocrinol.Metab.* **81** 3855-3860.

Pikuleva IA, Babiker A, Waterman MR & Bjorkhem I 1998 Activities of recombinant human cytochrome P450c27 (CYP27) which produce intermediates of alternative bile acid biosynthetic pathways. *J Biol.Chem.* **273** 18153-18160.

Pircher PC, Kitto JL, Petrowski ML, Tangirala RK, Bischoff ED, Schulman IG & Westin SK 2003 Farnesoid X receptor regulates bile acid-amino acid conjugation. *J Biol.Chem.* **278** 27703-27711.

Quattropani C, Vogt B, Odermatt A, Dick B, Frey BM & Frey FJ 2001 Reduced activity of 11 β-hydroxysteroid dehydrogenase in patients with cholestasis. *J Clin. Invest.* **108** 1299-1305.

Rask E, Olsson T, Söderberg S, Andrew R, Livingstone DEW, Johnson O & Walker BR 2001 Tissue-specific dysregulation of cortisol metabolism in human obesity. *J Clin.Endocrinol.Metab.* **86** 1418-1421.

Rask, E., Walker, B. R., Andrew, R., Soderberg, S., Johnson, O., and Olsson, T. 1999Altered peripheral metabolism of glucocorticoids, rather than central dysfunction of the hypothalamic-pituitary-adrenal (HPA) axis, in abdominal obesity in man. Proceedings of the Endocrine Society , P1-663..

Reaven GM 1988 Banting lecture 1988. Role of insulin resistance in human disease. *Diabetes* **37** 1595-1607.

Reichardt HM, Tronche F, Bauer A & Schutz G 2000 Molecular genetic analysis of glucocorticoid signaling using the Cre/loxP system. *Biol.Chem.* **381** 961-964.

Ren S, Marques D, Redford K, Hylemon PB, Gil G, Vlahcevic ZR & Pandak WM 2003 Regulation of oxysterol 7α-hydroxylase (CYP7B1) in the rat. *Metabolism* **52** 636-642.

Repa JJ & Mangelsdorf DJ 1999 Nuclear receptor regulation of cholesterol and bile acid metabolism. *Curr.Opin.Biotechnol.* **10** 557-563.

Ricketts ML, Shoesmith KJ, Hewison M, Strain A, Eggo MC & Stewart PM 1998 Regulation of 11 β-hydroxysteroid dehydrogenase type 1 in primary cultures of rat and human hepatocytes. *J Endocrinol.* **156** 159-168.

Russell DW 2003a The Enzymes, Regulation, and Genetics of Bile Acid Synthesis. *Annu.Rev.Biochem* 137-74.

Russell DW & Setchell KD 1992 Bile acid biosynthesis. *Biochemistry* **31** 4737-4749.

Russell, D. W. and Wilson, J. D. Steroid 5α-reductase: two genes / two enzymes. *Ann.Rev.Biochem.* 63, 25-61. 1994.

Sakai RR, Lakshmi V, Monder C & McEwen BS 1992 Immunocytochemical localization of 11beta-hydroxysteroid dehydrogenase in hippocampus and other brain regions of the rat. *J Neuroendocrinol.* **4** 101-106.

Sandeep TC, Andrew R, Homer NZ, Andrews RC, Smith K & Walker BR 2005 Increased in vivo regeneration of cortisol in adipose tissue in human obesity and effects of the 11β-hydroxysteroid dehydrogenase type 1 inhibitor carbenoxolone. *Diabetes* **54** 872-879.

Schlegel BP, Jez JM & Penning TM 1998 Mutagenesis of 3 alpha-hydroxysteroid dehydrogenase reveals a "push-pull" mechanism for proton transfer in aldo-keto reductases. *Biochemistry* **37** 3538-3548.

Seal CJ & Mathers JC 2001 Comparative gastrointestinal and plasma cholesterol responses of rats fed on cholesterol-free diets supplemented with guar gum and sodium alginate. *Br.J Nutr.* **85** 317-324.

Seckl JR, Morton NM, Chapman KE & Walker BR 2004 Glucocorticoids and 11β-hydroxysteroid dehydrogenase in adipose tissue. *Recent Prog.Horm.Res.* **59** 359-393.

Shackleton CHL & Stewart PM 1990 The hypertension of apparent mineralocorticoid excess syndrome. In *Endocrine hypertension*, pp 155-173. Eds EG Biglieri & JC Melby. New York: Raven Press.

Shafqat N, Elleby B, Svensson S, Shafqat J, Jornvall H, Abrahmsen L & Oppermann U 2003 Comparative Enzymology of 11β-hydroxysteroid dehydrogenase type 1 from glucocorticoid resistant (guinea pig) versus sensitive (human) species. *J Biol.Chem.* **278** 2030-2035.

Shefer S, Hauser S, Bekersky I & Mosbach EH 1969 Feedback regulation of bile acid biosynthesis in the rat. *J Lipid Res.* **10** 646-655.

Shimojo M, Whorwood CB & Stewart PM 1996 11β-Hydroxysteroid dehydrogenase in the rat adrenal. *J Mol.Endocrin.* **17** 121-130.

Staudinger JL, Goodwin B, Jones SA, Hawkins-Brown D, Mackenzie KI, LaTour A, Liu Y, Klaassen CD, Brown KK, Reinhard J, Will, Koller BH & Kliewer SA 2001 The nuclear receptor PXR is a lithocholic acid sensor that protects against liver toxicity. *Proc.Natl.Acad.Sci.U.S.A* **98** 3369-3374.

Stauffer AT, Rochat MK, Dick B, Frey FJ & Odermatt A 2002 Chenodeoxycholic acid and deoxycholic acid inhibit 11 β-hydroxysteroid dehydrogenase type 2 and cause cortisol-induced transcriptional activation of the mineralocorticoid receptor. *J Biol.Chem.* **277** 26286-26292.

Stewart PM, Boulton A, Kumar S, Clark PMS & Shackleton CHL 1999 Cortisol metabolism in human obesity: impaired cortisone - cortisol conversion in subjects with central adiposity. *J Clin.Endocrinol.Metab.* **84** 1022-1027.

Stewart PM, Corrie JET, Shackleton CHL & Edwards CRW 1988 Syndrome of apparent mineralocorticoid excess: a defect in the cortisol-cortisone shuttle. *J Clin. Invest.* **82** 340-349.

Stewart PM, Krozowski ZS, Gupta A, Milford DV, Howie AJ, Sheppard MC & Whorwood CB 1996 Hypertension in the syndrome of apparent mineralocorticoid excess due to mutation of the 11β-hydroxysteroid dehydrogenase type 2 gene. *Lancet* **347** 88-91.

Stewart PM, Murry BA & Mason JI 1994 Type 2 11β-hydroxysteroid dehydrogenase in human fetal tissues. *J Clin.Endocrinol.Metab.* **78** 1529-1532.

Stewart PM, Valentino R, Wallace AM, Burt D, Shackleton CHL & Edwards CRW 1987 Mineralocorticoid activity of liquorice: 11β-hydroxysteroid dehydrogenase deficiency comes of age. *Lancet* **ii** 821-824.

Stolz A, Hammond L, Lou H, Takikawa H, Ronk M & Shively JE 1993 cDNA cloning and expression of the human hepatic bile acid-binding protein. A member of the monomeric reductase gene family. *J Biol.Chem.* **268** 10448-10457.

Stravitz RT & Sanyal AJ 2003 Drug-induced steatohepatitis. *Clin.Liver Dis.* **7** 435-451.

Stroup D, Crestani M & Chiang JY 1997a Identification of a bile acid response element in the cholesterol 7 α-hydroxylase gene CYP7A. *Am.J Physiol.* **273** G508-G517.

Stroup D, Crestani M & Chiang JY 1997b Orphan receptors chicken ovalbumin upstream promoter transcription factor II (COUP-TFII) and retinoid X receptor (RXR) activate and bind the rat cholesterol 7α-hydroxylase gene (CYP7A). *J Biol.Chem.* **272** 9833-9839.

Stulnig TM, Oppermann U, Steffensen KR, Schuster GU & Gustafsson JA 2002 Liver X receptors downregulate 11beta-hydroxysteroid dehydrogenase type 1 expression and activity. *Diabetes* **51** 2426-2433.

Takahashi K-I, Sasano H, Fukushima K, Hirasawa G, Miura H, Sasaki I, Matsuno S, Krozowski ZS & Nagura H 1998 11 βhydroxysteroid dehydrogenase type II in human colon: A new marker of fetal development and differentiation in neoplasms. *Anticancer Research* **18** 3381-3388.

Thigpen AE, Silver RI, Guileyardo JM, Casey ML, McConnell JD & Russell DW 1993 Tissue distribution and ontogeny of steroid 5-reductase isozyme expression. *J Clin. Invest.* **92** 903-910.

Tomkins GM 1956 The enzymatic reduction of delta 4-3-ketosteroids. *J Biol.Chem.* **225** 13-24.

Tomlinson JW 2005 11β-hydroxysteroid dehydrogenase type 1 in human disease: a novel therapeutic target. *Endocr. Rev.* **30** 37-46.

Tomlinson JW, Crabtree N, Clark PM, Holder G, Toogood AA, Shackleton CH & Stewart PM 2003 Low-dose growth hormone inhibits 11 β-hydroxysteroid dehydrogenase type 1 but has no effect upon fat mass in patients with simple obesity. *J Clin.Endocrinol.Metab.* **88** 2113-2118.

Tomlinson JW, Moore J, Cooper MS, Bujalska I, Shahmanesh M, Burt C, Strain A, Hewison M & Stewart PM 2001 Regulation of expression of 11β-hydroxysteroid dehydrogenase type 1 in adipose tissue: tissue-specific induction by cytokines. *Endocrinology* **142** 1982-1989.

Trauner M & Boyer JL 2003 Bile salt transporters: molecular characterization, function, and regulation. *Physiol. Rev.* **83** 633-671.

Tsilchorozidou T, Honour JW & Conway GS 2003 Altered cortisol metabolism in polycystic ovary syndrome: insulin enhances 5α-reduction but not the elevated adrenal steroid production rates. *J Clin.Endocrinol.Metab. b* **88** 5907-5913.

Turley SD & Dietschy JM 1984 Modulation of the stimulatory effect of pregnenolone-16 α-carbonitrile on biliary cholesterol output in the rat by manipulation of the rate of hepatic cholesterol synthesis. *Gastroenterology* **87** 284-292.

Ubeda M, Matzilevich MM, Atucha NM, Garcia-Estan J, Quesada T, Tang SS & Ingelfinger JR 1994 Renin and angiotensinogen mRNA expression in the kidneys of rats subjected to long-term bile duct ligation. *Hepatology* **19** 1431-1436.

Ulick S, Tedde R & Wang JZ 1991 Defective Ring A Reduction of Cortisol as the Major Metabolic Error in the Syndrome of Apparent Mineralocortiocid Excess. *J Clin.Endocrinol.Metab.* **74** 593-599.

Ulick S, Levine LS, Gunczler P, Zanconato G, Ramirez LC, Rauh W, Rosler A, Bradlow HL & New MI 1979 A syndrome of apparent mineralocorticoid excess associated with defects in the peripheral metabolism of cortisol. *J Clin.Endocrinol.Metab.* **49** 757-764.

Ulick S, Ramirez LC & New MI 1977 An abnormality in steroid reductive metabolism in a hypertensive syndrome. *J Endocrinol.Metab.* **44** 799-802.

Ulven SM, Dalen KT, Gustafsson JA & Nebb HI 2005 LXR is crucial in lipid metabolism. *Prostaglandins Leukot.Essent.Fatty Acids* **73** 59-63.

van Heek M, Farley C, Compton DS, Hoos LM, Smith-Torhan A & Davis HR 2003 Ezetimibe potently inhibits cholesterol absorption but does not affect acute hepatic or intestinal cholesterol synthesis in rats. *Br. J Pharmacol.* **138** 1459-1464.

Vlahcevic ZR, Jairath SK, Heuman DM, Stravitz RT, Hylemon PB, Avadhani NG & Pandak WM 1996 Transcriptional regulation of hepatic sterol 27-hydroxylase by bile acids. *Am.J Physiol* **270** G646-G652.

Wake DJ, Rask E, Livingstone DE, Soderberg S, Olsson T & Walker BR 2003 Local and systemic impact of transcriptional up-regulation of 11β-hydroxysteroid dehydrogenase type 1 in adipose tissue in human obesity. *J Clin.Endocrinol.Metab.* **88** 3983-3988.

Walker BR, Aggarwal I, Stewart PM, Padfield PL & Edwards CRW 1995a Endogenous inhibitors of 11β-hydroxysteroid dehydrogenase in hypertension. *J Clin.Endocrinol.Metab.* **80** 529-533.

Walker BR, Connacher AA, Lindsay RM, Webb DJ & Edwards CRW 1995b Carbenoxolone increases hepatic insulin sensitivity in man: a novel role for 11-oxosteroid reductase in enhancing glucocorticoid receptor activation. *J Clin.Endocrinol.Metab.* **80** 3155-3159.

Walker BR & Edwards CRW 1994 Licorice-induced hypertension and syndromes of apparent mineralocorticoid excess. *Endocrin.Metab.Clin. N Amer.* **23 (2)** 359-377.

Walker BR, Soderberg S, Lindahl B & Olsson T 2000 Independent effects of obesity and cortisol in predicting cardiovascular risk factors in men and women. *J Intern.Med* **247** 198-204.

Wang DQ & Carey MC 2002 Susceptibility to murine cholesterol gallstone formation is not affected by partial disruption of the HDL receptor SR-BI. *Biochim.Biophys.Acta* **1583** 141-150.

Watanabe M, Houten SM, Mataki C, Christoffolete MA, Kim BW, Sato H, Messaddeq N, Harney JW, Ezaki O, Kodama T, Schoonjans K, Bianco AC & Auwerx J 2006 Bile acids induce energy expenditure by promoting intracellular thyroid hormone activation. *Nature* **439** 484-489.

Waxman DJ, Attisano C, Guengerich FP & Lapenson DP 1988 Human liver microsomal steroid metabolism: Identification of the major microsomal steroid hormone 6β-hydroxylase cytochrome P-450 enzyme. *Arch.Biochem.Biophy* **263** 424-436.

Webb NR, Connell PM, Graf GA, Smart EJ, de Villiers WJ, de Beer FC & van der Westhuyzen DR 1998 SR-BII, an isoform of the scavenger receptor BI containing an alternate cytoplasmic tail, mediates lipid transfer between high density lipoprotein and cells. *J Biol.Chem.* **273** 15241-15248.

Webb NR, de Villiers WJ, Connell PM, de Beer FC & van der Westhuyzen DR 1997 Alternative forms of the scavenger receptor BI (SR-BI). *J Lipid Res.* **38** 1490-1495.

Westerbacka J, Yki-Jarvinen H, Vehkavaara S, Hakkinen AM, Andrew R, Wake DJ, Seckl JR & Walker BR 2003 Body fat distribution and cortisol metabolism in healthy men: enhanced 5β-reductase and lower cortisol/cortisone metabolite ratios in men with fatty liver. *J Clin.Endocrinol.Metab.* **88** 4924-4931.

Whorwood CB, Franklyn JA, Sheppard MC & Stewart PM 1992 Tissue localization of 11β-hydroxysteroid dehydrogenase and its relationship to the glucocorticoid receptor. *J Ster.Biochem.* **41** 21-28.

Willy PJ, Umesono K, Ong ES, Evans RM, Heyman RA & Mangelsdorf DJ 1995 LXR, a nuclear receptor that defines a distinct retinoid response pathway. *Genes Dev.* **9** 1033-1045.

Wilson RC, Krozowski ZS, Li K, Obeyesekere VR, Razzaghy-Azar M, Harbison MD, Wei JQ, Shackleton CH, Funder JW & New MI 1995 A mutation in the HSD11B2 gene in a family with apparent mineralocorticoid excess. *J Clin.Endocrinol.Metab* **80** 2263-2266.

Woollett LA, Wang Y, Buckley DD, Yao L, Chin S, Granholm N, Jones PJ, Setchell KD, Tso P & Heubi JE 2006 Micellar solubilisation of cholesterol is essential for absorption in humans. *Gut* **55** 197-204.

Wu P, Zhang Y, Liu Y, Wang X, Guo Z, Zhang Y, Liang X & Lai W 1999 Effects of cholic acid on blood pressure and production of vascular aldosterone and corticosterone. *Steroids* **64** 291-295.

Xie W & Evans RM 2001 Orphan nuclear receptors: The exotics of xenobiotics. *J Biol.Chem.* **276** 37739-37742.

Yamagata K, Daitoku H, Shimamoto Y, Matsuzaki H, Hirota K, Ishida J & Fukamizu A 2004 Bile acids regulate gluconeogenic gene expression via small heterodimer partner-mediated repression of hepatocyte nuclear factor 4 and Foxo1. *J Biol.Chem.* **279** 23158-23165.

Ye P, Kenyon CJ, MacKenzie SM, Seckl JR, Fraser R, Connell JM & Davies E 2003 Regulation of aldosterone synthase gene expression in the rat adrenal gland and central nervous system by sodium and angiotensin II. *Endocrinology* **144** 3321-3328.

Zhang Y, Lee FY, Barrera G, Lee H, Vales C, Gonzalez FJ, Willson TM & Edwards PA 2006 Activation of the nuclear receptor FXR improves hyperglycemia and hyperlipidemia in diabetic mice. *Proc.Natl.Acad.Sci.U.S.A* **103** 1006-1011.

PUBLICATIONS

1. **Inhibitory effects of bile acids on glucocorticoid metabolism**
McNeilly A D, Kenyon C, Mitic T, Walker B R, Andrew R. *Endocrinology Submitted*

2. **Alterations in cholesterol utilisation and metabolism in the adrenal gland**
McNeilly A D, Walker B R, Andrew R. Kenyon C *In Preparation*

CONFERENCE PRESENTATIONS

88th Annual Meeting of the American Endocrine Societies – Boston, US – June 2006
McNeilly AD, MacKenzie S, Walker BR, Andrew R & Kenyon CJK
Aldosterone metabolism in the obese Zucker rat.
Poster Presentation

8th European Congress of Endocrinology – Glasgow, UK – April 2006
McNeilly AD, Kenyon CJ, Livingstone DEW, Davies E, MacKenzie S, Walker BR & Andrew R
Alterations in Scavenger Receptor B1 and steroidogenic enzymes within the adrenal gland in response to dietary bile acids.
Poster Presentation

8th European Congress of Endocrinology – Glasgow, UK – April 2006
Kenyon CJ, McNeilly AD, Livingstone DEW, Davies E, MacKenzie S, Walker BR & Andrew R
Adrenocortical function in obese Zucker rats.

Poster Presentation

87th Annual Meeting of the American Endocrine Societies – San Diego, US – June 2005
McNeilly AD, Mitic T, Walker BR & Andrew R

Impact of bile acids on glucocorticoid metabolism and activation of the hypothalamic-pituitary-adrenal axis.

Poster Presentation

Annual Meeting of British Endocrine Societies – Harrogate, UK – March, 2005

McNeilly AD, Walker BR & Andrew R

Impact of dietary chenodeoxycholic acid on the hypothalamic- pituitary-adrenal axis in rats
Oral Presentation

Annual Meeting of British Endocrine Societies – Brighton, UK – March, 2004

McNeilly AD, Walker BR & Andrew R (2004)

The inhibitory effect of bile acids on glucocorticoid metabolism
Poster Presentation

Scottish Society for Experimental Medicine- Glasgow, UK – January 2004

McNeilly AD, Livingstone DEW, Walker BR & Andrew R

Inhibition of steroid 5β-reductase by bile acids.
Poster Presentation-Prize winner